arXiv:hep-th/9910259v1 1 Nov 1999

Equilibrium and Non-equilibrium Quantum Field Theory

Petr Jizba

Summary

This dissertation is concerned with various aspects of equilibrium and non–equilibrium quantum field theory.

We first focus in Chapter 2 on infrared effects in finite–temperature quantum field theory. We propose a simple mathematical method (based on the largest–time equation and the Dyson–Schwinger equations) which allows systematic calculations of the change of density in energy/particles in heat–bath during a scattering/decay of external particles within the heat bath. A careful analysis reveals that the resulting changes in the energy density are finite even in the case of massless heat–bath particles (no infrared catastrophe).

As a next point we re–consider in Chapter 3 the usual method of pressure calculations. We use the so called hydrostatic pressure (or pressure at a point) which is defined via the energy–momentum tensor. We go through all delicate points which one must deal with in the context of quantum field theory. Namely the renormalisation of composite operators and the vital role of renormalisation for a consistent quantum field theoretical definition of pressure are discussed. We finally apply the whole procedure to a toy model system; $\lambda\Phi^4$ theory with $O(N)$ internal symmetry. In the case of the large–N limit (also Hartree–Fock approximation) the pressure is an exactly solvable quantity. Using the Mellin transform technique we then perform the large–temperature expansion of the pressure to all orders.

The hydrostatic pressure can be naturally extended to non–equilibrium systems. Using the Jaynes–Gibbs principle of maximal entropy and the (non–equilibrium) Dyson–Schwinger equations we derive generalised Kubo–Martin–Schwinger equations and set up a calculational scheme for pressure calculations away from thermal equilibrium. As an example we explicitly evaluate in Chapter 4 the pressure for our $O(N)$ $\lambda\Phi^4$ theory in the large–N limit in the case of two translationally invariant non–equilibrium systems.

There follow five appendices which collect together much of the background material required in the main body of the thesis. The important part is the detailed analysis in Appendix A.1 of the Dyson–Schwinger equations. The derivation there shows how the Dyson–Schwinger equations may be recast into a very useful functional form. In Appendices B and C we clarify some finer mathematical manipulations needed in Chapter 3. The fundamentals of the information or Shannon entropy are presented in Appendix D. Appendix E covers the elements of dimensional regularisation and special functions which underlie much of the material presented in the earlier chapters.

Equilibrium and Non-equilibrium Quantum Field Theory

Petr Jizba

Fitzwilliam College

A dissertation submitted for the degree of Doctor of Philosophy

University of Cambridge

March, 1999

Declaration of Originality

This dissertation contains the results of research carried out in the Department of Applied Mathematics and Theoretical Physics, University of Cambridge, between October, 1995 and March, 1999.

Excluding introductory section the research described in this dissertation is original unless where explicit reference is made to the work of others. Some of this work was carried out in collaboration. I further state that no part of this dissertation or anything substantially the same has been submitted for any qualification other than the degree of Doctor of Philosophy at the University of Cambridge. Some of the research in this dissertation has been, or is to be, published. The results in Chapter 2 appeared in [J1]. The material presented in Chapter 3 has been accepted to Phys. Rev. **D** [J2]. Chapter 4 results from a collaboration with Dr. E.S. Tututi [JT1], [JT2], [JT3].

[J1] P. Jizba, Phys. Rev. **D57**: 3634, 1998.

[J2] P. Jizba, `hep-th/9801197`, Phys. Rev. **D** (in press).

[JT1] P. Jizba and E.S. Tututi, `hep-th/9809110`, in *Proceedings of the 5th Int. Workshop on Thermal Field and Their Applications, Regensburg, 1998.*

[JT2] P. Jizba and E.S. Tututi, Phys. Rev. **D60**: 105013, 1999.

[JT3] E.S. Tututi and P. Jizba, `DAMTP-1998-163`, in *Proceedings of the VIII Mexican School of the Particles and Fields, Mexico city, 1998.*

Acknowledgement

I would like to express my respectful thanks to my research supervisor, Prof. P.V. Landshoff, for his careful guidance throughout my whole Ph.D., from the primitive inception of the research to its writing–up in this dissertation. I wish to extend my gratitude to Dr. E.S. Tututi and Dr. M. Blasone with whom I have enjoyed a relaxed and stimulating collaboration and who, among others, shared the many up–and–downs of my professional and personal life.

My fundamental gratitude to my mother goes beyond the limit words can capture. I would like to dedicate this dissertation to her.

Finally, it is a pleasure to thank to all my friends. Particularly the encouragement and support that I gained from Marketa Mazakova was invaluable. I also acknowledge the financial assistance that I have received from the Cambridge Overseas Trust, Fitzwilliam College and the Board of Graduate Studies, University of Cambridge.

To my mother

The scientist does not study nature because it is useful; he studies it because he delights in it, and he delights in it because it is beautiful. If nature were not beautiful, it would not be worth knowing, and if nature were not worth knowing, life would not be worth living.

Henri Poincaré

Contents

1 Introduction and overview **1**

2 Heat–bath particle number spectrum **11**

2.1 Basic tools . . . 13

2.1.1 Mean statistical value . . . 13

2.1.2 Largest–time equation at T=0 . . . 14

2.1.3 Thermal Wick's theorem (the Dyson–Schwinger equation) . . . 21

2.1.4 Thermal largest–time equation . . . 22

2.2 Heat–Bath particle number spectrum:
general framework . . . 26

2.3 Modified cut diagrams . . . 28

2.4 Model process . . . 36

2.4.1 Basic assumptions . . . 37

2.4.2 Calculations . . . 37

2.5 Conclusions . . . 50

3 Pressure at thermal equilibrium **53**

3.1 Introduction . . . 53

3.2 Renormalisation 57

3.3 Hydrostatic pressure 72

3.3.1 Mass renormalisation 72

3.3.2 Coupling constant renormalisation 77

3.3.3 The pressure 80

3.4 Hydrostatic pressure in $D = 4$ (high–temperature expansion) 86

3.5 Conclusions 93

4 Pressure in out–of–equilibrium media 96

4.1 Basic formalism 98

4.1.1 Off–equilibrium Dyson–Schwinger equations 99

4.1.2 The Jaynes–Gibbs principle of maximal entropy 101

4.2 The $O(N)$ Φ^4 theory 108

4.3 The large–N limit 110

4.4 Out–of–equilibrium pressure 112

4.4.1 Equilibrium 112

4.4.2 Off–equilibrium I 115

4.4.3 Off–equilibrium II 125

4.5 Conclusions 127

5 Summary and outlooks 130

A Finite–temperature Dyson–Schwinger equations 135

A.1 Functional formalism 135

A.2 Graphical formalism 142

A.3 Comparison 148

B Surface term in Eq.(4.69) 153

C High–temperature expansion of the gap equation 155

D Derivation of the Shannon (information) entropy 157

E Some mathematical formulae 169

E.1 Integrals in D dimensions 169

E.2 Special functions and important relations 171

List of figures

FIG.2.1 A one loop triangle diagram. p.15

FIG.2.2 An example of a cut diagram in the φ^3 theory which does not contribute to the RHS's of (2.12)–(2.13). Arrows indicate the flow of energy. p.19

FIG.2.3 Generic form of the cut diagram at the $T = 0$. Shadow is on the 2nd type vertex area. p.19

FIG.2.4 An example of non–vanishing cut diagrams at the $T \neq 0$. The heat–bath consists of two different particles. External particles are not thermalized. p.25

FIG.2.5 The cut diagram from FIG.2.3 c) demonstrates that the cut can be defined in many ways but the number of crossed lines is still the same. p.25

FIG.2.6 The numerator of (2.32) and (2.33) can be calculated using the modified cut diagrams for $\langle \mathbb{T}^{\dagger} \mathbb{P} \, \mathbb{T} \rangle_{p_1 p_2}$. As an example we depict all the possible contributions to the numerator derived from the cut diagram on Fig.2.4 c). The wavy lines and thin lines describe the heat-bath particles. The crossed lines denote the substituted propagators, in this case we wish to calculate the thin–line particle number spectrum. p.35

FIG.2.7 The modified cut diagrams involved in an order–e^2 contribution to the photon number spectrum. Dashed lines: photons. Solid lines: ϕ, $\phi^{\dagger}$ particles. Bold lines: Φ particles. p.38

FIG.2.8 The diagram a) with a corresponding kinematics. p.38

FIG.2.9 The lowest–order cut diagram for $\langle \mathbb{T} \mathbb{P} \mathbb{T}^{\dagger} \rangle_{p_1 p_2}$. p.41

FIG.2.10 The generating thermal diagrams involved in an order–e^4 contribution to the electron number spectrum. Dashed lines: photons. Thin lines: ϕ, $\phi^\dagger$ particles. Bold lines: Φ particles. Half–bold lines: electrons. p.46

FIG.2.11 The non–vanishing modified cut diagrams from FIG.2.10c). p.47

FIG.3.1 The graphical representation of $D^{\mu\nu}(p^n|p)$. p.59

FIG.3.2 Counterterm renormalisation of the last two diagrams in Eq.(2.17). (Cut legs indicate amputations.) p.67

FIG.3.3 The Keldysh–Schwinger time path. p.81

FIG.3.4 First few bubble diagrams in the $\mathfrak{M}$ expansion. p.83

FIG.4.1 A plot of $\langle\beta\rangle$ vs. $\mathcal{M}$ at $\sigma = 100$ MeV. p.119

FIG.4.2 A plot of the Eq.(4.60): a) the general shape, b) a small x behaviour. p.121

FIG.4.3 A plot of pressure as a function of T, σ for $m_r = 100$MeV. The gray line corresponds to equilibrium pressure, the black line corresponds to pressure (4.62). p.122

FIG.4.4 A plot showing the difference of equilibrium and non-equilibrium pressures for $m_r = 100$MeV. p.123

FIG.4.5 Behaviour of the pressure (4.67) as a function of α and T_0 at $m_r = 100$MeV. p.126

FIG.A.1 Diagrammatic equivalent of Eq.(A.20). The cut separates areas constructed out of $F[\psi]$ and $G[\psi]$. p.141

Notation

Natural units $\hbar = c = k_B = 1$ will be used throughout this dissertation. The following sub and superscripts will be used to label various quantities in the following text.

Subscripts

$_{s}$	Schrödinger picture
$_{H}$	Heisenberg picture
$_{C}$	Closed–time path (also the Keldysch–Schwinger path)
$_{fix}$	Gauge–fixing term
$_{in}$	Interaction component
$_{hb}$	Heat–bath component
$_{r}$	Renormalised object (operators, vertex functions, etc.)
$_{V}$	Volume

Superscripts

†	Hermitian conjugation
*	Complex conjugation (except for the $\mathcal{T}^*$–ordering)
^{T}	4–dimensional transverse components
^{L}	4–dimensional longitudinal components
^{D}	Symbol for a dimension

Either

μ, ν, λ	4–dimensional spacetime index
i, j	3–dimensional space index
α, β	Closed–time path indices :$\alpha, \beta = \{+, -\}$ for non-equilibrium, and $\alpha, \beta = \{1, 2\}$ for equilibrium
a, b, c, d	Internal symmetry indices

Some of the important fields and functionals which will be used are.

$H = \int d^3x \, \mathcal{H}(x)$	Hamiltonian
$\mathcal{L}(x)$	Lagrange density
$\mathbb{P}$	Projection operator onto final particle states
$\mathbb{S}$	$\mathbb{S}$–matrix ($\mathbb{S} = \mathbb{1} + i\mathbb{T}$)
$\mathbb{T}$	$\mathbb{T}$–matrix
$U(t;t')$	Ket evolution operator
ρ	Density matrix
$\Theta^{\mu\nu}$	General energy–momentum tensor
$\Theta_c^{\mu\nu}$	Canonical energy–momentum tensor
Φ, ϕ, ψ	General fields

Various other notations that will be used are.

$\mathbb{D}$	Full thermal propagator for scalar fields in the closed-time formalism (i.e. 2×2 matrix)
$\mathbb{D}^c$	Connected thermal 2–point Green's function, i.e. connected part of $\mathbb{D}_F$
$\mathbb{D}_F$	Free thermal propagator for scalar fields in the closed-time formalism (i.e. 2×2 matrix)
$\mathbb{D}^{(n)}$	Full thermal n–point Green's function
$G^{(n)}$	Non–equilibrium n–point connected Green's function
$\mathbb{G}$	Non–equilibrium propagator in the closed–time path formalism (i.e. 2×2 matrix)
f_B	Bose–Einstein distribution
f_F	Fermi–Dirac distribution
$\boldsymbol{\mathfrak{z}}$	Information content
$I(\ldots)$	Shannon (information) entropy
$\Im(\ldots)$	Amount of information conveyed by a single message
$\mathbb{M}$	Bogoliubov matrix
$\boldsymbol{\mathfrak{m}}$	Massieu function $= -\beta\times$ (Helmholtz) free energy
$\mathcal{O}(z)$	Order z
$p(T)$	Thermodynamic pressure at the temperature T
$p(x,T)$	Hydrostatic pressure at the temperature T
$\mathcal{P}(T)$	Hydrostatic pressure for translationally invariant media
S_F	Feynman (causal) propagator for spin–$\frac{1}{2}$ particles; ($T = 0$)
S^+	Positive energy part of S_F
S^-	Negative energy part of S_F
S_G	von Neumann–Gibbs entropy

$\mathcal{T}$	Time ordering symbol
$\mathcal{T}^*$	The $\mathcal{T}^*$ (or covariant) ordering
W	Generating functional for $G^{(n)}$
Z	(Grand) partition function
$\mathcal{Z}$	The Jaynes–Gibbs partition function
Z_Φ	Wave function renormalisation
β	Inverse temperature $1/T$
Γ	Generating functional for $\Gamma^{(n)}$ (i.e. the effective action)
$\Gamma^{(n)}$	n–point vertex function (i.e. 1PI n–point Green's function)
$\frac{\overrightarrow{\delta}}{\delta\psi(z)}$	Left–handed variation
$\frac{\overleftarrow{\delta}}{\delta\psi(z)}$	Right–handed variation
$\delta^{\pm}(\ldots)$	Positive (+), negative (−) frequency parts of Dirac's δ–function
Δ_F	Feynman (causal) propagator for scalar fields; ($T = 0$)
Δ^+	Positive energy part of Δ_F
Δ^-	Negative energy part of Δ_F
μ	Chemical potential
ϕ^a_α	Expectation value of the Heisenberg field operator Φ^a_α in the presence of a c–number source J (i.e. $\phi^a_\alpha = \langle \Phi^a_\alpha \rangle$)
Σ	Proper self–energy for the scalar theory; ($T = 0$)
$\boldsymbol{\Sigma}$	Proper self–energy for the scalar theory at finite temperature in the closed-time path formalism (i.e. 2×2 matrix)
$\tilde{\boldsymbol{\Sigma}}$	Self–energy for the scalar theory at finite temperature
Ω	Grand (canonical) potential. In the case when the canonical ensemble is in question, Ω is (Helmholtz) free energy
$\langle \ldots \rangle$	Expectation value
$\langle \ldots \rangle_{\{p_k\}}$	Thermal expectation value. Particles with momenta $\{p_k\}$ are unheated

- The Minkowski metric used throughout is $g^{\mu\nu} = g_{\mu\nu} = \mathrm{diag}(1, -1, -1, -1)$

$$g_{\mu\nu} g^{\mu\nu} = \delta^\mu_{\ \mu} = \mathrm{Tr}(g) = 4, \;\; g_{\mu\mu} = g^{\mu\mu} = -2$$

- Derivatives with respect to x^μ or x_μ are abbreviated as

$$\partial_\mu \equiv \partial/\partial x^\mu, \quad \partial^\mu \equiv \partial/\partial x_\mu$$

Chapter 1

Introduction and overview

The development of the theory of quantised fields at finite temperature and density (also thermal quantum field theory) over the past forty years or so has led to fundamental changes in the understanding of a wide number of physical phenomena. Among those one may mention symmetry restoration during high–temperature phase transitions [1–3] which has found significant application in early universe cosmology, and we may also mention applications in neutron–star [4] and supernova [5] astrophysics. However, perhaps one of the most important applications of thermal quantum field theory nowadays is to quantum chromodynamics (QCD).

The reason for this interest may be traced to the mid–70's when the notion of asymptotic freedom of QCD started to emerge. At zero temperature and chemical potential the low–energy and/or momentum transfer behaviour of QCD is characterised by confinement (i.e. strong interaction among QCD constituents). The internal scale that determines the boundary between small and large energy in QCD is $\sim \Lambda_{QCD} \sim 0.2\text{GeV}$. As the energy and/or momentum transfer increases, QCD begins to be characterised by asymptotic freedom, i.e., the coupling evolves as

$$\lambda_{QCD}(Q^2, T = 0 = \mu) \overset{Q^2 \to \infty}{\longrightarrow} 0,$$

(Q^μ is the four–momentum transfer, $Q^2 > 0$) and so quarks and gluons behave like weakly interacting, massless particles[1] in high–energy and/or large Q^2 processes. This behaviour is usually tested experimentally by means of deep inelastic electron–nucleon scattering.

If one starts to study QCD at finite temperature and/or finite baryon density one automatically introduces new (intensive) variables, namely the temperature T and the quark chemical potential μ. These bring an additional mass scale with which the coupling λ_{QCD} can run. It was Collins and Perry who first showed in [4] that strong interactions become weak not only at high energy–momentum transfer, as in the deep inelastic scattering, but also at very high baryon density. This reasoning was quickly extended to finite temperature [3, 8] where it was shown that

$$\lambda_{QCD}(Q^2 = 0, T, \mu) \to 0,$$

provided that $T \gg \Lambda_{QCD}$ and/or $\mu \gg \Lambda_{QCD}$. Thus at a sufficiently high temperature and/or baryon number density QCD systems consist of free quarks and gluons, regardless of the energy–momentum transfer. This "deconfined" phase of QCD is called the quark–gluon plasma. As was just mentioned, the temperature and/or chemical potential must be greater than the QCD fundamental mass scale Λ_{QCD}. In practice this means that the temperature for creation of the quark–gluon plasma must be at least of the order $\sim 0.2\text{GeV} \sim 10^{12}\text{K}$ and/or the baryon number density must be of order $\sim \Lambda_{QCD}^3 \sim 0.8(\text{GeV})^3 \sim 10^{42}\,\text{cm}^{-3}$.

---

[1] Because quarks become massless, the deconfined phase leads to chiral–symmetry restoration (under normal circumstances the chiral flavour group $SU_L(N) \times SU_R(N)$, with N the number of quark flavours, is broken to a vector–like subgroup $SU_V(N)$). The chiral phase transition is expected to be particularly interesting at high temperatures and/or densities [6, 7].

Such temperatures prevailed in the very early stage of the universe ($\sim 10^{-6}$s $-$ 10^{-5}s after the Big–Bang) and such densities are expected to be present, for instance, in the core of neutron stars [4].

Apart from the cosmological and astrophysical implications, the quark–gluon plasma naturally offers an important laboratory for the study of asymptotic freedom. This fact has led to the construction of a Relativistic Heavy Ion Collider (RHIC) at Brookhaven National Laboratory, where it is expected that two on–head colliding beams of ^{197}Au will generate a sufficient centre–of–mass energy density which, when properly thermalized, will allow the formation of a quark–gluon plasma. Similar experiments are planned in the Large Hadron Collider (LHC) at CERN with colliding Pb beams.

So far we have only outlined possible applications of QFT to systems which are in thermodynamical equilibrium. However, during the last several years there has been a steadily growing awareness that the usual equilibrium (or thermodynamical) approaches in quantum field theory fail to describe correctly such fundamental phenomena as realistic phase transitions (both in condensed matter physics and in high–energy physics), quantum electrodynamical (QED) plasma evolution (and the related problem of hot thermonuclear fusion), heat transfer in stars, etc. Presently, the most important applications of non–equilibrium QFT, however, are in the physics of the early universe. The reason why it is so important to go beyond conventional equilibrium approaches in describing the universe is the extreme conditions present in the early period of its evolution [9]. It is now well recognised that at the very early times the universe was very hot with energy densities approaching the Planck mass density $\sim 5.2 \times 10^{93}\,\mathrm{g\ cm}^{-3}$, and it then cooled rapidly due to the expansion. Because of this fact, it is expected that the matter fields went through a hierarchy of phase transitions before reaching the present status quo [10]. It is obvious that if the matter fields involved in the phase transitions interacted at a rate much smaller than the typical cooling (or relaxation) rate of the universe, the evolution would proceed in an out–of–equilibrium manner. Such non–equilibrium dynamics may, in turn, lead to many crucial physical consequences. One such example is the baryon asymmetry [9, 11, 12]. If one assumes that the relative abundance of baryonic matter over antibaryonic matter is not created *a priori* via the initial–time conditions, then one must find a physical mechanism which could generate such an asymmetry. It was A.D. Sakharov [13] who proposed more than thirty years ago that, in order to explain a biased production of baryons over anti–baryons, one needs to take into account the non–equilibrium evolution of the universe since baryons and anti–baryons are produced in equal number in any equilibrium process. This is one of the celebrated Sakharov criteria [11, 13, 14] for baryogenesis.

Another extremely interesting example of application of non–equilibrium QFT in cosmology is the production of topological defects during phase transitions. Interest in this area stems from the belief that topological defects, such as cosmic strings, might provide an explanation of structure formation and the cosmic microwave background radiation anisotropies in the universe [15]. The domain structure of a ferromagnet is known to become very different when the sample is cooled adiabatically through the Curie temperature compared to when it is cooled rapidly. In analogy one may expect that the production of topological defects and their evolution will depend strongly on the cooling rate of the universe. The formation of defects and their dynamics can be beautifully mimicked in quantum liquids [16, 17] such as helium ^{3}He or ^{4}He, in liquid nematic crystals [18] or in superconductors [19]. Recent experiments [16] with ^{3}He have confirmed that the density of vortex lines nucleated during the phase transition from a normal ^{3}He liquid to its superfluid B–phase depends considerably on the cooling rate.

In the framework of non–equilibrium applications of QFT one should not forget the currently very important application to relativistic heavy–ion collisions, which, as we have mentioned, are expected to produce a sufficient thermal environment for creation of a quark–gluon plasma. The major indication that a non–equilibrium description seems to be necessary comes from the expectation that the time scale at which the quark–gluon plasma should exhibit itself will be too short for its macroscopic equilibration. The point is that the energy density in the reaction zone, once the plasma begins to thermalise, will create a pressure which will consequently lead to explosive expansion of the plasma. The associated expansion time is estimated to be only 10 or 100 times longer than the time scale of microscopic equilibration processes [20]. This introduces a basic uncertainty as to whether an equilibrium treatment may be used safely. On the other hand, if a non–equilibrium description proves crucial, then one must face the question to what extent a small, short–lived, fast expanding system of quarks and gluons can be called a quark–gluon plasma. One should honestly admit that there does not presently exist any generally accepted model which would satisfactorily describe the quark–gluon plasma dynamics.

All the mentioned non–equilibrium processes are characterised by the rate at which a system changes (e.g. expansion rate, dissipative rate, the rate at which particles are exchanged with an external environment) which is comparable to or greater than the rate at which microscopic interactions (i.e. the equilibrating mechanism) are happening. In practice this means that the relaxation time scale (i.e. the mean time in which the system relaxes to equilibrium) is much longer than the time scale at which observations are performed, and consequently a system does not evolve adiabatically (i.e. it does not go through a sequence of states each of which is at thermal equilibrium). It is needless to say that many of phenomena in Nature are precisely of this character.

Whereas for the description of matter in equilibrium one has at one's disposal a systematic and unified approach based upon the formalism of the Gibbs (micro– or grand–) canonical density matrices, no such simple way seems to exist in a non–equilibrium theory because of the variety of phenomena and of the complexity of the evolution processes. This is to be expected, as there is basically no limitation on the amount of questions that may be asked about time–dependent phenomena unless one clearly specifies which degrees of freedom (or what degree of reduction) one will adopt for the description of the evolution of a system. Within such a reduced description, however, the dynamics has been shown to be capable of prediction. In this framework there have steadily crystallised two major (and mutually distinct) approaches [21–23].

The first one, which we mostly refer to in our thesis, is the, so called, 'Maxent school' (or maximal entropy school) founded by E.T.Jaynes *et al.* [24–27]. The basic philosophy behind this approach is rooted in the fact that the prediction of the future macroscopic evolution of a system cannot be done with certainty on the basis of the initial macroscopic data because of the existing correlations with the parameters or data that are discarded in the given reduced description. The corresponding statistical inference about the system is not deduced from the underlying microscopic dynamics but instead is rather based on information theory. There the algorithm of entropy maximalisation leads to the density matrix (or probability distribution) with the least informative content subject to the prior knowledge which one has about the system. Generally one may, at different times, adopt different macroscopic parameters describing the system (i.e. at different times one may choose a different level or reduction in the description). If this is the case, the maximalisation of entropy naturally leads to a more complex form of the density matrix. This branch of the Maxent school (and its various modifications) is also known as the *projection operator* *technique* [28].

The second school, the so called 'Brussels school', is associated with I.Prigogine, R.Balescu *et al.* [23, 29, 30]. The basic emphasis is here put on the microscopic dynamics (i.e. Hamilton, Schrödinger or Liouville equations), and all other non–dynamical approaches, such as those coming from information theory, are discarded: everything should be derived from the dynamics alone. The ultimate aim is a dynamical separation into the parameters to be retained on the desired level of description, and those to be discarded. This separation, if it exists, should emerge the from dynamics as an asymptotic property valid for the large (i.e. observational) time scales. It is well known since the time of Boltzmann that the latter may be achieved by introducing a certain hypothesis about the microscopic behaviour of the system; e.g. Boltzmann's "Stosszahlansatz" (random collision hypothesis) [31], Ehrenfest's coarse graining hypothesis [32], or Bogoliubov's no initial–time correlations hypothesis [33]. This line of reasoning is basically inherited and progressed by the Brussels school. It should be noted that all the statistical inferences or hypotheses here have a strictly dynamical nature (they are directly motivated by the underlying dynamics), but on the other hand they are in a certain respect *ad hoc*, because only certain probabilistic features of the microscopic dynamics are emphasised.

Synopsis

We first focus in Chapter 2 on infrared effects in finite–temperature QFT. We propose a simple mathematical method (based on the largest–time equation and the Dyson–Schwinger equations) which allows systematic calculations of the change of energy density (or particle density) in a heat–bath during a decay (or scattering) of the external particle(s) within the heat bath. The applied method naturally leads to an interpretation of the change of density of energy (particles) in terms of three additive contributions: stimulated emission, absorption and fluctuations of the heat–bath particles. This result is completely non–perturbative. A careful analysis reveals that the resulting change in the energy density is finite even in the case of massless heat–bath particles. This means that there is no infrared catastrophe.

As the next point we re–consider in Chapter 3 the problem of calculating pressure. We use the so–called hydrostatic pressure (or pressure at a point) which is defined via the energy–momentum tensor. The obvious advantage is a possible extension into a non–equilibrium medium. We go through all the delicate points that must be dealt with in the context of quantum field theory. Renormalisation of composite operators and in general the vital role of renormalisation for a consistent quantum field–theoretical definition of pressure is discussed. We finally apply the whole procedure to a toy–model system: $\lambda\Phi^4$ theory with $O(N)$ internal symmetry. In the case of the large–N limit (also the Hartree–Fock approximation) the pressure is exactly solvable. Using the Mellin transform technique we perform the large–temperature expansion of the pressure to all orders in T.

The hydrostatic pressure can be naturally extended to non–equilibrium systems. Using the Jaynes–Gibbs principle of maximal entropy and the (non–equilibrium) Dyson–Schwinger equations we derive in Chapter 4 the generalised Kubo–Martin–Schwinger equations and set up a calculational scheme for pressure calculations away from thermal equilibrium. As an example we explicitly evaluate pressure for the $O(N)$ $\lambda\Phi^4$ theory in the large–N limit in two cases of translationally invariant non–equilibrium systems.

There follow five appendices which comprise much of the background material required in the main body of the thesis. The important part is the detailed analysis in Appendix A.1 of the Dyson–Schwinger equations. The derivation there shows how the Dyson–Schwinger equations may be formulated in a very useful functional form. We also outline the connection with the more conventional approaches. In Appendices B and C we clarify some finer mathematical manipulations needed in Chapter 3. The fundamentals of information or Shannon entropy are presented in Appendix D. Appendix E covers the elements of dimensional regularisation and special functions which underlie much of the material presented in the earlier chapters.

Epilogue

A reader of this dissertation might be disappointed by the fact that he or she will not find a usual pedagogical introduction to the subject. The omission of such an introduction was dictated mainly by two considerations. Firstly, we have not felt very competent to provide a good account of the fundamentals of both equilibrium and non–equilibrium quantum field theory. The subjects themselves are currently immensely vast and the number of problems involved quickly approaches the "thermodynamic limit". We therefore take a more pragmatic point of view and proceed by sampling a few definite problems, which we develop and analyse in great detail. Secondly, and most importantly, we personally hold the opinion that a dissertation should reflect student's ability to cope with a subject and creatively apply it to practical problems rather than write an essay on mathematical or physical foundations of the subject in question. Any such attempts would lead (at least in our case) to pure epigonism since we do not feel that we could add anything substantially new to existing (and pedagogically excellent) textbooks and review articles; see for example Refs. [31,34–42] for equilibrium quantum field theory and statistical physics and Refs. [23,30,43,44] for non–equilibrium quantum field theory and statistical physics.

To end, we wish to make one more remark. We are perfectly aware that the presented work is incomplete in many respects. Our ignorance or lack of understanding of many important topics is of course in part responsible for this weakness. In particular, we refer here to discussions and applications of such crucial areas as the imaginary–time (Euclidean or Matsubara) formalism, (non–equilibrium) thermofield dynamics, hard thermal loops, the theory of temperature–induced phase transitions, linear response theory, stochastic approaches to non–equilibrium dynamics, quantum transport equations, theory of transport coefficients and many more, which are definitely missing in this dissertation. Although we had originally planned to include some of the aforementioned issues (namely those which directly concern or resonate with our present research), neither space nor time has allowed us to fulfil this wish.

Chapter 2

Heat–bath particle number spectrum

In recent years much theoretical effort has been invested in the understanding relativistic heavy ion collisions as these can create critical energy densities which are large enough to produce the quark–gluon plasma (the deconfined phase of quarks and gluons) [34, 36].

A natural tool for testing the quark–gluon plasma properties would be to look for the particle number spectrum formed when a particle decays within the plasma itself. As the plasma created during heavy ion collisions is, to a very good approximation, in thermodynamical equilibrium [34] (somewhat like a "microwave oven" or a heat bath), one can use the whole machinery of statistical physics and QFT in order to predict the final plasma number spectrum. Such calculations, derived from first principles, were carried out by Landshoff and Taylor [45].

Our aim is to find a sufficiently easy mathematical formalism allowing us to perform mentioned calculations to any order. Because unstable particles treated in [45] can not naturally appear in asymptotic states, we demonstrate our approach on a mathematically more correct (but from practical point of view less relevant) process; namely on the scattering of two particles inside of a heat bath. The method presented here however, might be applied as well to a decay itself (provided that the corresponding decay rate is much less than any of the characteristic energies of the process). In this chapter we formulate the basic diagrammatic rules for the methodical perturbative calculus of plasma particle number spectrum $d\langle N(\omega)\rangle/d\omega$ and discuss it in the simple case of a heat bath comprised of photons and electrons, which are for simplicity treated as scalar particles.

In Section 2.1 we review the basic concepts and techniques needed from the theory of the largest-time equation (both for $T = 0$ and $T \neq 0$) and the Dyson–Schwinger equations. Rules for the cut diagrams at finite–temperature are derived and subsequently extended to the case when unheated fields are present. It was already pointed out in [46] that the thermal cut diagrams are virtually the Kobes–Semenoff diagrams [34] in the Keldysh formalism [47]. This observation will allow us to identify type 1 vertices in the real time finite—temperature diagrams with the uncircled vertices used in the (thermal) cut diagrams, and similarly type 2 vertices will be identified with the circled, cut diagram vertices. As we want to restrict our attention to only some particular final particle states, further restrictions on the possible cut diagrams must be included. We shall study these restrictions in the last part of Section 2.1.

As we shall show in Section 2.2, the heat–bath particle number spectrum can be conveniently expressed as a fraction. Whilst it is possible to compute the denominator by means of the thermal cut diagrams developed in Section 2.1, the calculation of the numerator requires more care. Using the Dyson–Schwinger equations, we shall see in Section 2.3 that it can be calculated through modified thermal cut diagrams. The modification consists of the substitution in turn of each heat bath particle propagator by an altered one. We also show that there must be only one modification per diagram. From this we conclude that from each individual cut diagram we get n modified ones (n stands for the total number of heat–bath particle propagators in the diagram). Furthermore, in the case when more types of the heat bath particles are present, one might be only interested in the number spectrum of some of these. The construction of the modified cut diagrams in such cases follow the same procedure as in the previous situation. We find that only the propagators affiliated to the desired fields must be altered.

In Section 2.4 the presented approach is applied to a toy model in which a gluon plasma is simulated by scalar photons, and we calculate the resulting changes in the number spectrum of the 'plasma' particles. Section 2.4 ends with a qualitative discussion of the quark–gluon plasma simulated by scalar photons and electrons.

For reader's convenience, the chapter is accompanied with Appendix A.1 where we derive, directly from the thermal Wick's theorem, the (thermal) Dyson–Schwinger equations as well as other useful functional identities valid at finite temperature.

2.1 Basic tools

2.1.1 Mean statistical value

The central idea of thermal QFT is based on the fact that one can not take the expectation value of an observable A with respect to some pure state as generally all states have non-zero probability to be populated and consequently one must consider instead a mixture of states generally described by the density matrix ρ. The mean statistical value of A is then

$$\langle A \rangle = Tr(\rho A), \tag{2.1}$$

where the trace has to be taken over a complete set of *physical* states. For a statistical system in thermodynamical equilibrium ρ is given by the Gibbs (grand–) canonical distribution

$$\rho = \frac{e^{-\beta(H-\mu N)}}{Tr(e^{-\beta(H-\mu N)})} = \frac{e^{-\beta K}}{Z}, \tag{2.2}$$

here Z is the partition function, H is the Hamiltonian, N is the conserved charge (e.g. baryon or lepton number), μ is the chemical potential, $K = H - \mu N$, and β is the inverse temperature: $\beta = 1/T$.

2.1.2 Largest–time equation at T=0

An important property inherited from zero–temperature QFT is *the largest–time equation* (LTE) [48–50]. Although the following sections will mainly hinge on the *thermal* LTE, it is instructive to start first with the zero–temperature one. The LTE at $T = 0$ is a generally valid identity which holds for any individual diagram constructed with propagators satisfying certain simple properties. For instance, for the scalar theory with a coupling constant g one can define the following rules:

$$\begin{array}{lcl}
x\ \underline{1\qquad\qquad\qquad 1}\ y & \sim & i\,\Delta_F\,(x\text{-}y)\\
x\ \underline{1\qquad\qquad\qquad 2}\ y & \sim & i\,\Delta^-\,(x\text{-}y)\\
x\ \underline{2\qquad\qquad\qquad 1}\ y & \sim & i\,\Delta^+\,(x\text{-}y)\\
x\ \underline{2\qquad\qquad\qquad 2}\ y & \sim & -i\,\Delta^*_F\,(x\text{-}y)
\end{array}$$

Here $i\Delta_F$ is the Feynman propagator, $i\Delta^+$ ($i\Delta^-$) is corresponding positive (negative) energy part of $i\Delta_F$, the '$*$' means complex conjugation and index 1 (2) denotes *type–1* (*type–2*) vertex; type–1 vertex has attached a factor $-ig$ whilst type–2 bears a factor ig. Using this prescription, we can construct diagrams in configuration space. With each diagram then can be associated a function $F(x_1, \ldots x_n)$ having all the 2nd type vertices underlined. For example, for the triangle diagram in FIG.2.1 we have

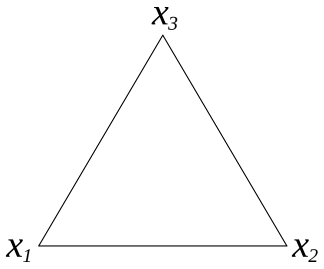

Figure 2.1: A one loop triangle diagram.

$$\begin{aligned}
F(x_1,x_2,x_3) &= (-ig)^3\, i\Delta_F(x_1-x_2)\, i\Delta_F(x_1-x_3)\, i\Delta_F(x_2-x_3) \\
F(\underline{x_1},x_2,x_3) &= (-ig)^2(ig)\, i\Delta^+(x_1-x_2)\, i\Delta^+(x_1-x_3)\, i\Delta_F(x_2-x_3) \\
F(\underline{x_1},\underline{x_2},x_3) &= (ig)^2(-ig)\, (-i)\Delta_F^*(x_1-x_2)\, i\Delta^+(x_1-x_3)\, i\Delta^+(x_2-x_3) \\
F(\underline{x_1},\underline{x_2},\underline{x_3}) &= (ig)^3\, (-i)\Delta_F^*(x_1-x_2)\, (-i)\Delta_F^*(x_1-x_3)\, (-i)\Delta_F^*(x_2-x_3).
\end{aligned}$$

etc.

The LTE then states that for a function $F(x_1,\ldots,x_n)$ corresponding to some diagram with n vertices

$$F(\ldots,\underline{x_i},\ldots) + F(\ldots,x_i,\ldots) = 0, \tag{2.3}$$

provided that x_{i0} is the largest time and all other underlinings in F are the same. The proof of Eq.(2.3) is based on an observation that the propagator $i\Delta_F(x)$ can be decomposed into positive and negative energy parts, i.e.

$$\begin{aligned} i\Delta_F(x) &= \theta(x_0)i\Delta^+(x) + \theta(-x_0)i\Delta^-(x), && (2.4) \\ i\Delta^\pm(x) &= \int \frac{d^4k}{(2\pi)^3} e^{-ikx}\theta(\pm k_0)\delta(k^2 - m^2). && (2.5) \end{aligned}$$

Incidentally, for x_{i0} being the largest time this directly implies

$$\begin{aligned} i\Delta_F(x_j - x_i) &= i\Delta^-(x_j - x_i), \\ -i\Delta_F^*(x_i - x_j) &= i\Delta^-(x_i - x_j), \\ i\Delta_F(0) &= -i\Delta_F^*(0). && (2.6) \end{aligned}$$

As $F(\ldots, \underline{x_i}, \ldots)$ differs from $F(\ldots, x_i, \ldots)$ only in the propagators directly connected to x_i - which are equal (see Eq.(2.6)) - and in the sign of the x_i vertex, they must mutually cancel.

Summing up Eq.(2.3) for all possible underlinings (excluding x_i), we get the LTE where the special rôle of the largest time is not manifest any more, namely

$$\sum_{index} F(x_1, x_2, \ldots, x_n) = 0. \tag{2.7}$$

The sum $\sum_{index}$ means summing over all possible distributions of indices 1 and 2 (or equivalently over all possible underlinings). The zero–temperature LTE can be easily reformulated for the $\mathbb{T}$–matrices. Let us remind that the Feynman diagrams for the $\mathbb{S}$–matrix ($\mathbb{S} = \mathbb{1} + i\mathbb{T}$) can be obtained by multiplying the corresponding $F(x_1, \ldots, x_n)$ with the plane waves for the incoming and outgoing particles, and subsequently integrate over $x_1 \ldots x_n$. Thus, in fixed volume quantisation a typical n–vertex Feynman diagram is given by

$$\int \prod_{i=1}^{n} dx_i \prod_j \frac{e^{-ip_j x_{m_j}}}{\sqrt{2\omega_{p_j} V}} \prod_k \frac{e^{iq_k x_{m_k}}}{\sqrt{2\omega_{q_k} V}} F(x_1, \ldots, x_n). \tag{2.8}$$

Here the momenta $\{p_j\}$ are attached to incoming particles at the vertices $\{x_{m_j}\}$, while momenta $\{q_k\}$ are attached to outgoing particles at the vertices $\{x_{m_k}\}$. In order to distinguish among various functions $F(x_1,\ldots,x_n)$ with the same variables $x_1,\ldots,x_n$, we shall attach a subscript l_n to each function F. For instance, the function $F_{1_4}(x_1,\ldots,x_4)$ corresponding to the diagram

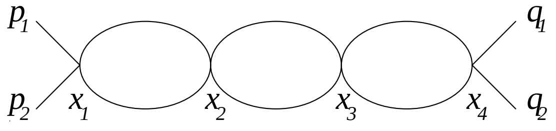

contributes to $\langle q_1q_2|i\mathbb{T}|p_1p_2\rangle$ by

$$\int\prod_{i=1}^{4}dx_i\frac{e^{-i(p_1+p_2)x_1}}{V\sqrt{4\omega_{p_1}\omega_{p_2}}}\frac{e^{i(q_1+q_2)x_4}}{V\sqrt{4\omega_{q_1}\omega_{q_2}}}(i\Delta_F(x_1-x_2))^2(i\Delta_F(x_2-x_3))^2(i\Delta_F(x_3-x_4))^2,$$

similarly, the function $F_{2_4}(x_1,\ldots,x_4)$ corresponding to the diagram

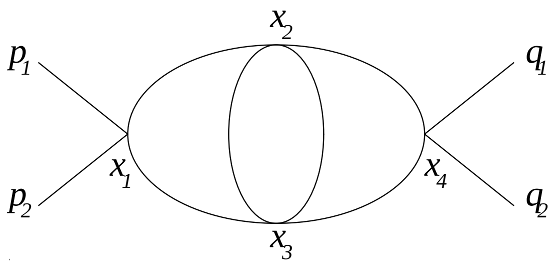

contributes to $\langle q_1q_2|i\mathbb{T}|p_1p_2\rangle$ by

$$\int\prod_{i=1}^{4}dx_i\frac{e^{-i(p_1+p_2)x_1}}{V\sqrt{4\omega_{p_1}\omega_{p_2}}}\frac{e^{i(q_1+q_2)x_4}}{V\sqrt{4\omega_{q_1}\omega_{q_2}}}i\Delta_F(x_1-x_2)i\Delta_F(x_1-x_3)(i\Delta_F(x_2-x_3))^2$$
$$\times\, i\Delta_F(x_4-x_3)i\Delta_F(x_4-x_2),$$

etc.

This can be summarised as

$$\langle\{q_k\}|i\mathbb{T}|\{p_j\}\rangle = \sum_n \int \ldots \int \prod_{i=1}^{n} dx_i \sum_{l_n} \prod_j \frac{e^{-ip_j x_{m_j}}}{\sqrt{2\omega_{p_j}V}} \prod_k \frac{e^{iq_k x_{m_k}}}{\sqrt{2\omega_{q_k}V}} F_{l_n}(x_1, \ldots, x_n). \tag{2.9}$$

Consider now the case $|\{p_j\}\rangle = |\{q_k\}\rangle$ (let us call it $|a\rangle$). From the unitarity condition: $\mathbb{T} - \mathbb{T}^\dagger = i\mathbb{T}^\dagger\mathbb{T}$, we get

$$\langle a|\mathbb{T}|a\rangle - \langle a|\mathbb{T}|a\rangle^* = i\langle a|\mathbb{T}^\dagger\mathbb{T}|a\rangle. \tag{2.10}$$

On the other hand, by construction $F(\underline{x_1}, \ldots, \underline{x_n}) = F^*(x_1, \ldots, x_n)$, and thus (see (2.7))

$$F(x_1, \ldots, x_n) + F^*(x_1, \ldots, x_n) = -\sum_{index'} F(x_1, \ldots, x_n). \tag{2.11}$$

The prime over *index* in (2.11) indicates that we sum neither over diagrams with all type 1 vertices nor diagrams with all type 2 vertices. Using (2.9), and identifying $|\{q_k\}\rangle$ with $|\{p_k\}\rangle$ $(= |a\rangle)$ we get

$$\langle a|\mathbb{T}|a\rangle - \langle a|\mathbb{T}|a\rangle^* = -\sum_{index'} \langle a|\mathbb{T}|a\rangle, \tag{2.12}$$

or (see (2.10))

$$\langle a|\mathbb{T}^\dagger\mathbb{T}|a\rangle = i\sum_{index'} \langle a|\mathbb{T}|a\rangle. \tag{2.13}$$

Eq.(2.12) is the special case of the LTE for the $\mathbb{T}$–matrices. The finite–temperature extension of (2.13) will prove crucial in Section 2.3.

Owing to the $\theta(\pm k_0)$ in $\Delta^{\pm}(x)$ (see Eq.(2.5)), energy is forced to flow only towards type 2 vertices. From both the energy–momentum conservation in each vertex and from the energy flow on the external lines, a sizable class of the diagrams on the RHS's of (2.12)-(2.13) will be automatically zero. Particularly regions of either 1st or 2nd type vertices which are not connected to any external line violate the energy conservation and thus do not contribute (no islands of vertices), see FIG.2.2. Consequently, the only surviving diagrams are those whose any 1st type vertex area is connected to incoming particles and any 2nd type vertex area is connected to outgoing ones. From historical reasons the border between two regions with different type of vertices is called *cut* and corresponding diagrams are called *cut diagrams*.

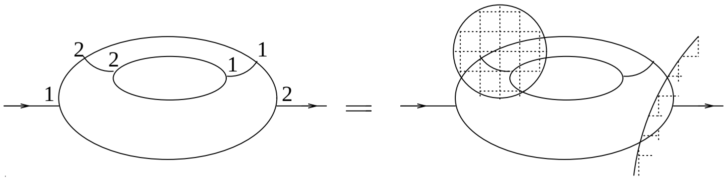

Figure 2.2: An example of a cut diagram in the φ^3 theory which does not contribute to the RHS's of (2.12)–(2.13). Arrows indicate the flow of energy.

We have just proved a typical feature of $T = 0$ QFT, namely any cut diagram is divided by the cut into two areas only, see FIG.2.3. Eq.(2.12), rewritten in terms of the cuttings is so called *cutting equation* (or Cutkosky's cutting rules) [48–50].

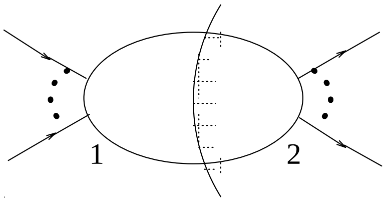

Figure 2.3: Generic form of the cut diagram at the $T = 0$. Shadow is on the 2nd type vertex area.

One point should be added. Inserting the completeness relation $\sum_f |f\rangle\langle f| = 1$ into the

LHS of (2.13), we get

$$\sum_f \langle a|\mathbb{T}^\dagger|f\rangle\langle f|\mathbb{T}|a\rangle = i\sum_{cuts}\langle a|\mathbb{T}|a\rangle. \tag{2.14}$$

It may be shown [46, 48] that all the intermediate particles in $|f\rangle$ correspond to cut lines. This has a natural extension when $\langle a|\mathbb{T}^\dagger\mathbb{T}|a\rangle \rightarrow \langle a|\mathbb{T}^\dagger\mathbb{P}\,\mathbb{T}|a\rangle$ with $\mathbb{P}$ being a projection operator ($\mathbb{P} = \mathbb{P}^\dagger = \mathbb{P}^2$) which eliminates some of the states $|f\rangle$. It is easy to see that in such case

$$\langle a|\mathbb{T}^\dagger\mathbb{P}\,\mathbb{T}|a\rangle = i\tilde{\sum_{cuts}}\langle a|\mathbb{T}|a\rangle, \tag{2.15}$$

where tilde over the $\sum_{cuts}$ indicates that one sums over the diagrams which do not have the cut lines corresponding to particles removed by $\mathbb{P}$.

There is no difficulty in applying the previous results to spin–$\frac{1}{2}$ [48, 49]. The LTE follows as before: the diagram with only iS_F propagators (and $-ig$ per each vertex) plus the diagram with only $(i\hat{S}_F)$ propagator [1] (and ig per each vertex) equals to minus the sum of all diagrams with one up to $n-1$ the type 2 vertices (n being the total number of vertices). For gauge fields more care is needed. Using the Ward identities one can show [48] that type 1 and type 2 vertices in (2.12)–(2.13) may be mutually connected only by *physical particle* propagators (i.e. neither through the propagators corresponding to particles with non–physical polarisations or Fadeev–Popov ghosts and antighosts).

---

[1] The function $i\hat{S}_F(x)$, similarly as $(i\Delta_F)^*(x)$, interchanges the rôle S^+ and S^-. Unlike bosons, for fermions $i\hat{S}_F(x)$ is not equal to $(iS_F)^*(x)$. Despite that, Eq.(2.12) still holds [48].

2.1.3 Thermal Wick's theorem (the Dyson–Schwinger equation)

The key observation at finite temperature is that for systems of *non–interacting* particles in thermodynamical equilibrium Wick's theorem is still valid, i.e. one can decompose the $2n$–point (free) thermal Green function into a product of two–point (free) thermal Green functions. This may be defined recursively by

$$\langle \mathcal{T}(\psi(x_1)\ldots\psi(x_{2n}))\rangle = \sum_{\substack{j \\ j\neq i}} \varepsilon_P \langle \mathcal{T}(\psi(x_i)\psi(x_j))\rangle \; \langle \mathcal{T}(\prod_{k\neq i;j} \psi(x_k))\rangle, \tag{2.16}$$

where ε_P is the signature of the permutation of fermion operators ($= 1$ for boson operators) and $\mathcal{T}$ is the standard time ordering symbol (for generalisation to the contour–time–path ordering see Appendix A.1). Note that the choice of "i" in (2.16) is completely arbitrary. The proof can be found for example in [34, 51, 52]. Similarly as at $T = 0$, Wick's theorem can also be written for the (free) thermal Wightman functions [51, 53], i.e.

$$\langle \psi(x_1)\ldots\psi(x_{2n})\rangle = \sum_{\substack{j \\ j\neq 1}} \varepsilon_P \langle \psi(x_1)\psi(x_j)\rangle \; \langle \prod_{k\neq 1;j} \psi(x_k)\rangle. \tag{2.17}$$

A particularly advantageous form of this is the so called Dyson–Schwinger equation (see Appendix A.1) which, at the $T \neq 0$, reads

$$\langle G[\psi]\psi(x)F[\psi]\rangle = \int dz \langle \psi(x)\psi(z)\rangle \left\langle G[\psi]\frac{\overrightarrow{\delta} F[\psi]}{\delta\psi(z)}\right\rangle + \int dz \langle \psi(z)\psi(x)\rangle \left\langle \frac{G[\psi]\,\overleftarrow{\delta}}{\delta\psi(z)} F[\psi]\right\rangle, \tag{2.18}$$

where $\psi(x)$ is an interaction–picture field and $G[\ldots]$ and $F[\ldots]$ are functionals of ψ. The arrowed variations $\frac{\delta}{\delta\psi(z)}$ are defined as formal operations satisfying two conditions, namely:

$$\frac{\overrightarrow{\delta}}{\delta\psi_n(z)}(\psi_m(x)\psi_q(y)) = \frac{\delta\psi_m(x)}{\delta\psi_n(z)}\psi_q(y) + (-1)^p\psi_m(x)\frac{\delta\psi_q(y)}{\delta\psi_n(z)}, \tag{2.19}$$

or

$$(\psi_m(x)\psi_q(y))\frac{\overleftarrow{\delta}}{\delta\psi_n(z)} = (-1)^p\frac{\delta\psi_m(x)}{\delta\psi_n(z)}\psi_q(y) + \psi_m(x)\frac{\delta\psi_q(y)}{\delta\psi_n(z)}, \tag{2.20}$$

with

$$\frac{\delta\psi_m(x)}{\delta\psi_n(y)} = \delta(x-y)\delta_{mn}. \tag{2.21}$$

The "p" is 0 for bosons and 1 for fermions; subscripts m, n suggest that several types of fields can be generally present. Note, for bosons $\frac{\overrightarrow{\delta} F}{\delta\psi} = \frac{F\overleftarrow{\delta}}{\delta\psi}$ which we shall denote as $\frac{\delta F}{\delta\psi}$. For more details see Appendix A.1.

2.1.4 Thermal largest–time equation

The LTE (2.13) can be extended to the finite–temperature case, too. Summing up in (2.13) over all the eigenstates of K $(= H - \mu N)$ with the weight factor $e^{-\beta K_i}$ (i labels the eigenstates), we get

$$\langle \mathbb{T}\mathbb{T}^\dagger \rangle = i \sum_{index'} \langle \mathbb{T} \rangle. \tag{2.22}$$

Let us consider the RHS of (2.22) first. The corresponding thermal LTE and diagrammatic rules (Kobes–Semenoff rules [34]) can be derived precisely the same way as at $T = 0$ using the previous, largest–time argumentation [34,54]. It turns out that these rules have basically identical form as those in the previous section, with an exception that now $\langle 0|\ldots|0\rangle \to \langle\ldots\rangle$. Note that labelling vertices by 1 and 2 we have naturally got a doubling of the number of degrees of freedom. This is a typical feature of the *real–time formalism* in thermal QFT (here, in so called *Keldysh version* [34]).

We should also emphasise that it may happen some fields are not thermalized. For example, external particles entering a heat bath or particles describing non–physical degrees of freedom [55]. Particularly, if some particles (with momenta $\{p_j\}$) enter the heat bath, the mean statistical value of an observable A is then

$$\begin{aligned}\sum_i \frac{e^{-\beta K_i}}{Z}\langle i;\{p_j\}|A|i;\{p_j\}\rangle &= Z^{-1}Tr(\rho_{\{p_j\}}\otimes e^{-\beta K}A),\\ \rho_{\{p_j\}} &= |\{p_j\}\rangle\langle\{p_j\}|,\end{aligned}$$

which we shall denote as $\langle A\rangle_{\{p_j\}}$. From this easily follows the generalisation of (2.22)

$$\langle \mathbb{T}\mathbb{T}^{\dagger}\rangle_{\{p_k\}} = i\sum_{index'}\langle\mathbb{T}\rangle_{\{p_k\}}. \tag{2.23}$$

Unlike $T=0$, we find that the cut diagrams have disconnected vertex areas and no kinematic reasonings used in the previous section can, in general, get rid of them. This is because the thermal part of $\langle\varphi(x)\varphi(y)\rangle$ describes[2] the absorption of on shell particle from the heat bath or the emission of one into it. Thus, at $T\neq 0$, there is no definite direction of transfer of energy from type 1 vertex to type 2 one as energy flows in both directions. Some cut diagrams nevertheless vanish. It is simple to see that only those diagrams survive in which the non–thermalized external particles "enter" a diagram via the 1st type vertices and "leave" it via the 2nd type ones. We might deduce this from the definition of $\langle\mathbb{T}\rangle_{\{p_j\}}$, indeed

---

[2] Note that $\langle\varphi(x)\varphi(y)\rangle = \langle:\varphi(x)\varphi(y):\rangle + \langle 0|\varphi(x)\varphi(y)|0\rangle$ and $\langle:\varphi(x)\varphi(y):\rangle = \int\frac{d^4k}{(2\pi)^3}f_B(k_0)\delta(k^2-m^2)e^{-ik(x-y)}$, with $f_B(k_0)=(e^{\beta|k_0|}-1)^{-1}$.

$$\sum_{index'} \langle \mathbb{T} \rangle_{\{p_j\}} = \sum_{index'} \sum_{i} \frac{e^{-\beta K_i}}{Z} \langle i; \{p_j\} | \mathbb{T} | i; \{p_j\} \rangle . \tag{2.24}$$

Note, we get the same set of thermal cut diagrams interchanging the summation $\sum_{index'}$ with $\sum_i$. It is useful to start then with $\sum_{index'} \langle i; \{p_j\} | \mathbb{T} | i; \{p_j\} \rangle$. This is, as usual, described by the ($T = 0$) cutting rules. In the last section we learned that the general structure of the corresponding cut diagrams is depicted in FIG.2.3, particularly the external particles enter the cut diagram via type 1 vertices and leave it via type 2 ones. Multiplying each diagram (with the external particles in the state $|i; \{p_j\}\rangle$) with the pre–factor $\frac{e^{-\beta K_i}}{Z}$ and summing subsequently over i, we again retrieve the thermal cut diagrams, though now it becomes evident that the particles $\{p_j\}$ enter such diagram only via type 1 vertices and move off only through type 2 ones, since the summation of the ($T = 0$) cut diagrams from which it was derived does not touch lines corresponding to unheated particles. Note, the latter analysis naturally explains why the unheated particles obey the ($T = 0$) LTE diagrammatic rules even in the thermal diagrams

Another vanishing comes from kinematic reasons. Namely three–leg vertices with all the on shell particles (1–2 lines) can not conserve energy–momentum and consequently the whole cut diagram is zero. As an illustration let us consider all the non–vanishing, topologically equivalent cut diagrams of given type involved in a three–loop contribution to $i \sum_{index'} \langle \mathbb{T} \rangle_{pq}$ (see FIG.2.4)[3]. Let us stress one more point. In contrast with $T = 0$, at finite temperature the cut itself neither is unique nor defines topologically equivalent areas, see FIG.2.5, only the number of crossed legs is, by definition, invariant. This ambiguity shows that the concept of the cut is not very useful at finite temperature and in the following we

---

[3] Let us emphasise that originally we had the 64 possible cut diagrams.

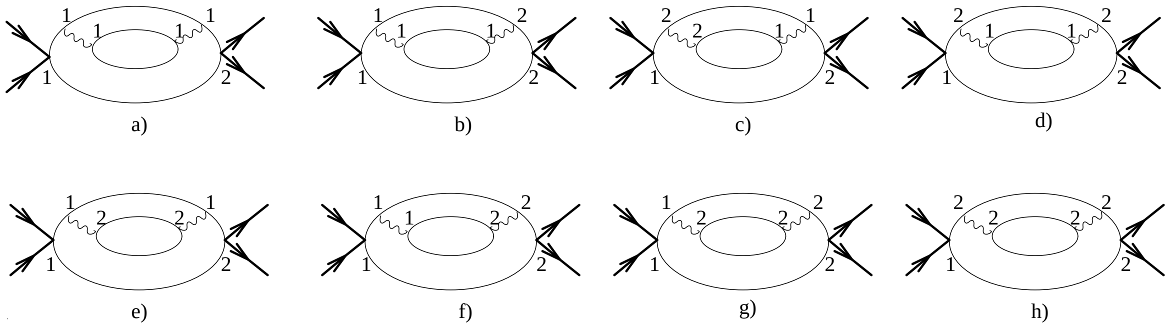

Figure 2.4: An example of non–vanishing cut diagrams at the $T \neq 0$. The heat–bath consists of two different particles. External particles are not thermalized.

shall refrain from using it.

In Section 2.3 it will prove useful to have an analogy of (2.23) for $\langle \mathbb{T}^{\dagger}\mathbb{P}\,\mathbb{T}\rangle$. Here $\mathbb{P}$

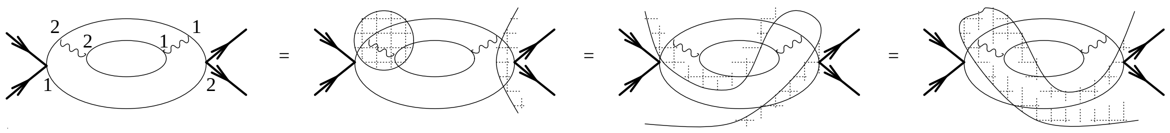

Figure 2.5: The cut diagram from Fig.2.3 c) demonstrates that the cut can be defined in many ways but the number of crossed lines is still the same.

is the projection operator defined as

$$\mathbb{P} = \sum_{j} |a; j\rangle\langle a; j| \,, \tag{2.25}$$

where "j" denotes the physical states for the heat–bath particles and "a" labels the physical states for the outgoing, non–thermalized particles. Let us deal with $\langle \mathbb{T}^{\dagger}\mathbb{P}\,\mathbb{T}\rangle$. Using (2.15), we acquire

$$\langle \mathbb{T}^{\dagger}\mathbb{P}\,\mathbb{T}\rangle = i \sum_{l} \frac{e^{-\beta K_l}}{Z} \tilde{\sum_{index'}} \langle l|\mathbb{T}|l\rangle \,. \tag{2.26}$$

Interchanging the summations, we finally arrive at

$$\langle \mathbb{T}^{\dagger}\mathbb{P}\,\mathbb{T}\rangle = i \tilde{\sum_{index'}} \langle \mathbb{T}\rangle, \tag{2.27}$$

where tilde over the $\sum_{index'}$ means that we are restricted to consider the cut diagrams, with only (1–2)–particle lines corresponding to the "a" and "j"particles (i.e. $\langle 0|\varphi(x)\varphi(y)|0\rangle$ and $\langle \psi(x)\psi(y)\rangle$, respectively). The extension of Eq.(2.27) to the case where some external, non–thermalized particles $\{p_k\}$ are present is obvious, and reads

$$\langle \mathbb{T}^{\dagger}\mathbb{P}\,\mathbb{T}\rangle_{\{p_k\}} = i \tilde{\sum_{index'}} \langle \mathbb{T}\rangle_{\{p_k\}}. \tag{2.28}$$

Finally, let us note that using the LTE, one may extend the previous treatment to various Green functions. The LTE for Green's functions is then a useful starting point for dispersion relations, see e.g. [34, 54].

2.2 Heat–Bath particle number spectrum: general framework

The cutting equation (2.28) can be fruitfully used for both the partition function Z and the heat–bath particle number spectrum $d\langle N(\omega)\rangle/d\omega$ calculations. To see that, let us for simplicity assume that two particles (say Φ_1, Φ_2) scatter inside a heat bath. We are interested in the heat–bath number spectrum after two different particles (say ϕ_1, ϕ_2) appear in the final state. Except for the condition that the external particles are different from the heat bath ones, no additional assumption about their nature is needed at this stage.

The initial density matrix ρ_i (i.e. the density matrix describing the physical situation before we introduce the particles $\Phi_1(p_1), \Phi_2(p_2)$ into the oven) can be written as

$$\rho_i = Z_i^{-1} \sum_j e^{-\beta K_j} |j; p_1, p_2\rangle\langle j; p_1, p_2|, \tag{2.29}$$

where "j" denotes the set of occupation numbers for the heat–bath particles. A long time after the scattering the final density matrix ρ_f reads

$$\rho_f = Z_f^{-1} \sum_j e^{-\beta K_j} \mathbb{P}\,\mathbb{S}|j; p_1, p_2\rangle\langle j; p_1, p_2|\mathbb{S}^\dagger \mathbb{P}^\dagger, \tag{2.30}$$

here $\mathbb{P}$ is the projection operator projecting out all the non–heat–bath final states except of $\phi_1(q_1), \phi_2(q_2)$ ones. The $\mathbb{S}$–matrix in (2.30) is defined in a standard way: $\mathbb{S} = 1\!\!\mathrm{I} + i\mathbb{T}$. The Z_f in (2.30) must be different from Z_i as otherwise ρ_f would not be normalised to unity. In order that ρ_f satisfy the normalisation condition $Tr(\rho_f) = 1$, one finds

$$Z_f = \sum_j e^{-\beta K_j} \langle j; p_1, p_2|\mathbb{S}^\dagger \mathbb{P}\,\mathbb{S}|j; p_1, p_2\rangle = \langle \mathbb{S}^\dagger \mathbb{P}\,\mathbb{S}\rangle_{p_1 p_2}\, Z_i = \langle \mathbb{T}^\dagger \mathbb{P}\,\mathbb{T}\rangle_{p_1 p_2}\, Z_i. \tag{2.31}$$

The key point is that we have used in (2.31) the $\mathbb{T}$–matrix because the initial state $|\Phi_1(p_1), \Phi_2(p_2)\rangle$ is, by definition, different from the final one $|\phi(q_1), \phi_2(q_2)\rangle$ and consequently $\mathbb{P}\,\mathbb{S}$ can be replaced by $i\mathbb{P}\,\mathbb{T}$. This allows us to calculate Z_f using directly the diagrammatic technique outlined in the preceding section.

From (2.1) and (2.30) one can directly read off that the number spectrum of the heat–bath particles is:

$$\begin{aligned} \frac{d\langle N_l(\omega)\rangle_f}{d\omega} &= \int \frac{d^3\mathbf{k}}{(2\pi)^3} \delta^+(\omega^2 - \mathbf{k}^2 - m_l^2) \sum_f \langle f|a_l^\dagger(\mathbf{k};\omega) a_l(\mathbf{k};\omega)\rho_f|f\rangle \\ &= \int \frac{d^3\mathbf{k}}{(2\pi)^3} \delta^+(\omega^2 - \mathbf{k}^2 - m_l^2) \frac{\langle \mathbb{T}^\dagger \mathbb{P} a_l^\dagger(\mathbf{k};\omega) a_l(\mathbf{k};\omega)\mathbb{T}\rangle_{p_1 p_2}}{\langle \mathbb{T}^\dagger \mathbb{P}\,\mathbb{T}\rangle_{p_1 p_2}}, \end{aligned} \tag{2.32}$$

and consequently

$$\langle N_l \rangle_f = \int \frac{d^4k}{(2\pi)^3} \delta^+(k^2 - m_l^2) \frac{\langle \mathbb{T}^\dagger \mathbb{P} a_l^\dagger(k) a_l(k) \mathbb{T} \rangle_{p_1 p_2}}{\langle \mathbb{T}^\dagger \mathbb{P}\, \mathbb{T} \rangle_{p_1 p_2}}, \tag{2.33}$$

where we have used the completeness relation for the final states $|f\rangle$ and $[\mathbb{P}; a^\dagger a] = 0$. The subscript "$l$" denotes which type of heat–bath particles we are interested in. In the following the index will be mostly suppressed.

2.3 Modified cut diagrams

To proceed further with (2.32) and (2.33), we expand the $\mathbb{T}$–matrix in terms of time–ordered interaction–picture fields, i.e.

$$\mathbb{T}[\psi] = \sum_n \int dx_1 \ldots \int dx_n \alpha_n(x_1 \ldots x_n) \mathcal{T}(\psi(x_1) \ldots \psi(x_n)). \tag{2.34}$$

Here ψ represents a heat–bath field in the interaction picture. Other fields (i.e. $\overline{\phi}$,ϕ and Φ) are included[4] in the α_n. An extension of (2.34) to the case where different heat–bath fields are present is natural. Employing (2.34) in $\langle \mathbb{T}^\dagger \mathbb{P}\, \mathbb{T} \rangle_{p_1 p_2}$, one can readily see that this factorises out in each term of the expansion a *pure* thermal mean value $\langle \ldots \rangle$. The general structure of each such thermal mean value is: $\langle G_m[\psi] F_n[\psi] \rangle$, where $F_n[\ldots]$ and $G_m[\ldots]$ are the operators with "n" chronological and "m" anti–chronological time ordered (heat–bath) fields, respectively. Analogous factorisation is true in the expansion of $\langle \mathbb{T}^\dagger \mathbb{P}^\dagger a^\dagger a \mathbb{P}\, \mathbb{T} \rangle_{p_1 p_2}$. The only difference is that the pure thermal mean value has the form $\langle G_m[\psi] a^\dagger a F_n[\psi] \rangle$

---

[4] When Fermi fields are involved, we have, for the sake of compactness, included in the argument of ψ the space–time coordinate, the Dirac index, and a discrete index which distinguishes ψ_α from $\overline{\psi}_\alpha$.

instead[5]. In case when various heat-bath fields are present, $m = m_1 + m_2 + \ldots + m_n$, with "$m_l$" denoting the number of the heat–bath fields of l–th type.

Applying the Dyson–Schwinger equation to $\langle G_m[\psi] a^\dagger a F_n[\psi]\rangle$ twice and summing over "n" and "m", we get cheaply the following expression (c.f. also (A.11))

$$
\begin{aligned}
&\langle \mathbb{T}^\dagger \mathbb{P} a_l^\dagger a_l \mathbb{T}\rangle_{p_1p_2} = \\
&= \int dxdy \{\langle \psi_l(x) a_l^\dagger\rangle \langle a_l \psi_l(y)\rangle + (-1)^p \langle \psi_l(x) a_l\rangle \langle a_l^\dagger \psi_l(y)\rangle\} \left\langle \frac{\mathbb{T}^\dagger \overleftarrow{\delta}}{\delta\psi_l(x)} \mathbb{P} \frac{\overrightarrow{\delta}\mathbb{T}}{\delta\psi_l(y)} \right\rangle_{p_1p_2} \\
&+ \int \frac{dxdy}{2} \{\langle \psi_l(x) a_l\rangle \langle \psi_l(y) a_l^\dagger\rangle + (-1)^p \langle \psi_l(x) a_l^\dagger\rangle \langle \psi_l(y) a_l\rangle\} \left\langle \frac{\mathbb{T}^\dagger \overleftarrow{\delta}^2}{\delta\psi_l(y)\delta\psi_l(x)} \mathbb{P}\,\mathbb{T} \right\rangle_{p_1p_2} \\
&+ \int \frac{dxdy}{2} \{\langle a_l \psi_l(x)\rangle \langle a_l^\dagger \psi_l(y)\rangle + (-1)^p \langle a_l^\dagger \psi_l(x)\rangle \langle a_l \psi_l(y)\rangle\} \left\langle \mathbb{T}^\dagger \mathbb{P} \frac{\overrightarrow{\delta}^2 \mathbb{T}}{\delta\psi_l(y)\delta\psi_l(x)} \right\rangle_{p_1p_2} \\
&+ \langle a_l^\dagger a_l\rangle \langle \mathbb{T}^\dagger \mathbb{P}\,\mathbb{T}\rangle_{p_1p_2}, \qquad (2.35)
\end{aligned}
$$

A similar decomposition for $\langle \mathbb{T}^\dagger \mathbb{P}\,\mathbb{T}\rangle_{p_1p_2}$ would not be very useful (cf.(A.19)); instead we define $\langle (\mathbb{T}^\dagger \mathbb{P}\,\mathbb{T})'\rangle_{p_1p_2}$ having the same expansion as $\langle \mathbb{T}^\dagger \mathbb{P}\,\mathbb{T}\rangle_{p_1p_2}$ except for the $\alpha_n(\ldots)\mathbb{P}\alpha_m^\dagger(\ldots)$ are replaced by $\alpha_n(\ldots)\mathbb{P}\alpha_m^\dagger(\ldots)\frac{n_l+m_l}{2}$. In this formalism $\langle (\mathbb{T}^\dagger \mathbb{P}\,\mathbb{T})'\rangle_{p_1p_2}$ reads

$$
\begin{aligned}
&\langle (\mathbb{T}^\dagger \mathbb{P}\,\mathbb{T})'\rangle_{p_1p_2} \\
&= \int dxdy \langle \psi_l(x)\psi_l(y)\rangle \left\langle \frac{\mathbb{T}^\dagger \overleftarrow{\delta}}{\delta\psi_l(x)} \mathbb{P} \frac{\overrightarrow{\delta}\mathbb{T}}{\delta\psi_l(y)} \right\rangle_{p_1p_2} \\
&+ \int \frac{dxdy}{2} \langle \overline{\mathcal{T}}(\psi_l(x)\psi_l(y))\rangle \left\langle \frac{\mathbb{T}^\dagger \overleftarrow{\delta}^2}{\delta\psi_l(y)\delta\psi_l(x))} \mathbb{P}\,\mathbb{T} \right\rangle_{p_1p_2} \\
&+ \int \frac{dxdy}{2} \langle \mathcal{T}(\psi_l(x)\psi_l(y))\rangle \left\langle \mathbb{T}^\dagger \mathbb{P} \frac{\overrightarrow{\delta}^2 \mathbb{T}}{\delta\psi_l(y)\delta\psi_l(x)} \right\rangle_{p_1p_2}, \qquad (2.36)
\end{aligned}
$$

---

[5] Remember that $\mathbb{P} = \mathbb{P}' \otimes \mathbb{P}'' = |q_1, q_2\rangle\langle q_1, q_2| \otimes \sum_j |j\rangle\langle j|$. Here $\mathbb{P}'' = \sum_j |j\rangle\langle j|$ behaves as an identity in the subspace of heat–bath states.

with the $\overline{\mathcal{T}}$ being the anti–chronological ordering symbol. Comparing (2.36) with (A.20), we can interpret the RHS of (2.36) as a sum over *all* possible distributions of one line (corresponding to ψ_l) inside of each given ($T \neq 0$!) cut diagram constructed out of $\langle \mathbb{T}^\dagger \mathbb{P}\, \mathbb{T} \rangle_{p_1 p_2}$. As (2.36) has precisely the same diagrammatical structure as

$$\langle \mathbb{T}^\dagger \mathbb{P} a^\dagger a \mathbb{T} \rangle_{p_1 p_2} - \langle a^\dagger a \rangle \ \langle \mathbb{T}^\dagger \mathbb{P}\, \mathbb{T} \rangle_{p_1 p_2}$$

(cf.(2.35)), it shows that in order to compute[6] the numerator of $\frac{d\Delta \langle N(\omega) \rangle}{d\omega} = \frac{d \langle N(\omega) \rangle_f}{d\omega} - \frac{d \langle N(\omega) \rangle_i}{d\omega}$ one can simply modify the usual $\langle \mathbb{T}^\dagger \mathbb{P}\, \mathbb{T} \rangle_{p_1 p_2}$ cut diagrams by the following one–line replacements (cf.(2.32)).

(i) For neutral scalar bosons:

$$\begin{aligned} \langle \varphi(x) \varphi(y) \rangle \ \ &\rightarrow \ \ \int \frac{d^3\mathbf{k}}{(2\pi)^3}\, \delta^+(\omega^2 - \mathbf{k}^2 - m^2) \{ \langle \varphi(x) a^\dagger(\mathbf{k};\omega) \rangle \langle a(\mathbf{k};\omega) \varphi(y) \rangle \\ &\quad + \langle \varphi(x) a(\mathbf{k};\omega) \rangle \langle a^\dagger(\mathbf{k};\omega) \varphi(y) \rangle \} \\ &= \ \ \int \frac{d^4k}{(2\pi)^3}\, \delta(k^2 - m^2) \, \{ f_B(\omega)(f_B(\omega) + 1) \\ &\quad \times \, (\delta^-(k_0 + \omega) + \delta^+(k_0 - \omega)) \\ &\quad + \delta^+(k_0 - \omega)(1 + f_B(\omega)) - \delta^-(k_0 + \omega) f_B(\omega) \big\} \, e^{-ik(x-y)}, \qquad (2.37) \end{aligned}$$

where $f_B(\omega)$ is the Bose–Einstein distribution: $f_B(\omega) = \frac{1}{e^{\beta|\omega|} - 1}$. Term $\theta(-k_0) f_B(\omega)$ describes the absorption of a heat–bath particle, so reduces the number spectrum, that is why the negative sign appears in front of it. Analogously,

---

[6] Here $\frac{d\langle N(\omega) \rangle_i}{d\omega} = \int \frac{d^3\mathbf{k}}{(2\pi)^3} \delta^+(\omega^2 - \mathbf{k}^2 - m^2) \langle a^\dagger(\omega, \mathbf{k}) a(\omega, \mathbf{k}) \rangle$, (cf. (2.32)).

$$
\begin{aligned}
\langle \mathcal{T}(\varphi(x)\varphi(y))\rangle \;\; &\rightarrow \;\; \int \frac{d^3\mathbf{k}}{(2\pi)^3}\, \delta^+(\omega^2 - \mathbf{k}^2 - m^2)\{\langle a^\dagger(\mathbf{k};\omega)\varphi(x)\rangle\langle a(\mathbf{k};\omega)\varphi(y)\rangle \\
&\quad + \langle a(\mathbf{k};\omega)\varphi(x)\rangle\langle a^\dagger(\mathbf{k};\omega)\varphi(y)\rangle\} \\
&= \int \frac{d^4k}{(2\pi)^3}\delta(k^2 - m^2)(1 + f_B(\omega))f_B(\omega)e^{-ik(x-y)} \\
&\quad \times\, (\delta^+(k_0 - \omega) + \delta^-(k_0 + \omega)). \qquad (2.38)
\end{aligned}
$$

Similarly, for $\Delta\langle N\rangle$ one needs the following replacements (cf.(2.33))

$$
\begin{aligned}
\langle \varphi(x)\varphi(y)\rangle \;\; &\rightarrow \;\; \int \frac{d^4k}{(2\pi)^3}\, \delta(k^2 - m^2)\, \{f_B(\omega_k)(f_B(\omega_k) + 1) \\
&\quad + \theta(k_0)(1 + f_B(\omega_k)) - \theta(-k_0)f_B(\omega_k)\}\, e^{-ik(x-y)}, \\
\langle \mathcal{T}(\varphi(x)\varphi(y))\rangle \;\; &\rightarrow \;\; \int \frac{d^4k}{(2\pi)^3}\, \delta(k^2 - m^2)(1 + f_B(\omega_k))f_B(\omega_k)e^{-ik(x-y)}, \\
& \qquad (2.39)
\end{aligned}
$$

with the dispersion relation $\omega_k = \sqrt{\mathbf{k}^2 - m^2}$.

(ii) For Dirac fermions:

The Dirac field is comprised of two different types of excitations (mutually connected via charge conjugation), so the corresponding number operator $N(\omega) = N_b(\omega) + N_d(\omega)$ with

$$
N_b(\omega) \;\; = \;\; \sum_{\alpha=1,2} \int \frac{d^3\mathbf{k}}{(2\pi)^3}\, \delta^+(\omega^2 - \mathbf{k}^2 - m^2)b^\dagger_\alpha(\mathbf{k};\omega)b_\alpha(\mathbf{k};\omega)
$$

$$N_d(\omega) = \sum_{\alpha=1,2}\int \frac{d^3\mathbf{k}}{(2\pi)^3}\,\delta^+(\omega^2-\mathbf{k}^2-m^2)d^\dagger_\alpha(\mathbf{k};\omega)d_\alpha(\mathbf{k};\omega).$$

Thus, the one–line replacements needed for $d\Delta\langle N_b(\omega)\rangle/d\omega$ are

$$\begin{aligned}
\langle\psi_\rho(x)\overline{\psi}_\sigma(y)\rangle \;\to\; & \sum_{\alpha=1,2}\int \frac{d^3\mathbf{k}}{(2\pi)^3}\,\delta^+(\omega^2-\mathbf{k}^2-m^2)\{\langle\psi_\rho(x)b^\dagger_\alpha(\mathbf{k};\omega)\rangle\langle b_\alpha(\mathbf{k};\omega)\overline{\psi}_\sigma(y)\rangle \\
& -\langle\psi_\rho(x)b_\alpha(\mathbf{k};\omega)\rangle\langle b^\dagger_\alpha(\mathbf{k};\omega)\overline{\psi}_\sigma(y)\rangle\} \\
= \; & \int \frac{d^4k}{(2\pi)^3}\,\delta^+(k^2-m^2)\,\delta(k_0-\omega)\,(\not{k}+m)_{\rho\sigma} \\
& \times\{(1-f_F(\omega))-f_F(\omega)(1-f_F(\omega))\}e^{-ik(x-y)},
\end{aligned} \tag{2.40}$$

where $f_F(\omega)$ is the Fermi–Dirac distribution: $f_F(\omega)=\frac{1}{e^{\beta(|\omega|-\mu)}+1}$, and

$$\begin{aligned}
\langle\mathcal{T}(\psi_\rho(x)\overline{\psi}_\sigma(y))\rangle \;\to\; & \sum_{\alpha=1,2}\int \frac{d^3\mathbf{k}}{(2\pi)^3}\,\delta^+(\omega^2-\mathbf{k}^2-m^2)\,\{\langle b_\alpha(\mathbf{k};\omega)\psi_\rho(x)\rangle\langle b^\dagger_\alpha(\mathbf{k};\omega)\overline{\psi}_\sigma(y)\rangle \\
& -\langle b^\dagger_\alpha(\mathbf{k};\omega)\psi_\rho(x)\rangle\langle b_\alpha(\mathbf{k};\omega)\overline{\psi}_\sigma(y)\rangle\} \\
= \; & -\int \frac{d^4k}{(2\pi)^3}\,\delta^+(k^2-m^2)\,\delta(k_0-\omega)\,(\not{k}+m)_{\rho\sigma} \\
& \times f_F(\omega)(1-f_F(\omega))e^{-ik(x-y)}.
\end{aligned} \tag{2.41}$$

Correspondingly, for $\Delta\langle N_b\rangle$ we need

$$\langle\psi_\rho(x)\overline{\psi}_\sigma(y)\rangle \;\to\; \int \frac{d^4k}{(2\pi)^3}\,\delta^+(k^2-m^2)\,(\not{k}+m)_{\rho\sigma}$$

$$\times \{(1 - f_F(\omega)) - f_F(\omega)(1 - f_F(\omega)\} e^{-ik(x-y)}$$

$$\langle \mathcal{T}(\psi_\rho(x)\overline{\psi}_\sigma(y))\rangle \quad \to \quad - \int \frac{d^4k}{(2\pi)^3}\, \delta^+(k^2 - m^2)\, (\not{k} + m)_{\rho\sigma} f_F(\omega)(1 - f_F(\omega)) e^{-ik(x-y)}. \tag{2.42}$$

For the d–type excitations the prescription is very similar, actually, in order to get $\frac{d\Delta\langle N_d(\omega)\rangle}{d\omega}$, the following substitutions must be performed in (2.40)–(2.42): $\theta(k_0) \to \theta(-k_0)$, $f_F \to (1 - f_F)$ and $\mu \to -\mu$.

(iii) For gauge fields in the axial temporal gauge ($A^0 = 0$):

The temporal gauge is generally incorporated in the gauge fixing sector of the Lagrangian and particularly

$$\mathcal{L}_{fix} = -\frac{1}{2\alpha}(A_0)^2; \alpha \to 0. \tag{2.43}$$

The principal advantage of the axial gauges arises from the decoupling the F–P ghosts in the theory. This statement is of course trivial in QED as any linear gauge (both for covariant and non–covariant case) brings this decoupling automatically [34]. Particular advantage of the temporal gauge comes from an elimination of non–physical scalar photons from the very beginning.

Let us decompose a gauge field $A_i, i = 1, 2, 3$ into the transverse and longitudinal part, i.e. $A_i = A_i^T + A_i^L$ with

$$A_i^T = \left(\delta_{ij} - \frac{\partial_i\partial_j}{\vec{\partial}^2}\right) A_j \;\text{ and }\; A_i^L = \frac{\partial_i\partial_j}{\vec{\partial}^2} A_j, \tag{2.44}$$

and use the sum over gauge–particle polarisations

$$\sum_{\lambda=1}^{2} \varepsilon_i^{(\lambda)}(k)\varepsilon_j^{(\lambda)}(k) = \delta_{ij} - \frac{k_i k_j}{\mathbf{k}^2}, \tag{2.45}$$

with $\varepsilon^{(\lambda)}(k)$ being polarisation vectors, then for $d\Delta\langle N^T(\omega)\rangle/d\omega$ we get the following one–line replacements

$$\begin{aligned}
\langle A_i^T(x)A_j^T(y)\rangle \quad &\rightarrow \quad \sum_{\lambda=1}^{2}\int \frac{d^3\mathbf{k}}{(2\pi)^3}\,\delta^+(\omega^2-\mathbf{k}^2-m^2)\langle A_i^T(x)a_\lambda^\dagger(\mathbf{k};\omega)\rangle\langle a_\lambda(\mathbf{k};\omega)A_j^T(y)\rangle \\
&\qquad + \langle A_i^T(x)a_\lambda(\mathbf{k};\omega)\rangle\langle a_\lambda^\dagger(\mathbf{k};\omega)A_j^T(y)\rangle_\beta\} \\
&= \quad \left(\delta_{ij} - \frac{\partial_i\partial_j}{\vec{\partial}^2}\right)(\text{Eq.}(2.37)) \\
\langle \mathcal{T}(A_i^T(x)A_j^T(y))\rangle \quad &\rightarrow \quad \sum_{\lambda=1}^{2}\int \frac{d^3\mathbf{k}}{(2\pi)^3}\,\delta^+(\omega^2-\mathbf{k}^2-m^2)\{\langle A_i^T(x)a_\lambda^\dagger(\mathbf{k};\omega)\rangle\langle A_i^T(y)a_\lambda(\mathbf{k};\omega)\rangle \\
&\qquad + \langle A_i^T(x)a_\lambda(\mathbf{k};\omega)\rangle\langle A_i^T(x)a_\lambda^\dagger(\mathbf{k};\omega)\rangle \\
&= \quad \left(\delta_{ij} - \frac{\partial_i\partial_j}{\vec{\partial}^2}\right)(\text{Eq.}(2.38)).
\end{aligned} \tag{2.46}$$

The replacements needed for $\Delta\langle N^T\rangle$ can be concisely expressed as

$$\langle \ldots \rangle \rightarrow \left(\delta_{ij} - \frac{\partial_i\partial_j}{\vec{\partial}^2}\right)(\text{Eq.}(2.39)) \tag{2.47}$$

As for the longitudinal (non–physical) degrees of freedom, it is obvious that

$$\langle A_i^L(x)A_j^L(y)\rangle; \;\; \langle \mathcal{T}(A_i^L(x)A_j^L(y))\rangle \rightarrow 0. \tag{2.48}$$

Eqs.(2.37)–(2.47) can be most easily derived in the finite–volume limit, e.g. for a scalar field we reformulate $\varphi(x)$ as

$$\varphi(x)=\sum_r \frac{A_r}{\sqrt{2E_rV}}e^{-iE_rt+i\mathbf{k}_r\mathbf{x}}+\frac{A_r^\dagger}{\sqrt{2E_rV}}e^{iE_rt-i\mathbf{k}_r\mathbf{x}},$$

rescaling the annihilation and creation operators by defining $a(k)=\sqrt{2E_kV}A_k$ in such a way that $[A_k;A^\dagger_{k'}]=\delta_{kk'}$ (so that $\langle A^\dagger_kA_{k'}\rangle=\delta_{kk'}f_B(k_0)$), while $\int\frac{d^3\mathbf{k}}{(2\pi)^3}\to\frac{1}{V}\sum_{\mathbf{k}}$.

The replacements (2.37)–(2.47) are meant in the following sense: firstly one constructs all the $T\neq 0$ diagrams for $\langle\mathbb{T}^\dagger\mathbb{P}\,\mathbb{T}\rangle_{p_1p_2}$, using the LTE (2.28) and the rules mentioned therein. In order to calculate the numerator of (2.32) or (2.33) we simply replace (using corresponding prescriptions) *one* heat–bath particle line in each cut diagram and this replacement must sum for all the possible heat–bath particle lines in the diagram. If more types of heat–bath particles are present, we replace only those lines which correspond to particles whose number spectrum we want to compute (see FIG.2.6).

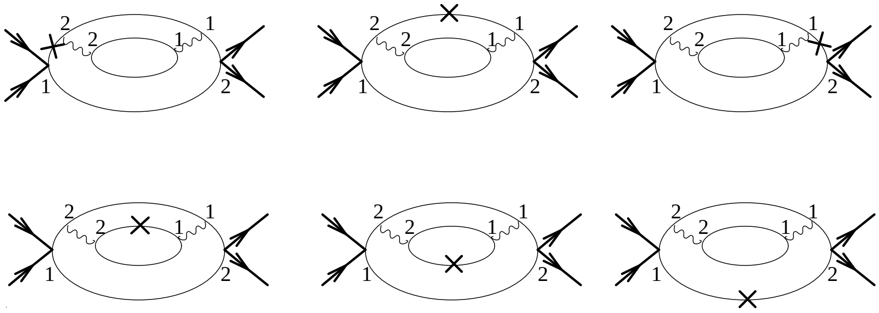

Figure 2.6: The numerator of (2.32) and (2.33) can be calculated using the modified cut diagrams for $\langle\mathbb{T}^\dagger\mathbb{P}\,\mathbb{T}\rangle_{p_1p_2}$. As an example we depict all the possible contributions to the numerator derived from the cut diagram on Fig.2.4 c). The wavy lines and thin lines describe the heat–bath particles. The crossed lines denote the substituted propagators, in this case we wish to calculate the thin–line particle number spectrum.

The terms in the replacements (2.37)–(2.47) have a direct physical interpretation. The $f(\omega_k)$ and $(1+(-1)^pf(\omega_k))$ can be viewed as the absorption and emission of the heat–

bath particles respectively [45]. The term $f(\omega_k)(1+(-1)^p f(\omega_k))$ describes the fluctuations of the heat bath particles. This is because for the non–interacting heat–bath particles $\langle (n_k - \langle n_k\rangle)^2\rangle = f(\omega_k)(1+(-1)^p f(\omega_k))$. The substituted propagators can be therefore schematically depicted as

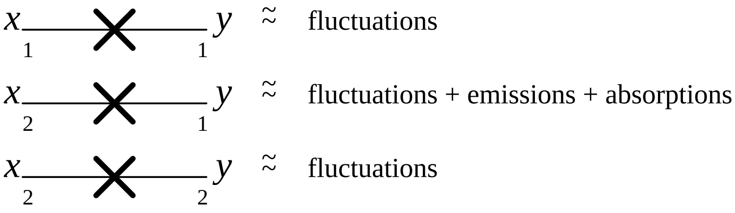
x_1 — y_1 ≈ fluctuations
x_2 — y_1 ≈ fluctuations + emissions + absorptions
x_2 — y_2 ≈ fluctuations

Collecting all the contributions from emissions, absorptions and fluctuations separately, one can schematically write

$$\frac{d\langle N(\omega)\rangle_f}{d\omega} = \frac{d\langle N(\omega)\rangle_i}{d\omega} + F^{emission}(\omega) + F^{absorption}(\omega) + F^{fluc}(\omega), \tag{2.49}$$

where, for instance for neutral scalar bosons

$$F^{emission}(\omega) = Z_f^{-1}\int \frac{d^4k}{(2\pi)^3}\delta^+(k^2-m^2)\delta(k_0-\omega)(1+f_B(\omega))\left\langle \frac{\mathbb{T}^\dagger\overleftarrow{\delta}}{\delta\psi(x)}\mathbb{P}\frac{\overrightarrow{\delta}\mathbb{T}}{\delta\psi(y)}\right\rangle_{p_1p_2}.$$

Using (2.38), it is easy to write down the analogous expressions for the $F^{absorption}$ and F^{fluc}. To the lowest perturbative order, the form (2.49) was obtained by Landshoff and Taylor [45].

2.4 Model process

2.4.1 Basic assumptions

To illustrate the modified cut diagram technique, we shall restrict ourselves to a toy model, namely to a scattering of two neutral scalar particles Φ (pions) within a photon heat bath, with a pair of scalar charged particles $\phi, \overline{\phi}$ ('muon' and 'antimuon') left as a final product. Both initial and final particles are supposed to be unheated. We further assume that the heat–bath photons A are scalars, i.e. the heat–bath Hamiltonian has form

$$H^{hb} = \frac{1}{2}(\partial_\nu A)^2 - \frac{m_\gamma^2}{2}A^2.$$

In order to mimic scalar electrodynamic, we have chosen the interacting Hamiltonian entering in the $\mathbb{T}$–matrix as

$$H_{in} = \frac{\lambda}{2}\Phi^2\phi\phi^\dagger + (eA + \frac{e^2}{2}A^2)\phi\phi^\dagger.$$

2.4.2 Calculations

We can now compute an order–e^2 contribution to the $\frac{d\Delta\langle N_\gamma(\omega)\rangle}{d\omega}$. The evaluation of the $\frac{d\Delta\langle N_\gamma(\omega)\rangle}{d\omega}$ is straightforward. In FIG.2.7 we list all the modified cut diagrams contributing to an order–e^2. Note that diagrams b) and c) are topologically identical. Similarly, diagrams e), f), h), i) and j) should be taken with combinatorial factor 2 (corresponding diagrams with a heat-bath particle line on the bottom solid line are not shown). Of course, diagram g) vanishes for kinematic reasons.

For instance, in order to calculate the contribution from diagram a) (see also FIG.2.8)

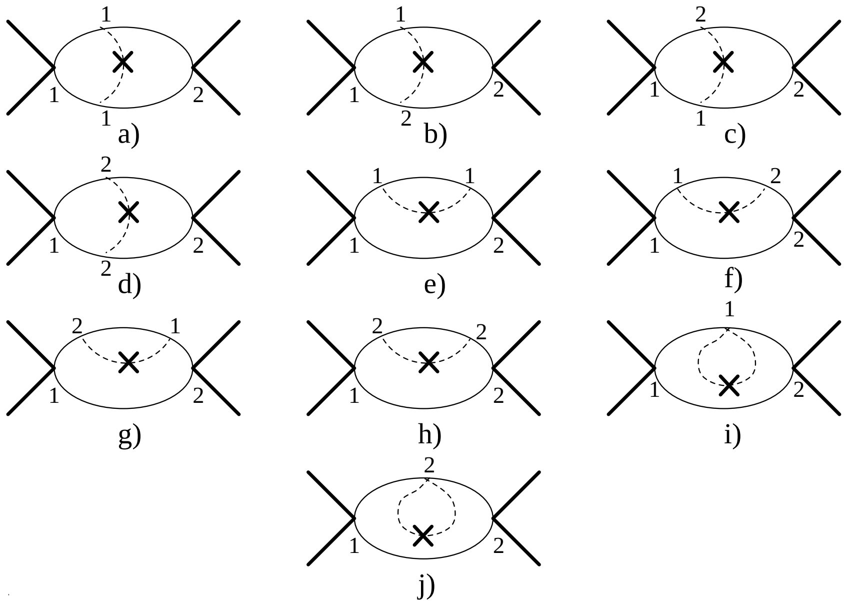

Figure 2.7: The modified cut diagrams involved in an order–e^2 contribution to the photon number spectrum. Dashed lines: photons. Solid lines: ϕ, $\phi^\dagger$ particles. Bold lines: Φ particles.

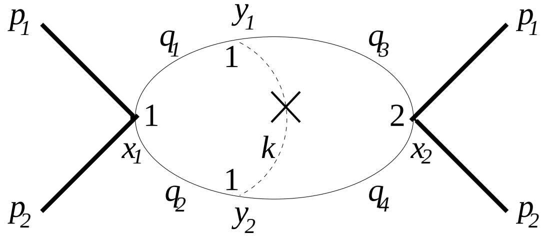

Figure 2.8: The diagram a) with a corresponding kinematics.

we go back to Eq.(2.9) and to prescriptions (2.37)–(2.38), so we get

$$
\begin{aligned}
\text{a)} = \quad & \frac{-\lambda^2 e^2}{V^2 4\omega_{p_1}\omega_{p_2}} \int d^4x_1 d^4x_2 d^4y_1 d^4y_2 \; e^{-i(p_1+p_2)x_1} \; e^{i(p_1+p_2)x_2} \; i\Delta_F(y_1 - x_1) \; i\Delta_F(y_2 - x_1) \\
\times \quad & i\Delta^-(y_1 - x_2) \; i\Delta^-(y_2 - x_2) \; \int \frac{d^4k}{(2\pi)^3} \delta(k^2 - m^2)(1 + f_B(\omega)) f_B(\omega) \\
\times \quad & (\delta^+(k_0 - \omega) + \delta^-(k_0 + \omega)) \; e^{-ik(y_1 - y_2)}
\end{aligned}
$$

$$
\begin{aligned}
= \quad & \frac{\lambda^2 e^2 t}{V 4\omega_{p_1}\omega_{p_2}(2\pi)^5} f_B(\omega)(1+f_B(\omega)) \int d^4k \; d^4q_3 \; d^4q_4 \; \delta^+(q_3^2 - m_\mu^2) \; \delta^+(q_4^2 - m_\mu^2) \\
\times \quad & \delta(k_0 - \omega) \left\{ \frac{1}{-2q_3k + m_\gamma^2} \; \frac{1}{2q_4k + m_\gamma^2} + \frac{1}{2q_3k + m_\gamma^2} \; \frac{1}{-2q_4k + m_\gamma^2} \right\} \\
\times \quad & \delta(k^2 - m_\gamma^2) \; \delta^4(-p_1 - p_2 + q_1 + q_2). \qquad (2.50)
\end{aligned}
$$

We have dropped the $i\epsilon$ prescription in the propagators since adding/ subtracting an on–shell momenta $q_{1;2}$ to/from an on–shell momenta k we can not fulfil the condition $(k \pm q_{1;2})^2 = m_\mu^2$. As it is usual, we have assumed that our interaction is enclosed in a 'time' and volume box (t and V respectively). Analogously one can calculate contributions from other diagrams in FIG.2.7. Let us emphasise that it is necessary to give sense to graphs e), h), i) and j) as these suffer with the pinch singularity; the muon–particle propagator $(p_{1;2}^2 - m^2)^{-1}$ has to be evaluated at its pole because of the presence of an on–shell line (1–2 line) with the same momenta. Some regularisation is obviously necessary. Using the formal identity [34]

$$
\frac{1}{x \pm i\epsilon}\delta(x) = -\frac{1}{2}\delta^{'}(x) \mp i\pi(\delta(x))^2, \qquad (2.51)
$$

we discover that the unwanted δ^2 mutually cancel between e) and h) diagrams (similarly for i) and j) diagrams). An alternative (but lengthier) way of dealing with the latter pinch singularity; i.e. switching off the interaction with a heat bath in the remote past and future, is discussed in [56]. Evaluating all the diagrams (note, we should attach to each digram the factor $\frac{1}{2!}$ coming from a Taylor expansion of the $\mathbb{T}$–matrix), we are left with (c.f. Eq.(2.49)):

$$\begin{aligned}F^{emission}(\omega) \quad + \quad & F^{absorption}(\omega) \\ = \quad & \frac{t\lambda^2 e^2}{\langle \mathbb{T}\,\mathbb{P}\,\mathbb{T}^\dagger \rangle_{p_1 p_2} V 8\omega_{p_1}\omega_{p_2}(2\pi)^5} \int d^4k \; \delta(k^2 - m_\gamma^2)\; \delta(k_0 - \omega) \\ & \times \int d^4q_1 d^4q_2 \; \delta^+(q_1^2 - m_\mu^2)\; \delta^+(q_2^2 - m_\mu^2) \\ & \times \; \big\{ K_1 (1 + f_B(\omega))\; \delta^4(-Q + q_1 + q_2 + k) \\ & - K_2 f_B(\omega)\; \delta^4(-Q + q_1 + q_2 - k) \big\} \qquad (2.52)\end{aligned}$$

and

$$\begin{aligned}F^{fluct}(\omega) \quad = \quad & \frac{t\lambda^2 e^2 f_B(\omega)(1 + f_B(\omega))}{\langle \mathbb{T}\,\mathbb{P}\,\mathbb{T}^\dagger \rangle_{p_1 p_2} V 8\omega_{p_1}\omega_{p_2}(2\pi)^5} \int d^4k \; \delta(k^2 - m_\gamma^2)\; \delta(k_0 - \omega) \\ & \times \int d^4q_1 d^4q_2 \; \delta^+(q_1^2 - m_\mu^2)\; \delta^+(q_2^2 - m_\mu^2) \\ & \times \big\{ \delta^4(-Q + q_1 + q_2 + k) K_1 + \delta^4(-Q + q_1 + q_2 - k) K_2 \\ & - \; 2\delta^4(-Q + q_1 + q_2) K_3 \big\} \\ \\ + \quad & \frac{t\lambda^2 e^2 f_B(\omega)(1 + f_B(\omega))}{\langle \mathbb{T}\,\mathbb{P}\,\mathbb{T}^\dagger \rangle_{p_1 p_2} V 8\omega_{p_1}\omega_{p_2}(2\pi)^5} \int d^4k \; \delta(k^2 - m_\gamma^2)\; \delta(k_0 - \omega) \\ & \times \int d^4q_1 d^4q_2 \; \delta^4(-Q + q_1 + q_2) \\ & \times \left\{ \left(1 - \frac{1}{2q_1k - m_\gamma^2} + \frac{1}{2q_1k + m_\gamma^2} \right) \delta^+(q_2^2 - m_\mu^2) \frac{\partial}{\partial m_\mu^2} \; \delta^+(q_1^2 - m_\mu^2) \right. \\ & \left. + (q_1 \leftrightarrow q_2) \right\} \qquad (2.53)\end{aligned}$$

with $K_1 = \left(\frac{1}{2q_1k + m_\gamma^2} + \frac{1}{2q_2k + m_\gamma^2} \right)^2$, $K_2 = \left(\frac{1}{2q_1k - m_\gamma^2} + \frac{1}{2q_2k - m_\gamma^2} \right)^2$, $K_3 = \frac{2}{(2q_1k - m_\gamma^2)(2q_2k + m_\gamma^2)}$ and $Q = p_1 + p_2$. The relevant (i.e. order–e^0) term (see FIG.2.9)

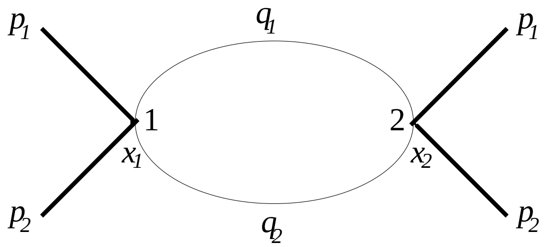

Figure 2.9: The lowest-order cut diagram for $\langle \mathbb{T}\mathbb{P}\mathbb{T}^\dagger\rangle_{p_1p_2}$.

for $\langle \mathbb{T}\,\mathbb{P}\,\mathbb{T}^\dagger\rangle_{p_1p_2}$ reads

$$\begin{aligned}\langle \mathbb{T}\,\mathbb{P}\,\mathbb{T}^\dagger\rangle_{p_1p_2} &= \frac{\lambda^2 t}{16\,V\omega_{p_1}\omega_{p_2}(2\pi)^2}\int d^4q_1 d^4q_2\ \delta^+(q_1^2-m_\mu^2)\ \delta^+(q_2^2-m_\mu^2)\ \delta^4(-Q+q_1+q_2)\\ &= \frac{\lambda^2 t}{64V\omega_{p_1}\omega_{p_2}|Q|(2\pi)}\sqrt{Q^2-4m_\mu^2}. \qquad (2.54)\end{aligned}$$

Eqs.(2.52) and (2.53) are analogous to the result obtained in [45] for the decay. In order to understand their structure, let us deal with the number spectrum[7] for small ω's. To do this, we change the integration variables

$$\begin{aligned} q_1 &\to q_1 \mp \frac{1}{2}k\\ q_2 &\to q_2 \mp \frac{1}{2}k. \qquad (2.55)\end{aligned}$$

These changes lead to

$$\begin{aligned}&(2q_ik \pm m_\gamma^2)\ \delta^+(q_1^2-m_\mu^2)\ \delta^+(q_2-m_\mu^2)\ \delta^4(-Q+q_1+q_2\pm k)\\ &\qquad\longrightarrow\ 2q_ik\ \delta^+(q_1^2-M^2\mp X)\ \delta^+(q_2^2-M^2\mp Y)\ \delta^4(-Q+q_1+q_2), \qquad (2.56)\end{aligned}$$

where $M^2 = m_\mu^2 - \frac{1}{4}m_\gamma^2$, $X = q_1k$ and $Y = q_2k$. In addition, transformations (2.55) have unite Jacobian. If one Taylor expands (2.56) in terms of X and Y then one gets successively higher ω–contributions to (2.52)–(2.53). Expanding (2.52) to the first order in X and Y, and keeping only temperature–dependent pieces, we have

---

[7] So we implicitly assume that the photon mass m_γ is sufficiently small.

$$\begin{aligned} &\langle \mathbb{T}\,\mathbb{P}\,\mathbb{T}^{\dagger}\rangle_{p_1p_2}\,\frac{8V\omega_{p_1}\omega_{p_2}}{t}\,\left(F^{emission}(\omega)+F^{absorption}(\omega)\right) \\ &\qquad\qquad \sim \frac{\lambda^2e^2}{(2\pi)^5}f_B(\omega)\,\int d^4q_1d^4q_2\;\delta(k^2-m_\gamma^2)\;\delta(k_0-\omega)\;A, \end{aligned} \tag{2.57}$$

with

$$A=\frac{\partial}{\partial_{M_1^2}}\int d^4q_1d^4q_2\;\delta^+(q_1^2-M_1^2)\;\delta^+(q_2^2-M_2^2)\;(4KX)\;\delta^4(Q-q_1-q_2)\,\Big|_{\,M_1=M_2=M}\;.$$

Here $K=\left(\frac{1}{2q_1k}+\frac{1}{2q_2k}\right)^2$ (we have performed transformation $q_1\leftrightarrow q_2$ in order to express (2.57) solely in terms of X). As A is a Lorentz scalar, it must depend on k only via product (kQ). One can thus evaluate A in the frame where $Q=(Q_0,\mathbf{0})$ and then replace ωQ_0 by (kQ) (see also [45]). Straightforward calculations show that

$$A=\frac{-(2\pi)(kQ)^3}{|Q|\sqrt{\frac{Q^2}{4}-M^2}\;\left(\frac{M}{|Q|}(kQ)^2+m_\gamma^2\left(\frac{|Q|^3}{4}-MQ^2\right)\right)^2}. \tag{2.58}$$

Recalling (2.54), we get

$$\begin{aligned} &F^{emission}(\omega)+F^{absorption}(\omega) \\ &\sim \frac{Q^2f_B(\omega)e^2}{\pi^2M^2\sqrt{Q_0^2-Q^2}\sqrt{Q^2-4M^2}\sqrt{Q^2-4m_\mu^2}} \\ &\times\left\{\ln\left(\frac{(\omega Q_0+|\mathbf{k}||\mathbf{Q}|)^2+m_\gamma^2\frac{Q^2}{M^2}\left(\frac{Q^2}{4}-M^2\right)}{(\omega Q_0-|\mathbf{k}||\mathbf{Q}|)^2+m_\gamma^2\frac{Q^2}{M^2}\left(\frac{Q^2}{4}-M^2\right)}\right)+\frac{m_\gamma^2\left(\frac{Q^2}{4}-M^2\right)}{\frac{M^2}{Q^2}(\omega Q_0-|\mathbf{k}||\mathbf{Q}|)^2+m_\gamma^2\left(\frac{Q^2}{4}-M^2\right)}\right. \end{aligned}$$

$$- \left. \frac{m_\gamma^2 \left(\frac{Q^2}{4} - M^2\right)}{\frac{M^2}{Q^2}(\omega Q_0 + |\mathbf{k}||\mathbf{Q}|)^2 + m_\gamma^2 \left(\frac{Q^2}{4} - M^2\right)} \right\} \tag{2.59}$$

with $|\mathbf{k}| = \sqrt{\omega^2 - m_\gamma^2}$ and $|\mathbf{Q}| = \sqrt{Q_0^2 - Q^2}$. Eq.(2.59) takes a particularly simple form if m_γ is negligibly small (i.e. if $m_\gamma \ll \omega$), then

$$\begin{aligned} &F^{emission}(\omega) + F^{absorption}(\omega) \\ &\qquad \sim \frac{2 f_B(\omega) e^2}{\pi^2} \frac{Q^2}{m_\mu^2 \sqrt{Q_0^2 - Q^2}\,(Q^2 - 4m_\mu^2)} \ln\left(\frac{Q_0 + \sqrt{Q_0^2 - Q^2}}{Q_0 - \sqrt{Q_0^2 - Q^2}}\right). \end{aligned} \tag{2.60}$$

Similarly as in the previous case we can evaluate F^{fluct}. Performing transformation (2.55), and expanding (2.53) to the first order in X and Y, we get

$$\begin{aligned} &\langle \mathbb{T}\,\mathbb{P}\,\mathbb{T}^\dagger \rangle_{p_1 p_2} \frac{8V\omega_{p_1}\omega_{p_2}}{t}\, F^{fluct}(\omega) \\ &\qquad \sim \frac{\lambda^2 e^2}{(2\pi)^5} f_B(\omega)(1 + f_B(\omega)) \int d^4q_1 d^4q_2\; \delta(k^2 - m_\gamma^2)\; \delta(k_0 - \omega)\; B, \end{aligned} \tag{2.61}$$

with

$$\begin{aligned} B \;=\; & \int d^4q_1 d^4q_2\; \delta^4(Q - q_1 - q_2) \left(\frac{\partial}{\partial m_\mu^2}\right) \delta^+(q_1^2 - m_\mu^2)\; \delta^+(q_2^2 - m_\mu^2) \\ + & \int d^4q_1 d^4q_2\; \delta^4(Q - q_1 - q_2) \left\{ \left(\frac{\partial}{\partial M}\right)^2 \right. \\ - & \left. 2\left(\frac{Qk}{q_1 k}\right) \frac{\partial^2}{\partial M_1 \partial M_2} \right\} \delta^+(q_1^2 - M_1^2)\; \delta^+(q_2^2 - M_2^2) \Big|_{\,M_1 = M_2 = M} . \end{aligned}$$

Direct calculations lead to

$$B = \frac{2\pi\ (kQ)^2}{Q^2(Q^2-4M^2)^{\frac{3}{2}}}\left\{\frac{M^2}{\left(\frac{M^2}{Q^2}(kQ)^2+m_\gamma^2\left(\frac{Q^2}{4}-M^2\right)\right)}-\frac{(\frac{Q^2}{4}-M^2)(2M^2-Q^2)\ m_\gamma^2}{\left(\frac{M^2}{Q^2}(kQ)^2+m_\gamma^2\left(\frac{Q^2}{4}-M^2\right)\right)^2}\right\}$$
$$-\frac{\pi}{|Q|\sqrt{Q^2-4M^2}}-\frac{2\pi}{|Q|(Q^2-4M^2)^{\frac{3}{2}}}.$$

After some analysis we finally get

$$F^{fluct}(\omega) \sim \frac{f_B(\omega)(1+f_B(\omega))\ m_\gamma\ e^2}{4\pi^2\ M^2\ \sqrt{Q_0^2-Q^2}\ \sqrt{Q^2-4m_\mu^2}}\left\{\frac{|Q|}{M}\left[\text{arctg}\left(\frac{\frac{M}{|Q|}(\omega Q_0+|\mathbf{k}||\mathbf{Q}|)}{m_\gamma\sqrt{\frac{Q^2}{4}-M^2}}\right)\right.\right.$$
$$\left.-\ \text{arctg}\left(\frac{\frac{M}{|Q|}(\omega Q_0-|\mathbf{k}||\mathbf{Q}|)}{m_\gamma\sqrt{\frac{Q^2}{4}-M^2}}\right)\right]$$
$$+\ \frac{(2M^2-Q^2)\ m_\gamma}{2\sqrt{Q^2-4M^2}}\left[\frac{\omega Q_0+|\mathbf{k}||\mathbf{Q}|}{\frac{M^2}{Q^2}(\omega Q_0+|\mathbf{k}||\mathbf{Q}|)^2+m_\gamma^2(\frac{Q^2}{4}-M^2)}\right.$$
$$\left.\left.-\ \frac{\omega Q_0-|\mathbf{k}||\mathbf{Q}|}{\frac{M^2}{Q^2}(\omega Q_0-|\mathbf{k}||\mathbf{Q}|)^2+m_\gamma^2(\frac{Q^2}{4}-M^2)}\right]\right\}$$
$$-\ \frac{f_B(\omega)(1+f_B(\omega))|\mathbf{k}|\ e^2}{\pi^2\ (Q^2-4m_\mu^2)}. \tag{2.62}$$

Expression (2.62) considerably simplifies in the limit $m_\gamma \to 0$. In the latter case

$$F^{fluct} \sim -\frac{f_B(\omega)(1+f_B(\omega))\ \omega\ e^2}{\pi^2(Q^2-4m_\mu^2)}, \tag{2.63}$$

so the leading behaviour for F^{fluct} at small ω and $m_\gamma \ll \omega$ is dominated by ω^{-1}. Note that separate contributions to the 0–th order of a Taylor expansion of F^{fluc} behave as ω^{-2} but they cancel between themselves leaving behind parts proportional at worst to ω^{-1}. The minus sign in (2.63) reflects the fact that the fluctuations tend to suppress an increase in the particle number spectrum when ω is small. On the other hand, from (2.60) we see that the emissions and absorptions stimulate an increase in the particle number spectrum for small ω.

A result similar to (2.60) and (2.63) has been derived by Landshoff and Taylor [45] for a decay using proper scalar electrodynamics, though in their case a contribution from the emission and absorption dominated over fluctuations for small ω. Note that in our model both contributions are of comparable size at $\omega \sim 0$. The former feature is inherently connected with the fact that our 'photons' are scalar particles. If photons were vector particles an additional photon momentum k_μ would go with each three–line photon–muon vertex and so one might expect that the contributions (2.60) and (2.63) would be 'soften' at small ω. We have checked explicitly that for zero–mass photons in the axial temporal gauge (i.e. $A^0 = 0$) this is indeed the case, and it was found that $F^{emission} + F^{absorption} \propto \omega^{-1}$ whilst $F^{fluct} \propto \omega$.

Until now we have supposed that our heat bath contains only (scalar) photons in thermal equilibrium. However, one could similarly treat a heat bath which is comprised of photons and charged particles, let say electrons, mutually coexisting in thermal equilibrium. To be more specific, let us assume that the heat–bath photons A and electrons Ψ are both scalars so the heat–bath Hamiltonian takes form

$$\begin{aligned} H^{hb} &= H^{\gamma} + H^{e} + eA\Psi\Psi^{\dagger} + \frac{e^2}{2}A^2\Psi\Psi^{\dagger} \\ H^{e} &= \partial_\nu\Psi\partial^\nu\Psi^{\dagger} - m_e^2\Psi\Psi^{\dagger} \\ H^{\gamma} &= \frac{1}{2}(\partial_\nu A)^2 - \frac{m_\gamma^2}{2}A^2, \end{aligned} \tag{2.64}$$

and the $\mathbb{T}$–matrix interacting Hamiltonian H_{in} reads

$$H_{in} = \frac{\lambda}{2}\Phi^2\phi\phi^\dagger + (eA + \frac{e^2}{2}A^2)\Psi\Psi^\dagger + (eA + \frac{e^2}{2}A^2)\phi\phi^\dagger.$$

It is usually argued [57,58] that the interacting pieces in H^{hb} can be dropped provided that $t_i \to -\infty$ and $t_f \to \infty$. Since we assume that 'pions' are prepared in the remote past and 'muons' are measured in the remote future, we shall accept in the following this omission.

We can now approach to calculate both the photon and electron number spectrum, i.e. $\frac{d\Delta\langle N_\gamma(\omega)\rangle}{d\omega}$ and $\frac{d\Delta\langle N_e(\omega)\rangle}{d\omega}$ respectively. As for $\frac{d\Delta\langle N_\gamma(\omega)\rangle}{d\omega}$, an order–$e^2$ contribution is clearly done only by diagrams in Fig.2.7 as there are no relevant graphs with electron vertices contributing to this order, so (2.59) and (2.62) still remain true. On the other hand, there is no order–e^2 contribution to $\frac{d\Delta\langle N_e(\omega)\rangle}{d\omega}$. The lowest order in e (keeping λ^2 fixed) is e^4. This brings richer diagrammatic structure then in the photon case. In FIG.2.10 we list all the generating thermal diagrams contributing to an order–e^4.

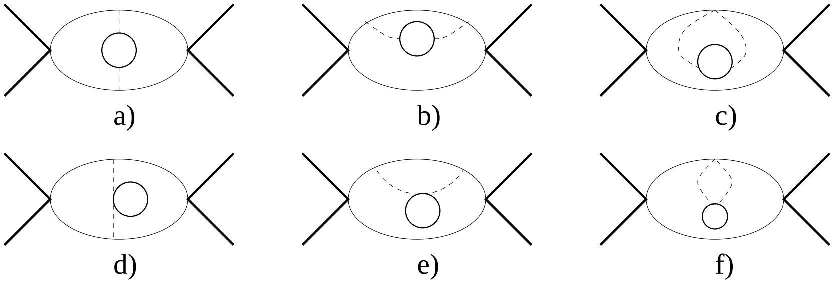
a) b) c) d) e) f)

Figure 2.10: The generating thermal diagrams involved in an order–e^4 contribution to the electron number spectrum. Dashed lines: photons. Thin lines: ϕ, $\phi^\dagger$ particles. Bold lines: Φ particles. Half–bold lines: electrons.

It is easy to see that out of these 6 generating thermal diagrams we get 43 non–vanishing and topologically inequivalent modified cut diagrams; for example from FIG.2.10c) we have only those diagrams which are depicted in FIG.2.11.

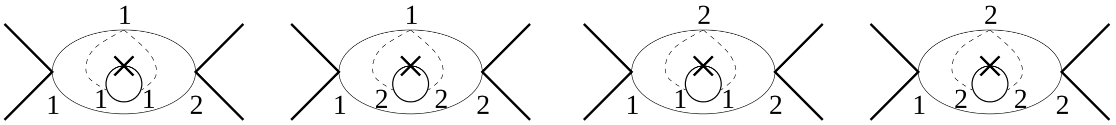

Figure 2.11: The non–vanishing modified cut diagrams from FIG.4.4c).

Note, the graphs of FIG.2.11 must be multiplied by a factor of four as there are two equivalent insertions of the modified electron line and two equivalent distributions of the photon–muon vertex (so together with $\frac{1}{2!}$ from a Taylor expansion of the $\mathbb{T}$–matrix we get the symmetry factor 2). Analogously we get 10 inequivalent modified cut diagrams from FIG.2.10a); 7 from b); 8 from d); 6 from e) and 8 from f).) The actual electron number spectrum calculations are thus rather involved. Nevertheless, one might evaluate fairly quickly $F^{emission}(\omega_e) + F^{absorption}(\omega_e)$ as there are only three diagrams which contribute, namely:

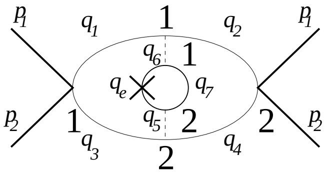

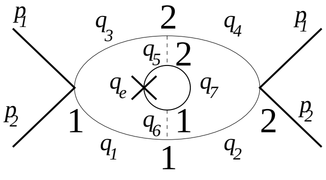

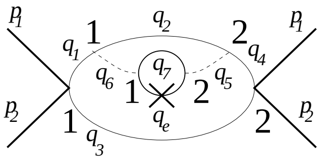

Let us remind that in the finale state we must have, apart from the heat-bath particles, only two 'muons', and so the diagram

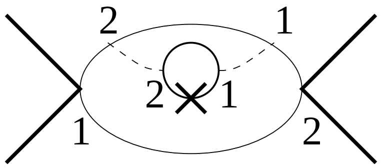

can not contribute to $\frac{d\Delta\langle N_e(\omega)\rangle}{d\omega}$. Subtracting a temperature independent part, we are left with

$$\begin{aligned}
&F^{emission}(\omega_e) + F^{absorption}(\omega_e) \\
&\quad = \frac{t\lambda^2 e^4 \, f_B(\omega_e)}{\langle T\mathcal{P}T^\dagger\rangle_{p_1p_2}\, V\omega_{p_1}\omega_{p_2}(2\pi)^8} \int d^4q_7 \; d^4q_e \; \delta^+(q_7^2 - m_e^2)\; \delta(q_e^2 - m_e^2)\; \delta(q_e^0 - \omega_e) \\
&\quad \times \int d^4q_2 \; d^4q_3 \; \delta^+(q_2^2 - m_\mu^2)\; \delta^+(q_3^2 - m_\mu^2) \;\; \big\{K_1 \; \delta^4(-Q + q_2 + q_3 + q_7 - q_e) \\
&\quad -K_2 \;\; \delta^4(-Q + q_2 + q_3 + q_7 + q_e)\big\}\,, \qquad (2.65)
\end{aligned}$$

with

$$\begin{aligned}
K_1 &= \frac{1}{(-q_2Q + Q^2 + i\epsilon)} \; \frac{1}{(-q_3Q + Q^2 - i\epsilon)} \; \frac{1}{(-2q_7q_e + 2m_e^2 - m_\gamma^2)^2} \\
K_2 &= K_1(q_e \to -q_e).
\end{aligned}$$

If we are interested in the qualitative behaviour of (2.65) at small ω's, we need to perform an integration over p_e only. In order to keep our calculations as simple as possible, let us assume that $m_e = m_\gamma = 0$. Eq.(2.65) can now be handled in a similar way as in the photon heat bath case. We first perform a transformation

$$\begin{aligned}
q_7 &\to q_7 \mp q_e, \\
q_e &\to q_e.
\end{aligned}$$

So (2.65) now reads

$$\begin{aligned}
(2.65) \quad = \quad & \frac{t\lambda^2 e^4 \, f_B(\omega_e)}{\langle \mathbb{TPT}^\dagger\rangle_{p_1p_2}\, V\omega_{p_1}\omega_{p_2}(2\pi)^8} \int \; d^4q_2 \; d^4q_3 \; \delta^+(q_2^2 - m_\mu^2)\; \delta^+(q_3^2 - m_\mu^2) \\
& \times \frac{1}{(-q_2Q + Q^2 + i\epsilon)} \; \frac{1}{(-q_3Q + Q^2 - i\epsilon)} \; B, \qquad (2.66)
\end{aligned}$$

where

$$B = \int \frac{d^4q_7\, d^4q_e}{(2q_7q_e)^2} \left\{ \delta^+(q_7^2 + X) - \delta^+(q_7^2 - X) \right\}\, \delta(q_e^2)\, \delta(q_7^0 - \omega_e)\, \delta^4(-Q + q_2 + q_3 + q_7),$$

with $X = 2q_7q_e$. As before we might expand B in terms of X. First surviving term reads

$$\begin{aligned} B &\sim \int d^4q_7\, d^4q_e\, \left(\partial_{q_7^2}\delta(q_7^2)\right) \delta^4(-Q + q_2 + q_3 + q_7)\, \frac{2X}{(2q_7q_e)^2} \\ &= -\omega_e^0\, \partial_{m^2} \int d^4q_7\, \delta(q_7^2 - m^2)\, \delta^4(-Q + q_2 + q_3 + q_7)\, \frac{1}{|\mathbf{q}_7|} \ln\left(\frac{q_7^0 - |\mathbf{q}_7|}{q_7^0 + |\mathbf{q}_7|}\right)\Bigg|_{m=0}, \end{aligned} \tag{2.67}$$

so $B \propto \omega_e^0$, and consequently $F^{emission}(\omega_e) + F^{absorption}(\omega_e) \propto \omega_e^{-1}$. Straightforward application of the previous mathematical operations to $F^{fluct}(\omega_e)$ reveals that $F^{fluct}(\omega_e) \propto \omega_e^{-1}$ as well. Let us mention that the separate contributions present in $F^{emission}(\omega_e)$, $F^{absorption}(\omega_e)$ and $F^{fluct}(\omega_e)$ behave as ω_e^{-2} but they mutually cancel leaving behind terms proportional at worst to ω_e^{-1}.

Surprisingly enough, we have found that, for small ω, our heat bath (2.64) changes due to scattering $\Phi\Phi \to \phi\bar{\phi}$ in such a way that the rate of change in the electron number spectrum has qualitatively similar behaviour (i.e. ω^{-1}) as the rate of change in the photon number spectrum. This is so provided one assumes that both electrons and photons are massless particles. Clearly, ω^{-2} behaviour would be disastrous as it would suggest that the energy density $\omega dN/d\omega$ of the heat–bath particles behaves as ω^{-1} which would, if integrated, produce an infinite contribution to the total energy carried off by the heat–bath particles.

2.5 Conclusions

In this chapter we have formulated a systematic method for studying the heat–bath particle number spectrum using modified cut diagrams. In particular, for the quark–gluon plasma in thermodynamical equilibrium our approach should be useful as an effective alternative to the Landshoff and Taylor [45] approach. The method used in [45] (i.e. to start from first principles) suffers from the lack of a systematic computational approach for higher orders in coupling constants. One of the corner stones of our formalism is the largest–time equation (LTE). We have shown how the zero–temperature LTE can be extended to finite temperature. During the course of this analysis, we have emphasised some important aspects of the finite–temperature extension which are worth mentioning. Firstly, many of kinematic rules valid for zero–temperature diagrams can not be directly used in the finite–temperature ones. This is because the emission or absorption of heat–bath particles make it impossible to fix some particular direction to a diagrammatic line. It turns out that one finds more diagrams then one used to have at zero temperature. The most important reductions of the diagrams have been proved. The rather complicated structure of the finite–temperature diagrams brings into play another complication: uncutable diagrams. It is well known that at zero temperature one can always make only one cut in each cut diagram (this can be viewed as a consequence of the unitarity condition). This is not true however at finite temperature. We have found it as useful to start fully with the LTE analysis which is in terms of type 1 and type 2 vertices. This language allows us to construct systematically all the cut diagrams. We have refrained from an explicit use of the cuts in finite–temperature diagrams as those are ambiguous and therefore rather obscure the analysis.

The second, rather technical, corner stone are the (functional) thermal Dyson–Schwinger equations. We have developed a formalism of the *arrowed* variations acting directly on field operators. This provides an elegant technique for dealing in a practical fashion with expectation values (both thermal and vacuum) whenever functions or functionals of fields admit the decomposition (A.1). The merit of the Dyson–Schwinger equations is that they allow us to rewrite an expectation value of some functional of field in terms of expectation values of less complicated functionals. Some illustrations of this and further thermal functional identities are derived in Appendix A.1.

When we have studied the heat–bath particle number spectrum, we applied the Dyson–Schwinger equations both to numerator and denominator of corresponding expression. The results were almost the same. The simple modification of one propagator rendered both equal. We could reflect this on a diagrammatical level very easily as the denominator was fully expressible in terms of thermal cut diagrams. Our final rule for the heat–bath particle spectrum is

$$\frac{d\Delta\langle N(\omega)\rangle}{d\omega} = \frac{\langle \mathbb{T}^{\dagger}\mathbb{P}\,\mathbb{T}\rangle^{M}_{p_1p_2}}{\langle \mathbb{T}^{\dagger}\mathbb{P}\,\mathbb{T}\rangle_{p_1p_2}}, \tag{2.68}$$

with $\mathbb{T}$ being the $\mathbb{T}$–matrix, $\mathbb{P}$ being the projection operator onto final states, p_1, p_2 being the momenta of particles in the initial state, β being the inverse temperature and M being abbreviation for the modified diagrams. Modification of the cut diagrams consist of the substitution in turn of each heat–bath particle line by an altered one. This substitution must be done in each cut diagram. Replacement must be only one per modified diagram. Our approach is demonstrated on a simple model where two scalar particles ('pions') scatter, within a photon heat bath, into a pair of charged particles ('muon' and 'antimuon') and we explicitly calculate the resulting changes in the number spectra of the photons and. It is also discussed how the results will change if the photon heat bath is replaced with photon–electron one.

Chapter 3

Pressure at thermal equilibrium

3.1 Introduction

A significant quantity of physical interest that one may want to calculate in field theory at finite temperature, either at equilibrium or out of equilibrium, is pressure. In thermal quantum field theory (both in the real– and imaginary–time formalism) where one usually deals with systems in thermal equilibrium there is an easy prescription for a pressure calculation. The latter is based on the observation that for thermally equilibrated systems the grand canonical partition function Z is given as

$$Z = e^{-\beta\Omega} = Tr(e^{-\beta(H-\mu_i N_i)}), \tag{3.1}$$

where Ω is the grand canonical potential, H is the Hamiltonian, N_i are conserved charges, μ_i are corresponding chemical potentials, and β is the inverse temperature: $\beta = 1/T$. Using identity $\beta\frac{\partial}{\partial\beta} = -T\frac{\partial}{\partial T}$ together with (3.1) one gets

$$T\left(\frac{\partial\Omega}{\partial T}\right)_{\mu_i,V} = \Omega - E + \mu_i N_i, \tag{3.2}$$

with E and V being the averaged energy and volume of the system respectively. A comparison of (3.2) with a corresponding thermodynamic expression for the grand canonical potential [36, 37, 59] requires that entropy $S = -\left(\frac{\partial \Omega}{\partial T}\right)_{\mu_i, V}$, so that

$$d\Omega = -SdT - pdV - N_i d\mu_i \;\Rightarrow\; p = -\left(\frac{\partial \Omega}{\partial V}\right)_{\mu_i, T}. \tag{3.3}$$

For large systems one can usually neglect surface effects so E and N_i become extensive quantities. Eq.(3.2) then immediately implies that Ω is extensive quantity as well, so (3.3) simplifies to

$$p = -\frac{\Omega}{V} = \frac{\ln Z}{\beta V}. \tag{3.4}$$

The pressure defined by Eq.(3.4) is the so called thermodynamic pressure.

Since $\ln Z$ can be systematically calculated summing up all connected closed diagrams (i.e. bubble diagrams) [3, 36, 60], the pressure calculated via (3.4) enjoys a considerable popularity [34, 36, 61, 62]. Unfortunately, the latter procedure can not be extended to out of equilibrium as there is, in general, no definition of the partition function Z nor grand canonical potential Ω away from an equilibrium.

Yet another, alternative definition of the pressure not hinging on thermodynamics can be provided; namely the hydrostatic pressure which is formulated through the energy–momentum tensor $\Theta^{\mu\nu}$. The formal argument leading to the hydrostatic pressure in D space–time dimensions is based on the observation that $\langle \Theta^{0j}(x) \rangle$ is the mean (or macroscopic) density of momenta $\mathbf{p}^j$ at the point x^μ. Let $\mathbf{P}$ be the mean total $(D-1)$–momentum of an infinitesimal volume $V^{(D-1)}$ centred at $\mathbf{x}$, then the rate of change of j–component of $\mathbf{P}$ reads

$$\frac{d\mathbf{P}^j(x)}{dt} = \int_{V^{(D-1)}} d^{D-1}\mathbf{x}' \, \frac{\partial}{\partial x^0} \langle \Theta^{0j}(x^0, \mathbf{x}') \rangle = -\sum_{i=1}^{D-1} \int_{\partial V^{(D-1)}} d\mathbf{s}^i \, \langle \Theta^{ij} \rangle. \tag{3.5}$$

In the second equality we have exploited the continuity equation for $\langle \Theta^{\mu j} \rangle$ and successively we have used Gauss's theorem[1]. The $\partial V^{(D-1)}$ corresponds to the surface of $V^{(D-1)}$.

Anticipating a system out of equilibrium, we must assume a non–trivial distribution of the mean particle four–velocity $U^{\mu}(x)$ (hydrodynamic velocity). Now, a pressure is by definition a scalar quantity. This particularly means that it should not depend on the hydrodynamic velocity. We must thus go to the local rest frame and evaluate pressure there. However, in the local rest frame, unlike the equilibrium, the notion of a pressure acting equally in all directions is lost. In order to retain the scalar character of pressure, one customarily defines the *pressure at a point* (in the following denoted as $p(x)$) [64], which is simply the 'averaged pressure' [2] over all directions at a given point. In the local rest frame Eq.(3.5) describes j–component of the force exerted by the medium on the infinitesimal volume $V^{(D-1)}$. (By definition, there is no contribution to $d\mathbf{P}^j(x)/dt$ caused by the particle convection through $\partial V^{(D-1)}$.) Averaging the LHS of (3.5) over all directions of the normal $\mathbf{n}(\mathbf{x})$, we get[3]

$$
\begin{aligned}
\frac{1}{(S_1^{D-2})} \sum_{j=1}^{D-1} \int \frac{d\mathbf{P}^j(x)}{dt}\, \mathbf{n}^j \, d\Omega(\mathbf{n}) &= -\frac{1}{(S_1^{D-2})} \sum_{j,i=1}^{D-1} \int_{\partial V^{(D-1)}} ds \, \langle \Theta^{ij}(x') \rangle \int d\Omega(\mathbf{n}) \, \mathbf{n}^i \mathbf{n}^j \\
&= \frac{1}{(D-1)} \sum_{i=1}^{D-1} \int_{\partial V^{(D-1)}} ds \, \langle \Theta^i{}_i(x') \rangle, \qquad (3.6)
\end{aligned}
$$

where $d\Omega(\mathbf{n})$ is an element of solid angle about $\mathbf{n}$ and S_1^{D-2} is the surface of $(D-2)$–sphere with unit radius ($\int d\Omega(\mathbf{n}) = S_1^{D-2} = 2\pi^{\frac{D-1}{2}}/\Gamma(\frac{D-1}{2})$) . On the other hand, from the definition of the pressure at a point x^μ we might write

---

[1] The macroscopic conservation law for $\langle \Theta^{\mu\nu} \rangle$ (i.e. the continuity equation) has to be postulated. For some systems, however, the later can be directly derived from the corresponding microscopic conservation law [63].

[2] To be precise, we should talk about averaging the normal components of stress [64].

[3] The angular average is standardly defined for scalars (say, A) as; $\int A \, d\Omega(\mathbf{n}) / \int d\Omega(\mathbf{n})$, and for vectors (say, $\mathbf{A}^i$) as; $\sum_j \int \mathbf{A}^j \, \mathbf{n}^j \, d\Omega(\mathbf{n}) / \int d\Omega(\mathbf{n})$. Similarly we might write down the angular averages for tensors of a higher rank.

$$\left(S_1^{D-2}\right)^{-1}\sum_{j=1}^{D-1}\int \frac{d\mathbf{P}^j(x)}{dt}\,\mathbf{n}^j\,d\Omega(\mathbf{n}) = -p(x)\,\int_{\partial V^{(D-1)}} ds, \tag{3.7}$$

here the minus sign reflects that the force responsible for a compression (conventionally assigned as a positive pressure) has reversed orientation than the surface normals $\mathbf{n}$ (pointing outward). In order to keep track with the standard text–book definition of a sign of a pressure [37, 64] we have used in (3.7) the normal $\mathbf{n}$ in a contravariant notation (note, $\mathbf{n}^i = -\mathbf{n}_i$). Comparing (3.6) with (3.7) we can write for a sufficiently small volume $V^{(D-1)}$

$$p(x) = -\frac{1}{(D-1)}\sum_{i=1}^{D-1}\langle \Theta^i{}_i(x)\rangle. \tag{3.8}$$

We should point out that in equilibrium the thermodynamic pressure is usually identified with the hydrostatic one via the virial theorem [36,43]. In the remainder of this chapter we shall deal with the hydrostatic pressure at equilibrium. We shall denote the foregoing as $\mathcal{P}(T)$, where T stands for temperature. We consider the non–equilibrium case in the next chapter.

The plan of this chapter is as follows. In Section 3.2 we review the necessary mathematical framework needed for the renormalisation of the energy–momentum tensor.(For an extensive review see also refs. [36, 65, 66].) The latter is discussed on the $O(N)$ Φ^4 theory. As a byproduct we renormalise Φ_a^2, $\Phi_a\Phi_b$ and $\Theta^{\mu\nu}$ operators. The corresponding QFT extension of (3.8) is obtained.

Resumed form for the pressure in the large–N limit, together with the discussion of both coupling constant and mass renormalisation is worked out in Section 3.3. The discussion is substantially simplified by means of the Dyson–Schwinger equations.

In Section 3.4 we end up with the high–temperature expansion of the pressure. Calculations are performed for $D = 4$ (both for massive and massless fields) and the result is expressed in terms of renormalised masses $m_r(0)$ and $m_r(T)$. The former is done by means of the Mellin transform technique.

This chapter is furnished with two appendices. In Appendix B we clarify some mathematical manipulations needed in Section 3.3. For the completeness' sake we compute in Appendix C the high–temperature expansion of the thermal–mass shift $\delta m^2(T)$ which will prove useful in Section 3.4.

3.2 Renormalisation

If we proceed with (3.8) to QFT this leads to the notorious difficulties connected with the fact that $\Theta^{\mu\nu}$ is a (local) composite operator. If only a free theory would be in question then the normal ordering prescription would be sufficient to render $\langle \Theta^{\mu\nu} \rangle$ finite. In the general case, when the interacting theory is of interest, one must work with the Zimmerman 'normal' ordering prescription instead. Let us demonstrate the latter on the $O(N)$ Φ^4 theory. (In this section we keep N arbitrary.) Such a theory is defined by the bare Lagrange function

$$\mathcal{L} = \frac{1}{2} \sum_{a=1}^{N} \left((\partial \Phi_a)^2 - m_0^2 \Phi_a^2 \right) - \frac{\lambda_0}{8N} \left(\sum_{a=1}^{N} (\Phi_a)^2 \right)^2 , \tag{3.9}$$

we assume that $m_0^2 > 0$. The corresponding canonical energy–momentum tensor is given by

$$\Theta_c^{\mu\nu} = \sum_a \partial^\mu \Phi_a \partial^\nu \Phi_a - g^{\mu\nu} \mathcal{L} \, . \tag{3.10}$$

The Feynman rules for Green's functions with the energy–momentum insertion can be easily explained in momentum space. In the reasonings to follow we shall need the (thermal) composite Green's function[4]

$$D^{\mu\nu}(x^n|y) = \langle \mathcal{T}^* \left\{ \Phi_r(x_1) \dots \Phi_r(x_n) \Theta_c^{\mu\nu}(y) \right\} \rangle \, . \tag{3.11}$$

Here the subscript r denotes the renormalised fields in the Heisenberg picture (the internal indices are suppressed) and $\mathcal{T}^*$ is so called $\mathcal{T}^*$ product (or covariant $\mathcal{T}$ product) [53, 67–69]. The $\mathcal{T}^*$ product is defined in such a way that it is simply the $\mathcal{T}$ product with all differential operators $\mathcal{D}_{\mu_i}$ pulled out of the $\mathcal{T}$–ordering symbol, i.e.

$$\mathcal{T}^* \{ \mathcal{D}_{\mu_1}^{x_1} \Phi(x_1) \dots \mathcal{D}_{\mu_n}^{x_n} \Phi(x_n) \} = \mathcal{D}(i\partial_{\{\mu\}}) \mathcal{T} \{ \Phi(x_1) \dots \Phi(x_n) \} \, , \tag{3.12}$$

where $\mathcal{D}(i\partial_{\{\mu\}})$ is just a useful short–hand notation for $\mathcal{D}_{\mu_1}^{x_1} \mathcal{D}_{\mu_2}^{x_2} \dots \mathcal{D}_{\mu_n}^{x_n}$. In the case of thermal Green's functions, the $\mathcal{T}$ might be as well a contour–ordering symbol. It is the mean value of the $\mathcal{T}^*$ ordered fields rather than the $\mathcal{T}$ ones, which corresponds at $T = 0$ and at equilibrium to the Feynman path integral representation of Green's functions [69, 70].

A typical contribution to $\Theta_c^{\mu\nu}(y)$ can be written as

$$\mathcal{D}_{\mu_1} \Phi(y) \; \mathcal{D}_{\mu_2} \Phi(y) \dots \mathcal{D}_{\mu_n} \Phi(y) \, , \tag{3.13}$$

so the typical term in (3.11) is

$$\mathcal{D}(i\partial_{\{\mu\}}) \; \langle \mathcal{T}^* \left\{ \Phi_r(x_1) \dots \Phi_r(x_n) \Phi(y_1) \dots \Phi(y_k) \right\} \rangle \; |_{y_i = y} \, .$$

Performing the Fourier transform in (3.11) we get

---

[4] By Φ we shall mean the field in the Heisenberg picture. The subscript H will be introduced in cases when a possible ambiguity could occur.

$$D^{\mu\nu}(p^n|p) = \sum_{k=\{2,4\}} \int \left(\prod_{i=1}^{k} \frac{d^D q_i}{(2\pi)^D} \right) (2\pi)^D \, \delta^D(p - \sum_{j=1}^{k} q_j) \; \mathcal{D}^{\mu\nu}_{(k)}(q_{\{\mu\}}) \; D(p^n|q^k), \qquad (3.14)$$

where $\mathcal{D}^{\mu\nu}_{(k)}(\ldots)$ is a Fourier transformed differential operator corresponding to the quadratic (k=2) and quartic (k=4) terms in $\Theta^{\mu\nu}_c$. Denoting the new vertex corresponding to $\mathcal{D}^{\mu\nu}_{(k)}(\ldots)$ as $\otimes$, we can graphically represent (3.11) through (3.14) as

$$D^{\mu\nu}(p^n|p) =$$

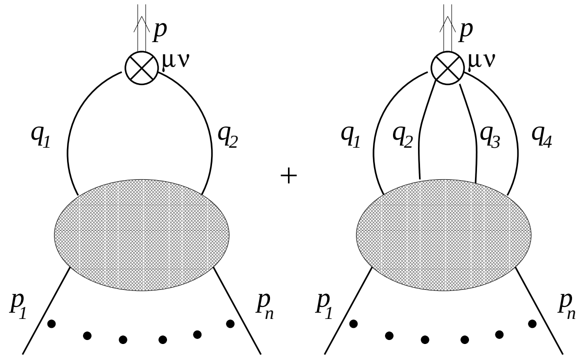

Figure 3.1: The graphical representation of $D^{\mu\nu}(p^n|p)$.

For the case at hand one can easily read off from (3.10) an explicit form of the bare composite vertices, the foregoing are

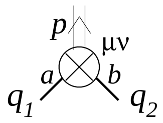

$$\sim \; \mathcal{D}^{\mu\nu}_{(2)}(q_{\{\mu\}}) = \tfrac{1}{2}\, \delta_{ab} \, \{2(q_1 - p)^\mu q_1^\nu - g^{\mu\nu}((q_1 - p)_\lambda q_1^\lambda - m_0^2))\}$$

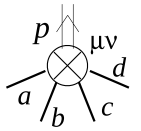

$$\sim \; \mathcal{D}^{\mu\nu}_{(4)}(q_{\{\mu\}}) = \tfrac{g^{\mu\nu}\lambda_0}{8N} \{2(\delta_{ab}\delta_{cd} + \delta_{ac}\delta_{bd} + \delta_{ad}\delta_{bc}) - 5\delta_{ab}\delta_{cd}\delta_{ac}\}$$

(For the internal indices we do not adopt Einstein's summation convention.) We have tacitly assumed in FIG.3.1 that the vacuum bubble diagrams present in the shaded blobs are divided out. We have also implicitly assumed that summation over internal indices is understood. Note that in the case of thermal composite Green's function, the new vertices are clearly of type–1 as the fields from which they are deduced have all a real–time argument[5] (type–1 fields).

Renormalisation of $\Phi_a(x)\Phi_b(x)$

Now, if there would be no $\Theta_c^{\mu\nu}$ insertion in (3.11), the latter would be finite, and so it is natural to define the renormalised energy–momentum tensor $[\Theta_c^{\mu\nu}]$ (or Zimmermann normal ordering) in such a way that

$$D_r^{\mu\nu}(x^n|y) = \langle \mathcal{T}^* \left\{ \Phi_r(x_1) \ldots \Phi_r(x_n) \, [\Theta_c^{\mu\nu}] \right\} \rangle ,$$

is finite for any $n > 0$. To see what is involved, we illustrate the mechanism of the composite operator renormalisation on $\Phi_a(x)\Phi_b(x)$. We shall use the mass–independent renormalisation (or minimal subtraction scheme – (MS)) which is particularly suitable for this purpose. In MS we can expand the bare parameters into the Laurent series which has a simple form [53, 66, 70], namely

$$\lambda_0 = \mu^{4-D} \, \lambda_r \left(1 + \sum_{k=1}^{\infty} \frac{a_k(\lambda_r; D)}{(D-4)^k} \right) \tag{3.15}$$

$$m_0^2 = m_r^2 \left(1 + \sum_{k=1}^{\infty} \frac{b_k(\lambda_r; D)}{(D-4)^k} \right) . \tag{3.16}$$

Here a_0 and b_0 are analytic in $D = 4$. The parameter μ is the scale introduced by the renormalisation in order to keep λ_r dimensionless. An important point is that both a_k's and b_k's are mass, temperature and momentum independent.

---

[5] For a brief introduction to the real–time formalism in thermal QFT see for example [38].

It was Zimmermann who first realized that the forest formula known from the ordinary Green's function renormalisation [53, 65] can be also utilised for the composite Green's functions rendering them finite [65,71]. That is, we start with Feynman diagrams expressed in terms of physical (i.e. finite) coupling constants and masses. As we calculate diagrams to a given order, we meet UV divergences which might be cancelled by adding counterterm diagrams. The forest formula then prescribes how to systematically cancel all the UV loop divergences by counterterms to all orders. However, in contrast to the coupling constant renormalisation, the composite vertex need not to be renormalised multiplicatively. We shall illustrate this fact in the sequel. Let us also observe that in the lowest order (no loop) the renormalised composite vertex equals to the bare one, and so to that order $A = [A]$, for any composite operator A.

Now, from (3.15) and (3.16) follows that for any function $F = F(m_r, \lambda_r)$ we have

$$\frac{\partial F}{\partial m_r^2} = \frac{\partial m_0^2}{\partial m_r^2}\,\frac{\partial F}{\partial m_0^2} = \frac{m_0^2}{m_r^2}\,\frac{\partial F}{\partial m_0^2}\,.$$

So particularly for

$$F = D(x_1, \ldots, x_n) = \langle \mathcal{T}^*\{\Phi_r(x_1)\ldots\Phi_r(x_n)\}\rangle,$$

one reads

$$\begin{aligned} m_r^2\,\frac{\partial}{\partial m_r^2}D(x_1,\ldots,x_n) &= m_0^2\,\frac{\partial}{\partial m_0^2}D(x_1,\ldots,x_n) \\ &= \left(-\frac{i}{2}\right)\mathcal{N}\int d^Dx\,\sum_{a=1}^{N}\int \mathcal{D}\phi\;\phi_r(x_1)\ldots\phi_r(x_n)\;m_0^2\phi_a^2(x)\,\exp(iS[\phi,T]) \\ &= \left(-\frac{i}{2}\right)\int d^Dx\,\sum_{a=1}^{N}\,D_a(x_1,\ldots,x_n|x;m_0^2)\,. \qquad (3.17) \end{aligned}$$

Here $\mathcal{N}^{-1}$ is the standard denominator of the path integral representation of Green's function. We should apply the derivative also on $\mathcal{N}$ but this would produce disconnected graphs with bubble diagrams. The former precisely cancel the very same disconnected graphs in the first term, so we are finally left with no bubble diagrams in (3.17). In the Fourier space (3.17) reads

$$m_r^2 \frac{\partial}{\partial m_r^2} D(p_1, \ldots, p_n) = \left(-\frac{i}{2}\right) \sum_{a=1}^{N} D_a(p_1, \ldots, p_n|0; m_0^2)\,. \tag{3.18}$$

As the LHS is finite, there cannot be any pole terms on the RHS either, and so $\sum_a m_0^2 \Phi_a^2$ is by itself a renormalised composite operator. We see that m_0^2 precisely compensates the singularity of $\sum_{a=1}^{N} \Phi_a^2$.

Now, it is well known that any second–rank tensor (say M_{ab}) can be generally decomposed into three irreducible tensors; an antisymmetric tensor, a symmetric traceless tensor and an invariant tensor. Let us set $M_{ab} = \Phi_a \Phi_b$, so the symmetric traceless tensor K_{ab} reads

$$K_{ab}(x) = \Phi_a(x)\Phi_b(x) - \delta_{ab}/N \sum_{c=1}^{n} \Phi_c^2(x)\,, \tag{3.19}$$

whilst the invariant tensor I_{ab} is

$$I_{ab}(x) = \delta_{ab}/N \sum_{c=1}^{N} \Phi_c^2(x)\,.$$

Because the renormalised composite operators have to preserve a tensorial structure of the bare ones, we immediately have that

$$K_{ab} = A_1[K_{ab}] \quad \text{and} \quad I_{ab} = A_2[I_{ab}]\,, \tag{3.20}$$

where both A_1 and A_2 must have structure $(1 + \sum(\text{poles}))$. The foregoing guarantees that to the lowest order $K_{ab} = [K_{ab}]$ and $I_{ab} = [I_{ab}]$. As we saw in (3.18), $m_0^2 I_{ab}$ is renormalised, and so from (3.20) follows that $m_0^2 I_{ab} = C\ [I_{ab}]$. Here C has dimension $[m^2]$ and is analytic in $D = 4$. We can uniquely set $C = m_r^2$ because only this choice fulfils the lowest order condition $I_{ab} = [I_{ab}]$ (c.f. Eq.(3.16)). Collecting our results together we might write

$$\sum_c \Phi_c^2 = Z_{\Sigma\Phi^2} \left[\sum_c \Phi_c^2\right] = Z_{\Sigma\Phi^2} \sum_c [\Phi_c^2]\,, \tag{3.21}$$

with $Z_{\Sigma\Phi^2} = A_2 = \frac{m^2 r}{m_0^2}$. In the second equality we have used an obvious linearity [65] of $[\ldots]$. From (3.19) and (3.21) follows that

$$\Phi_a(x)\Phi_b(x) = A_1[\Phi_a(x)\Phi_b(x)] - \frac{\delta_{ab}}{N}(A_1 - Z_{\Sigma\Phi^2}) \sum_{c=1}^{N} [\phi_c^2(x)]\,. \tag{3.22}$$

So particularly for Φ_a^2 one reads

$$\Phi_a^2 = \frac{1}{N}\left((N-1)A_1 + Z_{\Sigma\Phi^2}\right)\ [\Phi_a^2] - \frac{1}{N}\left(A_1 - Z_{\Sigma\Phi^2}\right) \sum_{c\neq a} [\Phi_c^2]\,. \tag{3.23}$$

From the discussion above it does not seem to be possible to obtain more information about A_1 without doing an explicit perturbative calculations, however, it is easy to demonstrate that $A_1 \neq Z_{\Sigma\Phi^2}$. To show this, let us consider the simplest non–trivial case; i.e. N=2, and calculate A_1 to order λ_r. For that we need to discuss the renormalisation of the n-point composite Green's function with, say, Φ_1^2 insertion. To do that, it suffices to discuss the renormalisation of the corresponding 1PI n–point Green's function. The perturbative expansion for the composite vertex to order λ_r can be easily generated via the Dyson–Schwinger equation [72] and it reads

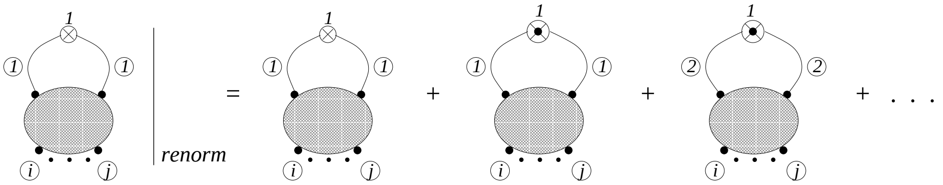

(3.24)

where

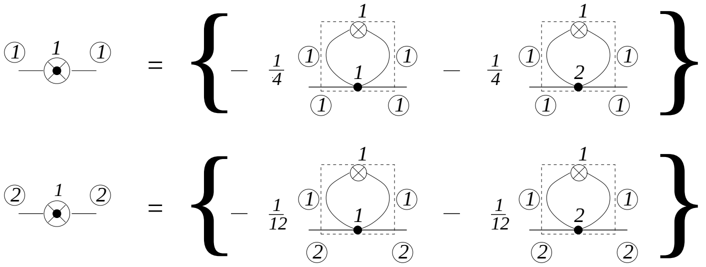

Here cross–hatched blobs refer to (renormalised) 1PI $(n+2)$–point Green's function, circled indices mark a type of the field propagated on the indicated line, and uncircled numbers refer to thermal indices (we explicitly indicate only relevant thermal indices). The counterterms, symbolised by a heavy dot, are extracted from the boxed diagrams (elementary Zimmermann forests). In MS scheme one gets the following results:

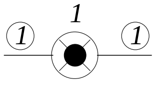

$$= \frac{i\,\lambda_r \mu^{4-D}}{4}\int \frac{d^D q}{(2pi)^D}\,\{\mathbb{D}_{11}(q)\mathbb{D}_{11}(-q) - \mathbb{D}_{12}(q)\mathbb{D}_{12}(-q)\}\,|_{\text{MS pole term}}$$

$$= -\frac{1}{4}\partial_{m_r^2}\left(\frac{\Gamma\left(1-\frac{D}{2}\right)}{(4\pi)^{\frac{D}{2}}}\,\lambda_r\,\mu^{4-D}\,m_r^{D-2}\right)|_{\text{MS}} = -\lambda_r\mu^{4-D}/2\;(D-4)\;(4\pi)^2$$

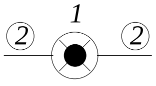

$$= -\lambda_r\mu^{4-D}/6\;(D-4)\;(4\pi)^2.$$

Here $\mathbb{D}_{11}$ and $\mathbb{D}_{12}$ are the usual thermal propagators in the real–time formalism [34, 36, 38] (see also Section 3.3). From (4.24) we can directly read off that

$$[\Phi_1^2] = \left(1 - \frac{\lambda_r \mu^{4-D}}{2\,(D-4)\,(4\pi)^2} + \mathcal{O}(\lambda_r^2)\right)\,\Phi_1^2 + \left(-\frac{\lambda_r \mu^{4-D}}{6\,(D-4)\,(4\pi)^2} + \mathcal{O}(\lambda_r^2)\right)\,\Phi_2^2\,.$$

As the coefficient before Φ_2^2 is not zero, we conclude that $A_1 \neq Z_{\Sigma\Phi^2}$. It is not a great challenge to repeat the previous calculations for the $\Phi_1\Phi_2$ insertion. The latter gives

$$A_1 = 1 - \frac{\lambda_r \mu^{4-D}}{3\,(D-4)\,(4\pi)^2} + \mathcal{O}(\lambda_r^2)\,.$$

Eq.(3.23) exhibits the so called operator mixing [53]; the renormalisation of Φ_a^2 cannot be considered independently of the renormalisation of Φ_c^2 ($c \neq a$). The latter is a general feature of composite operator renormalisation. Note, however, that $\Phi_a\Phi_b$ ($a \neq b$) do not mix by renormalisation, i.e. they renormalise multiplicatively. It can be shown that composite operators mix under renormalisation only with those composite operators which have dimension less or equal [53, 65, 71].

Unfortunately, if we apply the previous arguments to $n = 0$, the result is not finite; another additional renormalisation must be performed. The fact that the expectation values of $[\ldots]$ are generally UV divergent, in spite of being finite for the composite Green's functions[6], can be nicely illustrated with the composite operator $[\Phi^2]$ in the $N = 1$ theory. Taking the diagrams for $D(0|0)$ and applying successively the (unrenormalised) Dyson–Schwinger equation [72] we get

---

[6] Also called the matrix elements of $[\ldots]$.

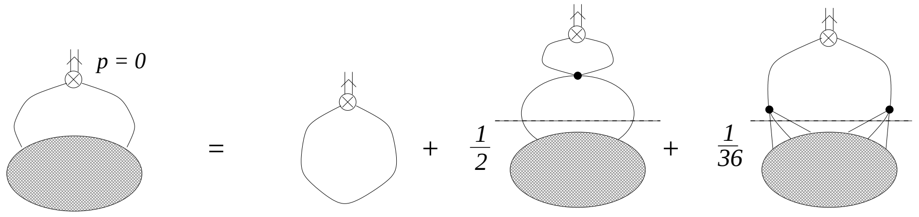

(3.25)

Eq.(3.25) might be rewritten as

$$
\begin{aligned}
D(0|0) \; = \; & D(0|0)|_{\lambda_r^0} \\
& + \frac{1}{2} \int \frac{d^D q_1}{(2\pi)^D} \frac{d^D q_2}{(2\pi)^D} \; \delta^D(q_1 + q_2) \; D^{amp}(q^2|0)|_{\lambda_r} \; D(q^2) \\
& + \frac{1}{36} \int \prod_{i=1}^{6} \frac{d^D q_i}{(2\pi)^D} \; \delta^D(\sum_{j=1}^{6} q_j) \; D^{amp}(q^6|0)|_{\lambda_r^2} \; D(q^6) \, , \qquad (3.26)
\end{aligned}
$$

where $D^{amp}(q^m|0)|_{\lambda_r^k}$ is the m–point amputated composite Green's function to order λ_r^k, and $D(q^m)$ is the full m–point Green's function. The crucial point is that we can write $D(0|0)$ as a sum of terms, which, apart from the first (free field) diagram, are factorised to the product of the composite Green's function with $n > 0$ and the full Green's function. (The factorisation is represented in (2.17) by the dashed lines.)

Now, utilising the counterterm renormalisation to the last two diagrams in (3.25) we get situation depicted in FIG.3.2. Terms inside of the parentheses are finite, this is because both the composite Green's functions ($n \geq 2$!) and the full Green's functions are finite after renormalisation. The counterterm diagrams, which appear on the RHS of the parentheses, precisely cancel the UV divergences coming from the loop integrations over momenta $q_1 \ldots q_i$ which must be finally performed. The heavy dots schematically indicates the corresponding counterterms. In the spirit of the counterterm renormalisation we should finally subtract the counterterm associated with the overall superficial divergence[7] related to the diagrams in question. But as we saw this is not necessary; individual counterterm diagrams (Zimmermann forests) mutually cancel their divergences leaving behind a finite result.

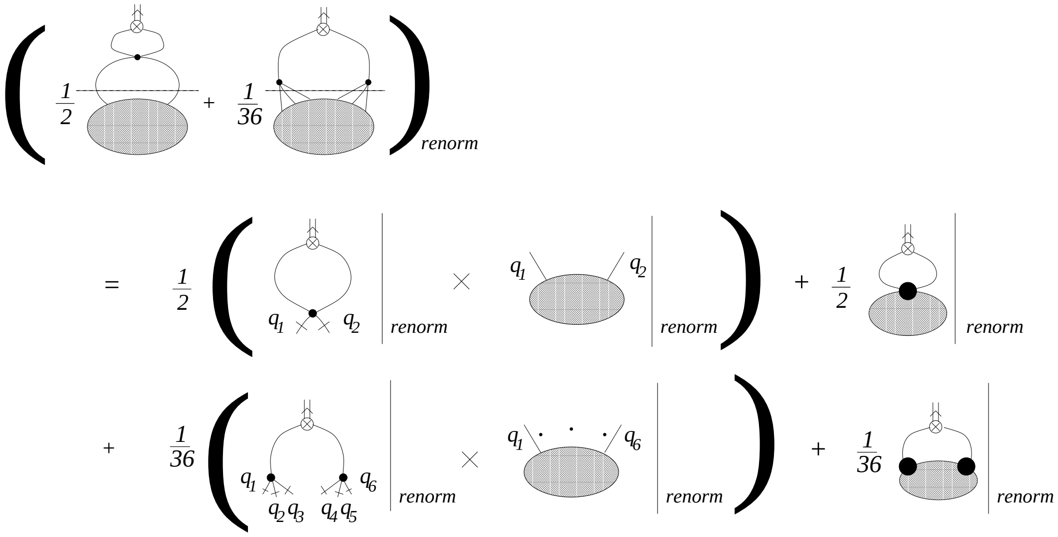

Figure 3.2: Counterterm renormalisation of the last two diagrams in Eq.(3.25). (Cut legs indicate amputations.)

So the only UV divergence in Eq.(3.25) which cannot be cured by existing counterterms is that coming from the first (i.e. free field or ring) diagram. The foregoing divergence is evidently temperature independent (to see that, simply use an explicit form of the free thermal propagator $\mathbb{D}_{11}$). Hence, if we define

---

[7] A simple power counting in the Φ^4 theory reveals [53] that for a composite operator A with dimension ω_A the superficial degree of divergence ω corresponding to an n-point diagram is $\omega = \omega_A - n$.

$$\langle \Phi^2 \rangle_{\text{renorm}} = \langle [\Phi^2] \rangle - \langle 0|[\Phi^2]|0 \rangle, \tag{3.27}$$

or, alternatively

$$\langle \Phi^2 \rangle_{\text{renorm}} = \langle [\Phi^2] \rangle - \langle [\Phi^2] \rangle|_{\text{free fields}}\,, \tag{3.28}$$

we get finite quantities, as desired. On the other hand, we should emphasise that

$$\langle \Phi^2 \rangle - \langle 0|\Phi^2|0 \rangle = Z_{\Phi^2} \left\{ \langle [\Phi^2] \rangle - \langle 0|[\Phi^2]|0 \rangle \right\} \neq \text{finite in } D{=}4\,. \tag{3.29}$$

An extension of the previous reasonings to any $N > 1$ is straightforward, only difference is that we must deal with operator mixing which makes (3.27) and (3.28) less trivial.

The important lesson which we have learnt here is that the naive "double dotted" normal product (i.e. subtraction of the vacuum expectation value from a given operator) does not generally give a finite result. The former is perfectly suited for the free theory ($Z_{\Sigma\Phi^2} = 1$) but in the interacting case we must resort to the prescription (3.27) or (3.28) instead.

Renormalisation of the energy–momentum tensor

In order to calculate the hydrostatic pressure, we need to find such $\langle \Theta_c^{\mu\nu} \rangle|_{\text{renorm}}$ which apart from being finite is also consistent with our derivation of the hydrostatic pressure performed in the introductory section. In view of the previous treatment, we cannot, however, expect that $\Theta_c^{\mu\nu}$ will be renormalised multiplicatively. Instead new terms with a different structure than $\Theta_c^{\mu\nu}$ itself will be generated during renormalisation. The latter must add up to $\Theta_c^{\mu\nu}$ in order to render $D^{\mu\nu}(x^n|y)$ finite[8].

---

[8] In fact it can be shown [36, 65] that the Noether currents corresponding to a given internal symmetry are renormalised, i.e $J^a = [J^a]$, however, this is not the case for the Noether currents corresponding to external symmetries (like $\Theta_c^{\mu\nu}$ is).

Now, the key ingredient exploited in Eq.(3.5) is the conservation law (continuity equation). It is well known that one can 'modify' $\Theta_c^{\mu\nu}$ in such a way that the new tensor $\Theta^{\mu\nu}$ preserves the convergence properties of $\Theta_c^{\mu\nu}$. Such a modification (the Pauli transformation) reads

$$\begin{aligned}\Theta^{\mu\nu} &= \Theta_C^{\mu\nu} + \partial_\lambda X^{\lambda\mu\nu} \\ X^{\lambda\mu\nu} &= -X^{\mu\lambda\nu}\,. \end{aligned} \tag{3.30}$$

For scalar fields, (3.30) is the only transformation which neither changes the divergence properties of $\Theta_c^{\mu\nu}$ nor the generators of the Poincare group constructed out of $\Theta_c^{\mu\nu}$ [36,53,63, 68]. Because the renormalised (or improved) energy momentum tensor must be conserved (otherwise theory would be anomalous), it has to mix with $\Theta_c^{\mu\nu}$ under renormalisation only via the Pauli transformation, i.e.

$$[\Theta_c^{\mu\nu}] = \Theta_c^{\mu\nu} + \partial_\lambda X^{\lambda\mu\nu}\,. \tag{3.31}$$

In order to determine $X^{\lambda\mu\nu}$, we should realize that its role is to cancel divergences present in $\Theta_c^{\mu\nu}$. Such a cancellation can be, however, performed only by means of composite operators which are even in the number of fields (note that $\Theta_c^{\mu\nu}$ is even in fields and Green's functions with the odd number of fields vanish). Recalling the condition that renormalisation can mix only operators with dimension less or equal, we see that the dimension of $X^{\lambda\mu\nu}$ must be $D-1$, and that $X^{\lambda\mu\nu}$ must be quadratic in fields. The only possible form which is compatible with tensorial structure (3.30) is then

$$X^{\lambda\mu\nu} = \sum_{a,b=1}^{N} c_{ab}(\lambda_r; D)\ \left(\partial^\mu g^{\lambda\nu} - \partial^\lambda g^{\mu\nu}\right)\ \Phi_a \Phi_b\,. \tag{3.32}$$

From the fact that both $\Theta_c^{\mu\nu}$ and $[\Theta_c^{\mu\nu}]$ are $O(N)$ invariant (see Eq.(3.10)), $\partial_\lambda X^{\lambda\mu\nu}$ must be also $O(N)$ invariant, so $c_{ab} = \delta_{ab} c$. Thus, finally we can write

$$[\Theta_c^{\mu\nu}] = \Theta_c^{\mu\nu} + c(\lambda_r; D) \sum_{a=1}^{N} \left(\partial^\mu \partial^\nu - g^{\mu\nu} \partial^2\right) \Phi_a^2 \, , \tag{3.33}$$

with $c = c_0 + \sum(\text{poles})$, here c_0 is analytic in D. Structure of $c(\lambda_r; D)$ could be further determined, similarly as in the $N = 1$ theory, employing a renormalisation group equation [66]. We do not intend to do that as the detailed structure of c will show totally irrelevant for the following discussion, however, it turns out to be important in non-equilibrium case.

Now, similarly as before, $[\Theta_c^{\mu\nu}]$ gives the finite composite Green's functions if $n > 0$ but the expectation value $\langle [\Theta_c^{\mu\nu}] \rangle$ is divergent (discussion for the $N = 1$ theory can be found in Brown [66]). The unrenormalised Dyson–Schwinger equation for $D^{\mu\nu}(0|0)$ reads

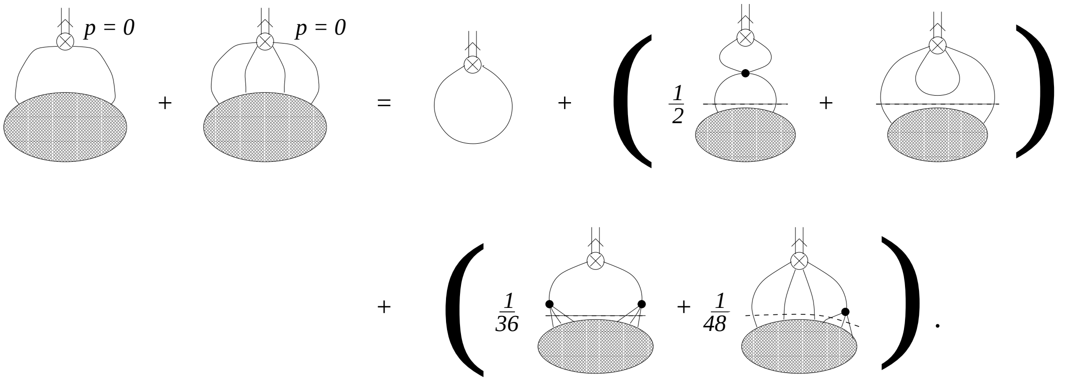

(3.34)

The structure of the composite vertices in (3.34) is that described at the beginning of this section. Note that the amputated composite Green's functions in individual parentheses are of the same order in λ_r. Performing the counterterm renormalisation as in the case of

$\langle[\Phi^2]\rangle$, we factorise the graphs inside of parentheses into the product of the renormalised 2– (and 6–) point composite Green's function and the renormalised full 2– (and 6–) point Green's function. The latter are finite. The UV divergences arisen during the integrations over momenta connecting both composite and full Green's functions are precisely cancelled by the remaining counterterm diagrams. The only divergence comes from the free–field contribution, more precisely from the $T = 0$ ring diagram. Defining

$$\langle\Theta_c^{\mu\nu}\rangle|_{\mathrm{renorm}} = \langle[\Theta_c^{\mu\nu}]\rangle - \langle 0|[\Theta_c^{\mu\nu}]|0\rangle, \tag{3.35}$$

or

$$\langle\Theta_c^{\mu\nu}\rangle|_{\mathrm{renorm}} = \langle[\Theta_c^{\mu\nu}]\rangle - \langle[\Theta_c^{\mu\nu}]\rangle|_{\text{free field}}, \tag{3.36}$$

we get the finite expressions. Note that the conservation law is manifest in both cases. In equilibrium (and in $T = 0$) we can, due to space–time translational invariance of $\langle\ldots\rangle$, write

$$\langle[\Theta_c^{\mu\nu}]\rangle = \langle\Theta_c^{\mu\nu}\rangle + \partial_\lambda\langle X^{\lambda\mu\nu}\rangle = \langle\Theta_c^{\mu\nu}\rangle\,. \tag{3.37}$$

Using (3.35) or (3.36) we get either the thermal interaction pressure or the interaction pressure, respectively. This can be explicitly written as

$$\mathcal{P}_{\mathrm{th.int.}}(T) = \mathcal{P}(T) - \mathcal{P}(0) = -\frac{1}{(D-1)}\sum_{i=1}^{D-1}\left\{\langle\Theta_{c\,i}^{i}\rangle - \langle 0|\Theta_{c\,i}^{i}|0\rangle\right\}, \tag{3.38}$$

or

$$\mathcal{P}_{\mathrm{int.}}(T) = \mathcal{P}(T) - \mathcal{P}_{\text{free field}}(T) = -\frac{1}{(D-1)}\sum_{i=1}^{D-1}\left\{\langle\Theta_{c\,i}^{i}\rangle - \langle\Theta_{c\,i}^{i}\rangle|_{\text{free field}}\right\}\,. \tag{3.39}$$

In order to keep connection with calculations done by Drummond *et al.* in [61] we shall in the sequel deal with the thermal interaction pressure only. If instead of an equilibrium, a non–equilibrium medium would be in question, translational invariance of $\langle \ldots \rangle$ might be lost, in that case either prescription (3.35) or (3.36) is obligatory, and consequently $c(\lambda_r; D)$ in (3.33) must be further specified.

3.3 Hydrostatic pressure

In the previous Section we have prepared ground for a hydrostatic pressure calculations in the $O(N)$ Φ^4 theory. In this section we aim to apply the previous results to the massive $O(N)$ Φ^4 theory in the large–N limit. Anticipating an out of equilibrium application, we shall use the real–time formalism even if the imaginary–time one is more natural in the equilibrium context. As we aim to evaluate the hydrostatic pressure in 4 dimensions, we use here, similarly as in the previous section, the usual dimensional regularisation to regulate the theory (i.e. here and throughout we keep D slightly away from the physical value $D = 4$).

Let us start first with some essentials of our model system at finite temperature.

3.3.1 Mass renormalisation

In the Dyson multiplicative renormalisation the fact that the complete propagator has a pole at the physical mass leads to the usual mass renormalisation prescription [53]:

$$m_r^2 = m_0^2 + \Sigma(m_r^2)\,, \tag{3.40}$$

where m_r is renormalised mass and $\Sigma(m_r^2)$ is the proper self–energy evaluated at the mass shell; $p^2 = m_r^2$. In fact, Eq.(3.40) is nothing but the statement that 2–point vertex function

$\Gamma_r^{(2)}$ evaluated at the mass–shell must vanish. The Dyson–Schwinger equations corresponding to the proper self–energies read [72–75]:

$$\Sigma^{aa} = \frac{1}{2}\sum_{b=1}^{N}$$

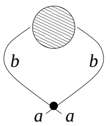

$$+$$

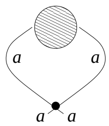

$$+\frac{i}{2}\sum_{b=1}^{N} \qquad (3.41)$$

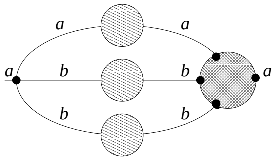

$$\Sigma^{ac}|_{a\neq c} = 0 \quad ; \qquad \times \sim \lambda_o/N$$

where hatched blobs represent 2–point connected Green's functions whilst cross-hatched blobs represent proper vertices $\Gamma_r^{(4)}$ (i.e. 1PI 4–point Green's functions). As Σ^{aa} are the same for all a, we shall simplify notation and write Σ instead. In the sequel the following convention is accepted:

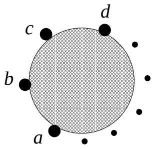

$$= \Gamma_r^{(n)\;abcd\ldots}$$

Note that the second term in (3.41) does not contribute in the large–N limit. It is easy to see that the third term does not contribute either. This is because each hatched blob behaves at most as N^0 whilst $\Gamma^{(4)}$ goes maximally[9] as N^{-1} . Consequently, various contributions from the first graph in (3.41) contribute at most N^0, whereas in the second graph the contributions contribute up to order N^{-1}. So the first diagram dominates, provided we retain only such 2–point connected Green's functions which are proportional to N^0 (as mentioned in the footnote, these are comprised only of 'tadpole' loops.). After neglecting the 'setting sun' graph, Eg.(3.41) generates upon iterating the so called superdaisy diagrams [61, 73, 76].

---

[9] In the Φ^4 theory there is a simple relation between the number of loops (L), vertices (V) and external lines (E); $4V = 2I + E$. Together with the Euler relation for connected graphs; $L = I - V + 1$ (here I is the number of internal lines), we have $L - V = \frac{2-E}{2}$. As each loop carries maximally a factor of N (this is saturated only for 'tadpole' loops) and each vertex carries a factor of N^{-1}, the overall blob contribution behaves at most as $N^{L-V} = N^{\frac{2-E}{2}}$.

Let us now define $\Sigma(m_r^2) = \lambda_0 \, \mathcal{M}(m_r^2)$. Because the 'tadpole' diagram in (3.2) can be easily resumed we observe that

$$\mathcal{M}(m_r^2) = \frac{1}{2}\int \frac{d^Dq}{(2\pi)^D}\,\frac{i}{q^2 - m_0^2 - \Sigma(m_r^2) + i\epsilon} = \frac{1}{2}\int \frac{d^Dq}{(2\pi)^D}\,\frac{i}{q^2 - m_r^2 + i\epsilon}\,, \tag{3.42}$$

hence we see that Σ is external–momentum independent. So if we had started with the renormalisation prescription: $i\Gamma_r^{(2)}(p^2 = 0) = -m_r^2$, we would arrived at (3.40) as well (this is not the case for $N = 1$!).

At finite temperature the strategy is analogous. Due to a doubling of degrees of freedom, the full propagator is a 2×2 matrix. The latter satisfies, similarly as at $T = 0$, Dyson's equation

$$\mathbb{D} = \mathbb{D}_F + \mathbb{D}_F\,(-i\mathbf{\Sigma})\,\mathbb{D}\,. \tag{3.43}$$

An important point is that there exists a real, non–singular matrix $\mathbb{M}$ (Bogoliubov matrix) [34, 36, 38] having a property that

$$\mathbb{D}_F = \mathbb{M}\begin{pmatrix} i\Delta_F & 0 \\ 0 & -i\Delta_F^* \end{pmatrix}\mathbb{M}\,. \tag{3.44}$$

Here Δ_F is the standard Feynman propagator and '*' denotes the complex conjugation. Consequently, the full matrix propagator may be written as

$$\mathbb{D} = \mathbb{M} \begin{pmatrix} \frac{i}{p^2 - m_0^2 - \Sigma_T + i\epsilon} & 0 \\ 0 & \frac{-i}{p^2 - m_0^2 - \Sigma_T^* - i\epsilon} \end{pmatrix} \mathbb{M}\,. \tag{3.45}$$

Similarly as in many body systems, the position of the (real) pole of $\mathbb{D}$ in p^2 fixes the temperature–dependent effective mass $m_r(T)$ [34, 41]. The latter is determined by the equation

$$m_r^2(T) = m_0^2 + \mathrm{Re}\left(\Sigma_T(m_r^2(T))\right)\ . \tag{3.46}$$

From the explicit form of $\mathbb{M}$ it is possible to show [34, 36] that $\mathrm{Re}\boldsymbol{\Sigma}_{11} = \mathrm{Re}\Sigma_T$. As before, the structure of the proper self–energy can be deduced from the corresponding Dyson–Schwinger equation. Following the usual real–time formalism convention (type–1 vertex $\sim -i\lambda_0$, type–2 vertex $\sim i\lambda_0$), the former reads:

$-i\boldsymbol{\Sigma}_{11} =$

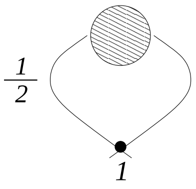

$;\ -i\boldsymbol{\Sigma}_{22} =$

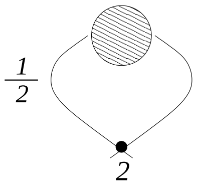

(3.47)

where

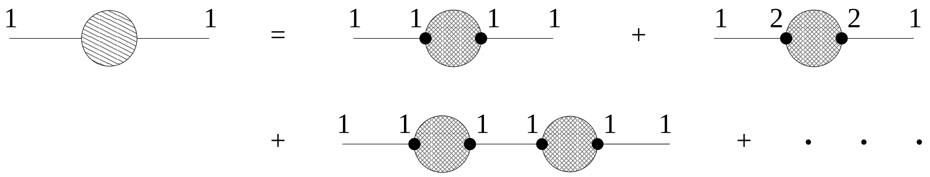

and similarly for $\mathbb{D}_{22}$. In (4.49) we have omitted diagrams which are of order $\mathcal{O}(1/N)$ or less.

Note that the fact that no ‘setting sun’ diagrams are present implies that the off–diagonal elements of $\mathbf{\Sigma}$ are zero. Inspection of Eq.(3.47) reveals that

$$\mathbf{\Sigma}_{11} = \frac{\lambda_0}{2} \int \frac{d^D q}{(2\pi)^D}\, \mathbb{D}_{11}(q;T) \quad \text{and} \quad \mathbf{\Sigma}_{22} = -\frac{\lambda_0}{2} \int \frac{d^D q}{(2\pi)^D}\, \mathbb{D}_{22}(q;T)\,. \tag{3.48}$$

It directly follows from Eq.(3.48) that both $\mathbf{\Sigma}_{11}$ and $\mathbf{\Sigma}_{22}$ are external–momentum independent and real[10]. If we define $\Sigma_T(m_r^2(T)) = \lambda_0\ \mathcal{M}_T(m_r^2(T))$, then Eq.(3.46) through Eq.(3.48) implies that

$$m_r^2(T) = m_0^2 + \lambda_0\, \mathcal{M}_T(m_r^2(T))\,. \tag{3.49}$$

A resumed version of $\mathbb{D}_{11}$ is easily obtainable from (3.45) [34, 36] and consequently (3.48) yields

$$\begin{aligned} \mathcal{M}_T(m_r^2(T)) &= \frac{1}{2} \int \frac{d^D q}{(2\pi)^D} \left\{ \frac{i}{q^2 - m_r^2(T) + i\epsilon} \ +\ (4\pi)\, \delta^+(q^2 - m_r^2(T))\, \frac{1}{e^{q_0\beta} - 1} \right\} \\ &= -\int \frac{d^D q}{(2\pi)^D}\, \frac{\varepsilon(q_0)}{e^{q_0\beta} - 1}\, \mathrm{Im} \frac{1}{q^2 - m_r^2(T) + i\epsilon}\,. \end{aligned} \tag{3.50}$$

Let us remark that (3.50) is manifestly independent of any particular real–time formalism version. This is because the various real–time formalisms [34, 36] differ only in the off–diagonal elements of $\mathbb{D}$.

In passing it may be mentioned that because $\mathbf{\Sigma}_{11}(m_r^2)$ is momentum independent, the wave function renormalisation $Z_\Phi = 1$. (The Källen–Lehmann representation requires the renormalised propagator to have a pole of residue i at $p^2 = m_r^2$. The former in turn implies that $Z_\Phi = (1 - \mathbf{\Sigma}'_{11}(p^2)|_{p^2=m_r^2})^{-1} = 1$.) Trivial consequence of the foregoing fact is that $\Gamma_r^{(2)} = \Gamma^{(2)}$ and $\Gamma_r^{(4)} = \Gamma^{(4)}$.

---

[10] Reality of $\mathbf{\Sigma}_{11}$ can be perhaps most easily seen from the largest–time equation. The LTE states that $\mathbf{\Sigma}_{11} + \mathbf{\Sigma}_{22} + \mathbf{\Sigma}_{12} + \mathbf{\Sigma}_{21} = 0$. Because no ‘setting sun’ graphs are present, $\mathbf{\Sigma}_{12} + \mathbf{\Sigma}_{21} = 0$, on the other hand $\mathbf{\Sigma}_{11} + \mathbf{\Sigma}_{22} = 2i\mathrm{Im}\mathbf{\Sigma}_{11}$ (see (3.44)).

3.3.2 Coupling constant renormalisation

Let us choose the coupling constant to be defined at $T = 0$. This will have the advantage that the high temperature expansion of the pressure (see Section 3.4) will become more transparent. In addition, such a choice allows us to stay on a safe ground as the renormalisation of the coupling constant at finite temperature is rather delicate [73].

By assumption the fields Φ_a have non–vanishing masses, so we can safely choose the renormalisation prescription for λ_r at $s = 0$ (s is the standard Mandelstam variable). For example, one may require that for the scattering $aa \rightarrow bb$

$$\Gamma^{(4)\; aabb}(s=0) = -\lambda_r/N, \qquad (b \neq a)\,. \tag{3.51}$$

The formula (3.51) clearly agrees with the tree level value $\Gamma^{(4)\; aabb}_{tree}(s=0) = -\lambda_0/N$. Let us also mention that Ward's identities corresponding to the internal $O(N)$ symmetry enforce $\Gamma^{(4)\; aaaa}$ to obey the constraint[11]

$$\begin{aligned}\Gamma^{(4)\; aaaa}(p_1;p_2;p_3;p_4) &= \Gamma^{(4)\; bbaa}(p_1;p_2;p_3;p_4) + \Gamma^{(4)\; baba}(p_1;p_2;p_3;p_4) \\ &+ \Gamma^{(4)\; baab}(p_1;p_2;p_3;p_4)\,,\end{aligned} \tag{3.52}$$

---

[11] Actually, Ward's identities read [42, 72] $\int d^Dx \, \frac{\delta\Gamma[\phi]}{\delta\phi_a(x)} \, \phi_b(x) = \int d^Dx \, \frac{\delta\Gamma[\phi]}{\delta\phi_b(x)} \, \phi_a(x)$ (here $\phi_a = \frac{\delta W}{\delta J_a}$; W is the generating functional of connected Green's functions). Performing successive variations with respect to $\phi_a(v), \phi_a(z), \phi_a(y)$ and $\phi_b(w)$, taking the Fourier transform, and setting the physical condition $\phi_c = 0$, we get directly (3.52).

for any $b \neq a$. The structure of $\Gamma^{(4)}$ is encoded in the Dyson–Schwinger equation which reads [53, 72]:

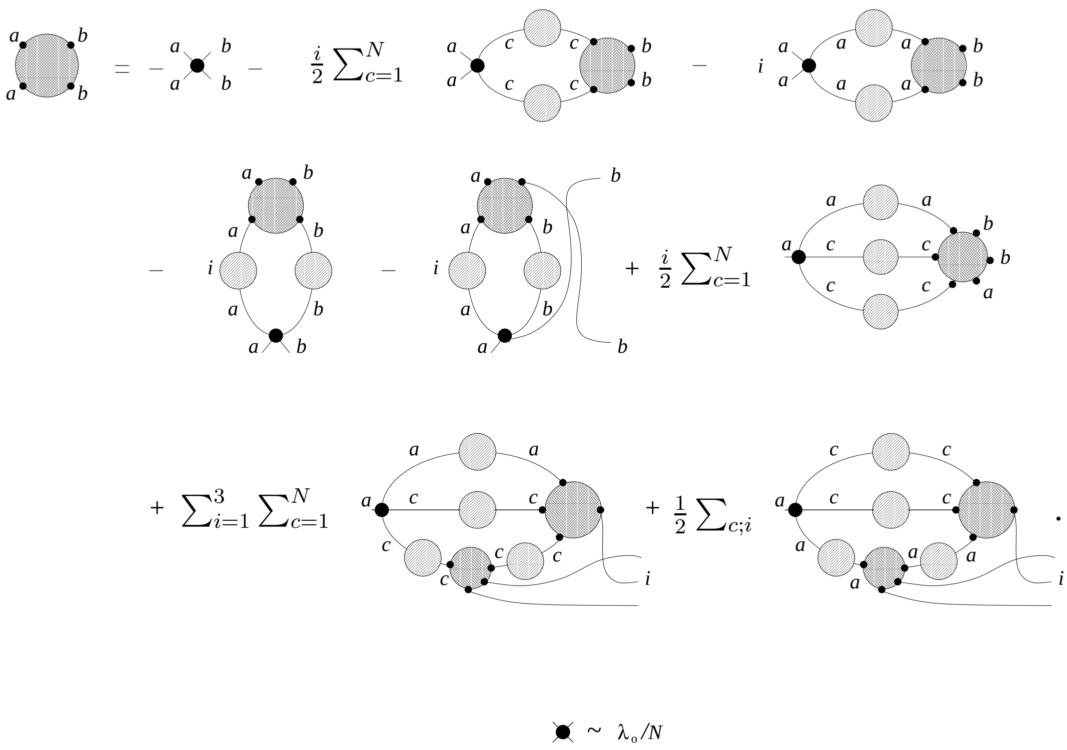
=
−
−
$\frac{i}{2}\sum_{c=1}^{N}$
−
i
−
i
−
i
+
$\frac{i}{2}\sum_{c=1}^{N}$
+
$\sum_{i=1}^{3}\sum_{c=1}^{N}$
+
$\frac{1}{2}\sum_{c;i}$
.
$\sim \lambda_{\circ}/N$

(3.53)

The sum $\sum_{i=1}^{3}$ schematically represents a summation over various scattering channels. Similarly as before, we can argue that the last three graphs contribute at most N^{-2}, whilst the second ('fish') graph may contribute up to order N^{-1}. So in the large–N limit the last three diagrams may be neglected, provided we keep in the 4–point vertex function only graphs proportional to N^{-1}. However, the former can be only fulfilled if we retain such a 'fish' graph where summation over internal index on the loop is allowed. Remaining 'fish' graphs (describing t and u scattering channel interactions) are suppressed by the factor

N^{-1} as the internal index on the loop is fixed. In this way we are left with the relation

$$\begin{aligned}
&\Gamma^{(4)\,aabb}(s=0) \\
&\quad = -\frac{\lambda_0}{N} - \frac{i\lambda_0}{2N}\sum_{c\neq b}\int \frac{d^Dq}{(2\pi)^D}\,\Gamma^{(4)\,bbcc}(s)\,\frac{i}{(q^2-m_r^2+i\epsilon)}\,\frac{i}{((q-Q)^2-m_r^2+i\epsilon)}\Bigg|_{s=0} \\
&\quad = -\frac{\lambda_0}{N} - \frac{\lambda_0\lambda_r(N-1)}{2N^2}\int_0^1 dx \int \frac{d^Dq}{(2\pi)^D}\;\frac{i}{(q^2-m_r^2+x(1-x)s+i\epsilon)^2}\Bigg|_{s=0}\,,
\end{aligned} \tag{3.54}$$

with $Q = p_1 + p_2$ and $s = Q^2$, p_1, p_2 are the external momenta. To leading order in $1/N$ we may equivalently write

$$\lambda_r = \lambda_0 + \lambda_0\lambda_r\,\mathcal{M}'(m_r^2)\,, \tag{3.55}$$

the prime means differentiation with respect to m_r^2; $\mathcal{M}(m_r^2)$ is defined by (3.42). Evaluating explicitly $\mathcal{M}'(m_r^2)$, we get from (3.55)

$$\lambda_0 = \frac{\lambda_r}{1 - \lambda_r\Gamma(2-\frac{D}{2})\,(m_r)^{D-4}/2\,(4\pi)^{\frac{D}{2}}}\,. \tag{3.56}$$

Assuming that both $\lambda_0 \geq 0$ and $\lambda_r \geq 0$, we can infer from (3.56) that

$$0 \geq \lambda_r \geq \frac{2(4\pi)^{\frac{D}{2}}(m_r)^{4-D}}{\Gamma(2-\frac{D}{2})}\,, \tag{3.57}$$

so for $D = 4$ we inevitably get that $\lambda_r = 0$. The latter indicates that the theory is trivial [42, 61, 77], or, in other words, the $O(N)$ Φ^4 theory is a renormalised free theory in the large–N limit. This conclusion is also consistent with the observation that the theory does not posses any non–trivial UV fixed point in the large–N limit [42, 77].

On the other hand, if we were assuming that $\lambda_0 < 0$, we would get a non–trivial renormalised field theory in $D = 4$ (actually, from (3.56) we see that $\lambda_0 \to 0_-$, provided that λ_r is fixed and positive and $D \to 4_-$). However, as it was pointed out in refs. [42,61,77,78], such a theory is intrinsically unstable as the ground–state energy is unbounded from below. This is reflected, for instance, in the existence of tachyons in the theory [61,77,78], therefore the case with negative λ_0 is clearly inconsistent.

The straightforward remedy for this situation was suggested by Bardeen and Moshe [77]. They showed that the only meaningful (stable) $O(N)$ Φ^4 theory in the large–N limit is that with $\lambda_r, \lambda_0 \geq 0$. This is provided that we view it as an effective field theory at momenta scale small compared to a fixed UV cut–off Λ. The cut–off itself is further determined by (3.55) because in that case (assuming $m_r \ll \Lambda$)

$$\lambda_0 = \frac{\lambda_r}{1 - \frac{\lambda_r}{32\pi^2}\ln(\frac{\Lambda^2}{m_r^2})}\,, \tag{3.58}$$

which implies that for $\lambda_r, \lambda_0 \geq 0$ we have $\Lambda^2 < m_r^2 \exp(\frac{32\pi^2}{\lambda_r})$. The case $\Lambda^2 = m_r^2 \exp(\frac{32\pi^2}{\lambda_r})$ corresponds to the Landau ghost [79] (tachyon pole [61,77]). For reasonably small λ_r, Λ is truly huge[12] and so it does not represent any significant restriction. The following discussion will be confined to such an effective theory.

3.3.3 The pressure

The partition function Z has a well known path–integral representation at finite temperature, namely

---

[12] For example, if $\lambda_r = 1$ and $m_r \approx 100$MeV, we get $\Lambda < 10^{141}$MeV or equivalently $\Lambda < 10^{131}$K (this is far beyond the Planck temperature - 10^{32}K).

$$
\begin{aligned}
Z[T] &= \exp(\mathfrak{M}[T]) = \int \mathcal{D}\phi \, \exp(iS[\phi;T]) \\
S[\phi;T] &= \int_C d^D x \, \mathcal{L}(x) \, .
\end{aligned}
\tag{3.59}
$$

Here $\mathfrak{M} = -\beta\Omega$ is the so called Massieu function [28, 36] and $\int_C d^D x = \int_C dx_0 \int_V d^{D-1}\mathbf{x}$ with the subscript C suggesting that the time runs along some contour in the complex plane. In the real–time formalism, which we adopt throughout, the most natural version is the so called Keldysh–Schwinger one [34, 36], which is represented by contour in FIG.3.3

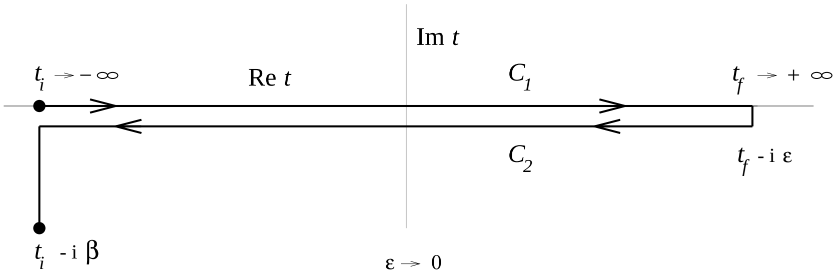

Figure 3.3: The Keldysh–Schwinger time path.

Let us mention that the fields within the path–integral (3.59) are further restricted by the periodic boundary condition (KMS condition) [34, 36, 38] which in our case reads:

$$
\phi_a(t_i - i\beta, \mathbf{x}) = \phi_a(t_i, \mathbf{x}) \, .
$$

As explained in Section 3.2, we can use for a pressure calculation the canonical energy–momentum tensor $\Theta_c^{\mu\nu}$. Employing for $\Theta_c^{\mu\nu}(x)$ its explicit form (3.10) together with (3.14), one may write

$$\langle \Theta_c^{\mu\nu} \rangle = \frac{N}{2} \int \frac{d^Dq}{(2\pi)^D} (2q^\mu q^\nu - g^{\mu\nu}(q^2 - m_0^2))\, \mathbb{D}_{11}(q;T) \; + \frac{\lambda_0}{8N} g^{\mu\nu} \left\langle \left(\sum_{a=1}^{N} \phi_a^2(0) \right)^2 \right\rangle \,, \tag{3.60}$$

where $\mathbb{D}_{11}$ is the Dyson–resumed thermal propagator [34, 36], i.e.

$$\mathbb{D}_{11}(q;T) = \frac{i}{q^2 - m_r^2(T) + i\epsilon} \; + (2\pi)\, \delta(q^2 - m_r^2(T))\, \frac{1}{e^{|q_0|\beta} - 1} \,. \tag{3.61}$$

Note that we have exploited in (3.60) the fact that the expectation value of $\Theta_c^{\mu\nu}(x)$ is x independent. On the other hand, in (3.61) we have used the fact that m_r^2 is q independent. In order to calculate the expectation value of the quartic term in Eq.(3.60), let us observe (c.f. (3.59)) that the derivative of $\mathfrak{M}$ with respect to the bare coupling λ_0 (taken at fixed m_0) gives

$$\frac{\partial \mathfrak{M}[T]}{\partial \lambda_0} = -\frac{i}{8\, N} \int_C d^Dx \left\langle \left(\sum_{a=1}^{N} \Phi_a^2(0) \right)^2 \right\rangle \,, \tag{3.62}$$

which implies that

$$\left\langle \left(\sum_{a=1}^{N} \Phi_a^2(0) \right)^2 \right\rangle = -\frac{N8}{\beta V}\, \frac{\partial \mathfrak{M}[T]}{\partial \lambda_0} \,. \tag{3.63}$$

The key point now is that we can calculate $\mathfrak{M}[T]$ in a non–perturbative form. (The latter is based on the fact that we know the Dyson–resumed propagator $\mathbb{D}_{11}(q;T)$ (see (3.61).) Indeed, taking derivative of $\mathfrak{M}$ with respect to m_0^2 (keeping λ_0 fixed) we obtain

$$\frac{\partial \mathfrak{M}[T]}{\partial m_0^2} \;=\; -\frac{iN}{2} \int_C d^Dx \, \langle \phi^2(0) \rangle = -\frac{\beta V N}{2} \int \frac{d^Dq}{(2\pi)^D}\, \mathbb{D}_{11}(q;T)$$

$$= \quad -\beta V N \, \mathcal{M}_T(m_r^2(T)) \, , \tag{3.64}$$

thus

$$\mathfrak{M}[T;\lambda_0;m_0^2] = \beta V N \int_{m_0^2}^{\infty} d\hat{m}_0^2 \, \mathcal{M}_T(\hat{m}_r^2(T)) \quad + \mathfrak{M}[T;\lambda_0;\infty] \, . \tag{3.65}$$

Let us note that $\mathfrak{M}[T;\lambda_0;\infty]$ is actually zero[13] because $\mathfrak{M}[T;\lambda_0;m_0^2]$ has the standard loop expansion [36, 72] depicted in FIG.3.4.

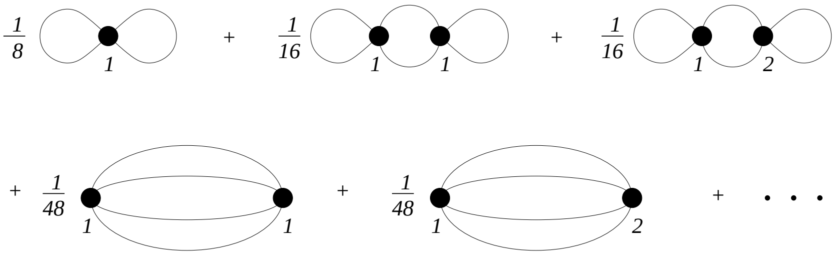

Figure 3.4: First few bubble diagrams in the $\mathfrak{M}$ expansion.

It is worth mentioning that in the previous expansion one must always have at least one type–1 vertex [36]. The RHS of FIG.3.4 clearly tends to zero for $m_0 \to \infty$ as all the (free) thermal propagators from which the individual diagrams are constructed tend to zero in this limit. The former result can be also deduced from the CJT effective action formalism [76] or from a heuristic argumentation based on a thermodynamic pressure [61]. Note that in the large–N limit the fourth and fifth diagrams in FIG.3.4 must be omitted.

The expectation value (3.63) can be now explicitly written as

---

[13] To be precise, we should also include in FIG.3.4 an (infinite) circle diagram corresponding to the free pressure [36, 73]. However the later is λ_0 independent (although m_0 dependent) and so it is irrelevant for the successive discussion (c.f. Eq.(3.63)).

$$\left\langle \left(\sum_{a=1}^{N} \Phi_a^2(0) \right)^2 \right\rangle = 8N^2 \int_{m_0^2}^{\infty} d\hat{m}_0^2 \int \frac{d^Dq}{(2\pi)^D} \frac{\varepsilon(q_0)}{e^{q_0\beta}-1} \, \mathrm{Im} \left(\frac{\frac{\partial \Sigma_T(\hat{m}_r^2(T))}{\partial \lambda_0}}{(q^2 - \hat{m}_r^2 + i\epsilon)^2} \right) . \tag{3.66}$$

In fact, the differentiation of the proper self–energy in (3.66) can be carried out easily. Using (3.49), we get

$$\frac{\partial \Sigma_T}{\partial \lambda_0} = \frac{\Sigma_T}{\lambda_0} + \lambda_0 \mathcal{M}_T' \frac{\partial \Sigma_T}{\partial \lambda_0} \quad \Rightarrow \quad \frac{\partial \Sigma_T}{\partial \lambda_0} = \frac{\Sigma_T}{\lambda_0 (1 - \lambda_0 \mathcal{M}_T')} \, .$$

From Eq.(3.49) it directly follows that

$$\frac{dm_r^2(T)}{dm_0^2} = \frac{1}{(1 - \lambda_0 \, \mathcal{M}_T')} \, ,$$

which, together with the definition of $\mathcal{M}_T$, gives

$$\begin{aligned} \left\langle \left(\sum_{a=1}^{N} \Phi_a^2(0) \right)^2 \right\rangle &= 8N^2 \int_{m_r^2(T)}^{\infty} d\hat{m}_r^2 \int \frac{d^Dq}{(2\pi)^D} \frac{\varepsilon(q_0)}{e^{q_0\beta}-1} \, \mathrm{Im} \frac{\mathcal{M}_T(\hat{m}_r^2)}{(q^2 - \hat{m}_r^2 + i\epsilon)^2} \\ &= -\, 8N^2 \int_{m_r^2(T)}^{\infty} d\hat{m}_r^2 \, \mathcal{M}_T(\hat{m}_r^2) \, \frac{\partial \mathcal{M}_T(\hat{m}_r^2)}{\partial \hat{m}_r^2} \\ &= 4N^2 \, \mathcal{M}_T^2(m_r^2(T)) \, , \end{aligned} \tag{3.67}$$

where we have exploited in the last line the fact that $\mathcal{M}_T^2(m_r^2 \to \infty) = 0$. Let us mention that the crucial point in the previous manipulations was that m_r is both real and momentum independent. Collecting our results together, we can write for the hydrostatic pressure per particle (cf. Eq.(3.38))

$$\begin{aligned}
\mathcal{P}(T)-\mathcal{P}(0) &= -\frac{1}{(D-1)N}\ \left(\langle\Theta_{c\,i}^{i}\rangle-\langle 0|\Theta_{c\,i}^{i}|0\rangle\right)\\
&= +\frac{1}{2}\int\frac{d^Dq}{(2\pi)^{D-1}}\left(\frac{2\mathbf{q}^2}{(D-1)}\right)\frac{\varepsilon(q_0)}{e^{q_0\beta}-1}\,\delta(q^2-m_r^2(T))\\
&\quad -\frac{1}{2}\int\frac{d^Dq}{(2\pi)^{D-1}}\left(\frac{2\mathbf{q}^2}{(D-1)}\right)\delta^{+}(q^2-m_r^2(0))\\
&\quad +\frac{1}{2\lambda_0}\left(\Sigma_T^2(m_r^2(T))-\Sigma^2(m_r^2(0))\right)\ . \qquad (3.68)
\end{aligned}$$

Applying the Green theorem to the last two integrals and eliminating the surface terms (for details see Appendix B) we find

$$\begin{aligned}
\mathcal{P}(T)-\mathcal{P}(0) &= \frac{1}{2}\int\frac{d^Dq}{(2\pi)^{D-1}}\,\frac{\varepsilon(q_0)}{e^{q_0\beta}-1}\,\theta(q^2-m_r^2(T))\\
&\quad -\frac{1}{2}\int\frac{d^Dq}{(2\pi)^{D-1}}\,\theta(q_0)\,\theta(q^2-m_r^2(0))\\
&\quad +\frac{1}{2\lambda_0}\left(\Sigma_T^2(m_r^2(T))-\Sigma^2(m_r^2(0))\right)
\end{aligned}$$

$$= \quad \mathcal{N}_T(m_r^2(T))-\mathcal{N}(m_r^2(0))+\frac{1}{2\lambda_0}\left(\Sigma_T^2(m_r^2(T))-\Sigma^2(m_r^2(0))\right)\ , \qquad (3.69)$$

where we have introduced new functions $\mathcal{N}_T(m_r^2(T)$ and $\mathcal{N}(m_r^2)$;

$$\begin{aligned}
\mathcal{N}_T(m_r^2(T)) &= \frac{1}{2}\int\frac{d^Dq}{(2\pi)^{D-1}}\,\frac{\varepsilon(q_0)}{e^{q_0\beta}-1}\,\theta(q^2-m_r^2(T))\\
\mathcal{N}(m_r^2) &= \lim_{T\to 0}\mathcal{N}_T(m_r^2(T))\,. \qquad (3.70)
\end{aligned}$$

Eq.(3.69) can be rephrased into a form which exhibits an explicit independence of bar quantities. Using the trivial identity:

$$\begin{aligned}
&\frac{1}{2\lambda_0}\,\left(\Sigma_T^2(m_r^2(T)) - \Sigma^2(m_r(0))\right)\\
&\qquad = \frac{1}{2\lambda_0}\,\left(\Sigma_T(m_r^2(T)) - \Sigma(m_r^2(0))\right)\left(\Sigma_T(m_r^2(T)) + \Sigma(m_r^2(0))\right)\\
&\qquad = \frac{\delta m^2(T)}{2}\,\left(\mathcal{M}_T(m_r^2(T)) + \mathcal{M}(m_r^2(0))\right)\,. \qquad (3.71)
\end{aligned}$$

we get

$$\mathcal{P}(T) - \mathcal{P}(0) = \mathcal{N}_T(m_r^2(T)) - \mathcal{N}(m_r^2(0)) + \frac{\delta m^2(T)}{2}\,\left(\mathcal{M}_T(m_r^2(T)) + \mathcal{M}(m_r^2(0))\right)\,, \quad (3.72)$$

where $\delta m^2(T) = m_r^2(T) - m_r^2(0)$. The result (3.72) has been previously obtained by authors [61] in the purely thermodynamic pressure framework.

3.4 Hydrostatic pressure in $D = 4$ (high–temperature expansion)

In order to obtain the high–temperature expansion of the pressure in $D = 4$, it is presumably the easiest to go back to equation (3.68) and employ identity (3.71). Let us split this task into two parts. We firstly evaluate the integrals with potentially UV divergent parts using the dimensional regularisation. The remaining integrals, with the Bose–Einstein distribution insertion, are safe of UV singularities and can be computed by means of the Mellin transform technique.

Inspecting (3.68) and (3.71), we observe that the only UV divergent contributions come from the integrals:

$$+ \quad \frac{1}{(D-1)}\int \frac{d^Dq}{(2\pi)^{D-1}}\,\mathbf{q}^2\,\left(\delta^+(q^2 - m_r^2(T)) - \delta^+(q^2 - m_r^2(0))\right)$$

$$+ \quad \frac{\delta m^2(T)}{4} \int \frac{d^D q}{(2\pi)^D} \left(\frac{i}{q^2 - m_r^2(T) + i\epsilon} + \frac{i}{q^2 - m_r^2(0) + i\epsilon} \right) , \tag{3.73}$$

which, if integrated over, give

$$\begin{aligned} (3.73) = \quad & + \quad \frac{\Gamma(\frac{-D}{2})\Gamma(\frac{D}{2}+\frac{1}{2})}{(D-1)\Gamma(\frac{D-1}{2})(4\pi)^{\frac{D}{2}}} \left((m_r^2(T))^{\frac{D}{2}} - (m_r^2(0))^{\frac{D}{2}} \right) \\ & + \quad \frac{\delta m^2(T)\ \Gamma(1-\frac{D}{2})}{4(4\pi)^{\frac{D}{2}}} \left((m_r^2(T))^{\frac{D}{2}-1} + (m_r^2(0))^{\frac{D}{2}-1} \right) . \end{aligned} \tag{3.74}$$

Taking the limit $D = 4 - 2\varepsilon \to 4$ and using expansions

$$\begin{aligned} \Gamma(-n+\varepsilon) &= \frac{(-1)^n}{n!} \left(\frac{1}{\varepsilon} + \sum_{k=1}^{n} \frac{1}{k} - \gamma + \mathcal{O}(\varepsilon) \right) \\ a^{x+\varepsilon} &= a^x \left(1 + \varepsilon\ \mathrm{ln} a + \mathcal{O}(\varepsilon^2) \right) , \end{aligned} \tag{3.75}$$

(γ is the Euler–Mascheroni constant) we are finally left with

$$(3.73)|_{D\to 4} = -\frac{m_r^2(0) m_r^2(T)}{64\ \pi^2} \ln\left(\frac{m_r^2(T)}{m_r^2(0)} \right) + \delta m^2(T)\ (m_r^2(T) + m_r^2(0))\ \frac{1}{128\ \pi^2} . \tag{3.76}$$

The fact that we get finite result should not be surprising as entire analysis of Section 3.2 was made to show that $\mathcal{P}(T) - \mathcal{P}(0)$ defined via $\Theta_c^{\mu\nu}$ is finite in $D = 4$.

We may now concentrate on the remaining terms in (3.68), the latter read (we might, and we shall, from now on work in $D = 4$)

$$\frac{1}{3}\int \frac{d^4q}{(2\pi)^3}\,\mathbf{q}^2\,\frac{1}{e^{|q_0|\beta}-1}\,\delta(q^2-m_r^2(T))+\frac{\delta m^2(T)}{4}\int\frac{d^4q}{(2\pi)^3}\,\frac{1}{e^{|q_0|\beta}-1}\delta(q^2-m_r^2(T))\,. \quad (3.77)$$

Our following strategy is based on the observation that the previous integrals have generic form:

$$\begin{aligned} I_{2\nu}(m_r) &= \int \frac{d^4q}{(2\pi)^3}\,\mathbf{q}^{2\nu}\,\frac{1}{e^{|q_0|\beta}-1}\,\delta(q^2-m_r^2), \\ &= \frac{m_r^{2+2\nu}}{2\,\pi^2}\int_1^\infty dx\,(x^2-1)^{\frac{1+2\nu}{2}}\,\frac{1}{e^{xy}-1}\,, \end{aligned} \quad (3.78)$$

with $\nu = 0, 1$ and $y = m_r\beta$. Unfortunately, the integral (3.78) can not be evaluated exactly, however, its small y (i.e. high–temperature) behaviour can be successfully analysed by means of the Mellin transform technique [36,73]. Before going further, let us briefly outline the basic steps needed for such a small y expansion.

The Mellin transform $\hat{f}(s)$ is done by the prescription [36,73,80–83]:

$$\hat{f}(s) = \int_0^\infty dx\, x^{s-1}\, f(x)\,, \quad (3.79)$$

with s being a complex number. One can easily check that the inverse Mellin transform reads

$$f(x) = \frac{1}{i(2\pi)}\int_{-i\infty+a}^{i\infty+a} ds\, x^{-s}\,\hat{f}(s)\,, \quad (3.80)$$

where the real constant 'a' is chosen in such a way that $\hat{f}(s)$ is convergent in the neighbourhood of a straight line $(-i\infty + a,\ i\infty + a)$. So particularly if $f(x) = \frac{1}{e^{xy}-1}$ one can find ([80]; formula I.3.19) that

$$\hat{f}(s) = \Gamma(s)\zeta(s)y^{-s} \qquad (\mathrm{Re}s > 1)\,, \tag{3.81}$$

where ζ is the Riemann zeta function ($\zeta(s) = \sum_{n=1}^{\infty} n^{-s}$). Now we insert the Mellin transform of $f(x) = \frac{1}{e^{xy}-1}$ to (3.78) and interchange integrals (this is legitimate only if the integrals are convergent before the interchange). As a result we have

$$\int_0^\infty dx\; g(x)\, \frac{1}{e^{xy}-1} = \int_{-i\infty+a}^{i\infty+a} \frac{ds}{i(2\pi)}\, \Gamma(s)\zeta(s)y^{-s}\hat{g}(1-s)\,, \tag{3.82}$$

with $g(x) = \theta(x-1)\,(x^2-1)^{\frac{1+2\nu}{2}}$. Using the tabulated result ([83]; formula 6.2.32) we find

$$\hat{g}(1-s) = \frac{1}{2}B(-\nu - 1 + \tfrac{1}{2}s; \tfrac{3}{2}+\nu) \qquad (\mathrm{Re}s > 2+2\nu)\,, \tag{3.83}$$

with $B(\ ;\ )$ being the beta function. Because the integrand on the RHS of (3.82) is analytic for Re$s > 2+2\nu$ and the LHS is finite, we must choose such a that the integration is defined. The foregoing is achieved choosing a $> 2+2\nu$. Another useful expressions for $\hat{g}(1-s)$ are ([83]; formula I.2.34 or I.2.37)

$$\begin{aligned} \hat{g}(1-s) &= B(\tfrac{3}{2}+\nu; -2-2\nu+s)\ \ {}_2F_1[-\tfrac{1}{2}-\nu; -2-2\nu+s; -\tfrac{1}{2}-\nu+s; -1] \\ &= 2^{\frac{1}{2}+\nu}\, B(\tfrac{3}{2}+\nu; -2-2\nu+s)\ \ {}_2F_1[-\tfrac{1}{2}-\nu; \tfrac{3}{2}+\nu; -\tfrac{1}{2}-\nu+s; \tfrac{1}{2}]\,, \end{aligned}$$

where ${}_2F_1$ is the (Gauss) hypergeometric function [83]. Using identity

$$\Gamma(2x) = \frac{2^{2x-1}}{\sqrt{\pi}}\,\Gamma(x)\Gamma(x+\tfrac{1}{2})\,,$$

we can write

$$(3.82) = \frac{\Gamma(\frac{3}{2}+\nu)}{4\sqrt{\pi}} \int_{-i\infty+a}^{i\infty+a} \frac{ds}{i(2\pi)} \Gamma(\tfrac{1}{2}s)\zeta(s)\left(\tfrac{1}{2}y\right)^{-s}\Gamma(-\nu-1+\tfrac{1}{2}s)\,. \tag{3.84}$$

The integrand of (3.84) has simple poles in $s=-2n$ $(n=1,2,\ldots)$, $s=1$, $s=-2n+2\nu+2$ $(n=0,1,\ldots,\nu)$ and double pole in $s=0$. An important point in the former pole analysis was the fact that $\zeta(s)$ has simple zeros in $-2m$ $(m>0)$ and only one simple pole in $s=1$. The former together with identity

$$\Gamma\left(\frac{x}{2}\right)\,\pi^{-\frac{x}{2}}\,\zeta(x) = \Gamma\left(\frac{1-x}{2}\right)\,\pi^{\frac{x-1}{2}}\,\zeta(1-x)\,,$$

shows that no double pole except for $s=0$ is present in (3.84). Now, we can close the contour to the left as the value of the contour integral around the large arc is zero in the limit of infinite radius (c.f. [80] and [84]; formula 8.328.1). Using successively the Cauchy theorem we obtain

$$\begin{aligned}
&\frac{4\sqrt{\pi}\,(3.82)}{\Gamma(\frac{3}{2}+\nu)} \\
&= \sum_{n=0}^{\nu} y^{2n-2\nu-2}\,\frac{\pi^{-2n+2\nu+2}(-n+\nu)!\,(-1)^{n}|B_{-2n+2\nu+2}|}{n!\,(-2n+2\nu+2)!\,2^{4n-4\nu-4}} \\
&+ \sum_{n=1}^{\infty} y^{2n}\,\frac{\pi^{-2n}\,(2n)!\,\zeta(1+2n)\,(-1)^{n+\nu+1}}{n!\,(n+1+\nu)!\,2^{4n-1}} \\
&+ y^{-1}\,\frac{\pi\,(-1)^{\nu+1}\,(\nu+1)!\,2^{2\nu+3}}{(2\nu+2)!} + \frac{2\,(-1)^{\nu+1}}{(\nu+1)!}\left\{\ln\left(\frac{y}{4\pi}\right)+\gamma-\tfrac{1}{2}\sum_{k=1}^{\nu+1}\frac{1}{k}\right\}\,,
\end{aligned} \tag{3.85}$$

where B_α's are the Bernoulli numbers. Let us mention that for $\zeta(2n+1)$ only numerical values are available.

Inserting (3.85) back to (3.77), we get for $\mathcal{P}(T) - \mathcal{P}(0)$

$$
\begin{aligned}
\mathcal{P}(T) - \mathcal{P}(0) &= (3.76) + \frac{1}{3}\, I_2(m_r(T)) + \frac{\delta m^2(T)}{4}\, I_0(m_r(T)) \\
&= \frac{T^4\, \pi^2}{90} - \frac{T^2}{24}\left(m_r^2(T) - \frac{\delta m^2(T)}{2}\right) + \frac{T\, m_r(T)}{4\,\pi}\left(\frac{m_r^2(T)}{3} - \frac{\delta m^2(T)}{4}\right) \\
&+ \frac{m_r^2(T)\, m_r^2(0)}{32\,\pi^2}\left(\ln\left(\frac{m_r(0)}{T\, 4\pi}\right) + \gamma - \frac{1}{2}\right) - \frac{m_r^4(0)}{128\,\pi^2} \\
&- \sum_{n=1}^{\infty}\left(m_r^2(T) - \tfrac{(n+2)}{2}\, \delta m^2(T)\right) \frac{m_r^{2n+2}(T)\, \pi^{-2n-2}\, (2n)!\, \zeta(1+2n)\, (-1)^{1+n}}{T^{2n}\, n!\, (n+2)!\, 2^{4n+4}}\,.
\end{aligned}
\tag{3.86}
$$

Note that (3.76) cancelled against the same term in $\frac{1}{3}\, I_2(m_r(T)) + \frac{\delta m^2(T)}{4}\, I_0(m_r(T))$. One can see that (3.86) rapidly converges for large T, so that only first four terms dominate at sufficiently high temperature. The aforementioned terms come from the poles nearby the straight line $(-i\infty + a,\ i\infty + a)$ (the more dominant contribution the closer pole). It is a typical feature of the Mellin transform technique that integrals of type

$$
\int_0^{\infty} dx\; g(x)\, \frac{1}{e^{xy} - 1}\,,
$$

can be expressed as an expansion which rapidly converges for small y (high–temperature expansion) or large y (low–temperature expansion)[14].

For a sufficiently large T we can use the high–temperature expansion of $\delta m^2(T)$ found in Appendix C. Inserting (C.6) to (3.86) we obtain

---

[14] By the same token we get the low–temperature expansion if the integral contour must be closed to the right.

$$\mathcal{P}(T)-\mathcal{P}(0)=\frac{T^4\,\pi^2}{90}-\frac{T^2\,m_r^2(T)}{24}+\frac{T^3\,m_r(T)}{12\pi}$$
$$+\frac{\lambda_r}{8}\left(\frac{T^4}{144}-\frac{T^3\,m_r(T)}{24\pi}+\frac{T^2\,m_r^2(T)}{16\pi^2}\right)+\mathcal{O}\left(m_r^4(T)\,\ln\left(\frac{m_r(T)}{T4\pi}\right)\right)\,. \qquad (3.87)$$

Up to a sign, the result (3.87) coincides with that found by Amelino–Camelia and Pi [85] for the effective potential[15]. Actually, they used instead of the $N\to\infty$ limit the Hartree–Fock approximation which is supposed to give the same V_{eff} as the leading $1/N$ approximation [79].

Note that the discussion of the mass renormalisation in Section 3.1 can be directly extended to the case when $m_r(0)=0$ (this does not apply to our discussion of λ_r!). Latter can be also seen from the fact that (3.86) is continuous in $m_r(0)=0$ (however not analytic). The foregoing implies that the original massless scalar particles acquire the thermal mass $m_r^2(T)=\delta m^2(T)$. From (3.86) one then may immediately deduce the pressure for massless fields Φ_a in terms of $\delta m(T)$. The latter reads

$$\begin{aligned}\mathcal{P}(T)-\mathcal{P}(0) \;&=\; \frac{T^4\,\pi^2}{90}-\frac{T^2\,(\delta m(T))^2}{48}+\frac{T\,(\delta m(T))^3}{48\,\pi}\\ &+\;\sum_{n=1}^{\infty}\frac{(\delta m(T))^{2n+4}\,\pi^{-2n-2}\,(2n)!\,\zeta(1+2n)\,(-1)^{n+1}}{T^{2n}\,(n-1)!\,(n+2)!\,2^{4n+5}}\,.\end{aligned} \qquad (3.88)$$

---

[15] Let us remind [75, 76, 85] that from the definition of V_{eff} the thermodynamic pressure is $-V_{eff}$. In order to obtain (3.87) from V_{eff} in [85], one must subtract the zero temperature value of V_{eff} and restrict oneself to vanishing field expectation value and positive bare mass squared.

This result is identical to that found by Drummond *et al.* in [61].

A noteworthy observation is that when the energy of a thermal motion is much higher then the mass of particles in the rest, then the massive theory approaches the massless one. This is justified in the first (high–temperature dominant) term of (3.86) and (3.88). This term is nothing but a half of the black body radiation pressure for photons [37,59] (photons have two degrees of freedom connected with two transverse polarisations). One could also obtain the temperature dominant contributions directly from the Stefan–Boltzmann law [36, 37, 59] for the density energy (i.e. $\langle \Theta^{00} \rangle$). The formal argument leading to this statement is based on the noticing that at high energy (temperature) the theory at hand is (classically) approximately conformally invariant, which in turn implies that the energy–momentum tensor is traceless [69]. Taking into account the definition of the hydrostatic pressure (3.8), we can with a little effort recover the leading high–temperature contributions for the massive case.

3.5 Conclusions

In the present chapter we have clarified the status of the hydrostatic pressure in (equilibrium) thermal QFT. The former is explained in terms of the thermal expectation value of the 'weighted' space–like trace of the energy–momentum tensor $\Theta^{\mu\nu}$. In classical field theory there is a clear microscopic picture of the hydrostatic pressure which is further enhanced by a mathematical connection (through the virial theorem) with the thermodynamic pressure. In addition, it is the hydrostatic pressure which can be naturally extended to a non–equilibrium medium. Quantum theoretic treatment of the hydrostatic pressure is however pretty delicate. In order to get a sensible, finite answer we must give up the idea of total hydrostatic pressure. Instead, thermal interaction pressure or/and interaction pressure must be used (see (3.38) and (3.39)). We have established this result for a special case when the theory in question is the scalar Φ^4 theory with $O(N)$ internal symmetry; but it can be easily extended to more complex situations. Moreover, due to a lucky interplay between the conservation of $\Theta^{\mu\nu}$ and the space–time translational invariance of an equilibrium (and $T = 0$) expectation value we can use the simple canonical (i.e. unrenormalised) energy–momentum tensor. In the course of our treatment in Section 3.2 we heavily relied on the counterterm renormalisation, which seems to be the most natural when one discusses renormalisation of composite Green's functions. To be specific, we have resorted to the minimal subtraction scheme which has proved useful in several technical points.

We have applied the prescriptions obtained for the QFT hydrostatic pressure to Φ^4 theory in the–large N limit. The former has the undeniable advantage of being exactly soluble. This is because of the fact that the large–N limit eliminates 'nasty' classes of diagrams in the Dyson–Schwinger expansion. The surviving class of diagrams (superdaisy diagrams) can be exactly resumed, because the (thermal) proper self–energy $\mathbf{\Sigma}$, as well as the renormalised coupling constant λ_r are momentum independent. We have also stressed that the $O(N)$ Φ^4 theory in the large–N limit is consistent only if we view it as an effective field theory. Fortunately, the upper bound on the UV cut–off is truly huge, and it does not represent any significant restriction. For the model at hand the resumed form of the pressure with $m_r(0) = 0$ was firstly derived (in the purely thermodynamic pressure context) by Drummond *et al.* in [61]. We have checked, using the prescription (3.38) for the thermal interaction pressure, that their results are in agreement with ours. The former is a nice vindication of the validity of the virial theorem even in the QFT context.

The expression for the pressure obtained was in a suitable form which allowed us to take advantage of the Mellin transform technique. We were then able to write down the high–

temperature expansion for the pressure in $D = 4$ (both for massive and massless fields) in terms of renormalised masses $m_r(T)$ and $m_r(0)$. We have explicitly checked that all UV divergences present in the individual thermal diagrams 'miraculously' cancel in accordance with our analysis of the composite operators in Section 3.2.

Chapter 4

Pressure in out–of–equilibrium media

In recent years significant progress has been made in understanding the behaviour of QFT systems away from thermal equilibrium. Motivation for the study of such systems comes both from the early universe as well as from the quark–gluon plasma (deconfined phase quarks and gluons). Non–equilibrium effects are expected to be relevant in the relativistic heavy–ion collisions planed at RHIC and LHC in the near future [86–89].

One of the significant physical variables, in the context of non–equilibrium QFT, is pressure. Pressure, as an easily measurable parameter[1], is expected to play an important role in a detection of phase transitions. This is usually ascribed to the fact that the pressure should exhibit a discontinuity in its derivative(s) when the local phase transition occurs. The aforementioned has found its vindication in solid state physics and fluid mechanics, and may play a crucial role, for instance, in various baryogenesis scenarios.

It is well known that for systems in thermal equilibrium, the pressure may be calculated via the partition function [34, 36, 62]. However, this procedure cannot be extended to off–equilibrium systems where is no such thing as the grand–canonical potential. In this chapter we consider an alternative definition of pressure, based on the energy–momentum tensor. This, so called, hydrostatic pressure is defined as the space–like trace of the energy–momentum tensor (see Chapter 3), and in equilibrium, it is identified with the thermodynamical pressure via the virial theorem [36]. There are several problems with the validity of this identification on the quantum level, indeed gauge theories suffer from a conformal (trace) anomaly and require special care [36]. However, we will avoid such difficulties by focusing on a scalar theory which is free of the mentioned complications [36,94]. The major advantage of defining pressure through the energy–momentum tensor stems from the fact that one may effortlessly extend the hydrostatic pressure to non–equilibrium systems (for discussion see Chapter 3).

---

[1] In this connection we may mention the piezo resistive silicon pressure sensors used, for instance, in superfluid helium [90, 91] or neutron (X–ray) diffraction technique used in solid state physics [92, 93].

The aim of this chapter is to provide a systematic prescription for the calculation of the hydrostatic pressure in non–equilibrium media. This requires three concepts; the Jaynes–Gibbs principle of maximal entropy, the Dyson–Schwinger equations and the hydrostatic pressure. In order to keep our discussion as simple as possible we illustrate the whole procedure on a toy model system, namely the $O(N)$ Φ^4 theory. The latter has advantage of being exactly solvable in the large–N limit, provided that we deal with a translationally invariant medium. As a result the hydrostatic pressure may be expressed in a closed form.

In order to provide meaningful results also for readers not entirely familiar with the off–equilibrium Dyson–Schwinger equations and the Jaynes–Gibbs principle of maximal entropy, we briefly summarise in Section 4.1 the basic essentials. (Detailed discussion of the equilibrium case may be found in Appendices A.1–A.3 or in Refs. [25,95,96].) As a byproduct we construct the generalised Kubo–Martin–Schwinger (KMS) conditions. Section 4.2 is devoted to the study of the (canonical–) energy momentum tensor in the $O(N)$ Φ^4 theory. If both the density matrix and the full Hamiltonian are invariant under $O(N)$ symmetry one obtains Ward's identities in a similar manner as in equilibrium. We show how these drastically simplify the expression for the pressure. In Section 4.3 we concentrate our analysis on the large–N limit. In this setting we derive a very simple expression for the pressure - pressure depends only on two–point Green functions. Section 4.4 then forms the vital part of this paper. Owing to the fact that the infinite hierarchy of the Dyson–Schwinger equations is closed (basically by chance) we obtain simple equations for two–point Green functions - Kadanoff–Baym equations. These are solved exactly for three illustrative density matrices ρ. We choose deliberately translationally invariant ρ's. The reason is twofold. Firstly, for a non–translationally invariant medium one must use the improved energy momentum tensor instead of the canonical one [94]. This is rather involved and it will be subject of our future work. Secondly, the Kadanoff–Baym equations turn out to be hyperbolic equations whose fundamental solution is well known. As a result we may evaluate, for the density matrices at hand, the hydrostatic pressure explicitly. The chapter ends with a discussion.

4.1 Basic formalism

The key object of our interest is the energy–momentum tensor $\Theta_{\mu\nu}(x)$. A typical contribution to $\Theta_{\mu\nu}(x)$ can be written as

$$\mathcal{D}_{\mu_1}\Phi(x)\;\mathcal{D}_{\mu_2}\Phi(x)\ldots\mathcal{D}_{\mu_n}\Phi(x)\,.$$

Here Φ is a field in the Heisenberg picture and $\mathcal{D}_{\mu_i}$ stands for a corresponding differential operator. Since $\mathcal{D}_{\mu_i}\Phi(x)$ and $\mathcal{D}_{\mu_j}\Phi(x)$ generally do not commute for $i \neq j$, one must prescribe the ordering in $\Theta_{\mu\nu}$. Our strategy is based on the observation that one can conveniently define such ordering via the non–local operator

$$\begin{aligned} &\lim_{x_i \to x} \mathcal{T}^*\{\mathcal{D}_{\mu_1}\Phi(x_1)\cdots\mathcal{D}_{\mu_n}\Phi(x_n)\} = \\ &\qquad \lim_{x_i \to x} \mathcal{D}(i\partial_{\{\mu\}})\mathcal{T}\{\Phi(x_1)\cdots\Phi(x_n)\}\,, \end{aligned} \tag{4.1}$$

where $\mathcal{D}(i\partial_{\{\mu\}})$ is just a useful short–hand notation for $\mathcal{D}_{\mu_1}\mathcal{D}_{\mu_2}\ldots\mathcal{D}_{\mu_n}$, and $\mathcal{T}^*$ is defined in Section 3.2. It is clear that both $\mathcal{T}^*$ and $\mathcal{T}$ coincide if all the arguments x_i are different, so $(\mathcal{T}^* - \mathcal{T})(\ldots)$ is an operator with a support at the contact points. The $\mathcal{T}^*$ ordering is in general a very useful tool whenever one deals with composite operators. In the sequel we shall repeatedly use this fact.

4.1.1 Off–equilibrium Dyson–Schwinger equations

Let us now briefly outline the derivation of the Dyson–Schwinger equations for systems away from equilibrium. For simplicity we illustrate this on a single scalar field Φ.

We start with the action $S[\Phi]$ where Φ is linearly coupled to an external source $J(x)$. Working with the fields in the Heisenberg picture, the operator equation of motion can be written as

$$\frac{\delta S}{\delta \Phi(x)}[\Phi = \Phi^J] + J(x) = 0\,, \tag{4.2}$$

where the index J emphasises that Φ is implicitly J–dependent. This dependence will be made explicit via a unitary transformation connecting Φ^J (governed by $H - J\Phi$) with Φ (governed by H). If $J(x)$ is switched on at time $t = t_i$ we have

$$\begin{aligned} \Phi^J(x) &= B^{-1}(t;t_i)\Phi(x)B(t;t_i) \\ &= B(t_i;t_f)B(t_f;t)\ \Phi(x)\ B(t;t_i) \\ &= T_C\left(\Phi(x)\ \exp\,(i\int_C d^4y\ J(y)\Phi(y))\right)\,. \end{aligned} \tag{4.3}$$

Here we have used the fact that

$$B(t_1;t_2) = T\left(\exp(i\int_{t_2}^{t_1} d^4y\ J(y)\Phi(y))\right) \qquad t_1 > t_2\,. \tag{4.4}$$

The close–time path C runs along the real axis from t_i to t_f (t_f is arbitrary, $t_f > t_i$) and then back to t_i. With this setting we can rewrite (4.2) as

$$\mathcal{T}_C^*\left(\left\{\frac{\delta S[\Phi_\pm]}{\delta\Phi} + J_\pm\right\}\exp(i\int d^4y\ (J_+(y)\Phi_+(y) - J_-(y)\Phi_-(y)))\right) = 0\,, \tag{4.5}$$

where, as it is usual [36, 44], we have labelled the field (source) with the time argument on the upper branch of C as Φ_+ (J_+) and that with the time argument on the lower branch of C as Φ_- (J_-). Introducing the metric $(\sigma_3)_{\alpha\beta}$ (σ_3 is the usual Pauli matrix and $\alpha,\beta = \{+;-\}$) we can write $J_+\Phi_+ - J_-\Phi_- = J_\alpha\ (\sigma_3)^{\alpha\beta}\ \Phi_\beta = J^\alpha\ (\sigma_3)_{\alpha\beta}\ \Phi^\beta$. For the raised and lowered indices we simply read: $\Phi_+ = \Phi^+$ and $\Phi_- = -\Phi^-$ (similarly for J_α). Taking $\mathrm{Tr}(\rho\ldots)$ with $\rho = \rho[\Phi, \partial\Phi, \ldots]$ being the density matrix, we obtain

$$\frac{1}{Z[J]}\frac{\delta S}{\delta\Phi(x)}\left[\Phi^\alpha(x) = -i\frac{\delta}{\delta J_\alpha(x)}\right] Z[J] = -J^\alpha(x)\,, \tag{4.6}$$

with $Z[J] = \mathrm{Tr}\left\{\rho\ \mathcal{T}_C \exp\ \left(i\int_C d^4y\ J(y)\Phi(y)\right)\right\}$ being the generating functional of Green's functions (which in the non–equilibrium context we shall denote az $\mathbb{G}$). Employing the commutation relation: $-i\frac{\delta}{\delta J_\alpha}Z = Z\,(\phi^\alpha - i\frac{\delta}{\delta J_\alpha})$, we may recast (4.6) into more convenient form, namely

$$-J^\alpha(x) = \frac{\delta S}{\delta\Phi(x)}\left[\phi^\alpha(x) + i\int d^4y\ \mathbb{G}^\alpha_\beta(x,y)\ (\sigma_3)^{\beta\gamma}\ \frac{\delta}{\delta\phi^\gamma(y)}\right]\mathbb{1}\,, \tag{4.7}$$

where the symbol $\mathbb{1}$ indicates the unit. As usual, the mean field, ϕ_α, is defined as the expectation value of the field operator: $\phi_\alpha(x) \equiv \langle \Phi_\alpha(x) \rangle$. Defining $Z[J] = \exp(iW[J])$, two–point Green functions are then defined as $\mathbb{G}_{\alpha\beta}(x,y) = -\delta^2 W/\delta J^\alpha(x)\delta J^\beta(y)$. Setting J in (4.6)–(4.7) to 0 (i.e. physical condition) we obtain a first out of infinite hierarchy of equations for Green's functions. Successive J variations of (4.6)–(4.7) generate higher order equations in the hierarchy. The system of these equations is usually referred to as the Dyson–Schwinger equations.

For the future reference is convenient to have the expression for the effective action $\Gamma[\phi_c]$. This is connected with $W[J]$ via the Legendre transform:

$$\Gamma[\phi_c] = W[J] - \int_C d^4y \; J(y)\phi_c(y)\,. \tag{4.8}$$

Following the previous reasonings, one can easily persuade oneself that the expectation value of $\Theta^{\mu\nu}$ reads

$$\langle \Theta^{\mu\nu}(x) \rangle = \langle \Theta^{\mu\nu}[\Phi(x)] \rangle = \Theta^{\mu\nu}[\phi_+(x) + i \int d^4y \; \mathbb{G}_{+\beta}(x,y) \; (\sigma_3)^{\beta\gamma} \; \frac{\delta}{\delta\phi^\gamma(y)}] \, \mathbb{1}\,. \tag{4.9}$$

We have automatically used the sub–index '+' as the fields involved in $\Theta^{\mu\nu}$ have, by definition, the time argument on the upper branch of C.

4.1.2 The Jaynes–Gibbs principle of maximal entropy

In this section we would like to review the Jaynes–Gibbs principle of maximal entropy (also maximum calibre principle) [24, 25, 31, 39], which we shall employ in the following. The formalism is a generalisation from an ordinary Gibbs's principle of maximal entropy to the systems out of equilibrium. The objective of the principle is to construct the 'most probable' density matrix which fulfils the constraints imposed by experimental/theoretical data.

The standard rules of statistical physics allows us to define the expectation value via the density matrix ρ as

$$\langle \ldots \rangle = \mathrm{Tr}(\rho \ldots)\,, \tag{4.10}$$

with the trace running over a complete set of *physical* states describing the ensemble in question at some initial time t_i. The specification (or reasonable approximation) of the density matrix is thus crucial for determining the macroscopic properties of a given system.

The usual approaches [97–100] trying to determine ρ start with the Schrödinger picture. The merit of this procedure is that one transforms the whole time dependence of the expectation value into the density matrix itself. Thus the time evolution of such an expectation value is equivalent to the time evolution of ρ, and we need not to solve separate equations for each observable[2].

Suppose that the system is prepared in such a way that at time t the probability of the system being in the state $|\psi_n; t\rangle$ is $p_n(t)$. The density matrix has then the standard form

$$\rho_s(t) = \sum_n p_n(t)\; |\psi_n; t\rangle\langle\psi_n; t|\,. \tag{4.11}$$

(by $\sum_n$ we mean; sum over discrete spectrum and integrate over continuous one). We should stress that the ensemble $\{|\psi_n; t\rangle\}$ in (4.11) not necessary consist of mutually orthogonal states, although the density matrix can always be formally diagonalised by selecting its eigenbasis (polar basis). Applying the Schrödinger equation to (4.11), the evolution of ρ_s reads

$$\frac{d\rho_s(t)}{dt} = i[\rho_s(t), H] + \frac{\partial \rho_s(t)}{\partial t}\,, \tag{4.12}$$

where

---

[2] This advantage does not seem to be relevant for Green's functions with different time arguments.

$$\frac{\partial \rho_s(t)}{\partial t} = \sum_n \frac{dp_n(t)}{dt} \, |\psi_n; t\rangle\langle\psi_n; t| \, . \tag{4.13}$$

For a closed Hamiltonian system $p_n(t)$ cannot be changed, and so (4.12) reduces to the celebrated von Neumann–Liouville equation

$$\frac{d\rho_s(t)}{dt} = i[\rho_s(t), H] \, . \tag{4.14}$$

Let us mention that the vanishing of the time derivative of $p_n(t)$ implies that the von Neumann–Gibbs entropy $S_G = -\mathrm{Tr}(\rho_s \ln \rho_s)$ is time independent. Indeed, in the latter case the evolution of ρ_s can be formally written (c.f. (4.12)) as

$$\rho_s(t) = U(t;t')\rho_s(t')U(t;t')^{-1} \, , \tag{4.15}$$

where the evolution operator is determined from the Schrödinger equation

$$i\frac{\partial}{\partial t}U(t;t') = H(t)U(t;t'), \qquad U(t', t') = 1 \, ,$$

and so using the property of a trace operation we have,

$$S_G(t') = -\mathrm{Tr}(\rho_s(t')\ln\rho_s(t')) = -\mathrm{Tr}(\rho_s(t)\ln\rho_s(t)) = S_G(t) \, . \tag{4.16}$$

The time dependence of $p_n(t)$ reflects the fact that the system in question interacts with an exterior – a heat bath (whose structure and dynamics are usually unknown). In order to determine $p_n(t)$ one would need to resort to some physical model [100] describing the dynamics of the environmental system – task by no means easy. In order to avoid these difficulties it is customary to apply a stochastic description of a system–bath interaction [101, 102], or equivalently use an irreversible "master equation" [102] for ρ.

To keep our ideas simple, we shall from the very outset assume that p_n is constant. This means that either no external environment interacts with our system or that the interaction is reflected only in the Hamiltonian H (e.g. effective external fields or time dependences) but the probability of the population of any state stays unchanged - adiabatic interaction.

Solving the von Neumann–Liouville equation would be a formidable task. One usually resorts either to variational method [100,103] with several trial ρ's, or one may recast (4.14) into an infinite hierarchy of integro–differential equations for two-particle, etc. distribution functions [30] (i.e. Bogoliubov–Born–Green–Kirkwood–Yvon or BBGKY hierarchy). In the latter approach one hopes that one can device an effective truncation of the hierarchy allowing to close the system of equations, and then solve it (usually perturbatively). However, in both aforementioned approaches we must specify the initial value data in order to solve uniquely the evolution equation(s). This is quite delicate task, and one usually uses the most simple (and not always physically well motivated) choices of ρ (e.g. Gibbs (grand–)canonical distribution [100], Gaussian distribution [95,98,99]).

Rather than following the previous path, we shall use the Heisenberg picture instead. This seems to be more suitable for our purpose. In our particular case the polar form of ρ_H reads

$$\rho_H = \sum_n p_n |\psi_n\rangle\langle\psi_n| \,. \tag{4.17}$$

In the following we shall denote ρ_H simply as ρ. In order to determine ρ explicitly we shall resort to the Jaynes–Gibbs principle of maximal entropy [24,25,31,39]. The latter allows one to construct ρ in a way which naturally extends the original Gibbs prescription [31,39] which refers only to equilibrium. The basic idea is 'borrowed' from the information theory. Let us assume that we have criterion of how to characterise the informative content of ρ. The most "probable" ρ is then selected out of those ρ which are consistent with 'whatever' we know about the system and which have the last informative content (Laplace's principle of insufficient reasons). Consistency with anything known about ρ must be kept; while to chose more informative ρ is to presume an extra information which we do not control, and to make unjustified implicit assumption concerning the information we do not know about.

It remains to characterise the *information content* (measure) $\mathfrak{I}[\rho]$ of ρ. This was done by C.E.Shannon [104], L.Brillouin [105] and L.Szilard [106] with the result

$$\mathfrak{I}[\rho] = \mathrm{Tr}(\rho \log_2 \rho)$$

The density matrix is then chosen to minimise $\mathfrak{I}[\rho]$. It is quite surprising that up to a (negative) multiplicative constant $\mathfrak{I}[\rho]$ coincides with $S_G[\rho]$, and thus the principle of insufficient reasons basically turns out to be the maximal entropy principle[3]. Note that no assumption about the nature of ρ was made; namely there was no assumption whether ρ describes equilibrium or non–equilibrium situation. (We were interested only in the information content of ρ, and not in the underlying dynamics of a system). To put more flesh on the bones, let us rephrase the former into more physical language [24,25]. What we actually need to do is to maximise S_G subject to the constraints imposed by our knowledge of expectation values of certain operators $P_1[\Phi, \partial\Phi], \ldots, P_n[\Phi, \partial\Phi]$. This yields a density matrix ρ which incorporates the fact that all the quantum states which are permitted by the constraints have equal probabilities [25]. In contrast to equilibrium, all $P_k[\ldots]$'s may be operators which are not the constants of the motion (both the position and time dependences are allowed). So namely if one knows that

---

[3] It Appendix D we show that the Shannon entropy (which is proportional to S_G) equals (in base 2 of logarithm) to the expected number of binary (yes/no) questions whose answer take us from our current state of knowledge to the one certainty. So, the bigger S_G, the more questions one has and consequently one possess a higher ignorance about a system.

$$\langle P_k[\Phi, \partial\Phi]\rangle = g_k(x_1, x_2, \ldots)\,, \tag{4.18}$$

the entropy maximalisation leads to

$$\rho = \frac{1}{\mathcal{Z}[\lambda_1, \ldots, \lambda_n]} \exp\left(- \sum_{i=1}^{n} \int \prod_{j} d^4x_j \; \lambda_i(x_1, \ldots) P_i[\Phi, \partial\Phi] \right)\,, \tag{4.19}$$

with the 'partition function'

$$\mathcal{Z}[\lambda_1, \ldots, \lambda_n] = \mathrm{Tr}\left(\exp(- \sum_{i=1}^{n} \int \prod_{j} d^4x_j \; \lambda_i(x_1, \ldots) P_i[\Phi, \partial\Phi]) \right)\,. \tag{4.20}$$

It is possible to show that the stationary solution of S_G is unique [27] and maximal. The latter goes on the account of the fact that S_G is a concave functional (see Appendix D). Both in (4.19) and (4.20) the time integration is not either present at all (so f_k is specified only in the initial time t_i), or is taken over the gathering interval $(-\tau, t_i)$ (i.e. as $\int_{\tau}^{t_i} dt \ldots$). If, instead, one has certain partial knowledge about the expectation value of $P_k[\Phi, \partial\Phi]$ at some discrete times prior t_i, the corresponding integration must be replaced by a discrete summation. Note that if we have no prior knowledge about the system, then $\rho = 1/\mathcal{W}$, where $\mathcal{W}$ is the number of accessible quantum states. Equivalently we may say that the no prior restrictions mean our total ignorance about the system and as a consequence we must affiliate with each quantum state an equal probability.

The Lagrange multipliers λ_k might be eliminated if one solves n simultaneous equations

$$g_k(x_1, \ldots) = - \frac{\delta \, \ln\mathcal{Z}}{\delta\lambda_k(x_1, \ldots)}\,. \tag{4.21}$$

Using the definition of the von Neumann–Gibbs entropy together with (4.19) we get

$$\begin{aligned} S_G[g_1,\ldots,g_n]|_{max} &= -\mathrm{Tr}(\rho\ \mathrm{ln}\rho)|_{max} \\ &= \mathrm{ln}\mathcal{Z}[\lambda_1,\ldots,\lambda_n] + \sum_{i=1}^{n}\int\prod_j d^4x_j\ \lambda_i(x_1,\ldots)g_i(x_1,\ldots)\,. \qquad (4.22)\end{aligned}$$

So one may view $S_{G\,max}$ as the Legendre transformation of ln$\mathcal{Z}$. In the equilibrium case the former is the standard relation between entropy and the grand–canonical potential. Having (4.22), the explicit solution of (4.21) may be formally written as

$$\lambda_k(x_1,\ldots) = \frac{\delta\ S_G[g_1,\ldots,g_n]|_{max}}{\delta g_k(x_1,\ldots)}\,. \qquad (4.23)$$

Now, in order to reflect the density matrix (4.19) in the Dyson–Schwinger equations, we need to construct the corresponding boundary conditions. This may be done quite straightforwardly. Using the cyclicity of Tr(...) together with the relation

$$e^A B e^{-A} = \sum_{n=0}^{\infty}\frac{1}{n!}C_n, \quad C_0 = B, C_n = [A, C_{n-1}]\,,$$

we can write the generalised KMS conditions for the n–point Green function as

$$\langle\Phi(x_1)\ldots\Phi(x_n)\rangle = \langle\Phi(x_2)\ldots\Phi(x_n)\Phi(x_1)\rangle + \sum_{k=1}^{\infty}\frac{1}{k!}\langle\Phi(x_2)\ldots\Phi(x_n)C_k(x_1)\rangle\,, \qquad (4.24)$$

where $A = \ln(\rho)$, $B = \Phi(x_1)$, $x_{10} = t_i$. So for the two–point Green functions we have[4]

$$\mathbb{G}_{+-}(x,y) = \mathbb{G}_{-+}(x,y) + \sum_{n=1}^{\infty}\frac{1}{n!}\mathrm{Tr}(\rho\ \Phi(x)C_n(y))\,.$$

---

[4] In special cases when $\rho = |0\rangle\langle 0|$ or $\rho = e^{-\beta H}/\mathcal{Z}(\beta)$ the boundary conditions are the well known Feynman and KMS boundary conditions, respectively.

In this chapter we aim to demonstrate that conditions (4.24) together with the causality condition are sufficient to determine Green's functions uniquely.

4.2 The $O(N)$ Φ^4 theory

The $O(N)$ Φ^4 theory is described by the bare Lagrangian

$$\mathcal{L} = \frac{1}{2}\sum_{a=1}^{N}\left((\partial\Phi^a)^2 - m_0^2(\Phi^a)^2\right) - \frac{\lambda_0}{8N}\left(\sum_{a=1}^{N}(\Phi^a)^2\right)^2 .$$

The corresponding canonical energy–momentum tensor is $\Theta_c^{\mu\nu} = \sum_a \partial^\mu\Phi^a\partial^\nu\Phi^a - g^{\mu\nu}\mathcal{L}$, and from Eqs.(4.1) and (4.9) its expectation value is

$$\begin{aligned}
\Theta_c^{\mu\nu}(\Phi_+(x)) &= \langle\Theta_c^{\mu\nu}(x)\rangle \\
&= i\sum_c \partial_x^\mu\partial_y^\nu\ \mathbb{G}^{cc}_{++}(x,y)|_{x=y} - \frac{g^{\mu\nu}i}{2}\sum_c\Big\{\partial_x^\alpha\partial_{\alpha y}\ \mathbb{G}^{cc}_{++}(x,y)|_{x=y} - m_0^2\mathbb{G}^{cc}_{++}(x,x)\Big\} \\
&+ \frac{g^{\mu\nu}\lambda_0}{8N}\sum_{c,d}\Big\{\Big((\phi_+^c(x))^2 + i\mathbb{G}^{cc}_{++}(x,x)\Big)\Big((\phi_+^d(x))^2 + i\mathbb{G}^{dd}_{++}(x,x)\Big) \\
&+ 2\Big(\phi_+^c(x)\phi_+^d(x) + i\mathbb{G}^{cd}_{++}(x,x)\Big)i\mathbb{G}^{cd}_{++}(x,x)\Big\} \\
&+ \text{terms with } \Gamma^3 \text{ and } \Gamma^4 . \qquad (4.25)
\end{aligned}$$

Before proceeding further with our development, we want to show how one can significantly simplify Eq.(4.25) provided that both the density matrix and the Hamiltonian are invariant under rotations in the N–dimensional vector space of fields. This situation would occur if the system was initially prepared in such a way that no field Φ^a was favoured over another. The fact that ρ is invariant under $O(N)$ transformations means that

$$U(\epsilon)\rho[\Phi,\partial\Phi,\ldots]U^{-1}(\epsilon) = \rho[\Phi,\partial\Phi,\ldots] , \qquad (4.26)$$

where the fields Φ^a transform under N–dimensional rotations: $U(\epsilon)\Phi^a U^{-1}(\epsilon) = R^{-1}(\epsilon)^{ab}\Phi^b = [\exp(\epsilon_i T_i)]^{ab}\Phi^b$, where $R(\epsilon)$ is the rotation matrix in the N–dimensional vector space, and the generators T_i are real and antisymmetric $N \times N$ matrices. It is obvious that the previous relation for Φ^c can be satisfied for all times only if the full Hamiltonian, which governs the evolution of Φ^a, is also invariant against the N–dimensional rotations.

Let us now consider the generating functional $Z[J]$ corresponding to the $O(N)$ symmetric density matrix. Employing the cyclic property of $\mathrm{Tr}(\ldots)$ together with the infinitesimal transformation, $\delta R(\epsilon) = 1 + \epsilon_i T_i$, we obtain that the variation of Z must vanish. The latter implies the following (unrenormalised) Ward's identities:

$$\int_C d^4y \; J^a(y) \frac{\delta W[J]}{\delta J^b(y)} = \int_C d^4y \; J^b(y) \frac{\delta W[J]}{\delta J^a(y)} \,. \tag{4.27}$$

Taking successive variations with respect to source J, we obtain the following results (see also [96]): n–point Green functions with n odd vanish, while for n even ($n = 2k, k = 1, 2, \ldots$) one has

$$\mathbb{G}^{a_1 a_2 \ldots a_{2k}}_{\alpha_1 \cdots \alpha_{(2k)}}(x_1, \ldots, x_{2k}) = \sum_{\text{all pairings}} \prod_{i<j} \delta_{a_i a_j} \mathbb{G}^{(2k)}_{\alpha_1 \cdots \alpha_{2k}}(x_1, \ldots, x_{2k}) \,, \tag{4.28}$$

where $\mathbb{G}^{(2k)}$ is a universal $2k$–point Green function. Similar results can be obtained for $\Gamma^{a_1 a_2 \ldots a_{2k}}_{\alpha_1 \alpha_2 \ldots \alpha_{2k}}(\ldots)$.

Finally note that these results enable the expression for the expectation value of the energy momentum tensor to be simplified significantly to

$$\begin{aligned} \langle \Theta^{\mu\nu}_c(x) \rangle &= iN \partial^\mu_x \partial^\nu_y \; \mathbb{G}_{++}(x,y)|_{x=y} - \frac{N+2}{8} \lambda_0 g^{\mu\nu} (\mathbb{G}_{++}(x,x))^2 \\ &- i\frac{N}{2} g^{\mu\nu} \Big(\partial^\mu_x \partial^\nu_y \; \mathbb{G}_{++}(x,y)|_{x=y} - m_0^2 \; \mathbb{G}_{++}(x,x) \Big) \end{aligned}$$

$$+ \ \ \text{terms with } \ \Gamma^{(4)} \, . \tag{4.29}$$

In the rest of this chapter we shall confine ourselves only to situations where both ρ and H are $O(N)$ invariant.

4.3 The large–N limit

Let us now examine behaviour of (4.29) to the order $\mathcal{O}(1/N)$. For this purpose it is important to know how either $G^{(n)}$ or $\Gamma^{(n)}$ behave in the $N \to \infty$ limit. At $T = 0$ or in equilibrium the Feynman diagrams are available [62, 74] and the corresponding combinatorics can be worked out quite simply. On the other hand, the situation in off–equilibrium cases is more difficult as we do not have at our disposal Wick's theorem. One may devise various diagrammatic approaches, e.g. kernel method [95], cumulant expansion [59], correlation diagrams [5], etc. Instead of relying on any graphical representation (as we done in Section 3.3) we show that for both equilibrium and off–equilibrium systems, the situation may be approached from far more general standpoint using only Ward's identities and properties of Γ and W.

In order to find the leading behaviour at large N it is presumably the easiest to consider the Legendre transform (4.8). The explicit N dependence may be obtained by setting $\phi^c = \phi$, which implies $J^c = J$ for all the group indices. Eq.(4.8) then indicates that both $\Gamma[\phi]$ and $W[J]$ are of order N. If we expand $\Gamma[\phi^a]$ in terms of ϕ^c taking into account Ward's identities we get

$$\begin{aligned}\Gamma[\phi] = \Gamma[0] \ \ &+ \ \ \frac{1}{2} N \int_C d^4x \; d^4y \; \Gamma^{(2)}(x,y) \; \phi(x)\phi(y) \\ &+ \ \ \frac{3}{4!} N^2 \int_C d^4x \; d^4y \; d^4z \; d^4q \; \Gamma^{(4)}(x,y,z,q) \\ &\times \ \ \phi(x)\phi(y)\phi(z)\phi(q) + \cdots \, .\end{aligned} \tag{4.30}$$

Since the LHS of (4.30) is of order N, $\Gamma^{(2)}$ must be of order N^0, $\Gamma^{(4)}$ of order N^{-1}, and, in general, $\Gamma^{(2n)}$ must be of order N^{1-n}. This suggests that in the expression for the energy–momentum tensor (4.29), terms containing $\Gamma^{(4)}$ can be ignored. The above argument can be repeated in a similar way for W.

Hence, collecting our results together, the expectation value of the energy–momentum tensor to leading order in N may be written as

$$\begin{aligned}\langle \Theta_c^{\mu\nu}(x)\rangle &= iN\partial_x^\mu \partial_y^\nu \; \mathbb{G}_{++}(x,y)\big|_{x=y} - \frac{N}{8}\lambda_0 g^{\mu\nu}(\mathbb{G}_{++}(x,x))^2 \\ &- i\frac{N}{2}g^{\mu\nu}\Big(\partial_x^\mu \partial_y^\nu \; \mathbb{G}_{++}(x,y)\big|_{x=y} - m_0^2 \; \mathbb{G}_{++}(x,x)\Big)\,. \qquad (4.31)\end{aligned}$$

This result is surprisingly simple: the expectation value of the energy–momentum tensor, and thus the hydrostatic pressure, is expressed purely in terms of two–point Green's functions. The latter can be calculated through the Dyson–Schwinger equations (4.7). Furthermore, these equations have a very simple form provided that both the large–N limit and Ward's identities are applied. If we perform a variation of (4.7) with respect to $J_\beta(y)$ we obtain, to order $\mathcal{O}(1/N)$, the following Dyson–Schwinger equations for two–point Green functions:

$$\begin{aligned}&\left(\Box + m_0^2 + \frac{i\lambda_0}{2}\; \mathbb{G}_{\alpha\alpha}(x,x)\right) \mathbb{G}_{\alpha\beta}(x,y) \\ &= -\delta(y-x)(\sigma_3)_{\alpha\beta}\,. \qquad (4.32)\end{aligned}$$

These dynamical equations for two–point Green functions are better known as the Kadanoff–Baym equations [40].

Let us mention one more point. The generalised KMS conditions for $\mathbb{G}_{\pm\mp}$ are significantly simple in the large–N limit. This is because in sum (4.24) only terms of order $\mathcal{O}(N^0)$ contribute. This implies that only quadratic operators $P_i[\Phi, \partial\Phi]$ in the density matrix are relevant. As a result, the Jaynes–Gibbs principle naturally provides a vindication of the popular Gaussian Ansatz [98–100].

4.4 Out–of–equilibrium pressure

The objective of the present section is to show how the outlined mathematical machinery works in the case of the hydrostatic pressure. In order to gain some insight we start with rather pedagogical, but by no means trivial examples; translationally invariant, non-equilibrium density matrices. We consider the more difficult case of translationally non–invariant density matrices in our future work.

4.4.1 Equilibrium

As an important special case we can choose the constraints

$$\langle P_k[\Phi, \partial\Phi]\rangle|_{t_i} = g_k = \text{constant}\,, \tag{4.33}$$

where t_i is arbitrary. Eq.(4.33) then implies that P_k's are integrals of motion. Since in the finite volume systems the spatial translational invariance is destroyed, the only integral of motion (apart from conserved charges) is the Hamiltonian. Thus the system is in thermal equilibrium and the laws of thermodynamics [37, 59] prescribe that $g = \int_0^T dT' C_V(T')$ (C_V is the heat capacity at constant volume V and T is temperature). Eq. (4.23) determines the Lagrange multiplier; $\lambda = 1/T = \beta$. The density matrix maximising the S_G is then the density matrix of the canonical ensemble: $\rho = \frac{\exp(-\beta H)}{\mathcal{Z}[\beta]}$. Due to the translational invariance of ρ, the Kadanoff–Baym equations read

$$\left(\Box_x + m_r^2(T)\right) \mathbb{G}_{\alpha\beta}(x-y) = -\delta(x-y)(\sigma_3)_{\alpha\beta}\,, \tag{4.34}$$

where the temperature–dependent renormalised mass is (see, for example [62,74]); $m_r^2(T) = m_0^2 + \frac{i\lambda_0}{2}\, \mathbb{G}_{\alpha\alpha}(0)$. The corresponding KMS boundary condition is

$$\mathbb{G}_{+-}(\mathbf{x}, t_i; \mathbf{y}, 0) = \mathbb{G}_{-+}(\mathbf{x}, t_i - i\beta; \mathbf{y}, 0)\,. \tag{4.35}$$

Because $m_r(T)$ is a spatial constant, a Fourier transform solves equations (4.34). The solutions of (4.34) subject to condition (4.35) are then the resumed propagators in the Keldysh–Schwinger formalism

$$\begin{aligned} i\mathbb{G}_{\pm\pm}(k) &= \frac{\pm i}{k^2 - m_r^2 \pm i\varepsilon} + 2\pi f_B(|k_0|)\delta(k^2 - m_r^2) \\ i\mathbb{G}_{\pm\mp}(k) &= 2\pi \left\{\theta(\mp k_0) + f_B(|k_0|)\right\} \delta(k^2 - m_r^2)\,, \end{aligned} \tag{4.36}$$

with $f_B(x) = (\exp(\beta x) - 1)^{-1}$ being the Bose–Einstein distribution.

Now, the total hydrostatic pressure in D dimensions is classically defined as [36, 74, 107]

$$p(x, T) = -\frac{1}{(D-1)} \langle \Theta^i{}_i(x) \rangle\,.$$

Because $\Theta_c^{\mu\nu}$ is a composite operator, a special renormalisation is required [36, 65, 66, 94]. As we have shown in [74], for translationally invariant systems the renormalised pressure coincides with the, so called, thermal interaction pressure $\mathcal{P}$ (see Eq.(3.38)). The latter reads

$$\mathcal{P}(T) = p(x, T) - p(x, 0) = -\frac{1}{(D-1)} \left\{ \langle \Theta_{c\,i}^{i} \rangle - \langle 0 | \Theta_{c\,i}^{i} | 0 \rangle \right\}\,. \tag{4.37}$$

Let us remind that the energy–momentum tensor $\Theta^{\mu\nu}$ need not to be the canonical one (however, the canonical one is usually the simplest one), c.f. Section 3.2. As a second point we should mention that prescription (4.37) retains its validity for non–equilibrium media as well. This is because the short–distance behaviour of $G_{++}(x, y)$, which is responsible for the singular behaviour of $\Theta^{\mu\nu}$, comes from the particular solution of the Kadanoff–Baym equation (4.34). The latter can be chosen to be completely independent of the boundary conditions (actually it is useful to chose the Feynman causal solution). On the other hand, the homogeneous solution of (4.34), which is regular at $|x-y| \to 0$, reflects all the boundary conditions. One may see then that the UV singularities which trouble $\Theta^{\mu\nu}$ may be treated in the same way as at the $T = 0$. Incidentally, the former is an extension of the well known fact that in order to renormalise a finite temperature QFT, it suffices to renormalise it at $T = 0$.

Inserting the solution (4.36) into the expression for the energy–momentum tensor (4.31) we arrive at the thermal interaction pressure per particle (compare Section 3.4, see also [85, 94])

$$\begin{aligned}\mathcal{P}(T) \;&=\; \frac{T^4\,\pi^2}{90} - \frac{T^2\,m_r^2(T)}{24} + \frac{T\,m_r^3(T)}{12\pi} + \frac{\lambda_r}{8}\left(\frac{T^4}{144} - \frac{T^3\,m_r(T)}{24\pi} + \frac{T^2\,m_r^2(T)}{16\pi^2}\right)\\ &+\; \mathcal{O}\left(m_r^4(T)\,\ln\left(\frac{m_r(T)}{T4\pi}\right)\right)\,, \qquad (4.38)\end{aligned}$$

where the renormalised coupling constant λ_r comes from the $T = 0$ renormalisation prescription: $\Gamma^{(4)}_{aa\to bb}(s = 0) = -\lambda_r/N$ (s is the usual Mandelstam variable). A direct calculation of $\Gamma^{(4)}$ in the large–N limit were performed in Section 3.2 with the result:

$$\lambda_r = \lambda_0 - \frac{1}{2}\lambda_0\lambda_r\frac{1}{(4\pi)^{D/2}}\Gamma\left[2 - D/2\right]\left(m_r^2\right)^{D/2-2}\,. \qquad (4.39)$$

To regularise the theory we have used the usual MS scheme with the dimensional regularisation ($D \neq 4$). The high temperature expansion of the pressure (4.38) to all orders can be found in Section 3.4 where the calculations, however, were approached from a different standpoint.

4.4.2 Off–equilibrium I

The next question to be addressed is how the above calculations are modified in the non–equilibrium case. To see that let us choose the following constraint

$$g(\mathbf{k}) = \langle \mathcal{H}(\mathbf{k}) \rangle |_{t_i} = \langle \tilde{\mathcal{H}}(\mathbf{k}) \rangle |_{t_i} \, . \tag{4.40}$$

Here t_i is arbitrary, and function $g(\mathbf{k})$ is specified by theory/experiment. The $\tilde{\mathcal{H}}(\mathbf{k})$ is a quadratic operator fulfilling the condition $\langle \mathcal{H} \rangle |_{N\to\infty} = \langle \tilde{\mathcal{H}} \rangle$. As $g(\mathbf{k})$ is finite, both $\mathcal{H}$ and $\tilde{\mathcal{H}}$ must be renormalised (i.e. we must subtract the zero temperature part). Obviously

$$\tilde{\mathcal{H}}(\mathbf{k}) = \omega_k a^{\dagger}(\mathbf{k}) a(\mathbf{k}) \, ,$$

with $\omega_k = \sqrt{\mathbf{k}^2 + \mathcal{M}^2}$ and

$$\mathcal{M}^2 = m_0^2 + \frac{i}{2}\lambda_0 \int \frac{d^d k'}{(2\pi)^d} \mathbb{G}_{++}(k') \, . \tag{4.41}$$

In the large–N limit the corresponding density matrix (4.19) reads

$$\rho = \frac{1}{\mathcal{Z}(\beta)} \exp\left(- \int \frac{d^3\mathbf{k}}{(2\pi)^3 2\omega_k} \beta(\mathbf{k}) \tilde{\mathcal{H}}(\mathbf{k}) \right) \, , \tag{4.42}$$

with $\beta(\mathbf{k})/2(2\pi)^3\omega_k$ being the Lagrange multiplier to be determined. Using Eq.(4.21), we find that

$$g(\mathbf{k}) = \frac{V}{(2\pi)^3} \frac{\omega_k}{e^{\beta(\mathbf{k})\omega_k} - 1} \, , \tag{4.43}$$

where V denotes the volume of the system. Clearly, expression (4.43) can be interpreted as the density of energy per mode. The fact that $\beta(\mathbf{k})$ is not constant indicates that different modes have different ‘temperatures’.

The Kadanoff–Baym equations coincide in this case with those in (4.34) provided $m_r(T) \rightarrow \mathcal{M}$. The boundary condition can be worked out simply using the prescription (4.24). This gives

$$\mathbb{G}_{+-}(k) = e^{-\beta(\mathbf{k})k_0}\mathbb{G}_{-+}(k)\,. \tag{4.44}$$

The fundamental solution of the Kadanoff–Baym equation is

$$\mathbb{G}_{\alpha\beta}(k) = \frac{(\sigma_3)_{\alpha\beta}}{k^2 - \mathcal{M}^2 + i\epsilon_{\alpha\beta}} - 2\pi i\delta(k^2 - \mathcal{M}^2)f_{\alpha\beta}(k)\,,$$

$$\epsilon_{\alpha\beta} = \epsilon(\sigma_3)_{\alpha\beta}\,. \tag{4.45}$$

Let us mention one more point. The boundary condition (4.44) is not by itself sufficient to determine $f_{\alpha\beta}$'s. (This fact is often overlooked even in the equilibrium QFT.) It is actually necessary to substitute this condition with an additional condition, namely the condition of causality. The causality condition, i.e. vanishing of the commutator $[\Phi(x), \Phi(y)]$ for $(x-y)^2 < 0$, importantly restricts the class of possible $f_{\alpha\beta}$'s. To see this, let us look at the Pauli–Jordan function $\langle\, [\Phi(x), \Phi(y)]\rangle$. The latter is the homogeneous solution of the Kadanoff–Baym equation with the initial–time value data: $\langle\, [\Phi(x), \Phi(y)]\rangle|_{x_0=y_0} = 0$ (i.e. causality condition) and $\partial_0\langle\, [\Phi(x), \Phi(y)]\rangle|_{x_0=y_0} = -\delta^3(\mathbf{x}-\mathbf{y})$. Thus the Pauli–Jordan function is uniquely determined and its Fourier transform reads

$$\text{F.T.}(\langle[\Phi(x), \Phi(y)]\rangle)(k) = -i2\pi\delta(k^2 - \mathcal{M}^2)\,\varepsilon(k_0)\,. \tag{4.46}$$

Relation (4.46) immediately implies that

$$f_{+-}(k) = \theta(-k_0) + \tilde{f}(k)$$

$$f_{-+}(k) = \theta(k_0) + \tilde{f}(k)\,, \tag{4.47}$$

with $\tilde{f}$ being, so far arbitrary, and for both f_{+-} and f_{-+} identical, function. The $\tilde{f}$ is then fixed via the generalised KMS condition (4.44). Similarly, the causality condition specifies that $\mathbb{G}_{++}(k) - \mathbb{G}_{--}(k) = \mathrm{PP}\{\,1/(k^2 - \mathcal{M}^2)\}$ (the symbol 'PP' denotes the principal part). By inspection of the definition of $\mathbb{G}_{\alpha\beta}$ one may easily realise that

$$\begin{aligned} \mathbb{G}_{++} + \mathbb{G}_{--} &= \mathbb{G}_{+-} + \mathbb{G}_{-+} \\ \mathbb{G}_{+-}(k) &= -(\mathbb{G}_{+-}(-k))^* \\ \mathbb{G}_{++}(k) &= -(\mathbb{G}_{--}(-k))^* \qquad . \end{aligned} \tag{4.48}$$

From these relations follows that $f_{++} = f_{--} = \tilde{f}$ and $\tilde{f}(k) = (\tilde{f}(-k))^*$. The $\tilde{f}$ is the same as in (4.47).

Since the divergences in $\mathbb{G}_{\alpha\beta}$ come from the first term in (4.45) (i.e. from the particular solution), we can shift the corresponding (zero temperature) poles at $D = 4$ to the bare mass. In this case we can write

$$\mathcal{M}^2 \equiv m_r^2 + \delta m^2\,, \tag{4.49}$$

where m_r is the renormalised mass in the vacuum and δm is the mass shift due to an interaction with the non–equilibrium medium. Inserting the '++' components of (4.45) into (4.41), we obtain

$$\mathcal{M}^2 = m_0^2 + \frac{1}{2}\lambda_0 \left[\frac{\mathcal{M}^{D-4}}{(4\pi)^{\frac{D}{2}}} \Gamma\left[1 - D/2\right] + N(\mathcal{M}^2) \right]\,, \tag{4.50}$$

where

$$N(\mathcal{M}^2) = \int \frac{d^D k}{(2\pi)^D} 2\pi\delta(k^2 - \mathcal{M}^2) f_{++}(k)\,. \tag{4.51}$$

In an equilibrium system f_{++} would be the Bose–Einstein distribution f_B. Note that because (4.51) corresponds to a homogeneous solution of the Kadanoff–Baym equation at $|x-y|=0$ it is automatically finite. Thus for a translationally invariant medium (both equilibrium and non–equilibrium) f_{++} must act as a regulator in the UV region.

Let us consider the expression for the expectation value of $\Theta^{\mu\nu}$ given in (4.31). It is a matter of a few lines to show that

$$\langle\Theta^{\mu\nu}\rangle_r = iN\int\frac{d^Dk}{(2\pi)^D}k^\mu k^\nu\left[\mathbb{G}_{++}(k)-\mathbb{G}(k)\right] - i\frac{N}{4}g^{\mu\nu}\delta m^2\int\frac{d^Dk}{(2\pi)^D}\left[\mathbb{G}_{++}(k)+\mathbb{G}(k)\right]\,, \tag{4.52}$$

with $\mathbb{G}$ being the $T=0$ causal Green function. Using (4.39), (4.41) and (4.45) one may directly check that Eq.(4.52) does not contain UV singularities when the limit $D\to 4$ is taken. This verifies our introductory remark, that (4.37) is finite even in non–equilibrium context. From the generalised KMS condition (4.44) and from (4.45) we obtain that f_{++} is

$$f_{++}(k)=\frac{1}{e^{\beta(\mathbf{k})\omega_k}-1}\,. \tag{4.53}$$

So far the results obtained were completely general and valid for any translationally invariant system. Let us now consider a system in which $g(\mathbf{k})=\frac{V\omega_k}{(2\pi)^3}\exp\left(-\omega_k/\sigma\right)$. As we shall see, this condition corresponds to systems where the lowest frequency modes depart from strict equilibrium, whilst the high energy ones obey standard Bose–Einstein statistics. This behaviour is typical of many off–equilibrium systems, eg. ionised atmosphere [108], laser stimulated plasma [109], hot fusion [110], etc. The σ is usually referred to as the ionisation half–width of the energetical spectrum. From (4.43) we can determine $\beta(\mathbf{k})$ as a function of the physical parameter σ:

$$\beta(\mathbf{k}) = \frac{1}{\sigma} + \frac{1}{\omega_k}\sum_{n=1}^{\infty}\frac{(-1)^{n+1}}{n}e^{-n\omega_k/\sigma}\,. \tag{4.54}$$

To proceed, some remarks on the interpretation of $\beta(\mathbf{k})$ are necessary. Firstly, Eq.(4.54) implies that for a sufficiently large ω_k ($\omega_k \gg \sigma$) the function $\beta(\mathbf{k})$ is approximately constant, and equals $1/\sigma$. Thus at high energies the distribution f_{++} approaches the Bose–Einstein distribution with the global temperature $T \approx \sigma$. In other words, only the soft modes were sensitive to processes which created the non–equilibrium situation. The interpretation of σ as an equilibrium temperature, however, fails whenever $\sigma \approx \omega_k$. Instead of σ one may alternatively work with the expectation value of $\beta(\mathbf{k})$, i.e.

$$\begin{aligned}\langle\beta\rangle &= \frac{\int d^3\mathbf{k}\,\beta(\mathbf{k})e^{-\omega_k/\sigma}}{\int d^3\mathbf{k}\,e^{-\omega_k/\sigma}}\\ &= \frac{1}{\sigma} + \frac{\sum_{n=1}^{\infty}\frac{(-1)^{n+1}}{n(n+1)}K_1((n+1)\mathcal{M}/\sigma)}{\mathcal{M}K_2(\mathcal{M}/\sigma)}\,,\end{aligned} \tag{4.55}$$

where K_n is the Bessel function of imaginary argument of order n. Because the system is for the significant part of the energetical spectrum in thermal equilibrium, $1/\langle\beta\rangle$ approximates the corresponding equilibrium temperature to high precision. An interesting feature of (4.55) is that it is quite insensitive to the actual value of $\mathcal{M}$. Dependence of $\langle\beta\rangle$ on $\mathcal{M}$ for a sample value $\sigma = 100$MeV is depicted in FIG.4.1. An important observation is that the asymptotic behaviour of $\langle\beta\rangle$ at $\sigma \to \infty$ goes like $\langle\beta\rangle \approx a/\sigma$, where $a = 1 + \frac{1}{2}\sum_{n=1}^{\infty}\frac{(-1)^{n+1}}{n(n+1)^2} = \ln 2 + \pi^2/24 \approx 1.1$.

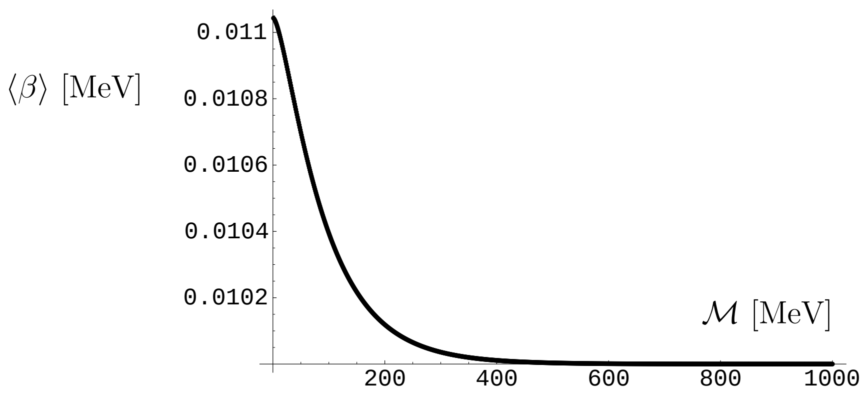

Figure 4.1: A plot of $\langle\beta\rangle$ vs. $\mathcal{M}$ at $\sigma = 100$ MeV.

Using (4.37) and (4.52) we get for the pressure per particle

$$\mathcal{P}(\sigma) = \frac{1}{2\pi^2}\left[\mathcal{M}^2\sigma^2 K_2(\mathcal{M}/\sigma) + \frac{\delta m^2}{4}\mathcal{M}\sigma K_1(\mathcal{M}/\sigma)\right] - \mathcal{P}_0\,, \tag{4.56}$$

where

$$\mathcal{P}_0 = \frac{1}{384\pi^2}(\delta m^2)m_r^2\left(2 + \frac{\delta m^2}{m_r^2}\right) + \frac{1}{64\pi^2}m_r^4\left(1 + \frac{\delta m^2}{m_r^2}\right)\ln\left(1 + \frac{\delta m^2}{m_r^2}\right)\,. \tag{4.57}$$

Note that $\mathcal{P}_0$ comes from the UV divergent parts of (4.52). Whilst the separate contributions are UV divergent, they cancel between themselves leaving behind the finite $\mathcal{P}_0$. As we already emphasised, the divergences come from the particular solutions of the Kadanoff–Baym equations. Because the former do not directly reflect the boundary conditions, the form of $\mathcal{P}_0$ must be identical for any translationally invariant medium. The non–trivial information about the non–equilibrium pressure is then encoded in terms in the brace [. . .] in (4.56).

Let us now perform the "high–temperature" expansion of the pressure (4.56). As a "temperature" parameter we may chose σ. In this case we have

$$\begin{aligned}
P(\sigma) &= \frac{\sigma^4}{\pi^2} - \frac{\sigma^2}{2\pi^2}\left(\mathcal{M}^2 - \frac{\delta m^2}{4}\right) \\
&- \ln\left(\frac{\mathcal{M}}{2\sigma}\right)\sum_{k=0}^{\infty} C_k(2\mathcal{M}^2 - \delta m^2\,(k+2)) \\
&- \sum_{k=0}^{\infty} C_k\left\{\delta m^2\left(\psi(k+1) + \frac{1}{2(k+1)}\right)(k+2)\right. \\
&- \left.\mathcal{M}^2\left(2\psi(k+1) + \frac{(2k+3)}{(k+1)(k+2)}\right)\right\} - \mathcal{P}_0\,,
\end{aligned} \tag{4.58}$$

where

$$C_k = \frac{\mathcal{M}^{2k+2}}{\pi^2 2^{2k+4} k!(k+2)!\,\sigma^{2k}}\,.$$

The $\psi(\ldots)$ is Euler's psi function. For a sufficiently large σ the leading behaviour of δm^2 may be easily evaluated. To do this, let us first assemble (4.39) and (4.49)–(4.51) together. This gives us the (renormalised) gap equation

$$\begin{aligned}
\delta m^2 &= \frac{1}{2\lambda_0}\left\{\frac{\Gamma[1-\frac{D}{2}]}{(4\pi)^{\frac{D}{2}}}\left(\mathcal{M}^{D-4} - m_r^{D-4}\right) + N(\mathcal{M}^2)\right\} \\
&= \frac{\lambda_r}{2}\left\{\tilde{\Sigma}(m_r^2, \delta m^2) + \frac{1}{2\pi^2}\sigma\mathcal{M}K_1[\mathcal{M}/\sigma]\right\}\,,
\end{aligned} \tag{4.59}$$

with

$$\frac{1}{2}\tilde{\Sigma}(\ldots) = \frac{1}{32\pi^2}\left\{(m_r^2 + \delta m^2)\ln\left(1 + \frac{\delta m^2}{m_r^2}\right) - \delta m_r^2\right\}\,.$$

Setting $x = \delta m^2/m_r^2$ and $s = \sigma/m_r$ we obtain the following transcendental equation for x

$$\lambda_r^{-1} = \frac{1}{32\pi^2}\left\{\frac{1}{x}\left[(1+x)\ln(1+x) - x + 8s\sqrt{1+x}\,K_1[\sqrt{1+x}/s]\,\right]\right\}\,. \tag{4.60}$$

The graphical representation of Eq.(4.60) is depicted in FIG.4.2.

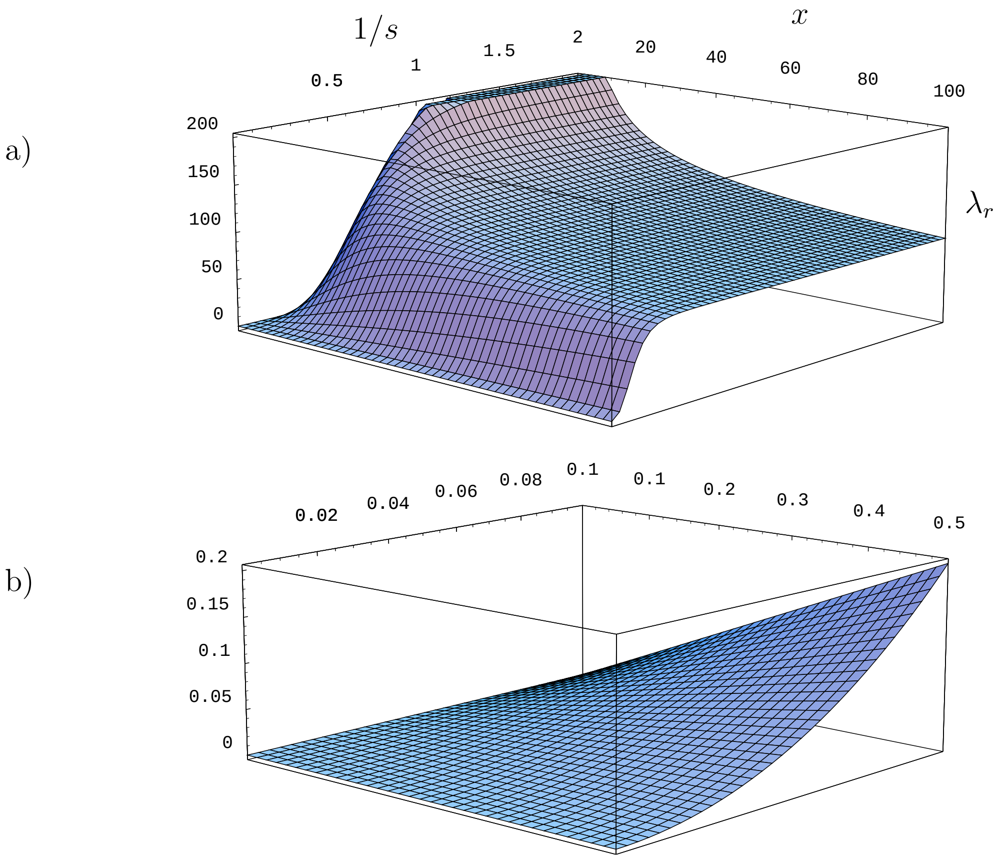

Figure 4.2: A plot of the Eq.(4.60): a) the general shape, b) a small x behaviour.

From this one may read off that for large x ($x > 50$) there exists a critical value of λ_r above which the gap equation has no solution. (The plateau is actually bent downward with a very gentle slope.) FIG.4.2b clearly shows that if $\lambda_r \ll 1/s < 1$ then $x \ll 1$. Using the asymptotic behaviour of $K_1[z]$ for $z \to 0$ ($K_1 \sim (z)^{-1}$) we arrive at more precise estimate of λ_r for which $x \ll 1$; namely $\lambda_r \approx 1/s^2 = m_r^2/\sigma^2$. This estimate is very helpful for the asymptotic expansion of δm^2. For a sufficiently high σ we may write

$$\begin{aligned} \delta m^2 &= \lambda_r \left\{ \frac{\frac{(\delta m^2)^2}{2m_r^2} - \frac{(\delta m^2)^3}{6m_r^4} + \frac{(\delta m^2)^4}{12m_r^6} + \ldots}{32\pi^2} + \frac{1}{4\pi^2}(\sigma\mathcal{M}\ K_1[\mathcal{M}/\sigma])|_{\sigma\to\infty} \right\} \\ &= \frac{\lambda_r \sigma^2}{4\pi^2} + \mathcal{O}(\mathcal{M}\ln(\mathcal{M}/\sigma))\,. \end{aligned} \tag{4.61}$$

Inserting this back into (4.56) we get

$$\mathcal{P}(\sigma) = \frac{\sigma^4}{\pi^2} - \frac{\sigma^2\,\mathcal{M}^2}{2\pi^2} + \frac{\lambda_r}{8}\left(\frac{\sigma^2\mathcal{M}^2}{64\pi^4} - \frac{\sigma^4 3}{4\pi^4}\right) + \mathcal{O}\left(\mathcal{M}^2\ln(\mathcal{M}/\sigma); \lambda_r^2\right)\,. \tag{4.62}$$

It is interesting to note that $1/\pi^2 \approx \pi^2/97$ which is almost the Stefan–Boltzmann constant. This once more vindicates our interpretation of σ as a "temperature". A plot of the pressure as a function of σ is depicted in FIG.4.3.

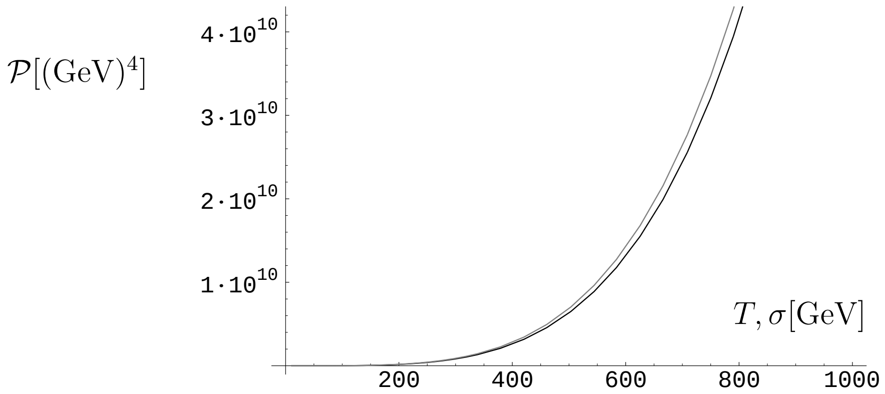

Figure 4.3: A plot of pressure as a function of T, σ for $m_r = 100$MeV. The gray line corresponds to equilibrium pressure, the black line corresponds to pressure (4.62).

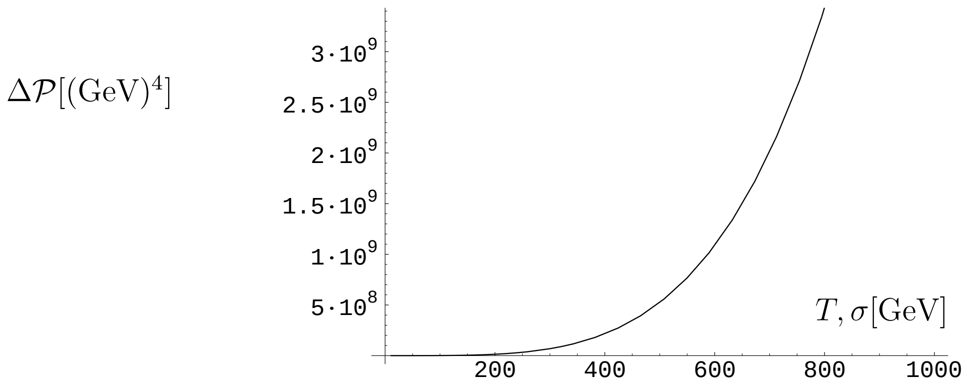

Figure 4.4: A plot showing the difference of equilibrium and non–equilibrium pressures for $m_r =$ 100MeV.

It is due to the low frequence modes contribution to the pressure that $P(\sigma) < P(T)$. This is a direct result of our choice of $g(\mathbf{k})$, namely that σ cannot be interpreted as temperature for the low frequence modes (i.e. $\omega_k < \sigma$). The smaller σ is the less important contribution from non–equilibrium soft modes and so the smaller difference between both pressures.

The result (4.62) can be alternatively rewritten in terms of $\langle\beta\rangle$. Using, for instance, the Padé approximation [111] for $\langle\beta\rangle$, we arrive at

$$\begin{aligned}
\mathcal{P}(\langle\beta\rangle) &= 0.0681122\,\langle\beta\rangle^{-4} - 0.0415368\,\langle\beta\rangle^{-2}\mathcal{M}^2 \\
&+ \lambda_r\left(-0.000647\,\langle\beta\rangle^{-4} + 0.0000164\,\langle\beta\rangle^{-2}\,\mathcal{M}^2\right) \\
&+ \mathcal{O}\left(\mathcal{M}^2\ln(\mathcal{M}\langle\beta\rangle);\lambda_r^2\right) . \qquad (4.63)
\end{aligned}$$

The coefficient $0.0681122 \approx \pi^2/145$ is 1.6 times smaller than the required value for the Stefan–Boltzmann constant, so the parameter $\langle\beta\rangle$ is a slightly worse approximation of the equilibrium temperature than σ. In practice, however, it is a matter of taste and/or a particular context which of the above two descriptions is more useful.

4.4.3 Off–equilibrium II

As was noted above, it is the specific form of the constraint $g(\mathbf{k})$ which prescribes the behaviour of $\beta(\mathbf{k})$. Let us now turn our attention to systems which depart 'slightly' from equilibrium, i.e. when $g(\mathbf{k})$ in (4.40) deviates a little from the equilibrium density of energy per mode. In this case the constraint (4.40) reads

$$g(\mathbf{k}) = \frac{V}{(2\pi)^3}\,\frac{\omega_k}{e^{\beta_0\omega_k}-1} + \delta g(\mathbf{k});\quad \delta g(\mathbf{k}) \ll g(\mathbf{k})\,, \tag{4.64}$$

with $\beta_0 = 1/T_0$ being an inverse of the equilibrium temerature. As a special example of (4.64) we choose

$$g(\mathbf{k}) = \frac{V}{(2\pi)^3}\,\frac{\omega_k}{e^{\beta_0\omega_k}\alpha^{-1}(\mathbf{k})-1};\quad \alpha(\mathbf{k},\beta_0) \approx 1\,. \tag{4.65}$$

The inverse mode "temperature" $\beta(\mathbf{k})$ is then $\beta_0 - \ln(\alpha(\mathbf{k}))/\omega_k$. So $\ln(\alpha)$ measures (in units of ω_k) the deviation of the mode temperature from the equilibrium one. The particular value of $\alpha(\mathbf{k},\beta_0)$ depends on the actual way in which the system is prepared. To avoid unnecessary technical complications, we select $\alpha(\mathbf{k},\beta_0)$ to be a momentum–space constant (generalisation is, however, straightforward). This choice represents the change in the mode temperature which is now inversely proportional to ω_k; the deviation is bigger for soft modes and is rapidly suppressed for higher modes. Obviously, T_0 becomes the global temperature if $\omega_k \gg \ln(\alpha)$. The generalised KMS conditions (4.44) together with solutions (4.45) determine f_{++} as

$$f_{++}(k) = \frac{\alpha}{e^{\beta_0\omega_k}-\alpha}\,. \tag{4.66}$$

Eq.(4.66) is a reminiscent of the, so called, Jüttner distribution[5] with fugacity α [112, 113].

---

[5] It should be mentioned that this similarity is rather superficial. The Jütner distribution describes

Now, using (4.37) and (4.52) we get for the pressure per particle

$$\mathcal{P}(T_0) + \mathcal{P}_0 = \frac{1}{2\pi^2}\left[\frac{\mathcal{M}^2}{\beta_0^2}\sum_{n=1}^{\infty}\frac{\alpha^n}{n^2}K_2(n\mathcal{M}\beta_0) + \frac{\mathcal{M}\delta m^2}{4\beta_0}\sum_{n=1}^{\infty}\frac{\alpha^n}{n}K_1(n\mathcal{M}\beta_0)\right], \tag{4.67}$$

where δm^2 satisfies the gap equation

$$\delta m^2 = \frac{\lambda_r}{2}\left(\tilde{\Sigma}(m_r^2, \delta m^2) + \frac{1}{2\pi^2}\int_0^{\infty}\frac{k^2 dk}{\omega_k}\frac{\alpha}{e^{\beta_0\omega_k} - \alpha}\right). \tag{4.68}$$

If we set, as before, $x = \delta m^2/m_r^2$ and $s = 1/\beta_0 m_r$ we get the transcendental equation for x

$$\lambda_r^{-1} = \frac{1}{32\pi^2 x}\left\{(1+x)\ln(1+x) - x + 8(1+x)\int_1^{\infty} dz\,\sqrt{z^2-1}\,\frac{\alpha}{e^{z\sqrt{x+1}/s} - \alpha}\right\}. \tag{4.69}$$

The corresponding numerical analysis of (4.69) reveals that for $x \ll 1$, $1/s \ll 1$. So at $x \ll 1$, $\lambda_r \approx \delta m^2/T_0^2$. This estimate is important for the asymptotic expansion of δm^2. However, in order to carry out the asymptotic expansion of (4.68) (and consequently (4.67)) we need to cope first with the sum $\sum_{n=1}^{\infty}\alpha^n K_k(n\mathcal{M}\beta_0)/n^k$ $(k = 1, 2)$ (also called Braden's function). Expansion of $K_k(\ldots)$ yields a double series which is very slowly convergent, and so it does not allow one to easily grasp the leading behaviour in T_0. In this case it is useful to resume (4.67)–(4.68) by virtue of the Mellin summation technique [36]. (It is well known [36, 74, 82] that at equilibrium this resummation leads to a rapid convergence for high temperatures.) As a result, for a sufficiently large T_0 we get

$$\delta m^2 \;=\; \frac{\lambda_r T_0^2}{24} - \frac{\lambda_r T_0 \mathcal{M}}{4\pi}\left[\frac{1}{2}(1-r^2)^{1/2}\right.$$

---

systems which are in thermal but not chemical equilibrium. (As we do not have a chemical potential, chemical equilibrium is ill defined concept.) The fugacity then parametrises the deviation from chemical equilibrium.

$$
\begin{aligned}
&- \;\; r\left(1-\ln\left(\frac{\mathcal{M}}{2T_0}\right)\right) - (1-r^2)^{1/2}\arcsin(r)\Big] \\
&+ \;\; \mathcal{O}(\ln T_0)\,,
\end{aligned}
\tag{4.70}
$$

where we have set $r = \ln(\alpha)T_0/\mathcal{M}$. The corresponding expansion of the pressure (4.67) reads

$$
\begin{aligned}
\mathcal{P}(T_0) \;=\;& \frac{\pi^2 T_0^4}{90} + \frac{\mathcal{M}\zeta(3)}{\pi^2}T_0^3 r - \frac{T_0^2\mathcal{M}^2}{24}\left(1-2r^2\right) - \frac{\mathcal{M}^3 T_0}{4\pi^2} \\
\times\;& \Big[-\frac{1}{3}\left(1-r^2\right)^{\frac{3}{2}} + \frac{r}{2}\left(1-\frac{2}{3}r^2\right)\left(1-2\ln\left(\frac{\mathcal{M}}{2T_0}\right)\right) \\
-\;& \frac{2}{9}\left(1-r^2\right)\Big(-r^3+3-3\left(1-r^2\right)^{\frac{1}{2}}\Big)\arcsin(r)\Big] \\
+\;& \frac{(\delta m^2)^2}{2\lambda_r} + \mathcal{O}(\ln T_0)\,.
\end{aligned}
\tag{4.71}
$$

where $\zeta(3) \approx 1.202$. Note that for $\alpha = 1$ we regain the equilibrium expansion (4.38). The corresponding plot of $\mathcal{P}$ as a function of T_0 and α is depicted in FIG.4.5.

In passing it may be mentioned that the expansion (4.71) is mathematically justifiable only for $\alpha \approx e^{\sqrt{\lambda_r/24}\,r} \approx 1$.

4.5 Conclusions

In order to get a workable recipe for non–equilibrium pressure Jaynes–Gibbs principle of maximal entropy, the Dyson–Schwinger equations, and the hydrostatic pressure. The basic steps are as follows.

To find quantitative results for pressure one needs to know the explicit form of the Green's functions involved. These may be find if we solve the Dyson–Schwinger equations. The corresponding solutions are unique provided we specify the density matrix ρ (the construction of ρ is one of the cornerstones of our approach, and we tackled this problem

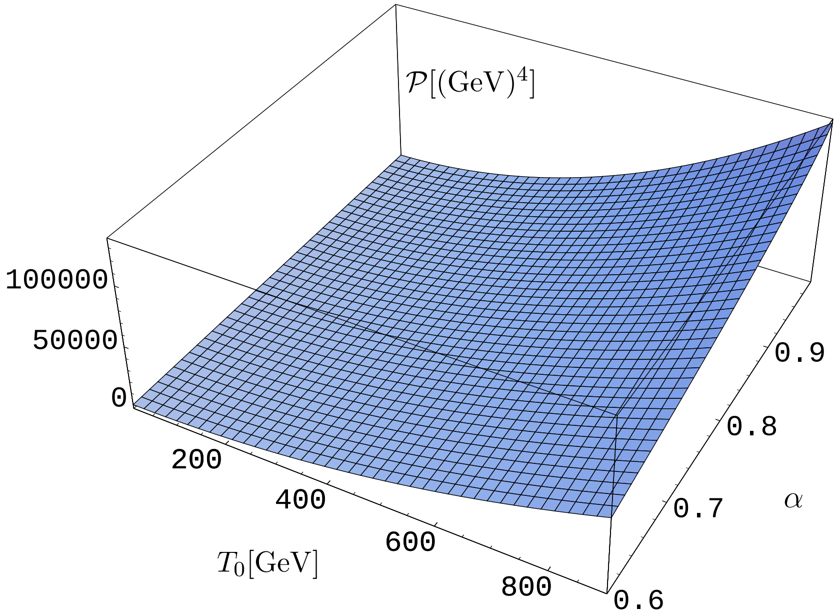

Figure 4.5: Behaviour of the pressure (4.67) as a function of α and T_0 at $m_r = 100$MeV.

using the Jaynes–Gibbs principle of maximal entropy). With ρ at our disposal we showed how to formulate the generalised Kubo–Martin–Schwinger (KMS) boundary conditions.

To show how the outlined method works we have illustrated the whole procedure on an exactly solvable model, namely $O(N)$ Φ^4 theory in the large–N limit. This model is sufficiently simple yet complex enough to serve as an illustration of basic characteristics of the presented method in contrast to other ones in use. In order to find the constraint conditions we have considered two gedanken experiments in which the system in question was prepared in such a way that only low frequence modes departed from the strict equilibrium behaviour. Such processes can be found, for example, in ionised atmosphere, in laser stimulated plasma or in hot fusion. In both alluded gedanken experiments we were able to work out the hydrostatic pressure exactly. Furthermore, after identifying a "temperature" parameter (virtually temperature of high modes) we carried out the corresponding high–temperature expansions.

As it was discussed, one of the main advantages of the Jaynes–Gibbs construction is that one starts with the (physical) constraints (i.e. parameters which are really controlled and measured in experiments). These constraints directly determine the density matrix and hence the generalised KMS conditions for the Dyson–Schwinger equations. This contrasts with the usual approaches where the density matrix is treated as the primary object. In these cases it is necessary to solve the von Neumann–Liouville equation. This is usually circumvent using either variational methods [100,103] with several trial ρ's or reformulating the problem in terms of the quantum transport equations for Wigner's functions [23]. It is, however, well known that the inclusion of constraints into transport equations is a very delicate and rather complicated task (the same is basically true about the variational methods) [23, 114].

Chapter 5

Summary and outlooks

In this dissertation we have explored various aspects of equilibrium and non–equilibrium quantum field theory.

In Chapter 2 we dealt with certain aspects of infrared effects in finite–temperature QFT. It is well known [34, 36] that these effects are far more subtle at finite temperature than at $T = 0$. The latter is ascribed to the fact that there is no finite–temperature Bloch–Nordsieck mechanism [53, 115] at our disposal. Intuitively, however, one might expect that if thermal QFT is a well posed theory, no infrared divergences should be present. This point was extensively studied on particles that decay and scatter inside a plasma (or heat bath). As a byproduct we proposed an easy mathematical formalism allowing one to calculate the plasma particle number spectrum formed when a particle(s) decays (scatter) within the plasma. This formalism which is based on the largest–time equation and the Dyson–Schwinger equations, is embodied in a one–line modification to the corresponding thermal cut diagrams. Such diagrams arise naturally when the imaginary part of a Green function is computed, and the whole calculations are immensely simplified by the observation that the thermal cut diagrams are virtually the same as the Kobes–Semenoff diagrams in the Keldysh formalism.

The vital part of Chapter 2 was dedicated to the study of the modifications which must be made in various quantum field contexts (scalar fields, spinor fields and gauge fields in temporal gauge). It was found that the modified propagators have an easy interpretation in terms of emission, absorption and fluctuation of the plasma particles. To demonstrate how the method works, we used various heat baths (photon, and electron–photon) in which two uncharged scalar particles scatter into a pair of charged particles. We calculated the leading ω behaviour for the resulting changes in the plasma particles number spectra. We also found that the energy density $\omega dN/d\omega$ is finite as ω tends to zero.

In Chapter 3 we have turned our attention to pressure. Pressure is undoubtedly one of the important parameters characterising quantum media at finite temperature. An extension of the pressure calculations to off–equilibrium systems should enhance our predicative ability in such areas as (realistic) phase transitions, early universe cosmology or hot fusion dynamics. Unfortunately, the standard approaches based on the partition function do not allow such an extension because there is no such thing as the grand–canonical potential away from equilibrium. We considered an alternative approach based on the, so called, hydrostatic pressure. As a warming up exercise we started with thermal equilibrium. The whole procedure was then illustrated on a toy model ($\lambda\Phi^4$ theory with $O(N)$ internal symmetry in the large–N limit). The result obtained matches that found in [61] for the thermodynamic pressure. (Whilst these two pressures agree in equilibrium , there is *no* thermodynamic pressure out of equilibrium.)

We took advantage to probe various mathematical techniques (composite operators renormalisation, Dyson–Schwinger diagrammatic equations, finite temperature coupling renormalisation, Mellin transform) which are indispensable in calculations of the hydrostatic pressure (most of them also being applicable to non–equilibrium as well). One of the key results obtained was the prescription for the renormalised pressure (Eqs.(3.36), (4.40) and (4.37)). This was achieved by means of the Zimmerman forest formula.

The model in question has the undeniable merit of being exactly solvable. In particular, one could find the pressure by means of a non–perturbative treatment. This is because of the fact that the large–N limit eliminates 'nasty' classes of diagrams in the Dyson–Schwinger expansions. The surviving class of diagrams (superdaisy diagrams) could be exactly resumed because the (thermal) proper self–energy $\mathbf{\Sigma}$ as well as the renormalised coupling constant λ_r were momentum independent. The resulting expression for the pressure obtained was then in a suitable form which allowed us to take advantage of the Mellin transform technique, and we were able to evaluate the pressure in $D = 4$ (both for massive and massless fields) to all orders in the high–temperature expansion.

As we have already mentioned, there are various motivations to be interested in the non–equilibrium pressure. One of them is based on the belief that the pressure (as an easily measurable parameter) should exhibit a discontinuity in its derivative(s) when a local phase transition occurs. This has been observed in solid state physics and fluid dynamics and it may play a central role in, for example, detection of the quark–gluon plasma or in various baryogenesis scenarios.

In Chapter 4 we approached the problem of pressure in a non–equilibrium quantum plasma by extending the notion of the hydrostatic pressure to systems out of equilibrium. On the equilibrium level the hydrostatic pressure; i.e. $p = -\frac{1}{3}\langle \Theta^{i}{}_{i} \rangle$ (here $\Theta^{\mu\nu}$ is the energy–momentum tensor of a system in question), has a well defined microscopic picture, which can be carried over to an off–equilibrium as we have showed in Chapter 3. Unlike in equilibrium, the non–equilibrium expectation value is sensitive to the particular choice of the energy–momentum tensor (see Chapter 3), though fortunately in translationally invariant media this sensitivity is not relevant. Our strategy for the calculation of pressure was simple. To find quantitative results for pressure one needs to know the explicit form of the Green's functions involved. These may be found if we solve the corresponding Dyson–Schwinger equations. The solution is unique provided we specify the density matrix ρ, and hence the generalised KMS conditions. In order to construct the density matrix we invoke the Jaynes–Gibbs principle of maximal entropy. The Jaynes–Gibbs principle is basically the Bayesian inference about the most probable density matrix ρ. This is based on the maximalisation of the Shannon (or information) entropy, subject to the prior knowledge which one has about the system (usually specified at some initial time t_i).

To show how the outlined method works we have illustrated the whole method on our favoured $O(N)$ Φ^4 theory in the large–N limit. In order to specify the initial–time constraints we have considered two gedanken experiments in which the system in question was prepared in such a way that only low frequency modes departed from the strict equilibrium behaviour. Such processes can be found, for example, in ionised atmosphere, in laser stimulated plasma or in hot fusion heated up by ultra–sound waves. Furthermore, after identifying a "temperature parameter" (virtually the temperature of the high modes) we carried out the corresponding high–temperature expansions. The leading high–temperature coefficients coincided to a good approximation with the Stefan–Boltzmann constant which is precisely what one would expect: at high "temperature" particles do no feel non–equilibrium "background" and consequently their distribution approaches the equilibrium one.

The next logical step in our investigation would be to calculate the pressure in a non–equilibrium, non–translationally invariant medium. In contrast to the previous situation, one is confronted now with two conceptual difficulties. As we have shown in Section 4.4.2, in order to get the renormalised pressure one has to consistently use the renormalised energy–

momentum tensor ($\Theta^{\mu\nu}$ is a composite operator). Unfortunately there are infinitely many renormalised energy–momentum tensors (generated from each other via Pauli's transformation), and these give rise to different pressures. The choice of the "correct" $\Theta^{\mu\nu}$ is then crucial for the next investigation. (As we discussed in Sections 3.2 and 4.4, in translationally invariant media pressure does not depend on a particular form of $\Theta^{\mu\nu}$.) Our future strategy is based on the observation that because the pressure is an observable, one should obviously work with an energy–momentum tensor which is an observable as well (or the corresponding Hermitian operator). We propose to use the Belinfante energy–momentum tensor. The fact that the physical significance of the Belinfante tensor (both in classical and quantum systems) is greater than that of other energy–momentum tensors was pointed out successively by Belinfante [116], Rosenfeld [117] and Jackiw [68]. In scalar QFT the Belinfante energy-momentum tensor coincides with the, so called, improved energy–momentum tensor [68]. The generic form of the improved energy–momentum tensor for the $O(N)$ Φ^4 theory was derived in Section 3.2 Eq.(3.33). Because the corresponding β function is exactly solvable in the–large N limit [13] we expect that constant $c(\lambda_r; D)$ is exactly solvable as well, and consequently the improved energy–momentum tensor can be written in closed form.

The second problem to be solved is connected with the fact that the corresponding Dyson–Schwinger equations are far more involved than in the translationally invariant case. Even, for the $O(N)$ Φ^4 theory in the large–N limit the Kadanoff–Baym are not any more hyperbolic equations. This fact, among others, complicates the renormalisation program (one cannot use the momentum space renormalisation). For this purpose we intend to resort to differential renormalisation [118]. Solving the renormalised Kadanoff–Baym equations (at least numerically) is the next step in our study.

Appendix A

Finite–temperature Dyson–Schwinger equations

A.1 Functional formalism

Eq.(2.18) gives us an alternative definition of Wick's theorem in terms of the "functional derivation" $\frac{\delta}{\delta\psi(x)}$. We refer to Eq.(2.18) as the Dyson–Schwinger equation because the classical $T = 0$ Dyson–Schwinger equations are implied by it (see Appendix A.3). Let us first show that (2.18) is consistent with Wick's theorem (2.16)–(2.17). To be specific, let us consider an ensemble of non–interacting particles in thermodynamical equilibrium. In order to keep the work transparent, we shall suppress all the internal indices. There is no difficulty whatsoever in reintroducing the necessary details. Let us first realize that for any (well behaved) functional the following Taylor's expansion holds [42]

$$X[\psi] = \sum_n \int dx_1 \dots \int dx_n \alpha^n(x_1 \dots x_n)\psi(x_1)\dots\psi(x_n)\,, \tag{A.1}$$

The same is true if ψ is an operator instead. In the latter case the $\alpha^n(\dots)$ are not generally symmetric in the x's [1]. When Fermi fields are involved, we might, for the sake of compactness, include in the argument of ψ the space-time coordinate, the Dirac index, and a discrete index which distinguishes ψ_α from $\overline{\psi}_\alpha$. In the latter case $\int dx \to \sum \int dx$, where summation runs over the discrete indices. With this convention, the expansion (A.1) holds even for the Fermi fields. An extension of (A.1) to the case where different fields are present is natural. Particularly important is the case when ψ is a field in the interaction picture, using Wick's theorem and decomposition (A.1) one can then write

---

[1] If $X = X[\psi, \partial\psi]$, the α^n may also contain derivations working on the various fields.

$$\begin{aligned}
&\langle G[\psi]\psi(x)F[\psi]\rangle = \\
&= \sum_{m,n} \left(\int dx\right)^n \left(\int dy\right)^m \alpha^n(x_1 \ldots x_n)\beta^m(y_1 \ldots y_m) \left\langle \left(\prod_k^n \psi(x_k)\right) \psi(x) \prod_{k'}^m \psi(y_{k'}) \right\rangle \\
&= \sum_n \left(\int dx\right)^n \alpha^n(x_1 \ldots x_n) \sum_l^n (\pm 1)^{n-l} \langle \psi(x_l)\psi(x)\rangle \left\langle \prod_{k\neq l}^n \psi(x_k) F[\psi] \right\rangle \\
&+ \sum_m \left(\int dy\right)^m \beta^m(y_1 \ldots y_m) \sum_l^m (\pm 1)^{l-1} \langle \psi(x)\psi(x_l)\rangle \left\langle G[\psi] \prod_{k'\neq l}^m \psi(y_{k'}) \right\rangle . \qquad \text{(A.2)}
\end{aligned}$$

with $\left(\int dx\right)^n = \int dx_1 \ldots \int dx_n$. The '$-$' stands for fermions and '$+$' for bosons. On the other hand, using the formal prescriptions (2.19) and (2.21) for $\frac{\overrightarrow{\delta}}{\delta\psi(x)}$ one can read

$$\begin{aligned}
&\int dz \langle \psi(x)\psi(z)\rangle \left\langle G[\psi] \frac{\overrightarrow{\delta} F[\psi]}{\delta\psi(z)} \right\rangle = \\
&= \sum_m \left(\int dy\right)^m \beta^m(y_1 \ldots y_m) \int dz \langle \psi(x)\psi(z)\rangle \sum_l^m (\pm 1)^{l-1} \delta(z - y_l) \left\langle G[\psi] \prod_{k'\neq l}^m \psi(y_{k'}) \right\rangle \\
&= \sum_m \left(\int dy\right)^m \beta^m(y_1 \ldots y_m) \sum_l^m (\pm 1)^{l-1} \langle \psi(x)\psi(y_l)\rangle \left\langle G[\psi] \prod_{k'\neq l}^m \psi(y_{k'}) \right\rangle . \qquad \text{(A.3)}
\end{aligned}$$

Similar expression holds for $\int dz \langle \psi(x)\psi(z)\rangle \left\langle \frac{G[\psi]\overleftarrow{\delta}}{\delta\psi(z)} F[\psi] \right\rangle$. Putting latter two together we get precisely (A.2). This confirms the validity of (2.18). It is easy to persuade oneself that exactly the same sort of arguments leads to

$$\langle\psi(x)F[\psi]\rangle = \int dz\langle\psi(x)\psi(z)\rangle \left\langle \frac{\overrightarrow{\delta} F[\psi]}{\delta\psi(z)} \right\rangle \tag{A.4}$$

$$\langle\mathcal{T}(\psi(x)F[\psi])\rangle = \int dz\langle\mathcal{T}(\psi(x)\psi(z))\rangle \left\langle \mathcal{T}\left(\frac{\overrightarrow{\delta} F[\psi]}{\delta\psi(z)}\right) \right\rangle \tag{A.5}$$

$$\begin{aligned}\langle G[\psi]\mathcal{T}(\psi(x)F[\psi])\rangle = \int dz\langle\mathcal{T}(\psi(x)\psi(z))\rangle \left\langle G[\psi]\mathcal{T}\left(\frac{\overrightarrow{\delta} F[\psi]}{\delta\psi(z)}\right) \right\rangle + \\ + \int dz\langle\psi(z)\psi(x)\rangle \left\langle \frac{G[\psi]\overleftarrow{\delta}}{\delta\psi(z)}\mathcal{T}(F[\psi]) \right\rangle ,\end{aligned} \tag{A.6}$$

etc.

with $\mathcal{T}$ being either the chronological or anti–chronological time ordering symbol. At this stage it is important to realize that from the definition of $\frac{\overrightarrow{\delta}}{\delta\psi(x)}$ directly follows that $[\frac{\overrightarrow{\delta}}{\delta\psi(x)}; \frac{\overrightarrow{\delta}}{\delta\psi(y)}]_{\mp} = 0$ ('$-$' holds for bosons and '$+$' for fermions). Indeed,

$$\begin{aligned}\frac{\overrightarrow{\delta}^2 F[\psi]}{\delta\psi(x)\delta\psi(y)} &= \sum_{n=2}\sum_{i<j}\left(\int dx\right)^{n-2}(\alpha^n(x_1 \ldots \overset{\overset{x_i}{\downarrow}}{x} \ldots \overset{\overset{x_j}{\downarrow}}{y} \ldots x_n) \pm \\ &\pm \quad \alpha^n(x_1 \ldots \overset{\overset{x_i}{\downarrow}}{y} \ldots \overset{\overset{x_j}{\downarrow}}{x} \ldots x_n))(\pm 1)^{i+j}\prod_{m\neq i,j}^{n}\psi(x_m) = \mp\frac{\overrightarrow{\delta}^2 F[\psi]}{\delta\psi(y)\delta\psi(x)} .\end{aligned} \tag{A.7}$$

Similarly $[\frac{\overleftarrow{\delta}}{\delta\psi(x)}; \frac{\overleftarrow{\delta}}{\delta\psi(y)}]_{\mp} = 0$. Analogously we might prove

$$\frac{F[\psi]\overleftarrow{\delta}^2}{\delta\psi(x)\delta\psi(y)} = \frac{\overrightarrow{\delta}^2 F[\psi]}{\delta\psi(x)\delta\psi(y)} , \tag{A.8}$$

and

$$\frac{\overrightarrow{\delta}^2(F[\psi]G[\psi])}{\delta\psi(x)\delta\psi(y)} = \frac{F[\psi]\overleftarrow{\delta}^2}{\delta\psi(x)\delta\psi(y)}G[\psi] + (-1)^p\frac{F[\psi]\overleftarrow{\delta}}{\delta\psi(x)}\frac{\overrightarrow{\delta} G[\psi]}{\delta\psi(y)}$$

$$+ \quad \frac{F[\psi]\overleftarrow{\delta}}{\delta\psi(y)}\frac{\overrightarrow{\delta}G[\psi]}{\delta\psi(x)} + F[\psi]\frac{\overrightarrow{\delta}^2 G[\psi]}{\delta\psi(x)\delta\psi(y)} \,. \tag{A.9}$$

The "p" is 0 for bosons and 1 for fermions. With (2.18) and (A.4)–(A.6) one can easily construct more complicated expectation values. For example, using (2.18) and (A.4) we get

$$\begin{aligned}
&\langle\psi(x)\psi(y)F[\psi]\rangle = \\
&= \int \frac{dz_1 dz_2}{2}(\langle\psi(x)\psi(z_1)\rangle\langle\psi(y)\psi(z_2)\rangle + (-1)^p\langle\psi(x)\psi(z_2)\rangle\langle\psi(y)\psi(z_1)\rangle) \\
&\times \left\langle \frac{\overrightarrow{\delta}^2 F[\psi]}{\delta\psi(z_1)\delta\psi(z_2)} \right\rangle + \langle\psi(x)\psi(y)\rangle\langle F[\psi]\rangle \,.
\end{aligned} \tag{A.10}$$

Similarly, using (2.18) and (anti–)commutativity of the arrowed $\frac{\delta}{\delta\psi(x)}$, we get

$$\begin{aligned}
&\langle G[\psi]\psi(x)\psi(y)F[\psi]\rangle = \\
&= \int \frac{dz_1 dz_2}{2}(\langle\psi(x)\psi(z_1)\rangle\langle\psi(y)\psi(z_2)\rangle + (-1)^p\langle\psi(x)\psi(z_2)\rangle\langle\psi(y)\psi(z_1)\rangle) \\
&\times \left\langle G[\psi]\frac{\overrightarrow{\delta}^2 F[\psi]}{\delta\psi(z_1)\delta\psi(z_2)} \right\rangle \\
&+ \int \frac{dz_1 dz_2}{2}(\langle\psi(z_1)\psi(x)\rangle\langle\psi(z_2)\psi(y)\rangle + (-1)^p\langle\psi(z_2)\psi(x)\rangle\langle\psi(z_1)\psi(y)\rangle) \\
&\times \left\langle \frac{G[\psi]\ \overleftarrow{\delta}^2}{\delta\psi(z_1)\delta\psi(z_2)}F[\psi] \right\rangle \\
&+ \int dz_1 dz_2(\langle\psi(z_1)\psi(x)\rangle\langle\psi(y)\psi(z_2)\rangle + (-1)^p\langle\psi(x)\psi(z_2)\rangle\langle\psi(z_1)\psi(y)\rangle) \\
&\times \left\langle \frac{G[\psi]\overleftarrow{\delta}}{\delta\psi(z_1)}\frac{\overrightarrow{\delta}F[\psi]}{\delta\psi(z_2)} \right\rangle + \langle\psi(x)\psi(y)\rangle\langle G[\psi]F[\psi]\rangle \,.
\end{aligned} \tag{A.11}$$

We could proceed further having still higher powers of fields and variations. However, there is a quite interesting generalisation in case when we have (anti–)time ordered operators. Let us have $F[\psi] = \mathcal{T}(F[\psi])$, in this case

$$\begin{aligned}
\langle F[\psi]\rangle &= \sum_n \left(\int dx\right)^n \alpha^n(\ldots)\langle \mathcal{T}(\prod_{i=1}^{n}\psi(x_i)\rangle \\
&= \sum_{n=1}\left(\int dx\right)^n \frac{\alpha^n(\ldots)}{n}\sum_{i,j}\varepsilon_P\langle\mathcal{T}(\psi(x_i)\psi(x_j))\rangle\langle\mathcal{T}(\prod_{m\neq i,j}^{n}\psi(x_m))\rangle + \alpha^0(\ldots) \\
&= \int dz_1 dz_2\langle\mathcal{T}(\psi(z_1)\psi(z_2))\rangle\left\langle\frac{\overrightarrow{\delta}^2\overline{F}[\psi]}{\delta\psi(z_2)\delta\psi(z_1)}\right\rangle + \langle F[0]\rangle\,, \qquad (A.12)
\end{aligned}$$

where $\overline{F}[\psi]$ differs from $F[\psi]$ in the replacement $\alpha^n(\ldots)\to\frac{\alpha^n(\ldots)}{n}$ (n starts from 1 !). In comparison with (A.4)–(A.11), the $\alpha^0(\ldots)$ (i.e. the pure $T=0$ contribution) does matter here. Note that $\alpha^0(\ldots)$ generally involves non–heat–bath fields with corresponding space-time integrations. Similar extension is true if $F[\psi]=\mathcal{T}_C(F[\psi])$, where $\mathcal{T}_C$ is the time path ordering symbol. In that case

$$\begin{aligned}
\langle F[\psi]\rangle &= \sum_n\left(\int_C dx\right)^n\alpha^n(\ldots)\langle\mathcal{T}_C(\prod_{p=1}^{n}\psi(x_p))\rangle \\
&= \int_C dz_1dz_2\langle\mathcal{T}_C(\psi(z_1)\psi(z_2))\rangle\left\langle\frac{\overrightarrow{\delta}^2\overline{F}[\psi]}{\delta\psi(z_2)\delta\psi(z_1)}\right\rangle \\
&+ \langle F[0]\rangle\,, \qquad (A.13)
\end{aligned}$$

with[2] $\int_C dx = \int_C dt\int_V d\mathbf{x}$ and $\frac{\delta\psi(x)}{\delta\psi(y)} = \delta_C(x-y)$. Wick's theorem for the $\mathcal{T}_C$–oriented product of fields has an obvious form

$$\langle\mathcal{T}_C(\psi(x_1)\ldots\psi(x_{2n}))\rangle = \sum_{\substack{j\\ j\neq i}}\varepsilon_P\langle\mathcal{T}_C(\psi(x_i)\psi(x_j))\rangle\ \langle\mathcal{T}_C(\prod_{k\neq i;j}\psi(x_k))\rangle\,. \qquad (A.14)$$

---

[2] A contour δ-function $\delta_C(x-y)$ is defined as $\int_C dz\delta_C(z-z^{'})f(z)=f(z^{'})$, see [51, 119].

This can be directly derived from Wick's theorem (2.17), realizing that

$$\mathcal{T}_C(\psi(x_1)\dots\psi(x_m)) = \sum_P \varepsilon_P \theta_C(t_{P_1},\dots,t_{P_m})\psi(x_{P_1})\dots\psi(x_{P_m}) \,, \tag{A.15}$$

where P refers to the permutation of the indices and $\theta_C(t_1,\dots,t_m)$ being a contour step function [73] defined as

$$\theta_C(t_1,\dots,t_m) = \begin{cases} 1 & (t_1,\dots,t_m \text{ are } \mathcal{T}_C\text{-oriented along } C) \\ 0 & (\text{otherwise}) \end{cases} \tag{A.16}$$

So for example (A.6) may be written as

$$\langle \mathcal{T}_C(\psi(x)F[\psi])\rangle = \int_C dz\,\langle \mathcal{T}_C(\psi(x)\psi(z))\rangle \left\langle \mathcal{T}_C\left(\frac{\vec{\delta}\ F[\psi]}{\delta\psi(z)}\right)\right\rangle \,. \tag{A.17}$$

Particularly important is the Keldysh–Schwinger path [34, 73, 120] (see FIG.3.3). In the latter case

$$\begin{aligned} \langle F[\psi]\rangle &= \int_{C_1} dz_1 dz_2 \langle \mathcal{T}(\psi(z_1)\psi(z_2))\rangle \left\langle \frac{\vec{\delta}^2\overline{F}[\psi]}{\delta\psi(z_2)\delta\psi(z_1)}\right\rangle \\ &+ \int_{C_2} dz_1 dz_2 \langle \overline{\mathcal{T}}(\psi(z_1)\psi(z_2))\rangle \left\langle \frac{\vec{\delta}^2\overline{F}[\psi]}{\delta\psi(z_2)\delta\psi(z_1)}\right\rangle \\ &+ 2\int_{C_2} dz_1 \int_{C_1} dz_2 \langle \psi(z_1)\psi(z_2)\rangle \left\langle \frac{\vec{\delta}^2\overline{F}[\psi]}{\delta\psi(z_2)\delta\psi(z_1)}\right\rangle \\ &+ \langle F[0]\rangle \,. \end{aligned} \tag{A.18}$$

Application to the product $G[\psi]F[\psi]$ with $F[\psi] = \mathcal{T}_{C_1}(F[\psi])$ and $G[\psi] = \mathcal{T}_{C_2}(G[\psi])$ is straightforward and reads

$$\begin{aligned}
\langle G[\psi]F[\psi]\rangle &= \int dz_1 dz_2 \langle \overline{\mathcal{T}}(\psi(z_1)\psi(z_2))\rangle \left\langle \overline{\frac{G[\psi]\overleftarrow{\delta}^2}{\delta\psi(z_2)\delta\psi(z_1)}F[\psi]} \right\rangle \\
&+ \int dz_1 dz_2 \langle \mathcal{T}(\psi(z_1)\psi(z_2))\rangle \left\langle \overline{G[\psi]\frac{\overrightarrow{\delta}^2 F[\psi]}{\delta\psi(z_2)\delta\psi(z_1)}} \right\rangle \\
&+ 2\int dz_1 dz_2 \langle \psi(z_1)\psi(z_2)\rangle \left\langle \overline{\frac{G[\psi]\overleftarrow{\delta}}{\delta\psi(z_1)}\frac{\overrightarrow{\delta}F[\psi]}{\delta\psi(z_2)}} \right\rangle \\
&+ \langle G[0]F[0]\rangle\,, \qquad \text{(A.19)}
\end{aligned}$$

where the overlining indicates that we work with $\frac{\alpha^n(\ldots)\beta^m(\ldots)}{n+m}$ instead of $\alpha^n(\ldots)\beta^m(\ldots)$, we have also abbreviated $\int_{C_1} dz$ to $\int dz \int_{C_1} dz$. We should also emphasise that $\frac{\delta\psi(x)}{\delta\psi(y)}$ used in (A.19) is $\delta(x-y)$ rather than $\delta_C(x-y)$.

In Eq.(2.36) it has been used the inverted version of (A.19), namely

$$\begin{aligned}
\langle (G[\psi]F[\psi])'\rangle &= \int \frac{dz_1 dz_2}{2} \langle \overline{\mathcal{T}}(\psi(z_1)\psi(z_2))\rangle \left\langle \frac{G[\psi]\overleftarrow{\delta}^2}{\delta\psi(z_2)\delta\psi(z_1)}F[\psi] \right\rangle \\
&+ \int \frac{dz_1 dz_2}{2} \langle \mathcal{T}(\psi(z_1)\psi(z_2))\rangle \left\langle G[\psi]\frac{\overrightarrow{\delta}^2 F[\psi]}{\delta\psi(z_2)\delta\psi(z_1)} \right\rangle \\
&+ \int dz_1 dz_2 \langle \psi(z_1)\psi(z_2\rangle \left\langle \frac{G[\psi]\overleftarrow{\delta}}{\delta\psi(z_1)}\frac{\overrightarrow{\delta}F[\psi]}{\delta\psi(z_2)} \right\rangle\,, \qquad \text{(A.20)}
\end{aligned}$$

Here $(G[\psi]F[\psi])'$ has the coefficients $\alpha^n(\ldots)\beta^m(\ldots)\frac{(n+m)}{2}$ instead of $\alpha^n(\ldots)\beta^m(\ldots)$. Note, that the $\alpha^0(\ldots)\beta^0(\ldots)$ does not contributes and thus we do not have any pure $T = 0$ contributions. Eq.(A.20) has a natural interpretation. Whilst the LHS tells us, that from each thermal diagram (constructed out of $\langle G[\psi]F[\psi]\rangle$) with $\frac{n+m}{2}$ internal heat–bath particle lines we must take $n+m$ identical copies, the RHS says, that this is virtually because we sum over all possible distributions of one heat-bath particle line inside of the given diagram. The pictorial expression of (A.20) is depicted in FIG.A.1 .

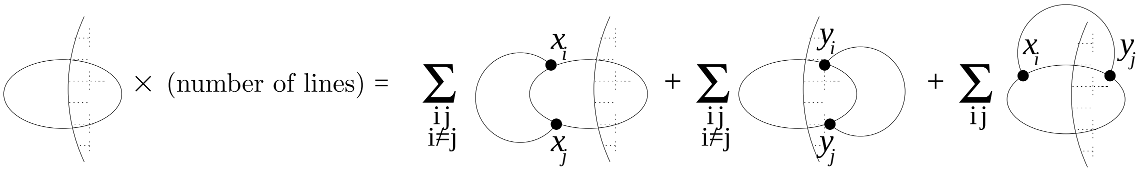

Figure A.1: Diagrammatic equivalent of Eq.(A.20). The cut separates areas constructed out of $F[\psi]$ and $G[\psi]$.

A.2 Graphical formalism

(This section is partially based on refs. [72, 121].)

In Chapter 3 we heavily used a graphical representation of the Dyson–Schwinger equations. In this section we provide a short derivation of such a representation and in the section to follow we perform a comparison with the functional Dyson–Schwinger equations of Section 2 and Appendix A.1.

The Dyson–Schwinger equations were originally constructed [122, 123] with the motivation that they could provide some information about the complete Green's functions outside the scope of perturbative theory. The basic philosophy is to directly use the equations of motion in order to construct the hierarchy of (integral) equations for full Green's functions. The usefulness of these equations is usually confined to the cases where some approximation (truncation) is available in order to bring them into manageable form. In this appendix we aim to derive the finite–temperature Dyson–Schwinger equations using the more intuitive path–integral formalism. The alternative derivation in the non–equilibrium context (based purely on operatorial approach) is discussed in Section 4.1.1.

Let us start with the ($T \neq 0$) generating functional of Green's functions $Z[J]$ (the partition functions with an external source J)

$$\begin{aligned} Z[T] &= \int \mathcal{D}\phi \, \exp\{i(S[\phi;T] + \int_C d^4x \, J(x)\phi(x))\} \\ S[\phi;T] &= \int_C d^4x \, \mathcal{L}(x) \, . \end{aligned} \tag{A.21}$$

Here $\int_C d^4x = \int_C dx_0 \int_V d^3\mathbf{x}$ with the subscript C indicating that the time runs along some contour in the complex plane. In the real–time formalism, which we adopt throughout, the most natural version is the so called Keldysh–Schwinger one [34,36], which is represented by the contour in FIG.3.3. Within the path–integral the c–number fields are further restricted by the periodic boundary condition (KMS condition) [34, 36, 38] which for bosonic fields reads:

$$\phi(t_i - i\beta, \mathbf{x}) = \phi(t_i, \mathbf{x}) \, . \tag{A.22}$$

The zero temperature generating functional may be recovered from (A.21) if we integrate over the close–time path (no vertical parts) and omit the KMS condition (A.22). Now, the LHS of (A.21) is independent of ϕ, thus particularly it is invariant under infinitesimal point transformation

$$\phi(x) \rightarrow \phi(x) + \varepsilon f(x) \, , \tag{A.23}$$

where f is an arbitrary (ϕ independent) function which fulfils the periodic boundary conditions

$$f(t_i - i\beta, \mathbf{x}) = f(t_i, \mathbf{x}) \, . \tag{A.24}$$

From (A.23) is obvious that the corresponding functional Jacobian is 1, i.e., $\mathcal{D}\phi = \mathcal{D}\phi'$. This immediately implies that

$$\begin{aligned} Z[J] &= \int \mathcal{D}\phi' \exp\left\{ i(S[\phi' - \varepsilon f] + \int_C d^4x\, J(x)\phi'(x) - \varepsilon \int_C d^4x\, J(x) f(x)) \right\} \\ &= -i\varepsilon \int \mathcal{D}\phi' \left\{ \int_C d^4x \left(\frac{\delta S}{\delta \phi'}(x) + J(x) \right) f(x) \right\} \exp(iS[\phi'] + i\int_C J\phi') + \mathcal{O}(\varepsilon^2) \\ &+ Z[J]\,, \\ \Rightarrow 0 &= \int \mathcal{D}\phi \left\{ \int_C d^4x \left(\frac{\delta S}{\delta \phi}(x) + J(x) \right) f(x) \right\} \exp(iS[\phi] + i\int_C J\phi)\,. \end{aligned} \tag{A.25}$$

As (A.25) is true for any $f(\ldots)$ fulfilling the condition (A.24) one may write

$$\begin{aligned} 0 &= \int_C d^4x \left\langle \frac{\delta S[\psi_H]}{\delta \phi}(x) + J(x) \right\rangle f(x)\,, \\ 0 &= \left\langle \frac{\delta S[\psi_H]}{\delta \phi}(x) + J(x) \right\rangle = \left(\frac{\delta S}{\delta \phi} \left[\frac{\delta}{i\delta J(x)} \right] + J(x) \right) Z[J]\,. \end{aligned} \tag{A.26}$$

Employing the commutation relation: $-i\frac{\delta}{\delta J}\, Z = Z(\phi - i\frac{\delta}{\delta J})$, we may recast (A.26) into more appropriate form, namely

$$- J(x) = \frac{\delta S}{\delta \phi} \left[\phi(x) - i\frac{\delta}{\delta J(x)} \right] \mathbb{1} = \frac{\delta S}{\delta \phi} \left[\phi(x) + i \int_C d^4z\, \mathbb{D}^c(x,z) \frac{\delta}{\delta \phi(z)} \right] \mathbb{1}\,. \tag{A.27}$$

So, for instance, for $\lambda\, \Phi^4$ theory we have

$$\begin{aligned} - J_\alpha(x) &= -(\Box + m_0^2)\phi_\alpha(x) - \frac{\lambda_0}{3!} \left\{ (\phi_\alpha(x))^3 + i3\phi_\alpha(x)\, \mathbb{D}^c_{\alpha\alpha}(x,x) \right. \\ &\quad \left. - \int d^4y\, d^4w\, d^4z\, \mathbb{D}^c_{\alpha\beta}(x,y)\, \mathbb{D}^c_{\alpha\gamma}(x,w)\, \Gamma^{(3)\ \beta\gamma\delta}(y,w,z)\, \mathbb{D}^c_{\delta\alpha}(z,x) \right\} \\ &= -(\Box + m_0^2)\phi_\alpha(x) - \frac{\lambda_0}{3!} \left\{ (\phi_\alpha(x))^3 + i3\phi_\alpha(x)\, \mathbb{D}^c_{\alpha\alpha}(x,x) - \mathbb{D}^{c\,(3)}_{\alpha\alpha\alpha}(x,x,x) \right\} \\ &= -(\Box + m_0^2)\phi_\alpha(x) + \frac{\lambda_0}{3!}\, \mathbb{D}^{(3)}_{\alpha\alpha\alpha}(x,x,x)\,, \end{aligned} \tag{A.28}$$

(no sum over α!)[3] or, using identity; $(\Box_x + m_0^2)\,\mathbb{D}_F^{\alpha\beta}(x,y) = -(\sigma_3)^{\alpha\beta}\delta(x-y)$, we may invert the differential operator and write equivalently

$$- \int d^4y\, J_\beta(y)\, \mathbb{D}_F^{\beta\alpha}(y,x) = \phi^\alpha(x) + \frac{\lambda_0}{3!} \int d^4y\, \mathbb{D}_F^{\alpha\beta}(x,y)\, \mathbb{D}^{(3)}_{\beta\beta\beta}(y,y,y). \tag{A.29}$$

Eq.(A.29) has the following graphical representation

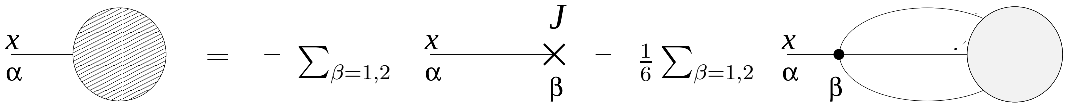

where the hatched blob refers to the (full) 1–point amputated Green's function, the dotted blob refers to the (full) 3–point amputated Green's function, the cross denotes the source J, while the heavy dot without coordinate indicates that the vertex must be integrated over all possible positions. The corresponding graphical representation in terms of the connected Green's functions reads (c.f. Eq.(A.28))

---

[3] In (A.28) we have implicitly used the identities;

$$\frac{1}{Z}\frac{\delta^n Z}{\delta J(x_1)\ldots\delta J(x_n)} = (-1)^{n+1} i\, \mathbb{D}^{(n)}(x_1,\ldots,x_n)$$
$$\frac{\delta^n W}{\delta J(x_1)\ldots\delta J(x_n)} = (-1)^{n+1}\, \mathbb{D}^{c\;(n)}(x_1,\ldots,x_n)$$
$$\frac{\delta\phi(x)}{\delta J(y)} = -\mathbb{D}^c(x,y)\,; \quad \frac{\delta^n \Gamma}{\delta\phi(x_1)\ldots\phi(x_n)} = \Gamma^{(n)}(x_1\ldots x_n)$$
$$\frac{\delta\,\mathbb{D}^c_{\alpha\beta}(x,y)}{\delta\phi_\gamma(z)} = -\int dy_1^4\, dy_2^4\, \mathbb{D}^c_{\alpha\delta}(x,y_1)\Gamma^{(3)\;\delta\kappa\gamma}(y_1,y_2,z)\,\mathbb{D}^c_{\kappa\beta}(y_2,y)\,.$$

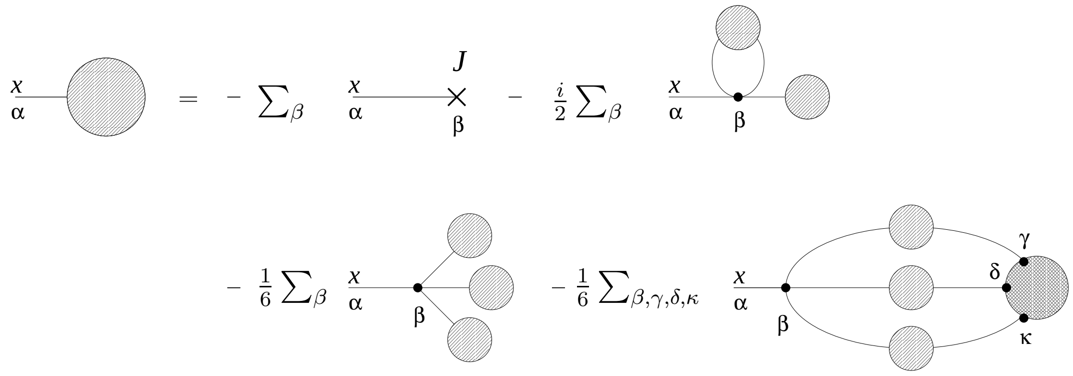
x
α
=
– $\sum_\beta$
x
α
J
β
– $\frac{i}{2}\sum_\beta$
x
α
β
– $\frac{1}{6}\sum_\beta$
x
α
β
– $\frac{1}{6}\sum_{\beta,\gamma,\delta,\kappa}$
x
α
β
γ
δ
κ

Here the double–hatched blob describe the 3–point vertex function and the hatched blobs refer, as before, to the connected (truncated) Green's functions.

To see how to obtain the corresponding Dyson–Schwinger equations for the 2–point (connected) Green's functions, let us perform in Eq.(A.27) (or, for simplicity's sake, in Eq.(A.28)) variation w.r.t. $J_\beta(y)$. This directly gives us

$$(\Box_x + m_0^2)\,\mathbb{D}^c_{\alpha\beta}(x,y) - \frac{\lambda_0}{3!}\,\mathbb{D}^{(4)}_{\alpha\alpha\alpha\beta}(x,x,x,y) + \frac{\lambda_0 i}{3!}\,\phi_\beta(y)\,\mathbb{D}^{(3)}_{\alpha\alpha\alpha}(x,x,x) = -(\sigma_3)_{\alpha\beta}\delta(x-y)\,,$$

or, inverting the differential operator, we may equivalently write

$$\begin{aligned}\mathbb{D}^c_{\alpha\beta}(x,y) = \mathbb{D}_{F\,\alpha\beta}(x,y) \quad &- \quad \frac{\lambda_0}{3!}\int d^4z\,\mathbb{D}_{F\;\alpha}^{\;\gamma}(x,z)\,\mathbb{D}^{(4)}_{\gamma\gamma\gamma\beta}(z,z,z,y)\\ &+ \quad \frac{\lambda_0 i}{3!}\int d^4z\,\mathbb{D}_{F\;\alpha}^{\;\gamma}(x,z)\,\mathbb{D}^{(3)}_{\gamma\gamma\gamma}(z,z,z)\,\phi_\beta(y)\,. \qquad \text{(A.30)}\end{aligned}$$

Eq.(A.30) is graphically represented as follows

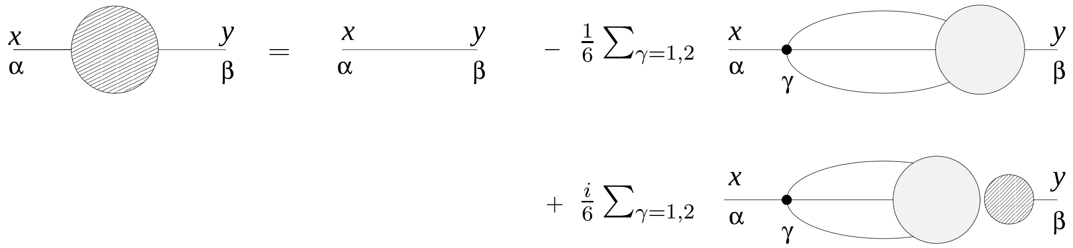

This may be reformulated purely in terms of the connected Green's functions and the vertex functions, indeed, performing variation w.r.t. $J_\beta(y)$ in first two lines in Eq.(A.28), and inverting the differential operator as before we obtain

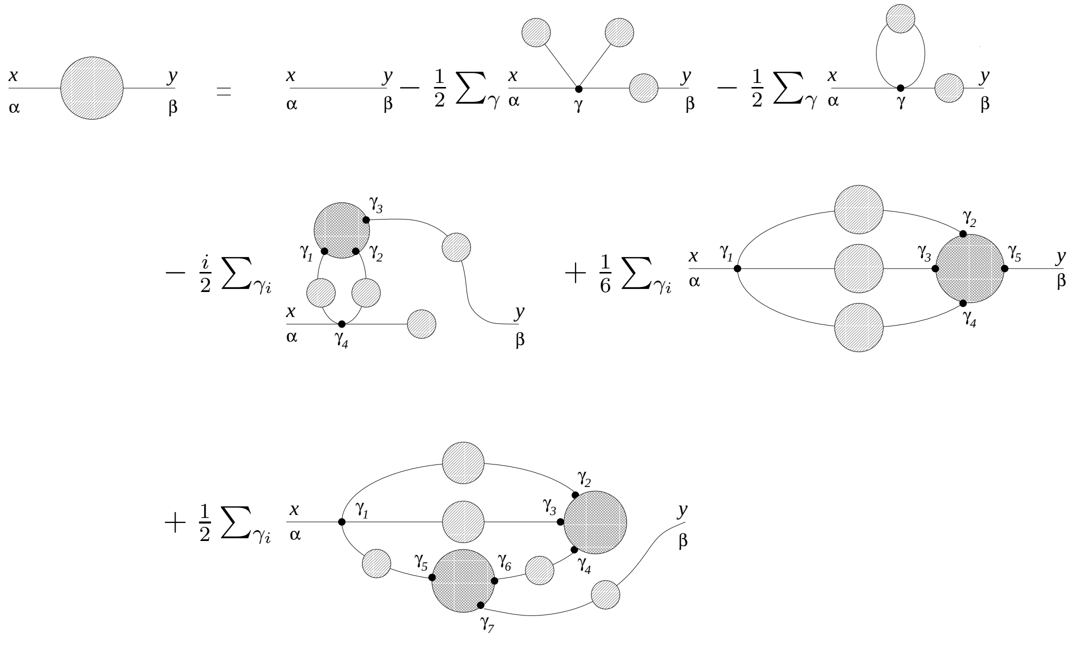

Note that if the symmetry is unbroken (i.e. when $m_0^2 > 0$) then after setting $J = 0$ the second, fourth and sixth term on the RHS will vanish.

It is important to mention that similarly as for the connected Green's functions we may write the Dyson–Schwinger equations for the vertex functions. Those may be obtained directly from Eq.(A.27) provided that one performs the corresponding number of variations w.r.t. ϕ. So, for instance, for the $\lambda\Phi^4$ theory the 1–point vertex function $\Gamma^{(1)}_{\alpha}(x) = \frac{\delta\Gamma}{\delta\phi^{\alpha}(x)} = -J_{\alpha}(x)$ is graphically represented (c.f. Eq.(A.28)) as

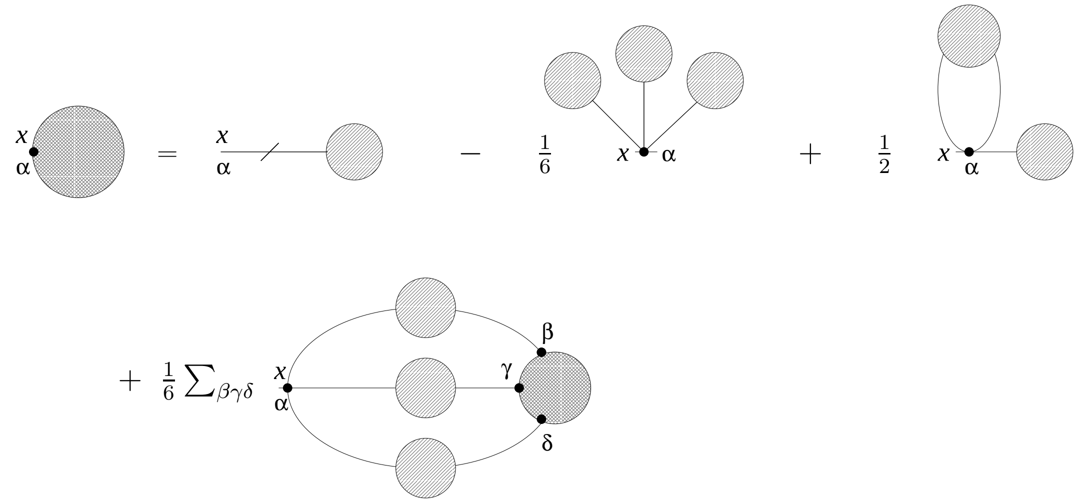

Here the slash stands for the inverse free thermal propagator. Particularly important examples are the 2– and 4–point vertex functions $\Gamma^{(2)}$ and $\Gamma^{(4)}$, respectively, which are indispensable in the renormalisation prescription (see Chapter 3). In the case of the $O(N)$ $\lambda\Phi^4$ in the large–N limit the corresponding graphical representations were explicitly calculated in Chapter 3 (see Sections 3.3.1–3.3.2).

A.3 Comparison

In order to find a link between the previous two approaches, let us start with the full n–point Green's function at $T = 0$. It is well known that in this case, the full Green's function may be expressed by means of the Gell–Mann and Low formula [53, 70, 115, 121]

$$\langle 0|\mathcal{T}(\psi_H(x_1)\dots\psi_H(x_n))|0\rangle = \frac{\left\langle 0\left|\mathcal{T}\left(\psi(x_1)\dots\psi(x_n)e^{i\int d^4x\mathcal{L}_I(x)}\right)\right|0\right\rangle}{\left\langle 0\left|\mathcal{T}\left(e^{i\int d^4x\mathcal{L}_I(x)}\right)\right|0\right\rangle}\,, \tag{A.31}$$

which may be equivalently rewritten in the Schwinger form [124] as

$$\langle 0|\mathcal{T}(\psi_H(x_1)\dots\psi_H(x_n))|0\rangle = \left\langle 0\left|\mathcal{T}_C\left(\psi(x_1)\dots\psi(x_n)e^{i\int_C d^4x\mathcal{L}_I(x)}\right)\right|0\right\rangle\,, \tag{A.32}$$

where ψ_H is a field operator in the Heisenberg picture, while ψ and $\mathcal{L}_I$, are operators in the interaction picture, the sub–index C denotes the Schwinger–Keldysh time contour. The Schwinger (but not the Gell–Mann and Low!) formula can be directly extended to finite temperature as we have mentioned in Chapters 2 and 4, the only difference is that $\langle 0|\dots|0\rangle \rightarrow \langle\dots\rangle$. The following results will be equally valid for both $T = 0$ and $T \neq 0$ provided we take into account corresponding expectation values. In order to be concise, we shall restrict ourselves to bosonic fields. The necessary extension to fermions and gauge fields is straightforward.

For one field ψ_H in the presence of an external resource $J(x)$ we have

$$\phi(x) = \langle\psi_H(x)\rangle = \left\langle\mathcal{T}_C\left(\psi(x)e^{i\int_C d^4x(\mathcal{L}_I(x)+J(x)\psi(x))}\right)\right\rangle. \tag{A.33}$$

Setting in (A.17) $F[\psi] = e^{i\int_C d^4x(\mathcal{L}_I(x)+J(x)\psi(x))}$, we get

$$\langle\psi_H(x)\rangle + \int_C d^4z\,\mathbb{D}_F(x,z)\left\langle\mathcal{T}_C\left(\frac{\delta\int_C d^4y\mathcal{L}_I(y)}{\delta\psi(z)}\right)_H\right\rangle = -\int_C d^4z\,\mathbb{D}_F(x,z)J(z)\,, \tag{A.34}$$

where $i\,\mathbb{D}_F(x,z) = \langle \mathcal{T}_C(\psi(x)\psi(z))\rangle$. For instance, for the $\lambda\Phi^4$ theory ($\mathcal{L}_I = -\frac{i\lambda_0}{4!}\Phi^4$) we have

$$\langle \Phi_H(x)\rangle - \frac{\lambda_0}{3!}\int_C d^4z\,\mathbb{D}_F(x,z)\langle\Phi_H^3(z)\rangle = -\int_C d^4z\,\mathbb{D}_F(x,z)J(z)\,, \tag{A.35}$$

or in the thermal–index notation; $\alpha,\beta,\gamma,\delta = \{1,2\}$,

$$\phi^\alpha(x) + \frac{\lambda_0}{3!}\int d^4z\,\mathbb{D}_F^{\alpha\delta}(x,z)\,\mathbb{D}^{(3)}_{\delta\delta\delta}(z,z,z) = -\int d^4z\,\mathbb{D}_F^{\alpha\delta}(x,z)J_\delta(z)\,. \tag{A.36}$$

In (A.36) we can recognise the Dyson–Schwinger equation (A.29) for the $\lambda\Phi^4$ theory from the previous section.

To get further equations in an infinite tower of couplet integral equations we may perform successive variations in (A.35) with respect to $J_\beta(y)$, or we may alternatively set in (A.17) $F[\psi] = \psi(y)\,e^{i\int_C d^4x\,(\mathcal{L}_I(x)+J(x)\psi(x))}$. In both cases we obtain for $\lambda\Phi^4$ theory the following identity

$$\begin{aligned}
\mathbb{D}^{\alpha\beta}(x,y) &= \mathbb{D}_F^{\alpha\beta}(x,y) - \frac{i\lambda_0}{3!}\int d^4z\,\mathbb{D}_F^{\alpha\delta}(x,z)\;(\sigma_3)_{\delta\gamma}\;\langle\mathcal{T}_C(\Phi_H^3(z)\Phi_H(y))\rangle^{\gamma\beta}\\
&\qquad + i\int d^4z\,\mathbb{D}_F^{\alpha\delta}(x,z)\;J_\delta(z)\;\phi^\beta(y)\\
\Leftrightarrow\qquad \mathbb{D}^{c\,\alpha\beta}(x,y) &= \mathbb{D}_F^{\alpha\beta}(x,y) - \frac{\lambda_0}{3!}\int d^4z\,\mathbb{D}_F^{\alpha\delta}(x,z)\,\mathbb{D}^{(4)\,\beta}_{\delta\delta\delta}(z,z,z,y)\\
&\qquad + \frac{i\lambda_0}{3!}\int d^4z\,\mathbb{D}_F^{\alpha\delta}(x,z)\,\mathbb{D}^{(3)}_{\delta\delta\delta}(z,z,z)\,\phi^\beta(y)\,.
\end{aligned} \tag{A.37}$$

Note that (A.37) precisely coincides with the Dyson–Schwinger equation (A.30) derived in the previous section.

Let us mention one more point in the connection with Eq.(A.37). If, instead of setting $F[\psi] = \psi(y)e^{i\int_C d^4x\,(\mathcal{L}_I(x)+J(x)\psi(x))}$, as we have done in the previous case, we would set $G[\psi]=1$, $F[\psi]=e^{i\int_C d^4x(\mathcal{L}_I(x)+J(x)\psi(x))}$ in (A.10) or (A.11), we would get somewhat different identity, namely

$$\begin{aligned}\mathbb{D}^{\alpha\beta}(x,y) &= \mathbb{D}_F^{\alpha\beta}(x,y) - \int d^4z_1 d^4z_2\, \mathbb{D}_F^{\alpha\gamma}(x,z_1)(\sigma_3)_{\gamma\delta} \\ &\times \left\langle \mathcal{T}_C\left(\frac{\delta^2(i\int_C d^4x(\mathcal{L}_I(x)+J(x)\psi(x)))_H}{\delta\psi(z_1)\delta\psi(z_2)}\right)\right\rangle^{\delta\iota}(\sigma_3)_{\iota\kappa}\,\mathbb{D}_F^{\kappa\beta}(z_2,y)\,, \quad (A.38)\end{aligned}$$

which in the case of $\lambda\Phi^4$ theory Eq.(A.38) may be explicitly written as

$$\begin{aligned}\mathbb{D}^{\alpha\beta}(x,y) = \mathbb{D}_F^{\alpha\beta}(x,y) &- \frac{i\lambda_0}{2}\int d^4z_1\,\mathbb{D}_F^{\alpha\gamma}(x,z_1)(\sigma_3)_{\gamma\delta}\left\langle\Phi_H^2(z_1)\right\rangle^{\delta\iota}(\sigma_3)_{\iota\kappa}\,\mathbb{D}_F^{\kappa\beta}(z_1,y) \\ &- \frac{\lambda_0^2}{(3!)^2}\int d^4z_1 d^4z_2\,\mathbb{D}_F^{\alpha\gamma}(x,z_1)(\sigma_3)_{\gamma\delta}\left\langle\mathcal{T}_C(\Phi_H^3(z_1)\Phi_H^3(z_2))\right\rangle^{\delta\iota}(\sigma_3)_{\iota\kappa}\,\mathbb{D}_F^{\kappa\beta}(z_2,y) \\ &- \int d^4z_1 d^4z_2\,\mathbb{D}_F^{\alpha\gamma}(x,z_1)\,J_\gamma(z_1)\,\mathbb{D}_F^{\delta\beta}(z_2,y)\,J_\delta(z_2)\,. \quad (A.39)\end{aligned}$$

It is, however, not complicated to persuade oneself that (A.39) is equivalent to (A.37). Indeed, using (A.36) we get the desired equality (A.37). In (A.38) we can recognise the Dyson equation with $\left\langle\mathcal{T}_C\left(\frac{\delta^2(i\int d^4x(\mathcal{L}_I(x)+J(x)\psi(x)))_H}{\delta\psi(z_1)\delta\psi(z_2)}\right)\right\rangle$ being the self–energy [41] $i\tilde{\mathbf{\Sigma}}(z_1,z_2)$. Introducing a proper self–energy $\mathbf{\Sigma}$, which is a self–energy that cannot be separated into two pieces by cutting a single line (i.e. in the matrix form $\tilde{\mathbf{\Sigma}} = \mathbf{\Sigma} + \mathbf{\Sigma}\mathbb{D}_F\mathbf{\Sigma} + \ldots$) the series (A.38) can be summed formally to yield

$$\mathbb{D}^{\alpha\beta}(x,y) = \mathbb{D}_F^{\alpha\beta}(x,y) + \int d^4z_1 d^4z_2\,\mathbb{D}_F^{\alpha\delta}(x,z_1)(-i\mathbf{\Sigma}_{\delta\gamma}(z_1,z_2))\mathbb{D}^{\gamma\beta}(z_2,y)\,,$$

which is the usual form of the (thermal) Dyson equation (c.f. equation (3.43)). So the second in the hierarchy of the Dyson–Schwinger equations is nothing but the Dyson equation for the full two–point Green's function. Analogous procedure can be repeated for the Dyson–Schwinger equations involving the higher–point Green functions. As a result we can see then that the usual Dyson–Schwinger equations emerge naturally as a special sub–class of identities derived in Appendix A.1. Another sub–class of identities which may be derived from the functional formalism of Appendix A.1 are thermal Ward's identities. For example, for the $O(N)\,\Phi^4$ theory we immediately get from (A.10) that $\mathbb{D}^{\alpha\beta}_{a\,a}(x,y) = \mathbb{D}^{\alpha\beta}_{b\,b}(x,y)$ and $\mathbb{D}^{\alpha\beta}_{a\,b}(x,y) = 0$ if $a \neq b$. We, however, do not intend to dwell on this point more.

We thus find that our functional formalism derived in Appendix A.1 provides a unifying framework embracing such diverse concepts as Wick's theorem, the Dyson–Schwinger equations and Ward's identities.

Appendix B

Surface term in Eq.(4.69)

In this appendix we give some details of the derivation of Eq.(3.69). We particularly show that the surface integrals arisen during the transition from (3.68) to (3.69) mutually cancel among themselves. As usual, the integrals will be evaluated for integer values of D and corresponding results then analytically continued to a desired (generally complex) D.

The key quantity in question is

$$\begin{aligned} &+ \frac{1}{2}\int \frac{d^D q}{(2\pi)^{D-1}} \left(\frac{2\mathbf{q}^2}{(D-1)}\right) \frac{\varepsilon(q_0)}{e^{\beta q_0}-1}\,\delta(q^2-m_r^2(T)) \\ &- \frac{1}{2}\int \frac{d^D q}{(2\pi)^{D-1}} \left(\frac{2\mathbf{q}^2}{(D-1)}\right) \delta^+(q^2-m_r^2(0)). \end{aligned} \tag{B.1}$$

$$\begin{aligned} (\text{B.1}) \;=\;& \mathcal{N}_T(m_r^2(T)) - \mathcal{N}(m_r^2(0)) \\ &+ \lim_{R\to\infty} \frac{1}{2(D-1)}\int \frac{dq_0}{(2\pi)^{D-1}} \int_{\partial S_R^{D-2}} d\mathbf{s}\,\mathbf{q}\;\theta(q^2-m_r^2(T))\,\theta(q_0)\,\left(\frac{2}{e^{\beta q_0}-1}+1\right) \\ &- \lim_{R\to\infty} \frac{1}{2(D-1)}\int \frac{dq_0}{(2\pi)^{D-1}} \int_{\partial S_R^{D-2}} d\mathbf{s}\,\mathbf{q}\;\theta(q^2-m_r^2(0))\,\theta(q_0). \end{aligned} \tag{B.2}$$

As usual, $\mathbf{ab} = \sum_{i=1}^{D-1}\mathbf{a}_i\mathbf{b}_i$ and S_R^{D-2} is a $(D-2)$-sphere with the radius R. The expressions for $\mathcal{N}_T$ and $\mathcal{N}$ are done by (3.70).

With the relation (B.2) we can show that the surface terms cancel in the large R limit. Let us first observe that

$$\begin{aligned}
&\lim_{R\to\infty} \int \frac{dq_0}{(2\pi)^{D-1}} \int_{\partial S_R^{D-2}} d\mathbf{s}\;\mathbf{q}\;\theta(q^2 - m_r^2(T))\,\frac{2\theta(q_0)}{e^{\beta q_0}-1}\\
=\;&\lim_{R\to\infty} \frac{2\pi^{\frac{D-1}{2}}R^{D-1}}{\Gamma\left(\frac{D-1}{2}\right)} \int \frac{dq_0}{(2\pi)^{D-1}}\,\theta(q_0^2 - R^2 - m_r^2(T))\,\frac{2\theta(q_0)}{e^{\beta q_0}-1}\\
=\;&\lim_{R\to\infty} \frac{\pi^{\frac{1-D}{2}}R^{D-1}}{2^{D-2}\Gamma\left(\frac{D-1}{2}\right)} \int_{\sqrt{R^2+m_r^2(T)}}^{\infty} dq_0\,\frac{2}{e^{\beta q_0}-1} \;=\; 0. \qquad \text{(B.3)}
\end{aligned}$$

In 2-nd line we have exploited Gauss's theorem and in the last line we have used L'Hôpital's rule as the expression is in the indeterminate form 0/0. The remaining surface terms in (B.2) read

$$\begin{aligned}
&\lim_{R\to\infty}\int \frac{dq_0}{(2\pi)^{D-1}} \int_{\partial S_R^{D-2}} d\mathbf{s}\;\mathbf{q}\;\left\{\theta(q^2 - m_r^2(T)) - \theta(q^2 - m_r^2(0))\right\}\;\theta(q_0)\\
=\;&\lim_{R\to\infty} \frac{\pi^{\frac{1-D}{2}}R^{D-1}}{2^{D-2}\Gamma\left(\frac{D-1}{2}\right)} \left\{\int_{\sqrt{R^2+m_r^2(T)}}^{\infty} - \int_{\sqrt{R^2+m_r^2(0)}}^{\infty}\right\} dq_0 \;=\; 0. \qquad \text{(B.4)}
\end{aligned}$$

The last identity follows either by applying L'Hôspital's rule or by a simple transformation of variables which renders both integrals inside of $\{\ldots\}$ equal. Expressions on the last lines in (B.3) and (B.4) can be clearly (single–valuedly) continued to the region Re$D > 1$ as they are analytic there. We thus end up with the statement that

$$\text{(B.1)} = \mathcal{N}_T(m_r^2(T)) - \mathcal{N}(m_r^2(0)).$$

Appendix C

High–temperature expansion of the gap equation

In this appendix we shall derive the high–temperature expansion of the mass shift $\delta m^2(T)$ in the case when fields Φ_a are massive (i.e. $m_r^2(0) \neq 0$).

Consider Eqs.(3.40) and (3.49). If we combine them together, we get easily the following transcendental equation for $\delta m^2(T)$

$$\delta m^2(T) = \lambda_0 \left\{ \mathcal{M}(m_r^2(T)) - \mathcal{M}(m_r^2(0)) + \frac{1}{2} I_0(m_r^2(0) + \delta m^2(T)) \right\}. \tag{C.1}$$

Here $\mathcal{M}$ and I_0 are done by (3.42) and (3.78), respectively.

Now, both λ_0 and $\mathcal{M}$ are divergent in $D = 4$. If we reexpress λ_0 in terms of λ_r, divergences must cancel, as $\delta m^2(T)$ is finite in $D = 4$. The latter can be easily seen if we Taylor expand $\mathcal{M}$, i.e.

$$\mathcal{M}(m_r^2(T)) = \mathcal{M}(m_r^2(0)) + \delta m^2(T)\, \mathcal{M}'(m_r^2(0)) + \hat{\mathcal{M}}(m_r^2(0); \delta m^2(T)). \tag{C.2}$$

Obviously, $\hat{\mathcal{M}}$ is finite in $D = 4$ as $\mathcal{M}$ is quadratically divergent. Inserting (C.2) to (C.1) and employing Eq.(3.55) we get

$$\delta m^2(T) = \lambda_r \left\{ \hat{\mathcal{M}}(m_r^2(0);\delta m^2(T)) + \frac{1}{2} I_0(m_r^2(0)+\delta m^2(T)) \right\} . \tag{C.3}$$

This is sometimes referred to as the renormalised gap equation. In order to determine $\hat{\mathcal{M}}$ we must go back to (C.2). From the former we read off that

$$\begin{aligned}
&\hat{\mathcal{M}}(m_r^2(T);\delta m^2(T)) \\
&\quad = \mathcal{M}(m_r^2(T)) - \mathcal{M}(m_r^2(0)) - \delta m^2(T)\, \mathcal{M}'(m_r^2(0)) \\
&\quad = \frac{\Gamma(1-\frac{D}{2})}{2(4\pi)^{\frac{D}{2}}} \left\{ (m_r^2(T))^{\frac{D}{2}-1} - (m_r^2(0))^{\frac{D}{2}-1} - \delta m^2(T)(\frac{D}{2}-1)\, (m_r^2(0))^{\frac{D}{2}-2} \right\} \\
&\quad \overset{D\to 4}{=} \frac{1}{32\pi^2} \left\{ m_r^2(T) \ln\left(\frac{m_r^2(T)}{m_r^2(0)}\right) - \delta m^2(T) \right\} .
\end{aligned} \tag{C.4}$$

So

$$\delta m^2(T) = \lambda_r \left\{ \frac{(m^2(0)+\delta m^2(T)) \ln\left(1+\frac{\delta m^2(T)}{m_r^2(0)}\right) - \delta m^2(T)}{32\pi^2} + \frac{1}{2} I_0 \right\} . \tag{C.5}$$

Eq.(C.5) was firstly obtained and numerically solved in [61]. It was shown that the solution is double valued. The former behaviour was also observed by Abbott *et al.* [78] at $T=0$, and by Bardeen and Moshe [77] at both $T=0$ and $T\neq 0$. The relevant solution is only that which fulfils the condition $\delta m^2(T) \to 0$ when $T \to 0$. For such a solution it can be shown (c.f. [61], FIG.3) that $\frac{\delta m^2(T)}{m_r^2(0)} \ll 1$ for a sufficiently high T. So the high–temperature expansion of (C.5) reads

$$\begin{aligned}
\delta m^2(T) &= \lambda_r \left\{ \frac{\frac{(\delta m^2(T))^2}{2m_r^2(0)} - \frac{(\delta m^2(T))^3}{6m_r^4(0)} + \frac{(\delta m^2(T))^4}{12m_r^6(0)} + \ldots}{32\pi^2} + \frac{1}{2} I_0 \right\} \\
&\doteq \frac{\lambda_r}{2} I_0 = \frac{\lambda_r T^2}{24} - \frac{\lambda_r m_r(T)}{8\pi}\, T + \mathcal{O}\left(m_r^2(T) \ln\left(\frac{m_r(T)}{T4\pi}\right)\right) .
\end{aligned} \tag{C.6}$$

Appendix D

Derivation of the Shannon (information) entropy

(This section is based on refs. [26, 28, 104, 125].)

In Chapter 4 we intensively used the concept of the Shannon (or information) entropy which we identified (up to a negative multiplicative constant) with an "information content" associated with a (macro–) system in question. The objective of the present appendix is to formulate mathematically more clearly the rather vague notion of "informative content" and to find a link between statistical physics and information theory. As a next step we derive the basic properties of the Shannon entropy.

Let us first introduce the concept of information in the context of probability calculus and of information theory. We shall consider a set of events (or ensemble of all possible messages) $\{x_1, \ldots, x_N\}$ with respective probabilities $\{p_1, \ldots, p_N\}$. So, for example, if only single letter messages are transmitted

$$\{x_1, \ldots, x_N\} = \{A, B, \ldots, Z\},$$

then the corresponding set of p's characterises a particular language[1]. Because events $\{x_i\}$

---

[1] For instance, $p(A)$ in English is 0.0703, 0.0645 in French is and 0.0693 in Czech, the least frequent

are all possible different messages which might be send from a sender to a recipient, the corresponding probabilities must sum up to one: $\sum_i^N p_i = 1$.

One says that $\Im_m$ is the amount of information conveyed by the message x_m if $\Im_m$ is a non–negative and continuous function $\Im$ of p_m defined on the range $0 < p_m \leq 1$. Moreover, the more likely a message is, the less information is conveyed by the knowledge of its actual occurrence (the more stereotypical a message is (i.e. the larger is the probability for being received), the less information it imparts). This implies that $\Im_m = \Im(p_m)$ must be decreasing function of p_m on the interval $[0, 1]$, and particularly $\Im(p_m = 1) = 0$.

In order to get more qualitative results let us consider first a simple system with only two possible messages x_1 and x_2 and the corresponding language $\{p_1, p_2\}$. Since the probability of receiving the amount of information $\Im_1$ is p_1 and that of $\Im_2$ is p_2, the expected averaged amount of information received is

$$I(p_1, p_2) = p_1 \Im(p_1) + p_2 \Im(p_2)\,,$$

or, more generally, for N mutually different messages $\{x_1, \ldots, x_N\}$ with the language $\{p_i\}$ the average amount of information received is[2]

$$I(p_1, \ldots, p_N) = p_1 \Im(p_1) + \ldots + p_N \Im(p_n)\,. \tag{D.1}$$

Let us note that (D.1) implies that $I(\ldots)$ is symmetric and continuous in all its arguments. As we shall see, these conditions will strongly restrict a possible class of feasible I's. A further, sever restriction on the possible form of $I(p_1, \ldots, p_N)$ is imposed by the, so called,

---

letter Z has $p(Z) = 0.0005$ in English, 0.0006 in French and 0.0008 in Czech. In information theory is usual to call a set of p's a *langue* even if a message itself is not composed of actual letters

[2] We may also say that the averaged amount of received information is the averaged gain of information associated with the transmitted message or equivalently, the ignorance of a receiver, that is removed by recipe of the message.

additivity law for information [92]. To understand the basic features of the latter, let us start with $N = 3$.

In order to determine the degree of uncertainty about the system (or equivalently, the expected amount of information received), we may, e.g., first evaluate the degree of uncertainty connected with the fact that we do not know whether x_1 or $\overline{x}_1$ (complement of x_1) occured and add the degree of uncertainty whether the message in $\overline{x}_1$ is x_2 or x_3. The amount of uncertainty due to (or information conveyed by) the first determination is obviously

$$I(p_1, \overline{p}_1) = p_1 \Im(p_1) + \overline{p}_1 \Im(\overline{p}_1)\,.$$

The amount of uncertainty due to the second determination is

$$I(x_1, x_2|\overline{x}_1) := I(p(x_2|\overline{x}_1), p(x_3|\overline{x}_1)) = p(x_2|\overline{x}_1)\Im(p(x_2|\overline{x}_1)) + p(x_3|\overline{x}_1)\Im(p(x_3|\overline{x}_1))\,.$$

Using the Bayes's formula for the conditional probabilities ($p(XY) = p(X)p(Y|X)$) and the fact that if $X \cap Y = X$ then $p(XY) = p(X)$ (X and Y denote sets of events) we may write

$$I(x_1, x_2|\overline{x}_1) = \frac{p(x_2)}{p(\overline{x}_1)} \Im\left(\frac{p(x_2)}{p(\overline{x}_1)}\right) + \frac{p(x_3)}{p(\overline{x}_1)} \Im\left(\frac{p(x_3)}{p(\overline{x}_1)}\right)\,. \tag{D.2}$$

However (D.2) is the amount of information conveyed only when the $\overline{x}_1$ event occurs, so the total amount of information conveyed on average must be

$$\begin{aligned} I(p_1, p_2, p_3) &= I(p_1, \overline{p}_1) + \overline{p}_1 I(x_2, x_3|\overline{x}_1) \\ &= I(p_1, \overline{p}_1) + \overline{p}_1\, I\left(\frac{p_2}{\overline{p}_1}, \frac{p_3}{\overline{p}_1}\right)\,. \end{aligned} \tag{D.3}$$

We shall now show that the additivity law (D.3) together with symmetry and continuity of $I(\ldots)$ suffice to determine $I(\ldots)$ uniquely up to a multiplicative constant. The proof will be done in three steps.

Step 1

Let us assume that we have events $\{x_1, \ldots, x_{N-1}, y_1, \ldots, y_M\}$ and the corresponding alphabet $\{p_1, \ldots, p_M, q_1, \ldots, q_M\}$. (The way we perform a splitting into x's and y's is actually irrelevant.) We shall show now that the following important identity holds

$$I(p_1, \ldots, p_{N-1}, q_1, \ldots, q_M) = I(p_1, \ldots, p_N) + p_N\, I\left(\frac{q_1}{p_N}, \ldots, \frac{q_M}{p_N}\right) , \qquad \text{(D.4)}$$

where $p_N = \sum_{i=1}^{M} q_i$. We may think of events $\{x_1, \ldots, x_{N-1}\}$ as a one composite event x. For $M = 1$ Eq.(D.4) is then trivially fulfilled. If $M = 2$, Eq.(D.4) coincides with Eq.(D.3) and so is true as well. Let us now take an induction step and let assume that (D.4) is true for a general $M > 2$ and let us prove that this must hold also for $M + 1$. Actually, due to the induction hypothesis we may directly write for $M + 1$

$$I(p_1, \ldots, p_{N-1}, q_1, \ldots, q_{M+1}) = I(p_1, \ldots, p_{N-1}, q_1, p'_N) + p'_N\, I\left(\frac{q_2}{p'_N}, \ldots, \frac{q_{M+1}}{p'_N}\right) , \qquad \text{(D.5)}$$

with $p'_N = \sum_{i=2}^{M+1} q_i$. Using now relation for $M = 2$ we may write the first term on the RHS of (D.5) as

$$I(p_1, \ldots, p_{N-1}, q_1, p'_N) = I(p_1, \ldots, p_N) + p_N I\left(\frac{q_1}{p_N}, \frac{p'_N}{p_N}\right) , \qquad \text{(D.6)}$$

with $p_N = q_1 + p'_N = \sum_{i=1}^{M+1} q_i$. Using the symmetry of $I(\ldots)$ and the induction hypothesis we may write

$$\begin{aligned} I\left(\frac{q_1}{p_N}, \ldots, \frac{q_{M+1}}{p_N}\right) &= I\left(\frac{q_1}{p_N}, \frac{p'_N}{p_N}\right) + \frac{p'_N}{p_N} I\left(\frac{q_2}{p'_N}, \ldots, \frac{q_{M+1}}{p'_N}\right) \\ \Leftrightarrow \quad p'_N I\left(\frac{q_2}{p'_N}, \ldots, \frac{q_{M+1}}{p'_N}\right) &= p_N I\left(\frac{q_1}{p_N}, \ldots, \frac{q_{N+1}}{p_N}\right) - p_N I\left(\frac{q_1}{p_N}, \frac{p'_N}{p_N}\right) . \qquad \text{(D.7)} \end{aligned}$$

Plugging both (D.6) into (D.7) into (D.5) we receive the desired relation for $M+1$, and so this proves that Eq.(D.4) holds.

Step 2

In this step we extend our reasoning to an arbitrary number, say n, of groups of the messages, i.e., we want to evaluate the amount of information

$$I(p_{1,1}, \ldots, p_{1,N_1}, p_{2,1}, \ldots, p_{2,N_2}, \ldots, p_{n,1}, \ldots, p_{n,N_n}) .$$

Using the result (D.4) we may directly write the former as

$$I(p_{1,1}, \ldots, p_{1,N_1}, \ldots, p_{n-1,1}, \ldots, p_{n-1,N_{n-1}}, p_n) + p_n I\left(\frac{p_{n,1}}{p_n}, \ldots, \frac{p_{n,N_n}}{p_n}\right) ,$$

where $p_n = \sum_{i=1}^{N_n} p_{n,i}$. If we now shift p_N to the very left in $I(\ldots)$ and iterate further we get

$$\begin{aligned} I(p_n, p_{1,1}, \ldots, p_{1,N_1}, \ldots, p_{n-1,1}, \ldots, p_{n-1,N_{n-1}}) &= I(p_n, p_{1,1}, \ldots, p_{n-2,N_{n-2}}, p_{n-1}) \\ &+ \; p_{n-1} I\left(\frac{p_{n-1,1}}{p_{n-1}}, \ldots, \frac{p_{n-1,N_{n-1}}}{p_{n-1}}\right) , \end{aligned}$$

with $p_{n-1} = \sum_{i=1}^{N_{n-1}} p_{n-1,i}$. Shifting p_{n-1} to the very left and repeating iteration we get

$$\begin{aligned} I(p_n, p_{n-1}, p_{1,1}, \ldots, p_{1,N_1}, \ldots, p_{n-2,N_{n-2}}) &= I(p_n, p_{n-1}, p_{1,1}, \ldots, p_{n-3,N_{n-3}} p_{n-2}) \\ &+ p_{n-2}\, I\left(\frac{p_{n-2,1}}{p_{n-2}}, \ldots, \frac{p_{n-2,N_{n-2}}}{p_{n-2}}\right) , \end{aligned}$$

with $p_{n-2} = \sum_{i=1}^{N_{n-2}} p_{n-2,i}$. Shifting p_{n-2} to the very left and repeating iteration, etc. up to p_1 we finally obtain

$$I(p_{1,1}, \ldots, p_{n,N_n}) = I(p_1, p_2, \ldots, p_n) + \sum_{i=1}^{n} p_i\, I\left(\frac{p_{i,1}}{p_i}, \ldots, \frac{p_{i,N_i}}{p_i}\right) . \tag{D.8}$$

Eq.(D.8) is the desired result.

Step 3

In this last step we shall actually solve Eq.(D.8). Before we start let us define one useful function. If all the messages were equiprobable, i.e., all $p_i = 1/n$ with n being the number of all possible messages, then we define

$$\sigma(n) := I\left(\frac{1}{n}, \ldots, \frac{1}{n}\right) ; \;\; n \geq 2; \;\; I(1) = 0 \, .$$

The first noticeable fact about $\sigma(x)$ is that it fulfils a very simple functional relation, namely

$$\begin{aligned} \sigma(mn) &= I\left(\frac{1}{mn}, \ldots, \frac{1}{mn}\right) = I\left(\frac{1}{n}, \ldots, \frac{1}{n}\right) + \sum_{i=1}^{n} \frac{1}{n}\, I\left(\frac{1}{m}, \ldots, \frac{1}{m}\right) \\ &= \sigma(n) + \sigma(m) \, , \end{aligned} \tag{D.9}$$

where in the first line we have used Eq.(D.8). The functional identity (D.9) has the well known solution[3]; $\sigma(x) = k \ln(x)$. The constant k is the only ambiguity which the solution possesses. We shall specify k latter on.

---

[3] A simple way how to solve (D.9) is to assume that $\sigma(x)$ is a continuous function. If we were able to

Let us now assume that probabilities $\{p_1, \ldots, p_n\}$ on the RHS of (D.8) are rational numbers, i.e., we may write $p_1 = N_1/N$, $p_2 = N_2/N, \ldots, p_n = N_n/N$ with $N = \sum_{i=1}^{n} N_i$. In this case

$$I(p_1, p_2, \ldots, p_n) = I\left(\frac{N_1}{N}, \ldots, \frac{N_n}{N}\right).$$

Inserting this back into Eq.(D.8) we may rewrite (D.8) as

$$\begin{aligned} I\left(\frac{1}{N}, \ldots, \frac{1}{N}\right) &= \sigma(N) = I\left(\frac{N_1}{N}, \ldots, \frac{N_n}{N}\right) + \sum_{i=1}^{n} \frac{N_i}{N} I\left(\frac{1}{N_i}, \ldots, \frac{1}{N_i}\right) \\ &= I\left(\frac{N_1}{N}, \ldots, \frac{N_n}{N}\right) + \sum_{i=1}^{n} \frac{N_i}{N} \sigma(N_i) \\ \Leftrightarrow \quad I\left(\frac{N_1}{N}, \ldots, \frac{N_n}{N}\right) &= \sigma(N) - \sum_{i=1}^{n} \frac{N_i}{N} \sigma(N_i) = -k \sum_{i=1}^{n} \frac{N_i}{N} \ln\left(\frac{N_i}{N}\right). \end{aligned} \tag{D.10}$$

As $I(\ldots)$ is by assumption continuous function we may analytically continue result (D.10) to irrational probabilities, and so generally

$$I(p_1, \ldots, p_n) = -k \sum_{i=1}^{n} p_i \ln(p_i). \tag{D.11}$$

Note that the structure of Eq.(D.11) is precisely that as in (D.1). Comparing both (D.1) and (D.11) we may identify the amount of information $\Im_m$ of the message x_m as $\Im(p_m) =$

---

find the solution of the relation $\sigma(xy) = \sigma(x) + \sigma(y)$ for continuous arguments we could at the end restrict our attention only to discrete ones. Assuming this continuity we may perform derivation w.r.t. x and get

$$\frac{d\sigma(yx)}{dx} = y\,\sigma'(yx) = \sigma'(x).$$

Setting $yx = z$ we obtain the differential equation

$$z\,\sigma'(z) = x\,\sigma'(x) = k,$$

where k is constant. So the solution is obvious: $\sigma(x) = k\ln(x)$.

$-k\ln(p_m)$. Because $\Im(\ldots)$ is a non–negative, decreasing function of its argument, the constant k must be positive[4].

The constant k clearly fixes the units of information. In information theory k is chosen to be 1 with the logarithm in the base 2, so $I(\ldots) = -\sum_i p_i \log_2(p_i)$. The reason for choice this is quite pragmatic. The messages are usually written in the binary characters ($\{0, 1\}$, yes/no). The most elementary message is composed of two equiprobable events (unbiased choice between two possible messages about which a receiver does not posses any further information). In this case the information entropy is $I(1/2, 1/2) = \sigma(1/2) = 1$. Thus the most elementary message carries the unit amount of information. This unit is called "bit" [5]. If one transmits only n–letter messages (i.e. $111\ldots11$, $111\ldots10$, $\ldots$, $000\ldots00$) then the amount of information is clearly $\sigma(2^n) = n$. Consequently such messages convey information with n bits.

As it was mentioned, in information theory Eq.(D.11) refers to the situation *after* the reception of a message. Accordingly we interpret (D.11) as the average gain in the information associated with the transmitted message (the greater the initial uncertainty, the greater the amount of information conveyed. If there is no initial uncertainty or doubt to be resolved, the alphabet $\{p_i\}$ shrinks to a single case $\{p_j = 1, p_{k\neq j} = 0\}$ and hence the Shannon entropy (gained information) is zero). Let us note that if events $\{x_i\}$ are equiprobable the information entropy equals to the expected number of binary (yes/no) questions whose answer take us from our current knowledge to the one of certainty[6].

---

[4] Note: If $k = \log_2 e$ the amount of information (D.11) is called both the Shannon and information entropy. For a different choice of k only notion of the Shannon entropy is used.

[5] If the base of the logarithm is e ($k = 1$), then the information is measured in "nats".

[6] For instance, for $I(1/2, 1/2)$ the binary question may sound: is it 1 which is transmitted ? In the case of the n–letter messages we may ask whether the transmitted message has on the first position 1 (yes/no),

In physical systems, however, no message is send, so to speak. We may, nonetheless, in accordance with the previous derivation view (D.11) as the mean information about the system which is not transmitted yet (i.e. the recipient is waiting for it). From this standpoint $I(\ldots)$ appears as entropy of the language, that is as uncertainty (or ignorance) about the ensemble of all possible messages which may be received. The only difference is that the uncertainty (ignorance) cannot never be completely removed, as in the case when the message is received, but it may be removed partially, namely when one performs a measurement on the system. We shall return to this point in a while.

Now, question stands what k we should choose in real (macroscopic) physical systems. It is clear that in statistical physics, the systems are too complex and the amount of all possible transmittable information is so vast that k must be chosen very small in order for one to get judiciously large numerical values of the Shannon entropy in typical processes. Because k should be a constant valid for all systems, its numerical value depends only on the choice of physical units and hence may be determined via arbitrary, but suitably chosen system. For example, we may define as a unit entropy the entropy corresponding to one mole of spins of free valence electrons in a piece of iron. Assuming that all the 2^{N_A} spin configurations are equiprobable (Avogadro's number $N_A = 0.6024 \times 10^{24}\ \text{mol}^{-1}$), then this yields $I(\ldots) = \sigma(2^{N_A}) = kN_A = 1\,\text{mol}^{-1}$. From this reasoning we would get $k \sim 10^{-24}$. In order to obtain a connection with the usual von Neumann–Gibbs entropy of statistical physics we may note that the Shannon entropy coincides with the von Neumann–Gibbs one provided we fix $k/\ln(2) = k_B = 1.3804 \times 10^{-23}\text{JK}^{-1}$.

In connection with statistical physics we may define a notion of *information content* $\mathfrak{I}$ inherent to a system of interest. Let us assume that the system had originally the

---

on the second position 1 (yes/no), ... , at the n-th position 1 (yes/no).

information entropy $I_0(\ldots)$ (i.e., entropy of the ensemble of all possible transmittable results or all possible results of a measurement). Entropy I_0 is often called a–priory entropy. Then measurement is made but because of experimental errors or impossibility to measure all phenomena there is a whole new ensemble of values, each of which could give rise to the one observed. The information entropy, say $I_1(\ldots)$ may be defined also for this a–posteriori ensemble. The latter expresses how much uncertainty still left unresolved after measurement. Let us now define the informative content $\mathfrak{Z}$ as an amount by which the uncertainty about a system has been reduced, i.e.

$$\mathfrak{Z} = I_0 - I_1\,,$$

or equivalently $I_1 = I_0 - \mathfrak{Z}$. After discarding the (constant) additive entropy I_0 the latter leads to the statement that the informative content is equivalent to negative entropy ("negatropy"). That is, as our information about a physical system increases, its entropy must decrease[7] . This result is due to Szilard [106] and Brillouin [105].

The passage to quantum mechanics is simple. If the macro–state of a system is represented by the density matrix

$$\rho_H = \sum_n p_n |\psi_n\rangle\langle\psi_n|\,, \tag{D.12}$$

then the information entropy turns out to be (for simplicity we omit from now on the sub–index H)

$$I(\rho) = -\mathrm{Tr}(\rho \log_2 \rho)\,, \tag{D.13}$$

and the information content

$$\mathfrak{Z} = \mathrm{Tr}(\rho \log_2 \rho)\,. \tag{D.14}$$

---

[7] Note that in information theory $I_1(\ldots) = 0$.

In the language of information theory the ensemble of all possible messages is set of all possible results of a measurement of a given system of observables. The corresponding alphabet is $\{p_1, p_2, \ldots\}$.

Some properties of the Shannon entropy

- **Concavity:** The Shannon entropy is concave on the set of ρ's on a given Hilbert space.

Concavity of $I(\rho)$ means that for any pair ρ_1 and ρ_2 and $0 < \lambda < 1$ we have

$$I(\lambda\rho_1 + (1-\lambda)\rho_2) \geq \lambda I(\rho_1) + (1-\lambda)I(\rho_2)\,.$$

This may be proven very simply with a help of the inequality

$$\mathrm{Tr}(X\log_2 Y) - \mathrm{Tr}(X\log_2 X) \leq (\mathrm{Tr}X - \mathrm{Tr}Y)\log_2 e\,.$$

(use the spectral decomposition of X and Y and the inequality $\ln x \leq (1-x)$) The generalised concavity identity reads

$$I(\sum_i \lambda_i \rho) \geq \sum_i \lambda_i I(\rho)\,,$$

where $\lambda_i > 0$ and $\sum_i \lambda_i = 1$.

- **Maximum:** If the possible kets in the spectral decomposition (D.12) span a finite $\mathcal{W}$–dimensional subspace of the Hilbert space then

$$I(\rho) \leq \log_2\mathcal{W}\,,$$

with the equality only in the case when all probabilities in (D.12) are equal, i.e. $p_i = p = 1/\mathcal{W}$.

To prove this we may look at the difference

$$I(\rho) - \log_2 \mathcal{W} = \mathrm{Tr}(\rho\,(\log_2 \rho^{-1}\mathcal{W}))\,.$$

Taking the spectral decomposition of ρ together with the inequality $\ln x \leq (1-x)$ (note the equality is fulfilled only when $x = 1$) we obtain $I(\rho) - \log_2 \mathcal{W} \leq 0$. The latter is equal to 0 if and only if $\mathcal{W}/p_i = 1$ for all p_i.

- **Minimum:** The Shannon entropy has a minimum equal to zero. This happen only when ρ describes a pure state.

Because $-\log_2(\ldots)$ is a convex function, one may use Jensens's inequality of statistical mathematics [37, 59]: if $f(\ldots)$ is a convex function then $\langle f(X)\rangle \geq f(\langle X\rangle)$. Thus $I(\rho) = -\langle \log_2 \rho\rangle \geq -\log_2\langle\rho\rangle = 0$, so

$$I(\rho) \geq 0\,.$$

$I(\rho) = 0$ only if there is no uncertainty about a message, i.e. when alphabet $\{p_i\}$ shrinks to a single case $\{p_j = 1, p_{i\neq j} = 0\}$, i.e. when ρ describes the pure state.

Appendix E

Some mathematical formulae

E.1 Integrals in D dimensions

(This section is based on refs. [42, 49, 50, 53].)[1]

Throughout our dissertation we frequently apply dimensional regularisation; i.e. we replace the dimension 4 by a lower dimension D where the corresponding (loop) integrals are convergent. Bellow we provide a short list of integrals which we found useful during our calculations (cf. Sections 3.2, 3.3, 3.4 and 4.4, Appendices B and C).

The paradigmatic integral of the dimensional regularisation is

$$\int \frac{d^D q_E}{(q_E^2 + X)^n} = \pi^{D/2} \frac{\Gamma(n - \frac{D}{2})}{\Gamma(n)} X^{-n+\frac{D}{2}} \, . \qquad n < 2 \, .$$

(use D–dimensional polar coordinates and the fact that $\int d\Omega = S^{D-1} = 2\pi^{\frac{D}{2}}/\Gamma(\frac{D}{2})$) Euclidean regime is defined via Wick's rotation as; $q^0 = iq_E^0, \mathbf{q} = \mathbf{q}_E, d^D q = id^D q_E$. Although the LHS as a D–dimensional integral is senseful only for integer values of D, the RHS has an analytic continuation for all $D \in \mathbb{C}$ with $D \neq 2n$ (so namely for $D = 4 - 2\varepsilon$ $(\varepsilon > 0, \varepsilon \to 0)$). Performing the change of variables $q_E \to q_E + l_E$ we get

---

[1] Note: All the quantities entering formulae bellow are dimensionless!!

$$\int \frac{d^D q_E}{(q_E^2+2l_E q_E+X)^n} = \pi^{D/2}\frac{\Gamma(n-\frac{D}{2})}{\Gamma(n)}(X-l_E^2)^{-n+\frac{D}{2}}\,.$$

Successive derivatives with respect to l_E^α then yield

$$\begin{aligned}
\int d^D q_E\,\frac{q^\mu}{(q^2+2l_E q_E+X)^n} &= -\pi^{D/2}\,l_E^\mu\,\frac{\Gamma(n-\frac{D}{2})}{\Gamma(n)}(X-l_E^2)^{-n+\frac{D}{2}}\,.\\
\int d^D q_E\,\frac{q^\mu q^\nu}{(q^2+2l_E q_E+X)^n} &= \frac{\pi^{D/2}}{\Gamma(n)}(X-l_E^2)^{-n+\frac{D}{2}}\\
&\times\left\{\Gamma(n-\tfrac{D}{2})l_E^\mu l_E^\nu+\frac{1}{2}\delta^{\mu\nu}\Gamma(n-1-\tfrac{D}{2})(X-l_E^2)\right\}\,.
\end{aligned}$$

The analytical continuation to Minkowski regime (i.e. Wick's rotation of both q_E^α and l_E^α) together with Eq.(3.75) gives

$$\begin{aligned}
\int\frac{d^D q}{(2\pi)^D}\frac{i}{q^2-m^2\pm i\epsilon} &= \frac{\Gamma(1-\frac{D}{2})}{(4\pi)^{D/2}}(m^2)^{D/2-1}\\
&= -\frac{m^2}{16\pi^2}\left(\Delta-\ln m^2+1+\mathcal{O}(\varepsilon)\right)\,,
\end{aligned}$$

with

$$\Delta=\frac{1}{\varepsilon}-\gamma+\ln 4\pi\,.$$

(for convenience we have introduced the usual factor $1/(2\pi)^D$) Previous results together with the Feynman parametrisation: $1/ab=\int_0^1 dt\,1/[at+b(1-t)]^2$, yield

$$\begin{aligned}
&\int\frac{d^D q}{(2\pi)^D}\frac{i}{(q^2-m^2+i\epsilon)((q+p)^2-m^2+i\epsilon)}\\
&\qquad\qquad= \frac{-1}{16\pi^2}\left(\Delta-\int_0^1 dt\ln(m^2+p^2(t^2-t))+\mathcal{O}(\varepsilon)\right)\\
&\int\frac{d^D q}{(2\pi)^D}\frac{i\,q^\mu}{(k^2-m^2+i\epsilon)((q+p)^2-m^2+i\epsilon)}\\
&\qquad\qquad= \frac{p^\mu}{32\pi^2}\left(\Delta-\int_0^1 dt\ln(m^2+p^2(t^2-t))+\mathcal{O}(\varepsilon)\right)\\
&\int\frac{d^D q}{(2\pi)^D}\frac{i\,q^\mu q^\nu}{(k^2-m^2+i\epsilon)((q+p)^2-m^2+i\epsilon)} = \frac{1}{16\pi^2}\left(g^{\mu\nu}A(p^2,m)+p^\mu p^\nu B(p^2,m)\right)\,,
\end{aligned}$$

with $A(p^2,m)$ and $B(p^2,m)$:

$$\begin{aligned}
A(p^2,m) &= \frac{1}{3}\Big\{-m^2\left[\tfrac{3}{2}\Delta - \tfrac{1}{2}\mathrm{ln}m^2 + \tfrac{3}{2} - \int_0^1 dt\,\ln(m^2+p^2(t^2-t))\right] \\
&\quad + \tfrac{1}{4}p^2\left[\Delta + \tfrac{2}{3} - \int_0^1 dt\,\ln(m^2+p^2(t^2-t))\right] + \mathcal{O}(\varepsilon)\Big\}
\end{aligned}$$

$$\begin{aligned}
B(p^2,m) &= \frac{4}{3p^2}\Big\{m^2\left[\tfrac{3}{2}\Delta - \tfrac{1}{2}\mathrm{ln}m^2 + 3 - \int_0^1 dt\,\ln(m^2+p^2(t^2-t))\right] \\
&\quad - \tfrac{1}{4}\left[\Delta + 1 - \int_0^1 dt\,\ln(m^2+p^2(t^2-t))\right] + \mathcal{O}(\varepsilon)\Big\}\,.
\end{aligned}$$

Note: the integral $\int_0^1 dt\,(\ldots)$ might be evaluated explicitly, the result reads

$$\int_0^1 dt\,\ln(m^2+p^2(t^2-t)) \;=\; \ln(m^2) - 2 + 2\sqrt{\frac{4-a}{a}}\,\arctan\left(\frac{\sqrt{a}}{\sqrt{4-a}}\right)\,,$$

with $a = p^2/m^2$.

E.2 Special functions and important relations

(This section is based on refs. [36, 41, 42, 53, 74, 80, 83, 84].)

The gamma function $\Gamma(x)$ and the Riemann zeta function $\zeta(x)$ are defined as follows:

$$\Gamma(x) = \int_0^\infty dt\,e^{-t}t^{x-1} \qquad \mathrm{Re}x > 0$$

$$\zeta(x) = \sum_{n=1}^\infty n^{-x} \qquad \mathrm{Re}x > 1\,.$$

The above definitions converge only in the specified regions of the complex plane, but they can be analytically (single–valuedly) continued. The following important relations (used in Section 3.4) are valid in the entire complex plane (save for the points $x = -n, (n = 0, 1, 2, \ldots)$ where the simple pole residue is $\frac{(-1)^n}{n!}$)

$$\begin{aligned}
&\Gamma(x+1) = x\Gamma(x) \\
&\Gamma(x)\Gamma(1-x) = \frac{\pi}{\sin(\pi x)} \\
&\Gamma\left(\frac{1}{2}+x\right)\Gamma\left(\frac{1}{2}-x\right) = \frac{\pi}{\cos(\pi x)} \\
&\Gamma(2x) = \frac{2^{2x-1}}{\sqrt{\pi}}\Gamma(x)\Gamma\left(x+\frac{1}{2}\right) \\
&\Gamma\left(\frac{x}{2}\right)\pi^{-\frac{x}{2}}\zeta(x) = \Gamma\left(\frac{1-x}{2}\right)\pi^{\frac{x-1}{2}}\zeta(1-x)\,.
\end{aligned}$$

For n being integer

$$\Gamma\left(\frac{1}{2}-n\right) = (-1)^n\frac{2^n\sqrt{\pi}}{(2n-1)!!}\,.$$

Important numerical values of $\zeta(x)$ used in the text are :

x	0	$\frac{3}{2}$	2	$\frac{5}{2}$	3	4	5
$\zeta(x)$	$\frac{1}{2}$	2.612	$\frac{\pi^2}{6}$	1.341	1.202	$\frac{\pi^4}{90}$	1.037

$$\zeta'(0) = \left(\frac{d\zeta(x)}{dx}\right)_{x=0} = -\tfrac{1}{2}\ln(2\pi)\,.$$

(note: only numerical values of $\zeta(2n+1)$ are available)

Important numerical values of $\Gamma(x)$ used in the text are :

x	$\frac{1}{2}$	1	$\frac{5}{4}$	$\frac{3}{2}$	$\frac{7}{4}$
$\Gamma(x)$	$\sqrt{\pi}$	1	0.906	$\frac{1}{2}\sqrt{\pi}$	0.919

Both $\zeta(x)$ and $\Gamma(x)$ appear in expansions of the following definite integrals used in the text ($n > 0$):

$$\begin{aligned}
&\int_0^\infty dt\,\frac{t^{n-1}}{e^t \pm 1} = (1-(1\mp 1)2^{-n})\Gamma(n)\zeta(n) \qquad \text{(Einstein's integrals)}\\
&\int_0^\infty dt\,\frac{t^{n-1}}{\mathrm{sinh}t} = 2(1-2^{-n})\Gamma(n)\zeta(n)\\
&\int_0^\infty dt\,\frac{t^{n-1}}{\mathrm{cosh}t} = 2\Gamma(n)\sum_{k=0}^{\infty}(-1)^k(2k+1)^n\\
&\int_0^\infty dt\,\frac{x^{n-1}}{\mathrm{cosh}^2 t} = 2^{2-n}(1-2^{2-n})\Gamma(n)\zeta(n-1)\,.
\end{aligned}$$

Euler's ψ function (or digamma) was used both in Section 3.4 and Section 4.4. $\psi(\ldots)$ is defined as the logarithmic derivation of Γ function:

$$\begin{aligned}
\psi(x) &= \frac{1}{\Gamma(x)}\frac{d\Gamma(x)}{dx}\\
&= \int_0^\infty \left(\frac{e^{-t}}{t} - \frac{e^{-zt}}{1-e^{-t}}\right) dt\,.
\end{aligned}$$

The former directly implies that

$$\begin{aligned}
\psi(x+1) &= \psi(x) + \frac{1}{x}\\
\psi(\tfrac{1}{2}) &= \psi(1) - 2\mathrm{ln}2\,,
\end{aligned}$$

or recursively (n is integer)

$$\psi(x+n) = \psi(x+1) + \frac{1}{1+x} + \frac{1}{2+x} + \ldots + \frac{1}{(n-1)+x}\,.$$

Defining the Euler–Mascheroni constant $\gamma = -\psi(1)$ (the only numerical value is known: $\gamma = 0.5772156649\ldots$), we get directly

$$\begin{aligned}
\psi(n) &= -\gamma + \sum_{k=1}^{n-1}\frac{1}{k}\\
\psi(\tfrac{1}{2}+n) &= -\gamma - 2\mathrm{ln}2 + 2\left(1 + \frac{1}{3} + \ldots + \frac{1}{2n-1}\right)\,.
\end{aligned}$$

In Section 4.4 we use functions K_n, which are the Bessel functions of imaginary argument of order n (we deal only with n being integer). K_n is defined as:

$$\begin{aligned} K_n(x) &= \frac{\sqrt{\pi}(\frac{1}{2}x)^n}{\Gamma(n+\frac{1}{2})}\int_0^\infty dt\, e^{-z\mathrm{cosh t}}\mathrm{sinh}^{2n}t \\ &= \frac{\sqrt{\pi}(\frac{1}{2}x)^n}{\Gamma(n+\frac{1}{2})}\int_0^\infty dt\, e^{-zt}(t^2-1)^{n-\frac{1}{2}}\,. \end{aligned}$$

The former implies the important relation: $K_0'(x) = K_1(x)$. In Section 4.4 we use the following relations:

$$\begin{aligned} \int_0^\infty dt\, \frac{e^{-pt}}{\sqrt{t(t+a)}} &= e^{\frac{ap}{2}}K_0\left(\frac{ap}{2}\right) \\ \int_m^\infty dt\, \frac{te^{-pt}}{\sqrt{t^2-m^2}} &= mK_1(mp) \\ \int_0^\infty dt\, \frac{(t+a)e^{-pt}}{\sqrt{t^2+2at}} &= ae^{ap}K_1(ap)\,. \end{aligned}$$

The limiting form for small arguments x (n fixed) reads:

$$K_n(x) \sim \tfrac{1}{2}\Gamma(n)(\tfrac{1}{2}x)^{-n}\,.$$

Some miscellaneous functions used in the text:

- Beta function $B(z;y)$ (see Section 3.4):

$$B(x;y) = \int_0^1 dt\, t^{x-1}(1-t)^{y-1} = \int_0^\infty \frac{t^{x-1}}{(1+t)^{x+y}} = \frac{\Gamma(x)\Gamma(y)}{\Gamma(x+y)}\,.$$

- Gauss' hypergeometric functions ${}_2F_1[\ldots]$ (see Section 3.4):

$$\begin{aligned} {}_2F_1[a,b;c;x] &= \frac{\Gamma(c)}{\Gamma(a)\Gamma(b)}\sum_{k=0}^\infty \frac{\Gamma(a+k)\Gamma(b+k)}{\Gamma(c+k)}\frac{x^k}{k!} \\ &= \frac{1}{B(b;c-b)}\int_0^1 dt\, t^{b-1}(1-t)^{c-b-1}(1-tx)^{-a}\,. \end{aligned}$$

(note: ${}_2F_1$ converges for $|x| < 1$ with a branch point at $x = 1$, for $c = -n (n = 0, 1, \ldots)$ ${}_2F_1$ is undetermined)

The following relations for ${}_2F_1$ are used in Section 3.4:

$$\begin{aligned} {}_2F_1[a, b; a-b+1; -1] &= 2^{-a}\sqrt{\pi}\frac{\Gamma(1+a-b)}{\Gamma(1+\frac{1}{2}a-b)\Gamma(\frac{1}{2}+\frac{1}{2}a)} \\ {}_2F_1[a, b; \tfrac{1}{2}a+\tfrac{1}{2}b+\tfrac{1}{2}; \tfrac{1}{2}] &= \sqrt{\pi}\frac{\Gamma(\frac{1}{2}+\frac{1}{2}a+\frac{1}{2}b)}{\Gamma(\frac{1}{2}+\frac{1}{2}a)\Gamma(\frac{1}{2}+\frac{1}{2}b)}\,. \end{aligned}$$

- Bernoulli numbers B_α (see Section 3.4) are defined through the series :

$$\frac{x}{e^x - 1} = \sum_{\alpha=0}^{\infty} B_\alpha \frac{x^\alpha}{\alpha!} \qquad |x| < 2\pi\,.$$

Important numerical values of B_α used in the text are :

α	0	1	2	4
B_α	1	$-\frac{1}{2}$	$\frac{1}{6}$	$-\frac{1}{30}$

Bibliography

[1] D. A. Kirzhnitz and A. Linde. *Phys. Lett.*, **B42**: 471, 1972.

[2] S. Weinberg. *Phys. Rev.*, **D9**: 3357, 1974.

[3] L. Dolan and R. Jackiw. *Phys. Rev.*, **D9**: 3320, 1974.

[4] J. C. Collins and M. Perry. *Phys. Rev. Lett.*, **34**: 1353, 1975.

[5] P.A. Henning. *Nucl. Phys.*, **B337**: 547, 1990.

[6] J. Berges and K. Rajagopal. `hep-ph/9804233`.

[7] M. A. Halasz, A. D. Jackson, R. E. Shrock, M. A. Stephanov and J. J. M. Verbaarschot. *Phys. Rev.*, **D58**: 096007, 1998.

[8] J. I. Kapusta. *Nucl. Phys.*, **B148**: 461, 1979.

[9] E. W. Kolb and M. S. Turner. *The Early Universe.* Addison–Wesley, London, 1994.

[10] T. W. B. Kibble. *Acta Phys. Polon.*, **B13**: 723, 1982.

[11] V. A. Rubakov and M. E. Shaposnikov. *Phys. Usp.*, **39**: 461, 1996.

[12] E. W. Kolb, A. Linde and A. Riotto. *Phys. Rev. Lett.*, **77**: 4290, 1996.

[13] A. D. Sakharov. *Pisma ZhETF*, **5**: 32, 1967.

[14] A. Riotto and M. Trodden. `hep-ph/9901362`.

[15] T. W. B. Kibble. *J. Phys.*, **A9**: 1389, 1976.

[16] V. M. H. Ruutu, V. B. Eltsov, A. J. Gill, T. W. B. Kibble, M. Krusius, Yu. G. Makhlin, B. Placais, G. E. Volovik and Wen Xu. *Nature*, **382**: 334, 1996.

[17] P. C. Hendry, N. S. Lawson, R. A. M. Lee, P. V. E. McClintock and C. D. H. Williams. *Nature*, **368**: 315, 1994.

[18] I. Chuang, R. Durrer, N. Turok and B. Yurke. *Science*, **251**: 1336, 1991.

[19] W. H. Zurek. *Acta Phys. Polon.*, **B24**:1301, 1993.

[20] U. Heinz. `hep-ph/9902424`.

[21] J. P. Dougherty. *Phil. Trans. Roy. Soc. London*, **346**: 259, 1993.

[22] W. T. Grandy. *Principle of maximal entropy and irreversible processes, 2 vols.* D.Reidel, Amsterdam, 1980.

[23] R. Balescu. *Equilibrium and Nonequilibrium Statistical Mechanics.* John Wiley & Sons, 1975.

[24] E.T. Jaynes. *Am. J. Phys.*, **33**: 391, 1965.

[25] E.T. Jaynes. *Phys. Rev.*, **106, 108**: 620, 171, 1957.

[26] E. T. Jaynes. *Papers on probability, statistics and statistical mechanics.* D.Reidel, Amsterdam, 1983.

[27] B. Buck and V.A. Macaulay. *Maximum Entropy in Action.* Oxford Press, Oxford, 1991.

[28] R. Balian. *From Microphysics to Macrophysics; Methods and Applications of Statistical Physics, Vol.II.* Springer–Verlag, London, 1992.

[29] I. Prigogine. *Introduction to Thermodynamics of Irreversible Processes.* Interscience, New York, 1969.

[30] R. Balescu. *Statistical Dynamics, Matter out of Equilibrium.* Imperial College Press, London, 1997.

[31] R.C. Tolman. *The principles of the Statistical Mechanics.* Clarendon Press, Oxford, 1938.

[32] P. Ehrenfest and T. Ehrenfest. *The conceptual foundations of the statistical approach to mechanics.* Cornell University Press, 1959.

[33] N. N. Bogoliubov. *Problems of a dynamical theory in statistical physics.* Nort-Holland, London, 1962.

[34] M. LeBellac. *Thermal Field Theory.* Cambridge University Press, Cambridge, 1996.

[35] A. Das. *Finite Temperature Field Theory.* World Scientific, London, 1997.

[36] N. P. Landsman and Ch. G. van Weert. *Physics Report*, **145**: 141, 1987.

[37] R. Kubo. *Statistical Mechanics.* North–Holland Publishing Company, Oxford, 1965.

[38] T. Altherr. *Int. J. Mod. Phys.*, **A8**: 5605, 1993.

[39] J.W. Gibbs. *Elementary Principles in Statistical Mechanics.* Dover Publications, New York, 1960.

[40] L.P. Kadanoff and G. Baym. *Quantum Statistical Mechanics.* Benjamin, reading, 1962.

[41] A.L. Fetter and J.D. Walecka. *Quantum Theory of Many Particle Systems.* McGraw-Hill, New York, 1971.

[42] P. Ramond. *Field Theory, A Modern Primer.* The Benjamin/Cummings Publishing Company, INC, London, 1981.

[43] D.N. Zubarev. *Nonequilibrium Statistical Thermodynamics.* Consultants Bureau, London, 1974.

[44] K.C. Chou, Z.B. Su, B.L. Hao and L.Yu. *Phys. Rep.*, **118**: 1, 1985.

[45] P. V. Landshoff. *Nucl. Phys.*, **B430**: 683, 1994.

[46] P. V. Landshoff. *Phys. Lett.*, **B386**: 291, 1996.

[47] L. V. Keldysh. *Sov. Phys. – JETP*, **20**: 1018, 1964.

[48] P. van Nieuwenhuizen. Canonical methods in quantized gauge field theories. Teyler's lectures, Leyden Univerity, 1992.

[49] M. Veltman. *Diagrammatica – The Path to Feynman Diagrams.* Cambridge University Press, Cambridge, 1994.

[50] G. 't Hooft and M. Veltman. Diagrammar. *CERN Jellow Report*, **73-9**, 1973.

[51] R. Mills. *Propagators for Many–Particle Systems.* Gordon and Breach, New York, 1969.

[52] T. S. Evans and D. A. Steer. *Nucl. Phys.*, **B476**: 481, 1996.

[53] C. Itzikson and J. B. Zuber. *Quantum Field Theory.* McGraw-Hill, New York, 1980.

[54] R. L. Kobes and G. W. Semenoff. *Nucl. Phys.*, **B272**: 329, 1986.

[55] P. V. Landshoff and A. Rebhan. *Nucl. Phys.*, **B410**: 23, 1993.

[56] M. Jacob and P. V. Landshoff. *Phys Lett.*, **B281**: 114, 1992.

[57] A. J. Niemi and G. W. Semenoff. *Nucl. Phys.*, **B230**: 181, 1984.

[58] T. S. Evans and A. C. Pearson. *Phys. Rev.*, **D52**: 4652, 1995.

[59] G. Morandi. *Statistical Mechanics, An Intermediate Course.* World Scientific Publishing Co. Pte. Ltd., London, 1995.

[60] M.C.J. Leermakers and Ch.G. van Weert. *Nucl. Phys.*, **B248**: 671, 1984.

[61] I.T. Drummond, R.R. Horgan, P.V. Landshoff and A. Rebhan. *Nucl. Phys.*, **B524**: 579, 1998.

[62] I.T. Drummond, R.R. Horgan, P.V. Landshoff and A. Rebhan. *Phys. Lett.*, **B398**: 326, 1997.

[63] W.A. van Leeuwen S.R. de Groot and Ch.G. van Weert. *Relativistic Kinetic Theory. Principles and Applications.* North-Holland Publishing Company, Oxford, 1980.

[64] G.K. Batchelor. *An Introduction to Fluid Dynamics.* Cambridge University Press, London, 1967.

[65] J. Collins. *Renormalization; An introduction to renormalization, the renormalization group, and the operator–product expansion.* Cambridge University Press, Cambridge, 1984.

[66] L.S. Brown. *Ann. Phys.*, **126**: 135, 1979.

[67] Y. Nambu. *Prog. Theor. Phys. (Kyoto)*, **7**: 131, 1952.

[68] R. Jackiw. In S.B. Treiman, R. Jackiw, B. Zumino and E. Witten, editor, *Current Algebra and Anomalies.* World Scientific Publishing Co. Pte.Ltd., Singapore, 1985.

[69] S. Coleman C.G. Callan and R. Jackiw. *Ann. Phys.*, **59**: 42, 1970.

[70] G. Sterman. *An Introduction to Quantum Field Theory.* Cambridge University Press, Cambridge, 1993.

[71] W. Zimmermann. In S.Deser et al., editor, *Lectures on Elementary Particles and Quantum Field Theory.* M.I.T. Press, Cambridge (Mass.), 1970.

[72] P. Cvitanovic. *Field Theory.* Nordita, Copenhagen, 1983.

[73] M. van Eijck. *Thermal Field Theory and the Finite-Temperature Renormalization Group.* PhD thesis, University of Amsterdam, 1995.

[74] P. Jizba. *Phys. Rev.*, **D57**: 3634, 1998.

[75] H.J. Schnitzer. *Phys. Rev.*, **D10**: 1800, 1974.

[76] J.M. Cornwall, R. Jackiw and E. Tomboulis. *Phys. Rev.*, **D10**: 2428, 1974.

[77] W.A. Bardeen and M. Moshe. *Phys.Rev.*, **D28**: 1372, 1983.

[78] L.F. Abbot, J.S. Kang and H.J. Schnitzer. *Phys. Rev.*, **D13**: 2212, 1976.

[79] G. Amelino Camelia. `hep-th/9811236`.

[80] F. Oberhettinger. *Tables of Mellin Transforms.* Springer, Berlin, 1974.

[81] H.W. Braden. *Phys. Rev.*, **D25**: 1028, 1982.

[82] H.E. Haber and H.A. Weldon. *J. Math. Phys.*, **23**: 1852, 1982.

[83] A. Erdélyi. *Tables of Integral Transformations I.* McGraw–Hill, London, 1954.

[84] I.S. Gradshteyn and I.M. Ryzhik. *Tables of Integrals, Series, and Products.* Academic Press, INC., London, 1980.

[85] G. Amelino Camelia and S.-A. Pi. *Phys. Rev.*, **D47**: 2356, 1993.

[86] T.D.Lee. pp 1–13. In W.C. Haxton and E.M. Hanley, editor, *Symmetries and fundamental interactions in nuclei.* Columbia University Press, 1997.

[87] S.N. White. *Nucl. Instrum. Methods*, **A409**: 618, 1998.

[88] H. Heiselberg and A.D. Jackson. to be published in the proceedings of 3rd Workshop on Continuous Advances in QCD (QCD98), Minneapolis, MN, 16–19 Apr. 1998.

[89] R. Hagedorn. *Z. Phys.*, **C17**: 265, 1983.

[90] T. Haruyama, N. Kimura and T. Nakamoto. to be published in the proceedings of 17th International Conference on Cryogenic Engineering (ICEC 17), Bornemounth, England, 14–17 Jul. 1998.

[91] T. Haruyama, N. Kimura and T. Nakamoto. to be published in the proceedings of the-Cryogenic Engineering Conference and International Cryogenic Materials Conference (CEC / ICMC 97), Portland, OR, 27 Jul – 1 Aug. 1997.

[92] S. Hull, D.A. Keen, R. Done and C.N. Uden. `RAL-91-089`. to be published.

[93] J. Staun Olsen, L. Gerward and U. Benedict. `DESY SR-84-22`. to be published.

[94] P. Jizba. `hep-th/9801197`. to be published in Phys. Rev. **D**.

[95] E. Calzetta and B.L. Hu. *Phys. Rev.*, **D37**: 2878, 1988.

[96] P. Jizba and E.S. Tututi. work in progress.

[97] F. Cooper, S. Habib, Y. Kluger, E. Mottola and J.P. Paz. `hep-ph/9405352`. to be published.

[98] F. Cooper and E. Mottola. *Phys. Rev.*, **D36**: 3114, 1987.

[99] F. Cooper, S. Habib, Y. Kluger and E. Mottola. *Phys. Rev.*, **D55**: 6471, 1997.

[100] O. Éboli, R. Jackiw and So–Young Pi. *Phys. Rev.*, **D37**: 3557, 1988.

[101] D.C. Brody and L.P. Hughston. to be published.

[102] C.W. Gardier. *Handbook of Stochastic Methods for Physics, Chemistry and the Natural Sciences*. Springer–Verlag, New York, 1985.

[103] F. Floreanini and R. Jackiw. *Phys. Rev.*, **D37**: 2206, 1988.

[104] C.E. Shannon and W. Weaver. *The Mathematical Theory of Communication*. University of Illinois Press, Urbana, 1949.

[105] L. Brillouin. *J. Applied Phys.*, **22**: 334, 1951.

[106] L. Szilard. *Z. Physik*, **53**: 840, 1929.

[107] G. Marc and W.G. McMillan. In I. Prigogine and S. Rice, editor, *Advances in Chemical Physics*, volume Vol. LVIII. Wiley, New York, 1985.

[108] V. Petviashvili and O. Pokhotelov. *Solitary Waves in Plasmas and in the Atmosphere.* Gordon and Breach Science Publishers, Philadelphia, 1992.

[109] S. Ichimaru. *Basic Principles of Plasma Physics, A Statistical Approach.* W.A.Benjamin, INC. London, 1973.

[110] M. Gavrila. *Atoms in Intense Laser Fields.* Academic Press, San Diego Ca., 1992.

[111] G.A. Baker. *Essentials of Padé Approximation.* Academic Press, London, 1975.

[112] R. Baier, M. Dirks, K. Redlich, and D. Schiff. *Phys. Rev.*, **D56**: 2548, 1997.

[113] M. Strickland. *Phys. Lett.*, **B331**: 245, 1994.

[114] J. Baacke, K. Heitmann and C.P. Pätzold. `hep-th/9711144`. to be published.

[115] M. LeBellac. *Quantum and Statistical Field Theory.* Clarendon Press, Oxford, 1991.

[116] F. J. Belinfante. *Physica*, **7**: 449, 1940.

[117] L. Rosenfeld. *Mem. Roy. Acad. Belg. Cl. Sci.*, **6**: 18, 1940.

[118] P. E. Haagenson and J. I. Latorre. `hep-ph/9203207`. to be published.

[119] A. J. Niemi and G. W. Semenoff. *Ann. Phys.*, **152**: 181, 1984.

[120] J. I. Kapusta and P. V. Landshoff. *Nucl. Part. Phys.*, **15**: 267, 1989.

[121] J. Zinn–Justin. *Quantum Field Theory and Critical Phenomena.* Oxford Science Publisher, Oxford, 1996.

[122] J. Schwinger. *Proc. Nat. Acad. Sc.*, **37**: 452, 1951.

[123] F. J. Dyson. *Phys. Rev.*, **75**: 1736, 1949.

[124] J. Schwinger. *J. Math. Phys*, **2**: 407, 1961.

[125] M. Rasetti. *Modern Methods in Equilibrium Statistical Machanics.* World Scientific Poblishing Co. Pte. Ltd., Singapore, 1986.